USGS
science for a changing world

Prepared in cooperation with Oregon Water Resources Department

Simulation of Groundwater Flow and the Interaction of Groundwater and Surface Water in the Willamette Basin and Central Willamette Subbasin, Oregon

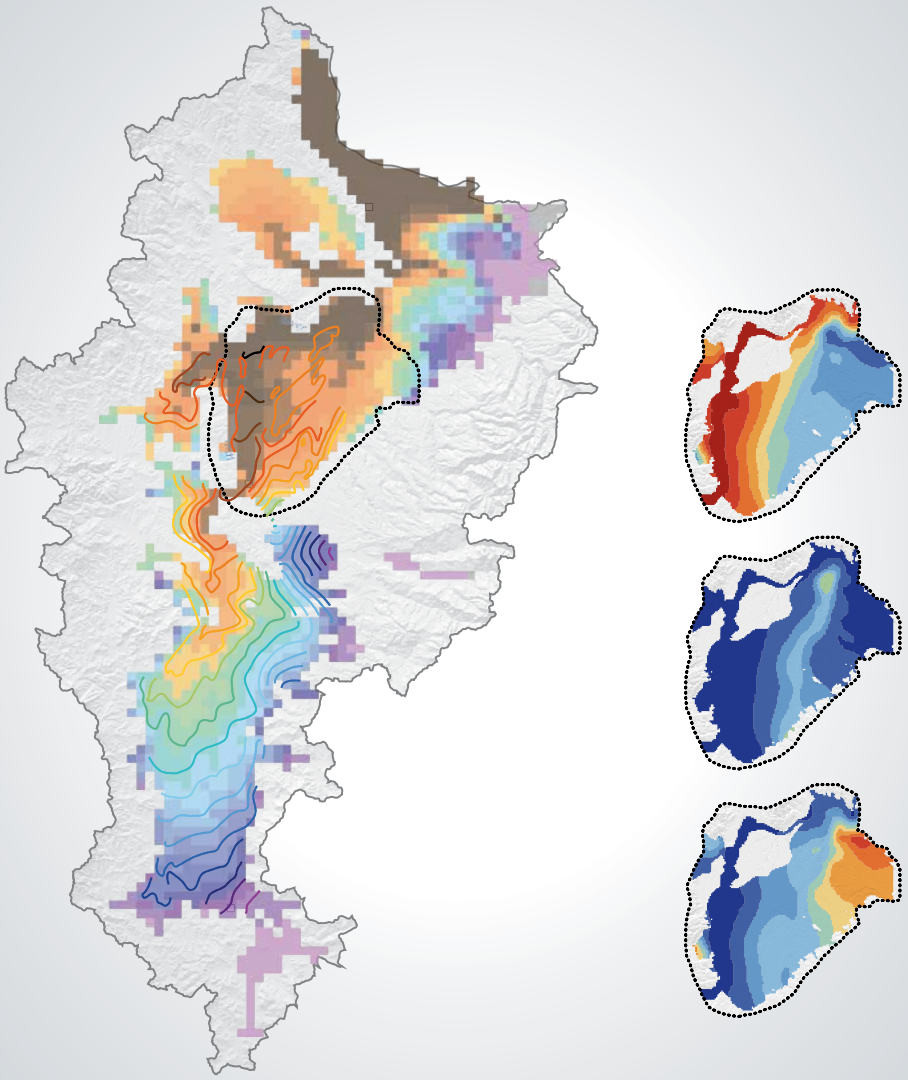

Scientific Investigations Report 2014–5136

U.S. Department of the Interior
U.S. Geological Survey

Cover

Left: Representation of simulated pre-development water-level elevations for the uppermost sedimentary model layer compared with 1935 pre-development water-table elevations of Piper (1942), Willamette Basin, Oregon.

Right: Representations of computed steady-state capture fraction that would result from withdrawal of water from model layer 3 at a constant rate in the Willamette, Pudding, and other selected rivers in the Central Willamette subbasin, Willamette Basin, Oregon.

Simulation of Groundwater Flow and the Interaction of Groundwater and Surface Water in the Willamette Basin and Central Willamette Subbasin, Oregon

By Nora B. Herrera, Erick R. Burns, and Terrence D. Conlon

Prepared in cooperation with Oregon Water Resources Department

Scientific Investigations Report 2014–5136

U.S. Department of the Interior
U.S. Geological Survey

U.S. Department of the Interior
SALLY JEWELL, Secretary

U.S. Geological Survey
Suzette M. Kimball, Acting Director

U.S. Geological Survey, Reston, Virginia: 2014

Suggested citation:
Herrera, N.B., Burns, E.R., and Conlon, T.D., 2014, Simulation of groundwater flow and the interaction of groundwater and surface water in the Willamette Basin and Central Willamette subbasin, Oregon: U.S. Geological Survey Scientific Investigations Report 2014–5136, 152 p., *http://dx.doi.org/10.3133/sir20145136*.

ISSN 2328-0328 (online)

Contents

Contents—Continued

Figures

Figures—Continued

Figures—Continued

Figures—Continued

Figures—Continued

Figures—Continued

Tables

Conversion Factors, Datums, Abbreviations and Acronyms, and Well or Spring Identification System

Conversion Factors

Multiply	By	To obtain
	Length	
inch (in.)	25.4	millimeter (mm)
foot (ft)	0.3048	meter (m)
mile (mi)	1.609	kilometer (km)
	Area	
acre	4,047	square meter (m^2)
square mile (mi^2)	2.590	square kilometer (km^2)
	Flow rate	
acre-foot per year (acre-ft/yr)	1,233	cubic meter per year (m^3/yr)
cubic foot per second (ft^3/s)	0.02832	cubic meter per second (m^3/s)
cubic foot per second per mile [(ft^3/s)/mi]	0.02832	cubic meter per second per mile [(m^3/s)/mi]
gallon per minute (gal/min)	0.06309	liter per second (L/s)
inch per year (in/yr)	25.4	millimeter per year (mm/yr)
	Hydraulic conductivity	
foot per day (ft/d)	0.3048	meter per day (m/d)
	Hydraulic gradient	
foot per mile (ft/mi)	0.1894	meter per kilometer (m/km)

Temperature in degrees Fahrenheit (°F) may be converted to degrees Celsius (°C) as follows:

$$°C = (°F - 32) / 1.8.$$

Datums

Vertical coordinate information is referenced to the National Geodetic Vertical Datum of 1929 (NGVD 29).

Horizontal coordinate information is referenced to the North American Datum of 1927 (NAD 27).

Elevation, as used in this report, refers to distance above the vertical datum.

Conversion Factors, Datums, Abbreviations and Acronyms, and Well or Spring Identification System

Abbreviations and Acronyms

BCU	basement confining unit
BUTTE_MONTR	streamflow gaging station, Butte Creek at Monitor, Oregon
CFC	chlorofluorocarbon
CLACK_ESTCDA	streamflow gaging station, Clackamas River at Estacada, Oregon
COYOTE_CROW	streamflow gaging station, Coyote Creek near Crow, Oregon
CRB	Columbia River basalt unit
CSS	composite scaled sensitivity
DEM	digital elevation model
DRAIN	MODFLOW drain package
DRN_BCU	drain bed vertical hydraulic conductivity (ft/d) of the basement confining unit in the Willamette Basin
DRN_CRB	drain bed vertical hydraulic conductivity (ft/d) of the Columbia River basalt unit in the Willamette Basin
DRN_CRB1	drain bed vertical hydraulic conductivity (ft/d) of the Columbia River basalt unit in the Central Willamette subbasin (layer 5 in local model)
DRN_CRB2	drain bed vertical hydraulic conductivity (ft/d) of the Columbia River basalt unit in the Central Willamette subbasin (layer 6 in local model)
DRN_CRB3	drain bed vertical hydraulic conductivity (ft/d) of the Columbia River basalt unit in the Central Willamette subbasin (layer 7 in local model)
DRN_LSU	drain bed vertical hydraulic conductivity (ft/d) of the lower sedimentary unit in the Willamette Basin (excluding the Portland subbasin)
DRN_MSU	drain bed vertical hydraulic conductivity (ft/d) of the middle sedimentary unit in the Willamette Basin (excluding the Portland subbasin)
DRN_USU	drain bed vertical hydraulic conductivity (ft/d) of the upper sedimentary unit in the Willamette Basin (excluding the Portland subbasin)
DRN_WSU	drain bed vertical hydraulic conductivity (ft/d) of the Willamette silt unit in the Willamette Basin (excluding the Portland subbasin)
ET	evapotranspiration
FISH_3LNX	streamflow gaging station, Fish Creek near Three Lynx, Oregon
HCU	high Cascade unit
HK_BCU	horizontal hydraulic conductivity (ft/d) of the basement confining unit in the Willamette Basin
HK_CRB	horizontal hydraulic conductivity (ft/d) of the Columbia River basalt unit in the Willamette Basin
HK_CRB1	horizontal hydraulic conductivity (ft/d) of the Columbia River basalt unit in the Central Willamette subbasin (layer 5 in local model)
HK_CRB2	horizontal hydraulic conductivity (ft/d) of the Columbia River basalt unit in the Central Willamette subbasin (layer 6 in local model)
HK_CRB3	horizontal hydraulic conductivity (ft/d) of the Columbia River basalt unit in the Central Willamette subbasin (layer 7 in local model)
HK_LSU	horizontal hydraulic conductivity (ft/d) of the lower sedimentary unit in the Willamette Basin (excluding the Portland subbasin)
HK_LSUP	horizontal hydraulic conductivity (ft/d) of the lower sedimentary unit in the Portland subbasin

Conversion Factors, Datums, Abbreviations and Acronyms, and Well or Spring Identification System

Abbreviations and Acronyms

HK_MLAY	horizontal hydraulic conductivity (ft/d) of pseudo-cells in the regional and local numerical models
HK_MSU	horizontal hydraulic conductivity (ft/d) of the middle sedimentary unit in the Willamette Basin (excluding the Portland subbasin)
HK_MSUP	horizontal hydraulic conductivity (ft/d) of the middle sedimentary unit in the Portland subbasin
HK_USU	horizontal hydraulic conductivity (ft/d) of the upper sedimentary unit in the Willamette Basin (excluding the Portland subbasin)
HK_USUP	horizontal hydraulic conductivity (ft/d) of the upper sedimentary unit in the Portland subbasin
HK_WSU	horizontal hydraulic conductivity (ft/d) of the Willamette silt unit in the Willamette Basin (excluding the Portland subbasin)
HRU	hydrologic-response unit
JHNSN_MILW	streamflow gaging station, Johnson Creek at Milwaukie, Oregon
JHNSN_SYCMR	streamflow gaging station, Johnson Creek at Sycamore, Oregon
Kh	horizontal hydraulic conductivity (ft/d)
Kv	vertical hydraulic conductivity (ft/d)
L_NSANT_MHMA	streamflow gaging station, Little North Santiam River near Mehama, Oregon
LSU	lower sedimentary unit
LSUP	lower sedimentary unit, Portland subbasin only
LTOM_MONROE	streamflow gaging station, Long Tom River at Monroe, Oregon
LTOM_NOTI	streamflow gaging station, Long Tom River near Noti, Oregon
LUCKMT_SUVER	streamflow gaging station, Luckiamute River near Suver, Oregon
MARYS_PHLMTH	streamflow gaging station, Marys River near Philomath, Oregon
MODFLOW	USGS groundwater-flow model program
MODPATH	USGS particle tracking program
MOLAL_CANBY	streamflow gaging station, Molalla River near Canby, Oregon
MOLAL_WILHT	streamflow gaging station, Molalla River above Pine Creek near Wilhoit, Oregon
MSU	middle sedimentary unit
MSUP	middle sedimentary unit, Portland subbasin only
NSANT_MHMA	streamflow gaging station, North Santiam River at Mehama, Oregon
OWRD	Oregon Water Resources Department
PART	a “streamflow partitioning” computer program to estimate base flow on unregulated streams
PRMS	Precipitation-Runoff Modeling System
PUDD_AUR	streamflow gaging station, Pudding River at Aurora, Oregon
PUDD_MT_ANG	streamflow gaging station, Pudding River near Mount Angel, Oregon
RCH_BCU	recharge parameter (array multiplier, unitless) value for the basement confining unit in the Willamette Basin
RCH_CRB	recharge parameter (array multiplier, unitless) value for the Columbia River basalt unit in the Willamette Basin
RCH_CRB1	recharge parameter (array multiplier, unitless) value for the Columbia River basalt unit in the Central Willamette subbasin (layer 5 in local model), transient model

Conversion Factors, Datums, Abbreviations and Acronyms, and Well or Spring Identification System

Abbreviations and Acronyms

RCH_CRB2	recharge parameter (array multiplier, unitless) value for the Columbia River basalt unit in the Central Willamette subbasin (layer 6 in local model), transient model
RCH_CRB3	recharge parameter (array multiplier, unitless) value for the Columbia River basalt unit in the Central Willamette subbasin (layer 7 in local model), transient model
RCH_LSU	recharge parameter (array multiplier, unitless) value for the lower sedimentary unit in the Willamette Basin
RCH_MSU	recharge parameter (array multiplier, unitless) value for the middle sedimentary unit in the Central Willamette subbasin, transient model
RCH_USU	recharge parameter (array multiplier, unitless) value for the upper sedimentary unit in the Central Willamette subbasin, transient model
RCH_USU_MSU	recharge parameter (array multiplier, unitless) value for the upper and middle sedimentary units in the Willamette Basin
RCH_WSU	recharge parameter (array multiplier, unitless) value for the Willamette silt unit in the Willamette Basin
RICKRL_DLLS	streamflow gaging station, Rickreall Creek near Dallas, Oregon
RIVER	MODFLOW river package
RIV_BCU	riverbed vertical hydraulic conductivity (ft/d) of the basement confining unit in the Willamette Basin
RIV_CRB	riverbed vertical hydraulic conductivity (ft/d) of the Columbia River basalt unit in the Willamette Basin
RIV_CRB1	riverbed vertical hydraulic conductivity (ft/d) of the Columbia River basalt unit in the Central Willamette subbasin (layer 5 in local model)
RIV_CRB2	riverbed vertical hydraulic conductivity (ft/d) of the Columbia River basalt unit in the Central Willamette subbasin (layer 6 in local model)
RIV_CRB3	riverbed vertical hydraulic conductivity (ft/d) of the Columbia River basalt unit in the Central Willamette subbasin (layer 7 in local model)
RIV_LSU	riverbed vertical hydraulic conductivity (ft/d) of the lower sedimentary unit in the Willamette Basin (excluding the Portland subbasin)
RIV_MSU	riverbed vertical hydraulic conductivity (ft/d) of the middle sedimentary unit in the Willamette Basin (excluding the Portland subbasin)
RIV_USU	riverbed vertical hydraulic conductivity (ft/d) of the upper sedimentary unit in the Willamette Basin (excluding the Portland subbasin)
RIV_WSU	riverbed vertical hydraulic conductivity (ft/d) of the Willamette silt unit in the Willamette Basin (excluding the Portland subbasin)
SANT_JFFSN	streamflow gaging station, Santiam River at Jefferson, Oregon
SILVER_SILVE	streamflow gaging station, Silver Creek at Silverton, Oregon
SS_BCU	specific storage parameter (ft-1) value for the basement confining unit in the Central Willamette subbasin
SS_CRB1	specific storage parameter (ft-1) value for the Columbia River basalt unit in the Central Willamette subbasin (layer 5 in local model)
SS_CRB2	specific storage parameter (ft-1) value for the Columbia River basalt unit in the Central Willamette subbasin (layer 6 in local model)
SS_CRB3	specific storage parameter (ft-1) value for the Columbia River basalt unit in the Central Willamette subbasin (layer 7 in local model)

Conversion Factors, Datums, Abbreviations and Acronyms, and Well or Spring Identification System

Abbreviations and Acronyms

SS_LSU	specific storage parameter (ft-1) value for the lower sedimentary unit in the Central Willamette subbasin
SS_MLAY	specific storage parameter (ft-1) value for pseudo-cells in the local transient numerical model
SS_MSU	specific storage parameter (ft-1) value for the middle sedimentary unit in the Central Willamette subbasin
SS_USU	specific storage parameter (ft-1) value for the upper sedimentary unit in the Central Willamette subbasin
SS_WSU	specific storage parameter (ft-1) value for the Willamette silt unit in the Central Willamette subbasin
SYAM_MCMINN	streamflow gaging station, South Yamhill River at McMinnville, Oregon
SYAM_WLLMNA	streamflow gaging station, South Yamhill River near Willamina, Oregon
THOM_SCIO	streamflow gaging station, Thomas Creek near Scio, Oregon
TUAL_DILLEY	streamflow gaging station, Tualatin River near Dilley, Oregon
TUAL_WLINN	streamflow gaging station, Tualatin River at West Linn, Oregon
USGS	U.S. Geological Survey
USU	upper sedimentary unit
USUP	upper sedimentary unit, Portland subbasin only
VK_BCU	vertical hydraulic conductivity (ft/d) of the basement confining unit in the Willamette Basin
VK_CRB	vertical hydraulic conductivity (ft/d) of the Columbia River basalt unit in the Willamette Basin
VK_CRB1	vertical hydraulic conductivity (ft/d) of the Columbia River basalt unit in the Central Willamette subbasin (layer 5 in local model)
VK_CRB2	vertical hydraulic conductivity (ft/d) of the Columbia River basalt unit in the Central Willamette subbasin (layer 6 in local model)
VK_CRB3	vertical hydraulic conductivity (ft/d) of the Columbia River basalt unit in the Central Willamette subbasin (layer 7 in local model)
VK_LSU	vertical hydraulic conductivity (ft/d) of the lower sedimentary unit in the Willamette Basin (excluding the Portland subbasin)
VK_MLAY	vertical hydraulic conductivity (ft/d) of pseudo-cells in the regional and local numerical models
VK_MSU	vertical hydraulic conductivity (ft/d) of the middle sedimentary unit in the Willamette Basin (excluding the Portland subbasin)
VK_USU	vertical hydraulic conductivity (ft/d) of the upper sedimentary unit in the Willamette Basin (excluding the Portland subbasin)
VK_WSU	vertical hydraulic conductivity (ft/d) of the Willamette silt unit in the Willamette Basin (excluding the Portland subbasin)
WELL	MODFLOW well package
WILL_ABV_SALEM	streamflow gaging station, Willamette River at Salem, Oregon
WILLAMETTE	streamflow gaging station, Willamette River at Portland, Oregon
WLLMNA_WLLMN	streamflow gaging station, Willamina Creek near Willamina, Oregon
WSU	Willamette silt unit

Well and Spring Identification System

Well or Spring Identification System
Public Land Survey System

Example well: 02S/03W-31ACB, YAMH 1127, 452120123060500

This well has three identification systems.
Public Land Survey System designation: **02S/03W-31ACB**, diagrammed below.
Oregon State designation: **YAMH 1127,** county name (Yamhill) and unique number within the county.
USGS identifier: **452120123060500**; first six digits are the latitude in degree-minute-seconds, the next seven digits are the longitude, and the last two digits indicate a unique number at that location.

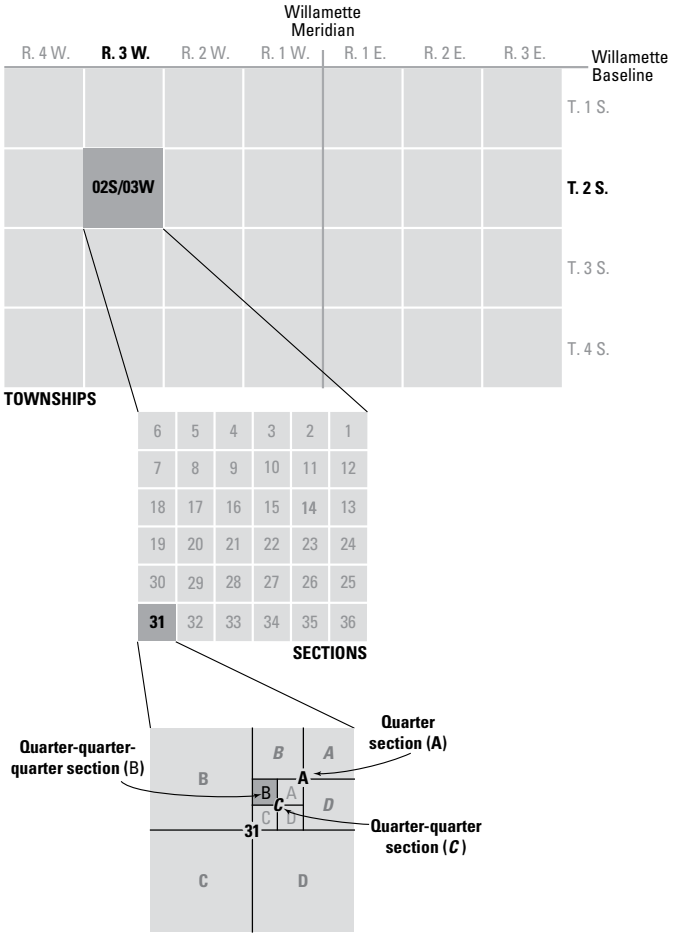

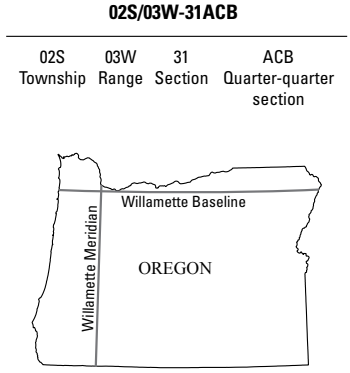

Simulation of Groundwater Flow and the Interaction of Groundwater and Surface Water in the Willamette Basin and Central Willamette Subbasin, Oregon

By Nora B. Herrera, Erick R. Burns, and Terrence D. Conlon

Summary

Full appropriation of tributary streamflow during summer, a growing population, and agricultural needs are increasing the demand for groundwater in the Willamette Basin. Greater groundwater use could diminish streamflow and create seasonal and long-term declines in groundwater levels. The U.S. Geological Survey (USGS) and the Oregon Water Resources Department (OWRD) cooperated in a study to develop a conceptual and quantitative understanding of the groundwater-flow system of the Willamette Basin with an emphasis on the Central Willamette subbasin. This final report from the cooperative study describes numerical models of the regional and local groundwater-flow systems and evaluates the effects of pumping on groundwater and surface-water resources. The models described in this report can be used to evaluate spatial and temporal effects of pumping on groundwater, base flow, and stream capture.

The regional model covers about 6,700 square miles of the 12,000-square mile Willamette and Sandy River drainage basins in northwestern Oregon—referred to as the Willamette Basin in this report. The Willamette Basin is a topographic and structural trough that lies between the Coast Range and the Cascade Range and is divided into five sedimentary subbasins underlain and separated by basalts of the Columbia River Basalt Group (Columbia River basalt) that crop out as local uplands. From north to south, these five subbasins are the Portland subbasin, the Tualatin subbasin, the Central Willamette subbasin, the Stayton subbasin, and the Southern Willamette subbasin. Recharge in the Willamette Basin is primarily from precipitation in the uplands of the Cascade Range, Coast Range, and western Cascades areas. Groundwater moves downward and laterally through sedimentary or basalt units until it discharges locally to wells, evapotranspiration, or streams. Mean annual groundwater withdrawal for water years 1995 and 1996 was about 400 cubic feet per second; irrigation withdrawals accounted for about 80 percent of that total. The upper 180 feet of productive aquifers in the Central Willamette and Southern Willamette subbasins produced about 70 percent of the total pumped volume.

In this study, the USGS constructed a three-dimensional numerical finite-difference groundwater-flow model of the Willamette Basin representing the six hydrogeologic units, defined in previous investigations, as six model layers. From youngest to oldest, and [generally] uppermost to lowermost they are the: upper sedimentary unit, Willamette silt unit, middle sedimentary unit, lower sedimentary unit, Columbia River basalt unit, and basement confining unit. The high Cascade unit is not included in the groundwater-flow model because it is not present within the model boundaries. Geographic boundaries are simulated as no-flow (no water flowing in or out of the model), except where the Columbia River is simulated as a constant hydraulic head boundary. Streams are designated as head-dependent-flux boundaries, in which the flux depends on the elevation of the stream surface. Groundwater recharge from precipitation was estimated using the Precipitation-Runoff Modeling System (PRMS), a watershed model that accounts for evapotranspiration from the unsaturated zone. Evapotranspiration from the saturated zone was not considered an important component of groundwater discharge. Well pumping was simulated as specified flux and included public supply, irrigation, and industrial pumping. Hydraulic conductivity values were estimated from previous studies through aquifer slug and permeameter tests, specific capacity data, core analysis, and modeling. Upper, middle and lower sedimentary unit horizontal hydraulic conductivity values were differentiated between the Portland subbasin and the Tualatin, Central Willamette, and Southern Willamette subbasins based on preliminary model results.

A regional steady-state model, one that describes the equilibrium condition of a groundwater flow system, was calibrated to average conditions from water years 1995 and 1996 using the Parameter Estimation Process in the USGS groundwater-flow model MODFLOW-2000. Water-level data from 488 observation wells and base flow estimates at 27 streamflow-gaging stations were used to calibrate the model. Modeled gradients and water levels in wells matched those determined by field measurements and previous studies within expected limits in most areas. Overall, the steady-state model reasonably simulates the regional groundwater system.

A transient model, one that describes a groundwater flow system that is in disequilibrium, was developed for the Central Willamette subbasin to understand the large seasonal fluctuations and the effect of pumping on groundwater discharge to streams. This finer scale "local model" required more detail to represent changes in the amount and timing of fluctuations in groundwater levels, base flow, and stream capture induced by seasonal variations in groundwater pumping and recharge. In the local model, the single layer representing the Columbia River basalt unit in the regional model was divided into three model layers to simulate vertical head gradients in the basalt. Lateral flux boundaries were selected to coincide with groundwater divides when present, and, where necessary, regional groundwater flow into and out of the lateral boundaries of the model was based on results from the regional model. Model parameter values were the same as used in the regional model. Initially, the local model was calibrated to steady-state conditions using average annual data for water years 1999 and 2000. After the addition of storage parameters that follow hydraulic conductivity zoning patterns, the local model was calibrated to transient conditions using traditional trial-and-error methods for water years 1999–2000 using 24 monthly stress periods. Time-series water-level measurements from 51 wells were used for calibration.

Long-term climate cycles may be a cause of variations in water levels in wells in the Central Willamette subbasin. Maximum water levels declined slightly from water year 1999 to water year 2000, reflecting an observed decrease in precipitation and the downward trend of the cumulative departure from average precipitation curve. This trend is reflected in the simulated water levels of the local model. Overall, simulated water levels in the sedimentary units of interest in the Central Willamette subbasin closely approximated measured water levels, and simulated water levels in the Columbia River basalt unit matched measured water levels within acceptable limits. Temporal variations in head gradients and groundwater discharge to streams were reasonable and distributed appropriately in the subbasin, although independent measurements were not available for quantitative comparisons.

The Central Willamette subbasin shows the greatest effects from pumping of any subbasin in the study area. Results from steady-state and transient simulations indicate that average annual groundwater levels have declined in most parts of the Central Willamette subbasin since pumping began. Water-use analysis by OWRD indicates that about one-half of all permitted water rights are in use. Model scenarios demonstrate that groundwater levels will continue to decline in the Central Willamette subbasin with full use of permitted water rights. Simulations show similar water-level declines for localized areas in the Portland and Southern Willamette subbasins.

Groundwater pumping in the Willamette Basin has caused an increase in stream capture, primarily in the lowland areas, with largest effects predominantly in the Central Willamette subbasin. All simulations indicated that pumping water from aquifers that are hydrologically connected to a significant water body result in less hydraulic head decline in the surrounding area because of captured flow that has been induced from, or would normally discharge to, that water body. Simulations of pumping from the upper, middle, and lower sedimentary units indicate that Willamette River capture may limit drawdown for wells completed in aquifers penetrated by the river, whether the wells are near to or distant from streams.

In steady-state and transient simulations in the Central Willamette subbasin, Willamette River capture is a significant groundwater source for pumping, except in the northeastern part of the subbasin, where Molalla River capture is a primary source of groundwater for pumping.

Where streams flow on or are incised into, but do not penetrate the confining Willamette silt unit, or have a poor hydrologic connection with the underlying aquifer, stream capture decreases, and the influence of pumping (drawdowns) can propagate greater distances.

In areas where the upper and middle sedimentary units are thin, simulated pumping causes large hydraulic head declines that can induce an increase in stream capture from streams that flow on the Willamette silt unit. Simulated pumping from the relatively thick, lower sedimentary unit in the Central Willamette subbasin, however, does not produce large hydraulic head declines because of its relatively high transmissivity. The high transmissivity allows pumping effects to propagate quickly to surface water boundaries. Additionally, the presence of the permeable middle sedimentary unit in conjunction with flow contributed from release of groundwater storage and restricted vertical groundwater movement from the overlying low permeability Willamette silt unit, results in relatively small effects to local streams with channels flowing on or incised into the Willamette silt unit. In the southeastern area of the Central Willamette subbasin where the thicknesses of the lower sedimentary unit and the middle sedimentary unit are similar, stream capture induced by pumping from either sedimentary unit is similar.

Transient simulations indicate that before development, minimum groundwater levels and base flow occurred during autumn, maximum groundwater levels occurred during late winter, and maximum base flow occurred during spring. Groundwater pumping in the Central Willamette subbasin during summer has caused minimum groundwater levels and base flow in the Willamette River to occur earlier in the year. Model simulations indicate that pumping causes an earlier minimum water level during summer and delayed maximum water level in winter as capture due to pumping decreases and recharge replenishes water removed from storage. For the

Pudding River watershed, the model results indicate that the presence of the Willamette silt unit has prevented a change to a summer-low/spring-high base flow pattern under current pumping conditions. However, if permitted groundwater rights are fully exercised, model scenarios indicate that increased pumping can override the effects of flow contributed from release of groundwater storage and impeded vertical groundwater movement by the Willamette silt unit and decrease Pudding River base flow.

Transient simulations with monthly stress periods provide information on the timing of stream capture in the Central Willamette subbasin. At average annual pumping rates for water years 1999 and 2000, net aquifer storage depleted by summer pumping is replenished by recharge which includes induced recharge from streams over the autumn, winter, and spring. Variations in hydrogeological characteristics in the subbasin, however, result in variations in stream capture during the summer irrigation season. Model simulation results indicate that because the Willamette River flows on and is in direct hydrologic connection with the upper, middle, and lower sedimentary units, Willamette River capture is directly related to seasonal pumping from those units, with greatest capture fraction occurring in summer.

In the Central Willamette subbasin, the continuous geometry of the lower sedimentary unit compared to the variable and sometimes absent upper and middle sedimentary units allows for better hydrologic connection to the Willamette River and increased Willamette River capture. Willamette River capture is greatest at locations close to the river, and decreases when the pumping location is farther from the stream. Stream capture is distributed more evenly over the year for pumping locations farther from the river. Pudding River capture is small compared to Willamette River capture, and pumping effects are distributed over the water year, with greatest capture fraction taking place in winter. Pumping from the middle sedimentary unit induces more Pudding River capture than pumping from the lower sedimentary unit. Simulation of interaction of groundwater and surface water near the Pudding River indicated that the presence of the low permeability Willamette silt unit restricts Pudding River capture, direct effects from seasonal pumping are minimal, and base flow and stream capture is controlled by storage requirements of the groundwater system. These results imply that careful location of a well can minimize the effects of pumping on stream capture during periods of historically high demand, and maximize stream capture during periods of historically high streamflows caused by precipitation and surface water runoff.

Large declines in heads in the upper and middle sedimentary units could lead to increased pumping costs, increased number of dry wells during times of high demand, and increased seasonal changes in aquifer storage. Large declines also could lead to movement of lower quality water from the basement confining unit.

Water resource managers can use the steady-state and transient simulations generated by this study to evaluate possible long-term effects of changes in groundwater pumping on water levels and streams in the Willamette Basin, and long-term, short-term, and seasonal effects of changes in groundwater pumping on water levels and streams in the Central Willamette subbasin. Water managers can use the capture maps developed during this study to evaluate where groundwater pumping will affect flows in the Willamette River, Pudding River, and other tributary streams.

The results from this study may be used to identify areas in the Willamette Basin where more data is needed to better understand groundwater and surface-water interactions. The scenarios in this study consider only changes in pumping as a cause of changes to groundwater levels, base flow, and stream capture. Other factors, such as climate cycles or changes in water-use patterns can alter results. This study and the modeling tools it provides can be used as a starting point for climate and water-withdrawal optimization studies, water management and policy discussions, and strategies to help avert future water scarcity in the Willamette Basin and Central Willamette subbasin.

Introduction

Background and Study Objectives

The Willamette Basin (fig. 1) is home to 3.0 million people—about three-fourths of the residents of Oregon. The population has increased by 0.1 million since the 2010 census (U.S. Census Bureau, 2014). The Willamette Basin also is a major agricultural area, with nearly 50 percent of Oregon's gross farm and ranch sales (Oregon Agricultural Statistics Service, 2014). The demand for groundwater is increasing because summer flows of the Willamette River and most tributaries are fully allocated and water users are increasingly turning to groundwater to meet new demands.

The Oregon Water Resources Department (OWRD) allocates surface water and groundwater by using a permit system based on the doctrine of prior appropriation. Because of competing demands for municipal, industrial, irrigation, and instream (pollution abatement and fish habitat) uses, many streams in the basin are administratively closed to additional appropriation in summer, when demand is high and streamflow is low. Groundwater is the only readily available resource to satisfy new demands for water in many areas. Various factors limit the capacity of the groundwater system to meet these demands, including potential reduction of streamflow by groundwater withdrawals and large seasonal and long-term declines in water levels in wells. Available information and tools have not been sufficient to quantify these limiting factors.

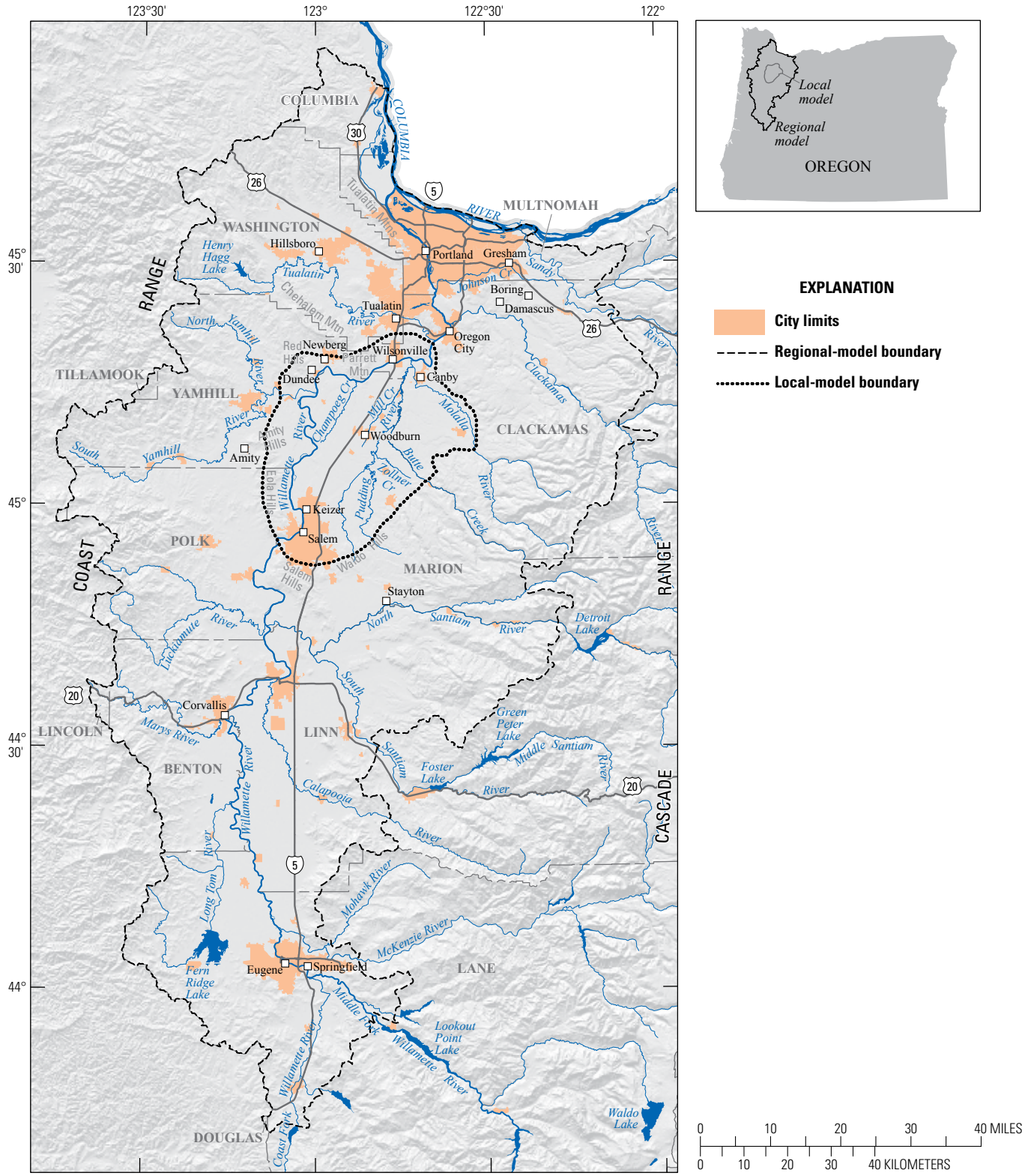

Base map modified from USGS and other digital data sources, various scales. Coordinate system: UTM, Zone 10N, Projection: Transverse Mercator; Datum: North American Datum of 1927.

Figure 1. Locations of the regional- and local-model boundaries in the Willamette Basin, Oregon.

The U.S. Geological Survey (USGS) and the OWRD began a cooperative study to develop a quantitative conceptual understanding of the groundwater-flow system of the Willamette Basin (fig. 1) and apply this knowledge with more detail in the Central Willamette subbasin (fig. 2), because of demands for water for irrigation and a growing population in this area. Numerical hydrologic models were developed to test the conceptualization of the groundwater-flow system and to provide tools to simulate its response to proposed groundwater development. These models and tools also may be used to support water-resource management decisions.

This report is the final report in a series that presents the results of the study. Previous publications from the study have documented the distribution of arsenic in groundwater (Hinkle and Polette, 1999); compiled water levels, groundwater chemistry, and geophysical logs (Orzol and others, 2000); described the origin, extent, and thickness of permeable sediments in the flood plain of the major tributaries of the basin (O'Connor and others, 2001); estimated groundwater recharge and the exchange of water between aquifers and streams (Lee and Risley, 2001); estimated groundwater discharge to streams using heat as a tracer (Conlon and others, 2003); and described the groundwater hydrology of the Willamette Basin (Conlon and others, 2005).

Purpose and Scope

This report describes the development of the groundwater-flow models for the Willamette Basin and Central Willamette subbasin, and the use of those models to simulate the responses of the groundwater-flow system to changes in groundwater pumping according to possible management scenarios. Simulated pumping scenarios were designed to represent pre-development conditions, full use of current groundwater rights, and possible increases in groundwater pumping and the potential resultant changes in groundwater flow. Two areas in the Willamette Basin were simulated. A regional, steady-state model, primarily of the lowland area in the Willamette Basin was developed to synthesize data over a large area, test the conceptual understanding of regional groundwater flow and its interaction with streams, and evaluate the steady-state response of the groundwater system under current and future conditions. Transient modeling of groundwater flow over the entire basin was beyond the scope of this study; consequently, a detailed transient-flow model was developed for analysis of the groundwater-flow system and seasonal interactions with surface water in the Central Willamette subbasin.

The Central Willamette subbasin was selected for a detailed analysis because of increasing demands for water for irrigation and for a growing population. Streamflow during summer is fully allocated for irrigation and instream needs, and there is an interest in exploring additional use of groundwater to satisfy the demand for water. Groundwater withdrawals in the Central Willamette subbasin are widely distributed and natural seasonal water-level fluctuations have increased by an estimated 10–55 ft since pumping began in the basin-fill sediments. Of particular interest are changes in the amount and timing of water-level fluctuations in the basin-fill sediments and groundwater discharge to streams induced by seasonal variations in recharge and groundwater pumping. Long-term changes in water levels and groundwater flow in the sedimentary and basalt units are included in the analysis.

All models use simplifying assumptions, have inherent uncertainty, and are constrained by the distribution in space and time of hydrologic data, such as aquifer geometry, and water level and flux. The numerical groundwater-flow model described in this report is based on the conceptual model discussed in Conlon and others (2005).

Location and General Features

The Willamette Basin study area comprises the Willamette and Sandy River drainage basins in northwestern Oregon (fig. 2). The Willamette Basin encompasses about 12,000 mi^2 and is bordered by two north-south trending mountain ranges, the Coast Range to the west and the Cascade Range to the east. It is bounded by the Columbia River to the north and by the intersection of the Coast Range and the Cascade Range to the south (fig. 1). The Central Willamette subbasin is located within the Willamette Basin between Salem and Canby, and is bounded by the Red, Amity, Eola, and Salem Hills to the west, Waldo Hills to the east and south, and Chehalem and Parrett Mountains to the north. The study area contains all or part of 13 Oregon counties: Columbia, Washington, Multnomah, Yamhill, Clackamas, Polk, Marion, Benton, Linn, Lane, Tillamook, Lincoln, and Douglas.

Land-surface elevation in the Willamette Basin ranges from near sea level at the Columbia River to more than 10,000 ft at the summit of volcanic peaks along the crest of the Cascade Range. Elevations in the Coast Range vary from 1,000 to 4,000 ft, in the western Cascade Range from 1,000 to 6,000 ft, and in the high Cascade Range from 4,000 to 10,000 ft. The lowland area of the basin between the Coast Range and Cascade Range is about 120-mi long and 20-mi wide, and elevations range from about 10 ft at Portland to about 400 ft near Eugene. The Portland, Tualatin, Central Willamette, Stayton, and Southern Willamette subbasins (fig. 2) are separated by upland areas of bedrock that reach elevations of 1,500 ft. The Clackamas, North and South Santiam, McKenzie, and Middle Fork Willamette Rivers drain the Cascade Range and are the major tributaries to the Willamette River. Smaller streams in the Cascade Range and Coast Range also flow into the Willamette River, which flows from south to north through the lowland to the Columbia River.

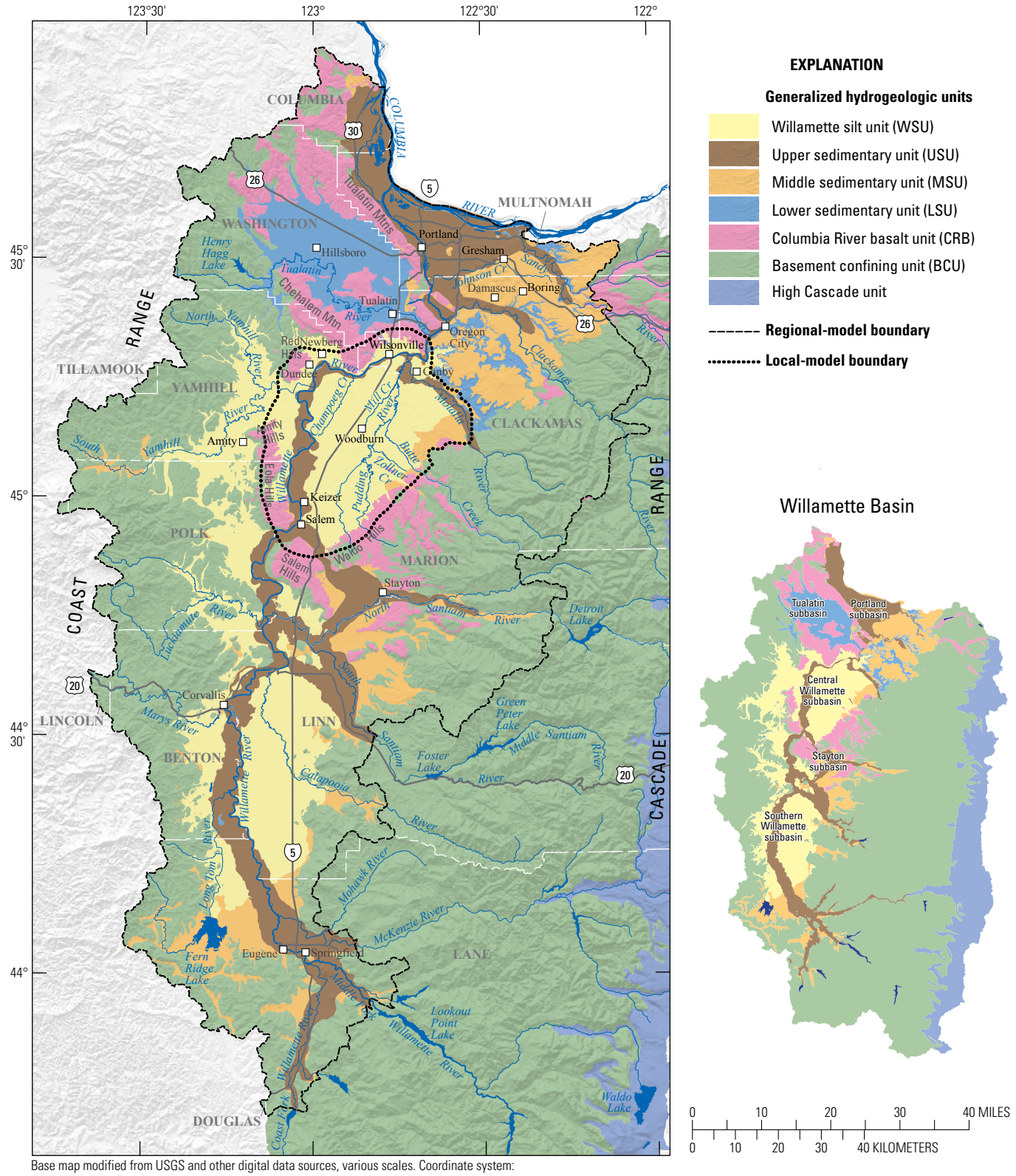

Base map modified from USGS and other digital data sources, various scales. Coordinate system: UTM, Zone 10N, Projection: Transverse Mercator; Datum: North American Datum of 1927.

Figure 2. Generalized hydrogeologic units and subbasins of the Willamette Basin, Oregon.

Climate in the Willamette Basin is characterized by cool, wet winters and warm, dry summers. Precipitation increases with elevation, with mean annual precipitation in the study area ranging from 40 to 130 in. in the Coast Range, about 40 in. in the lowland, 50 to 100 in. in the western Cascade Range, and as much as 130 in. at the crest of the Cascade Range. Heavy winter snow in the Cascade Range results in permanent snowfields and glaciers on the highest peaks. About 80 percent of the annual precipitation falls from October through March, and less than 5 percent falls in July and August (Wentz and others, 1998). A graph of average annual precipitation and the cumulative departure from average precipitation shows yearly and long-term variations in precipitation (fig. 3). Wet and dry periods coincide with above average years of total annual precipitation during the mid-1990s and with below average years of total annual precipitation in the years between 1999 and 2003. The trend of the precipitation line indicates a slightly wetter period during the first years of the study (1994 through 1998), and a slightly dryer period during the final years of the study (1999 through 2000). Mean monthly temperatures in the lowland range from 39 °F in January to 68 °F in August. In the Coast Range and western Cascade Range, mean monthly temperatures range from 37 °F in January to 64 °F in August. The mean monthly temperature in the high Cascade Range is 28 °F in January and 57 °F in August.

About 70 percent of the Willamette Basin is forested, including most of the Coast and Cascade Ranges (Hulse and others, 2002). Agricultural land encompasses 20 percent of the study area and generally is restricted to the lowland. The remaining land is urban, grasslands, open water, or permanent snowfields. Major population centers are the metropolitan areas of Portland, Salem-Keizer, Corvallis, and Eugene-Springfield (fig. 1). Of these communities, Springfield and Keizer rely solely on groundwater. Salem, Portland, and some suburban Portland communities use groundwater to supplement surface water supplies during summer. Many smaller communities rely on groundwater as the primary source of water for municipal use.

Agricultural crops in the Willamette Basin account for 62 percent of total crop sales in Oregon, and include field and grass seed, vegetables, filbert nuts, cut Christmas trees, berries, hops, grapes, and nursery stock (Oregon Agricultural Statistics Service, 2007). Historically, crops that do not require irrigation, such as wheat, were cultivated in the lowland, but high-value crops that do require irrigation became more common as markets and technology evolved. Except in the Stayton basin, irrigation canals are not widely used. Much of the lowland is irrigated with groundwater because surface water irrigation is limited to fields adjacent to streams. However, irrigation with groundwater is increasing adjacent to many smaller streams because of limitations placed on surface water withdrawals due to low streamflow in the summer.

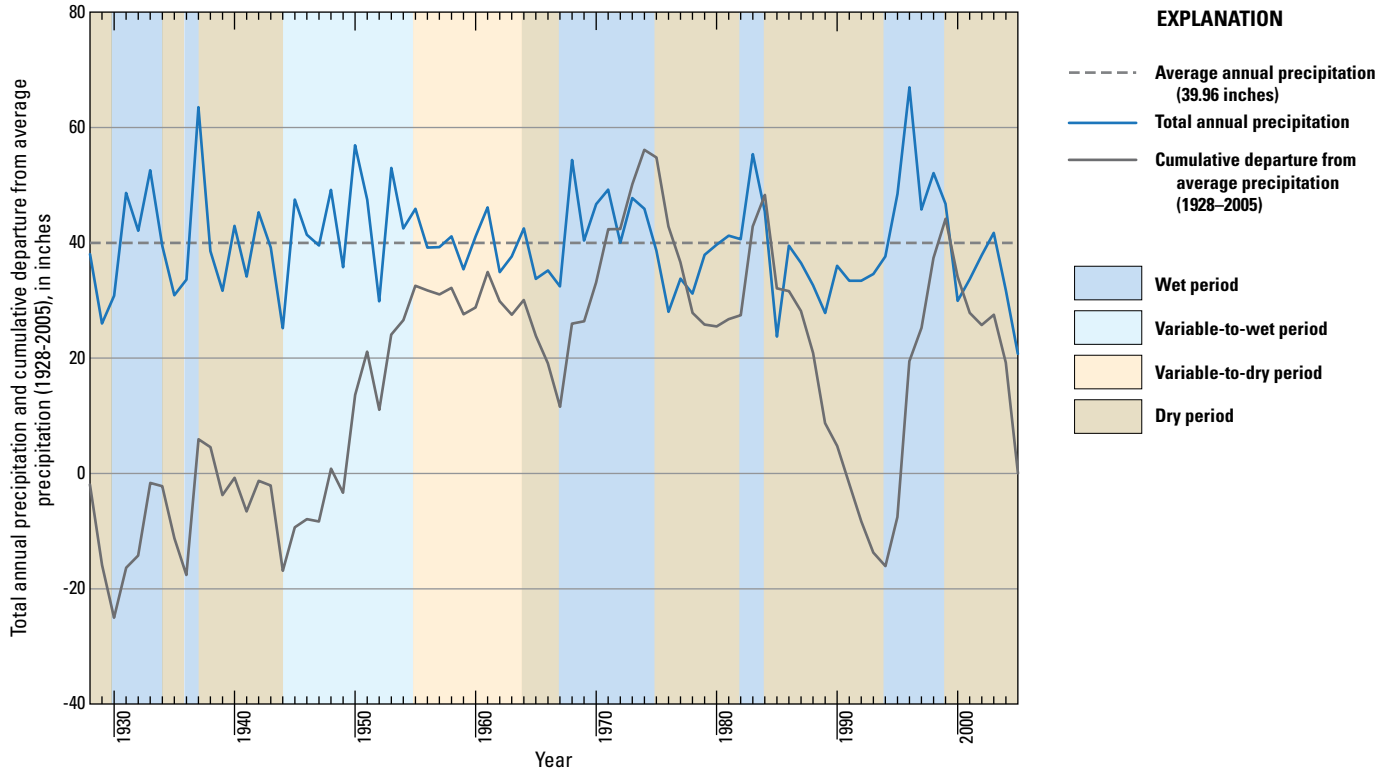

Figure 3. Total annual precipitation and cumulative departure from average precipitation at Salem, Oregon, 1928–2005.

Hydrogeologic Framework

Groundwater flow in the Willamette Basin is controlled primarily by the distribution of recharge, subsurface geology, and the geography of the steam network. The geology and hydrology of the Willamette Basin and the Central Willamette subbasin have been described by Piper (1942), Price (1967a, 1967b), Hampton (1972), Woodward and others (1998), and Conlon and others (2005). Detailed geologic histories are available in Orr and others (1992), Yeats and others (1996), Gannett and Caldwell (1998), and O'Connor and others (2001).

Geologic Setting

The Willamette Basin was formed by structural deformation of underlying early Cenozoic marine sedimentary, volcanic, and intrusive rocks of the Coast Range and older Cascade volcanic rocks of the Cascade Range that form the bedrock foundation of the lowland. Miocene Columbia River basalt is present at depth over the northern part of the basin and forms upland areas locally that divide the Willamette Basin lowland into five sedimentary subbasins (fig. 2). From north to south, these are the Portland subbasin (sometimes referred to locally and in previous reports as the "Portland Basin," the Tualatin subbasin, the Central Willamette subbasin, the Stayton subbasin, and the Southern Willamette subbasin. The Stayton subbasin is small and is included in the Southern Willamette subbasin in this report.

Fluvial and lacustrine sediment thickness exceeds 1,400 ft in the Portland, Tualatin, and Central Willamette subbasins, but generally is less than 500 ft in the Southern Willamette subbasin (Conlon and others, 2005). The bulk of the basin-fill sediments in the Willamette lowland consist of clays and silts that were deposited in low-energy depositional environments (Gannett and Caldwell, 1998). The uppermost basin-fill deposits resulted from Pleistocene glacial outburst Missoula Floods. These floods resulted from the repeated failures of a glacial ice dam that impounded the Clark Fork River in western Montana. Floodwater crossed central Washington and through the Columbia River Gorge into the Willamette Valley (Waitt, 1980). The floods emplaced deposits of sand and gravel in the Portland subbasin (more than 150 ft thick) and silts of the Willamette Silt unit (as much as 120 ft thick) elsewhere in the Willamette Basin. Reworking of basin deposits by the Willamette River and major tributaries during the Pleistocene and Holocene formed modern flood plains and newer sand and gravel deposits (Gannett and Caldwell, 1998; O'Connor and others, 2001). Fine-grained deposits predominate in the western areas of the lowland and at depth. Coarse-grained sediments are largely restricted to the eastern side of the basin, where high-gradient streams draining the Cascade Range enter the valley lowland. Extensive deposits of coarse-grained sediments are not associated with streams that drain the Coast Range on the west side of the valley. This lack of course-grained material is particularly evident in the Tualatin subbasin, where the bulk of the basin-fill sediments are fine-grained deposits eroded from local highlands in and adjacent to the subbasin (Wilson, 1997).

Hydrogeologic Units

For the purposes of this study, seven regional hydrogeologic units, which each consist of one or more geologic units with similar hydrogeologic properties at a regional scale, are defined in the Willamette Basin: (1) the Willamette silt unit (WSU), (2) the upper sedimentary unit (USU), (3) the middle sedimentary unit (MSU), (4) the lower sedimentary unit (LSU), (5) the Columbia River basalt unit (CRB), (6) the basement confining unit (BCU) and (7) the high Cascade unit (HCU) (fig. 2). This usage parallels that of Woodward and others (1998) with the addition of the HCU and the subdivision of the Willamette aquifer into a younger, more permeable USU, and an older, less permeable MSU. Previous investigators (Piper, 1942; Price, 1967a; 1967b; Frank, 1973; McFarland and Morgan, 1996; and Woodward and others, 1998) recognized that younger coarse-grained material had higher permeabilities than older coarse-grained material. Information from these studies and mapping by O'Connor and others (2001) allows a broad division of the coarse-grained basin-fill sediments (Willamette aquifer) into two regional hydrogeologic units (USU and MSU) based on permeability contrasts and age. The WSU, USU, MSU, and LSU are unconsolidated, nonmarine, basin-fill sediments that post-date the Columbia River Basalt Group. Descriptions of each hydrogeologic unit are presented in detail in Conlon and others (2005).

The WSU is composed primarily of fine-grained Missoula Flood deposits (O'Connor and others, 2001), and is at land surface in the lowland areas below about 400 ft elevation, except in the flood plains of large streams, where the unit has been removed by erosion. Although the WSU is present in the Tualatin subbasin, it cannot be recognized as a separate unit from other fine-grained deposits in the basin and is grouped together with the LSU. In the Central Willamette subbasin, the unit ranges from 60 to 120 ft thick, and generally is less than 20 ft thick in the Southern Willamette subbasin. The WSU has high porosity, low permeability, and is not generally used as an aquifer, but it may be a source of recharge to the underlying MSU. Little information on hydraulic properties is available; however, horizontal hydraulic conductivity values from Price (1967a), Wilson (1997), and Iverson (2002) provide ranges of 0.01 to 8 ft/d, 0.003 to 0.2 ft/d, and 0.3 to 1.4 ft/d, respectively. Specific yield values range from 0.2 to 0.3 (dimensionless). Vertical hydraulic conductivity is reported as 0.008 ft/d (Iverson, 2002).

Late Pleistocene and Holocene aged unconsolidated sands and gravels make up the high permeability, high porosity USU, which occurs at land surface in the Portland, Central Willamette and Southern Willamette subbasins, and is

absent in the Tualatin subbasin. In the Portland subbasin, the USU ranges from 50 to 150 ft thick. Hydraulic conductivity values range from 0.03 to 7,000 ft/d with a median hydraulic conductivity of 200 ft/d (McFarland and Morgan, 1996). In areas south of the Portland subbasin, the generally unconfined unit ranges in thickness from 20 to 40 ft and has a mean hydraulic conductivity of 600 ft/d (Woodward and others, 1998).

Pleistocene sands and gravels that predate the Missoula Floods make up the MSU. The unit generally overlies the fine-grained LSU and in turn is overlain by either the younger USU or WSU. In the Portland subbasin, the MSU consists of consolidated gravels of the upper Troutdale Formation, Pliocene to early Pleistocene volcaniclastic conglomerates from the Cascade Range, and the Pliocene to Pleistocene Boring Lavas. The unit is about 300–400 ft thick in the Portland subbasin, but can exceed 500 ft. In areas south of the Portland subbasin, the MSU includes pre-Missoula Floods sands and gravels, and Pliocene to Pleistocene fluvial gravels and alluvial fan remnants. In the lowland areas of the Central and Southern Willamette subbasins, the unit is generally less than 60 ft thick, but may exceed 200 ft thick where alluvial fan remnants are present. The unit tends to be unconsolidated in the upper part of the unit, but becomes more cemented with depth. Hydraulic conductivity values in the Portland subbasin range from 0.03 to 1,500 ft/d (McFarland and Morgan, 1996), and in other areas of the Willamette Basin range from 8 to 2,230 ft/d (Woodward and others, 1998). Storage coefficient values range from 0.0002 to 0.2 (Conlon and others, 2005), with larger values representing the specific yield of unconfined portions of the aquifers present where the overlying WSU is less than 20 ft thick. An aquifer test on well 06S/01W-08DAD01 in the Central Willamette subbasin indicated hydraulic conductivity values between 6 and 31 ft/d and a storage coefficient of 2×10^{-4} to 3×10^{-4} (Conlon and others, 2005, table 2).

The LSU is composed of a mix of fine grained units, and corresponds to the Willamette confining unit of Gannett and Caldwell (1998) and the lower sedimentary subsystem of Swanson and others (1993) in the Portland subbasin. The maximum thickness of the LSU is approximately 1,200 ft in the Portland subbasin. In the Tualatin subbasin, the LSU includes the Hillsboro Formation (Wilson, 1997) and flood deposits elsewhere included in the WSU, with a combined thickness of about 1,400 ft. In the Central and Southern Willamette subbasins, the LSU often contains stringers or thin beds of sand and gravel where the gradational unit boundary between it and the MSU is present. The LSU is generally considered a confining unit at a regional scale; however, at a local scale, the presence of productive but sparse sand and gravel interbeds allows for average to high well yields. Hydraulic conductivity values for the unit in the Portland subbasin range from 0.02 to 200 ft/d (McFarland and Morgan, 1996), in the Tualatin subbasin range from 0.8 to 32 ft/d (Wilson, 1997), and in the Central Willamette subbasin are as much as 220 ft/d. Because LSU wells tend to be completed in the coarse interbeds, the bulk hydraulic conductivity of this predominantly fine-grained unit likely is lower than reported aquifer test values. Reported storage coefficient values range from 0.00005 to 0.2 (Conlon and others, 2005). An aquifer test on well 05S/02W-08CBC01 in the Central Willamette subbasin indicated hydraulic conductivity values of 200–220 ft/d and a storage coefficient of 3×10^{-4} (Conlon and others, 2005, table 2).

The CRB consists of basaltic lava flows of Grande Ronde and Wanapum Formations of the Columbia River Basalt Group. The Wanapum flows are absent in the Tualatin subbasin (Beeson and others, 1989). More than 50 lava flows are present in the Portland subbasin, but only about a dozen are present in the Salem area (Beeson and others, 1989, Tolan and others, 1999, 2000). Individual basalt flows in the Willamette Basin range from 40 to 100 ft thick, but may exceed 250 ft in some areas (Beeson and others, 1989, Tolan and others, 1999, 2000). Total thickness of the CRB is more than 2,000 ft in the eastern area of the Portland subbasin, but generally ranges from 200 to 1,000 ft thick in other areas of the Willamette Basin. The CRB consists of thin, permeable, interflow zones representing flow tops and bottoms and associated sediments, separated by thick, low permeability flow interiors. Porosity of these zones, when considering bulk porosity of the entire flow, likely is less than 3 percent (Conlon and others, 2005). Hydraulic conductivity values from previous studies range from 10^{-3} to 10^{3} ft/d (Conlon and others, 2005). Selected aquifer tests reviewed for this study provide ranges of hydraulic conductivity values from 22 to 1,000 ft/d, and storage coefficient values from 0.0001 to 0.2 (Conlon and others, 2005).

Early Cenozoic marine sedimentary and volcanic rocks of the Coast Range and western Cascade Range make up the BCU (Gannett and Caldwell, 1998). The unit is exposed at surface in the Willamette Basin around the western perimeter of the study area and the eastern perimeter of the study area between the HCU and the sediment-filled basins of the Willamette lowland, and underlies the basin-fill sediment and the CRB in the Willamette Basin. The BCU has low permeability and low porosity, with hydraulic conductivity estimates of 10^{-5} to 10^{-2} ft/d in the western Cascade Range (Ingebritsen and others, 1994), and 0.2 to 0.3 ft/d near the Coast Range (Gonthier, 1983). The storage coefficient ranges from 0.00005 to 0.003 (Gonthier, 1983).

Pleistocene to Holocene volcanics make up the HCU along the crest of the Cascade Range on the eastern edge of the study area. The unit is greater than 1,000 ft thick. Hydraulic conductivity values range from 100 to 1,000 ft/d in the upper 100 ft of the unit and decrease to 0.1 ft/d at depth.

Hydrologic Setting

The processes that influence groundwater flow in the Willamette Basin include recharge by infiltration of precipitation and applied irrigation water, the exchange of

water between surface-water and groundwater systems, and discharge by evapotranspiration and wells. The estimated groundwater budgets for the Willamette Basin, the Willamette lowland, and the Central Willamette subbasin from Conlon and others (2005) are shown in table 1. The primary source of recharge is infiltration of precipitation in upland areas. Mean annual precipitation ranges from 40 in. in the lowland to 130 in. in the Coast Range and at the crest of the Cascade Range (Conlon and others, 2005). Recharge moves downward and laterally through sedimentary or basalt units until it discharges locally to pumping wells, evapotranspiration, streams, or to the regional sink, the Willamette River. Recharge also can be provided by infiltration of irrigation water, infiltration of storm water through drywells, and stream leakage. In this study, estimates of recharge from precipitation were based on watershed modeling using the Precipitation-Runoff Modeling System (PRMS) modified to incorporate irrigation water infiltration (Leavesley and others, 1983; Lee and Risley, 2001) except in the Portland subbasin, where recharge was based on regression equations developed by Snyder and others (1994). Snyder and others' regression equations used the average annual recharge calculated from estimates of deep percolation of precipitation, runoff into drywells, and septic systems in three areas in the Portland subbasin to derive an equation for calculating recharge in any area of the Portland subbasin. Average annual recharge values in the Willamette Basin were estimated for water years 1995 and 1996, and monthly recharge values in the Central Willamette Basin were estimated for water years 1999 and 2000. (The water year is a 12-month period beginning October 1 through September 30, designated by the calendar year in which it ends and which includes 9 of the 12 months.) Average annual recharge during water years 1995 and 1996 ranged from 7 in/yr in the lowland to more than 40 in/yr in the Coast Range and Cascade Range, and closely corresponds to observed precipitation patterns (Conlon and others, 2005).

Seepage between surface-water bodies and the groundwater system can take the form of recharge or discharge. When the elevation of the water table is above the elevation of the stream, seepage takes place as discharge into the stream from the groundwater system and the stream is classified as a gaining stream. When the elevation of the water table is below the elevation of the stream, seepage takes place from the stream as recharge into the groundwater system and the stream is classified as a losing stream. Base flow is a measure of the contribution of groundwater to streamflow. In Willamette Basin headwater streams in the higher elevations of the Cascade Range, seasonal variation in streamflow is less than 50 percent of mean annual flow and base flow is more than 80 percent of streamflow. Summer streamflow at these higher elevations is sustained by groundwater discharge and provides a large amount of the summer flow to the Willamette River. By contrast, the runoff-dominated, flashy, western Cascade Range, Coast Range, and Willamette lowland streams have small summer flows with seasonal variation in streamflow greater than 100 percent of mean annual flow, and base flow is less than 80 percent of streamflow (Lee and Risley, 2001).

In the Willamette lowland, both overland and base flow contributes to streamflow during the wet winters. Base flow is the main component of streamflow during the dry summers. Methods used to evaluate groundwater and surface-water interactions included seepage runs, seepage meters, and simulation of one-dimensional heat transport (Conlon and

Table 1. Groundwater budget for the Willamette Basin, Oregon, 1995–96.

[**Willamette Basin:** Upstream of Portland streamgage. Groundwater budget (from Conlon and others, 2005, table 6, p. 39). **Lowland:** Area defined in Conlon and others, 2005. Recharge = Evapotranspiration + well discharge + stream seepage (storage change assumed negligible). **Abbreviations:** M acre-ft/yr, million acre-feet per year; in/yr, inch per year; mi^2, square mile; PRMS, Precipitation-Runoff Modeling System]

	Willamette Basin (11,111 mi^2 area)		Lowland (3,394 mi^2 area)		Central Willamette subbasin (683 mi^2 area)	
	M acre-ft/yr	Recharge (percent)	M acre-ft/yr	Recharge (percent)	M acre-ft/yr	Recharge (percent)
Recharge	13.22		2.86		0.56	
Evapotranspiration[1,2]	0.46	3.4	0.46	15.9	0	0.0
Well discharge	0.28	2.1	0.28	9.8	0.14	25.0
Stream seepage	12.49	94.4	2.13	74.3	0.42	75.0

[1]Evapotranspiration from land surface and unsaturated zone simulated with PRMS.

[2]Evapotranspiration from water table (saturated zone) estimated in southern Willamette Basin to be 8 in/yr.

others, 2005). Results show that water levels in shallow wells near large streams track stream stage and indicate a good hydraulic connection between the stream and the underlying USU. In contrast, there is poor hydraulic connection between streams flowing on the WSU and the underlying sedimentary units due to the low hydraulic conductivity of the WSU. Groundwater discharge to these streams is small relative to streamflow and originates mostly in the WSU (Iverson, 2002). The limited hydraulic connection is apparent when local pumping from an underlying unit lowers groundwater levels below the stream stage of a stream flowing on the WSU. Recharge to the groundwater system from the stream is relatively small when compared to a stream flowing on the USU (Conlon and others, 2005).

Evapotranspiration from the unsaturated zone is accounted for in the PRMS model (Lee and Risley, 2001). Evapotranspiration from the saturated zone where the water table is less than 10 ft below land surface is relatively small in the Willamette Basin with most occurring in the lowland (table 1). In the Central Willamette, Tualatin, and Portland subbasins, shallow water levels are limited to local areas containing the stream flood plain and are assumed insignificant. In the Southern Willamette subbasin, shallow water levels could cover a more significant area, and evapotranspiration rates from the saturated zone might be as high as 8 in/yr (Conlon and others, 2005).

Well pumping, summarized in Conlon and others (2005), is mostly in the lowland with about half occurring in the Central Willamette subbasin (table 1). Pumping includes withdrawals for public supply, irrigation, and industrial uses. Domestic pumping generally returns to the aquifer through septic systems, and the consumptive amount of domestic use is assumed to be small. In this study, annual pumping for the Willamette Basin was estimated for water years 1995 and 1996. Monthly withdrawals were estimated for the Central Willamette subbasin for water years 1999 and 2000. Irrigation withdrawals were estimated on the basis of OWRD water right records and satellite imagery (Conlon and others, 2005).

Groundwater Flow

Two water-level contour maps were developed by Conlon and others (2005) to determine horizontal groundwater flow directions in the Willamette Basin: a water-table map for the basin-fill sediments and a generalized water-level map for the CRB. Water levels from shallow wells less than 150 ft deep and open to WSU, USU, MSU, and LSU were used to develop the basin-fill sediments water-table map.

In most areas of the Tualatin, Central Willamette, and Southern Willamette subbasins, the water table is within 20 ft of land surface. In the Southern Willamette subbasin, where the WSU is generally less than 20 ft thick, average annual water levels in the underlying MSU generally are within 10 ft of land surface. In the Central Willamette subbasin, where the WSU is as much as 120 ft thick, water levels in the WSU can be as much as 25 ft higher than in wells in the underlying sediments. Hydraulic heads generally are lower at greater depth in the lowland, and the low vertical permeability of the WSU impedes vertical flow. This increases differences in water levels between wells completed in the WSU and wells completed in the underlying sedimentary units. Water-level measurements indicate that the regional water table is present at shallow depths in the silt and all sediments below are fully saturated; hence, a perched water table does not exist as suggested by Piper (1942).

Groundwater flows from southeast to northwest in the Southern Willamette subbasin, and from east to west in the Stayton subbasin, with most flow approximately parallel to streams. Hydraulic gradients generally are less than 15 ft/mi due to the topography and high permeability of the USU and MSU. Chlorofluorocarbon (CFC) age dates of shallow groundwater are consistent with flow directions in the Southern Willamette subbasin. Relatively young water is at the eastern edge of the lowland where local recharge is the primary source of inflow, and relatively old water is to the west consistent with longer flow paths. The relatively young water in the USU may indicate infiltration of precipitation and surface water into the highly permeable flood plain deposits (Conlon and others, 2005).

A more complex flow system described by Conlon and others (2005) is evident in the Central Willamette subbasin. Streams incised into the WSU influence shallow water levels more than the less incised streams in the Southern Willamette subbasin. Small streams in the Central Willamette subbasin tend to occupy sharply cut and deep pathways in the WSU, which generally do not fully penetrate the silt. Water levels are commonly within 15 ft of land surface in the WSU, and hydraulic gradients range from 20 to 40 ft/mi; however, in areas adjacent to incised streams, hydraulic gradients may increase to as much as 500 ft/mi. Local flow systems are prevalent in the WSU where a small component of local recharge flows horizontally and discharges to local streams. In the USU where there is little resistance to flow in the flood plains of the Willamette River, hydraulic gradients generally are less than 2 ft/mi.

In the Tualatin subbasin, the water table in the basin-fill sediments is generally detected at depths of less than 20 ft. Groundwater flows from the margins of the basin to the center where it discharges to streams. Hydraulic gradients are steep due to the low permeability of the LSU. Although regional subbasin discharge is to the Tualatin River, some flow discharges to local streams.

In the Central and Southern Willamette subbasins, direction and elevation of flow as indicated by the water table in the sediments has not changed significantly in most areas since it was mapped by Piper in 1935 (Piper, 1942). This indicates that mean average annual water levels have remained stable in most areas of the Willamette Basin. Although Willamette Basin water levels generally show an absence of long-term declines, limited areas display long-term declines in water levels, which likely are the result of groundwater withdrawals (Conlon and others, 2005).

Water levels in the upper part of the USU, MSU and LSU where exposed at land surface are similar to the water table. The WSU acts as a confining unit where it is thick and overlies the MSU and LSU. Where overlain by the WSU, groundwater levels in the MSU and LSU represent the water levels of a confined aquifer and generally flow to the Willamette River, or discharge locally to the lower reaches of the Pudding and Molalla Rivers where the confining WSU is absent. In areas where the WSU is present, the underlying aquifers have poor hydraulic connection to the smaller streams (Piper, 1942). Although other studies have indicated a hydraulic connection to these streams (Price, 1967a; Woodward and others, 1998), the connection likely is minimal and on a local scale.

Groundwater in the CRB generally moves from exposed upland areas at basin perimeters toward the lowland areas in the basin interiors where it discharges to the Tualatin and the Willamette Rivers. The rate of discharge likely is low due to the low vertical permeability of the unit and the thickness of the overlying basin-fill sediments. Some discharge to small streams is likely in the upland areas where the streams are incised into the basalt. Horizontal gradients in the upland areas are expected to be less than 10 ft/mi compared to gradients in the lowlands of less than 6 ft/mi (Conlon and others, 2005). In the Wilsonville area, gradients have decreased by about 50 percent since pumping from the basalt aquifers ended in April 2002, which suggests that pumping from the CRB may cause a significant increase in the horizontal gradient. Under natural conditions, horizontal gradients are about 1 ft/mi. In the valley center, vertical gradients appear to be negligible and groundwater flow is essentially horizontal (Conlon and others, 2005). Water level fluctuations in upland and lowland CRB wells show similar fluctuations, which indicate a connection between deep interflow zones in the upland and lowland areas. Faulting in the CRB may act as barriers to flow on a local scale over short time intervals, especially when the unit is stressed by pumping; however, they may not act as flow barriers on a regional scale (Conlon and others, 2005).

Vertical groundwater flow is generally downward within the basin-fill sediments, except in narrow areas near streams incised into the WSU or other sedimentary units. Upward groundwater flow also takes place near the Willamette River, where discharge arises through the USU. Around and near the perimeter of the basins, groundwater flow in the CRB is downward; however, an upward component of flow to regional discharge areas is likely in the lowlands. The low vertical permeability of the basalt interior provides a resistance to vertical flow, and can cause substantial head differences between permeable zones.

Precipitation and snowmelt easily infiltrate the HCU and follow shallow, short flow paths through the highly transmissive shallow part of the HCU before discharging locally into springs. Deeper and longer flows through the HCU follow paths toward the west to the contact of the unit with the low permeability BCU, where most High Cascades groundwater exits the system (Conlon and others, 2005). Another much smaller component of these flow paths is presumed to continue through the BCU and to ultimately discharge to the Willamette River.

Groundwater Levels

Water levels in the Willamette Basin change in response to precipitation, stream stage, pumping or injection, changes in storage, and possible long-term climate effects. Water levels reflect variations in precipitation trends from year to year, but in most locations fluctuate around an average value that reflects a balance between recharge and discharge.

Wells in the basin show either a direct, rapid response to short term precipitation events or a gradual, indirect rise, or a combination of both, depending on the hydrogeologic conditions at the well location. Direct response wells exhibit a rapid water level rise in late autumn or early winter shortly after the start of the rainy season, with successive peaks that correlate to periodic storms during the rainy season. An indirect response to precipitation is indicated where a well shows a rising groundwater level that is proportional to cumulative precipitation, with water levels peaking and beginning to drop off in March. Wells in the USU, and in the upper part of the MSU in the Southern Willamette subbasin generally show a direct response to precipitation, which suggests that recharge is local, infiltration rates are rapid, and recharge paths are short. Wells completed in the confined or deeper parts of the MSU often show an indirect response to precipitation, which suggests more distant recharge sources, relatively slower infiltration rates, and longer recharge paths. Water levels in wells adjacent to large streams in the Willamette Basin generally show a hydraulic connection to stream stage. Water levels are slightly higher than river stage, suggesting discharge from the aquifer to the river; however, during short time intervals when river levels are high, the gradient is often reversed and suggests discharge from the river to the aquifer.

Aquifer water levels decline in response to groundwater removed from storage by pumping. If additional groundwater cannot be captured from stream discharge or induced recharge, water will continue to be removed from storage and groundwater levels will continue to decline. The magnitude of the decline is dependent on the properties of the aquifer, and the pumping duration and rate. Water levels affected by pumping show a steep decline in the summer followed by a broad recovery curve during winter and spring. Water levels in many wells open to confined basin-fill sediments and the CRB show a response to seasonal pumping. Conlon and others (2005) compared the seasonal fluctuations from Piper (1942) of 10 ft in the Central Willamette subbasin to fluctuations during the period 1997–98, which suggested that as much as 55 ft of additional seasonal fluctuation has been induced by groundwater withdrawals in areas where there was poor connection between local streams and the associated sedimentary unit.

Rising and declining water level trends in the Willamette Basin generally correlate to precipitation trends; however, water-level changes cannot be attributed to climatic cycles in some areas. Upper limits are imposed on high water levels in shallow long-term observation wells where the water table is near land surface, and response to winter precipitation appears to fully recharge these aquifers. Deeper water levels in upland observation wells are not limited by the elevation of land surface and resultant storage, and if a hydraulic connection is present, water levels may match precipitation trends. However, seasonal pumping in the Willamette Basin often affects well water levels, and can obscure climate trends.

Short pathways and quick infiltration of recharge has resulted in little change in groundwater levels in the Southern Willamette subbasin since pre-development (Piper, 1942). Seasonal irrigation pumping in the USU captures discharge to the Willamette River, and has less effect on nearby water levels. An increase in current pumping patterns in the Southern Willamette subbasin likely will result in additional capture from the major streams in the area.

Unconfined groundwater is present in the USU near the major streams in the Central Willamette subbasin, and the water table is present near land surface in the WSU. Confined groundwater generally is found in the underlying MSU and LSU. Seasonal pumping effects are evident and seasonal water-level fluctuations have increased over time. Long-term climatic trends are not obvious, but effects of short-term droughts are evident (Conlon and others, 2005). Large seasonal fluctuations are generally caused by pumping from the MSU where the unit is thin. The basinwide pattern of seasonal withdrawals indicates that pumping interferences overlap and produce a seasonal system-wide decline in water levels, rather than isolated areas of low water levels due to local well pumping. Water levels are more affected in the Central Willamette subbasin than in the Southern Willamette subbasin because pumping is more evenly distributed spatially and across aquifers in the Central Willamette subbasin, compared to pumping concentrated near the Willamette River in the USU and MSU in the Southern Willamette subbasin. Water-level declines in the basin-fill sediments are seen in several locations in the Central Willamette subbasin (Conlon and others, 2005), indicating that wells may capture groundwater otherwise discharging to streams, or induce increased recharge from streams. The WSU limits increased recharge from the smaller basin streams, so stream capture is likely primarily from the larger streams that penetrate the WSU. Increases in pumping could lead to larger seasonal water-level fluctuations and long-term declines in average annual water levels.

Water levels in the basin-fill sediments in the Tualatin and Portland subbasins appear to be relatively stable over time, with seasonal fluctuations of about 15 ft and response to periods of decreased precipitation. Although withdrawals in the Tualatin subbasin are limited, most groundwater withdrawals in the Portland subbasin are derived from the basin-fill sediments. Much of the pumping originates from relatively shallow wells near the large streams in the subbasin. Stream capture is the likely source of water for these wells, which decreases the drawdown of aquifer water levels in the subbasin. Areas in the Portland subbasin near Boring and Damascus show long-term effects from pumping from the confined MSU and LSU of about 20 ft over 35 years (Conlon and others, 2005).

The CRB, present only in the northern half of the Willamette Basin, has shown variability in water levels based on the effects from nearby pumping. The fluctuations evident in water levels in the CRB indicate an influence from local stresses rather than a basin-wide reduction in water levels from pumping. These fluctuations are caused by the small storage capacity of the CRB due to the restriction of pore space to interflow zones, and the lack of hydraulic connection with major streams in the basin or other close recharge sources. These conditions may cause significant declines in water levels in the area of influence of the pumping well.

Description of Numerical Models Used in this Study

Numerical flow models were developed to simulate the effects of changes in groundwater pumping on water levels, groundwater flow, and surface-water flow in the Willamette Basin. The USGS modular, three-dimensional, finite-difference numerical groundwater flow model MODFLOW-2000 (McDonald and Harbaugh 1988; modified by Harbaugh and others, 2000, and Hill and others, 2000), was used to simulate regional groundwater conditions in the Willamette Basin and local groundwater conditions in the Central Willamette subbasin. MODFLOW-2000 uses block-centered, finite-difference approximations to solve the three-dimensional equation of groundwater flow in a heterogeneous and anisotropic porous medium with a constant-density and viscosity fluid. It computes an approximation of the solution for water levels at specific points and times by solving a system of algebraic equations among all points. In this study, the geometric multigrid solver was used to simultaneously solve these equations. The sensitivity process (Hill and others, 2000) was used to calculate the sensitivity of model outputs to changes in model parameter values. The parameter estimation process (Hill and others, 2000) was used to calibrate the regional steady-state model and obtain parameter values that result in simulations that best match measurements of groundwater levels and base flow.

Approach to Model Development

Two models were developed for this study: a regional-scale model of the Willamette Basin and a more detailed model of the Central Willamette subbasin. The regional scale model was developed to simulate steady-state conditions in the Willamette Basin to test the conceptual model of groundwater flow and understand the effects of pumping on surface water and groundwater. The use of a steady-state model is appropriate when a system can be represented by an approximate equilibrium condition (Reilly and Harbaugh, 2004). (A steady-state flow model describes the hydrologic conditions in a groundwater-flow system in equilibrium; that is, a system in which there is no net change in hydraulic head.) In order to simulate the study area in steady state, the regional model of the Willamette Basin was constructed with estimates of model parameter values obtained from previous studies, as summarized in Conlon and others (2005, table 1). Average annual recharge and streamflow data from water years 1995 and 1996 (water years during which conditions were reasonably close to long-term average conditions and hydrologic data were collected basinwide) and water-level data collected during or near the seasonal low-flow period, November 1996, were used to calibrate the regional steady-state model using the parameter estimation and sensitivity processes (Hill and others, 2000). Chlorofluorocarbon-age data (Conlon and others, 2005, appendix B) were used to verify calibration results and adjust model parameters as indicated.

A finer scale transient model was developed for the Central Willamette subbasin to simulate potential effects on water levels and flows caused by pumping patterns in an area of increasing development. (A transient flow model describes the hydrologic conditions in a groundwater flow system that is in disequilibrium; that is, a system in which there is a change in hydraulic head due to changing stresses on the system, such as increasing pumping.) Spatially, the approximately 1.75-mi^2 (1,125-acre) regional model cells were subdivided into cells of approximately 0.04 mi^2 (23 acres) for the local model. This refinement allowed for the analysis of individual groundwater/stream interaction not possible in the regional model. The regional model layer representing the CRB was divided into three vertical layers for the local model, which allowed for the simulation and analysis of vertical gradients within the basalt. Groundwater flux estimates simulated by the regional model were applied to the boundary of the local model to simulate the regional flow entering and leaving the local model.

The local model was developed using calibrated parameters from the regional steady-state model, and this model was initially calibrated in steady state to test parameter assignment and provide initial conditions for the transient model. Updated water use information, average annual recharge, and water-level measurements from water years 1999–2000 were used to calibrate the local steady-state model. Further adjustment of model parameters (specifically, riverbed and drainbed vertical hydraulic conductivity) by trial-and-error allowed for the best fit between model simulated and measured groundwater levels and flows.

The local steady-state model of the Central Willamette subbasin was then converted to a transient model to simulate potential effects on water levels and flows caused by pumping patterns in an area of increasing development. Initial groundwater levels for the transient model were set equal to water levels simulated in the local steady-state model. The transient model was calibrated to monthly average hydraulic head conditions during water years 1999–2000 (24 stress periods) using parameter values from the local steady-state model and adjusting specific storage by trial-and-error. Following model calibration, to reach dynamic steady-state conditions the simulation was extended for a period of 50 years (600 stress periods) using and repeating monthly average data from water years 1999–2000. The simulated water levels at the end of the final stress period were assigned as initial water levels for predictive simulations.

Regional Groundwater Model

Regional Discretization

The regional steady-state model for the Willamette Basin has 7,000 ft by 7,000 ft grid cells (about 1,125 acres). The grid for the regional model contains 117 rows, 66 columns, and 6 layers, with a maximum of 3,887 cells active in a layer. All lateral boundaries of the regional model are no-flow boundaries. The boundaries were selected to coincide with the location of the groundwater divide along the crest of the Coast Range to the west and southwest and drainage basin boundaries (derived from the PRMS model used to estimate recharge for the Willamette Basin) to the east (fig. 4*A*). The eastern boundary was selected to include most of the basin-fill sediments and extend into the BCU. Rivers draining the HCU are simulated as flowing across the eastern boundary, but the amount of groundwater originating from the HCU that flows through the low permeability western Cascade Range is assumed to be negligible. The Columbia River was simulated as a constant head boundary to the north in layer 2 because average annual water levels in the Columbia River do not vary significantly from year to year.

Six layers were used to represent the six major hydrogeologic units within the regional model boundary (figs. 2 and 4*B*). Each layer varies in thickness throughout the model, except for layer 6. Layer 1, which represents the WSU, ranges from about 0- to 120-ft thick. Layers 2 and 3 (USU and MSU) range in thickness from about 10 to 900 ft. In the Central and Southern Willamette subbasins,

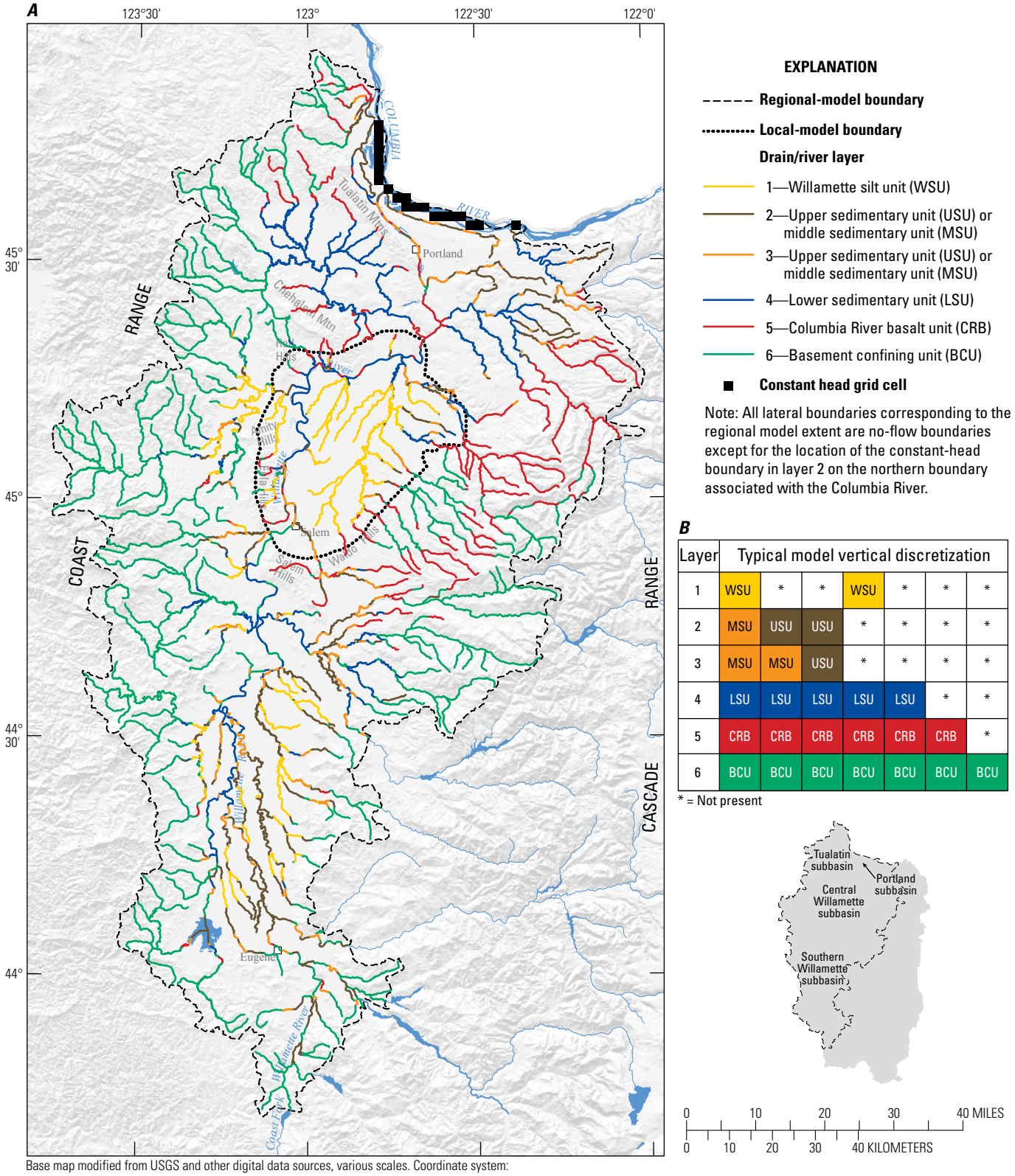

Base map modified from USGS and other digital data sources, various scales. Coordinate system: UTM, Zone 10N, Projection: Transverse Mercator; Datum: North American Datum of 1927.

Figure 4. (*A*) Locations of constant head, river, and drain cells, boundary conditions, and (*B*) typical vertical configurations of hydrogeologic units in model layers, Willamette Basin, Oregon. Stream reaches, simulated using river and drain cells, are color coded by layer and hydrogeologic unit. Gaps in the vertical configuration are simulated using thin pseudo-cells that easily transmit water in the vertical direction.

the unit thicknesses are limited to less than 60 and 200 ft, respectively. Layers 2 and 3 are thickest where alluvial fans are present in the Central and Southern Willamette subbasins and in the Portland subbasin where they include parts of the hydrologically similar unconsolidated sedimentary unit and Troutdale gravels. Layers 1 through 3 are not present in the Tualatin subbasin. Layer 4 represents the LSU and is thickest in the Central Willamette subbasin (as much as 1,600 ft) and the Portland and Tualatin subbasins (as much as 1,400 ft). It is also the only basin-fill sedimentary unit present in the Tualatin subbasin. Layer 5 represents the CRB; however, to the east, it also includes the Sardine Formation and younger volcanic deposits in the study area. Layer 5 is thickest in the Portland basin and northeastern area of the model (as much as about 5,000 ft), and ranges from 0 to about 1,000 ft thick in the Central Willamette and Tualatin subbasins; it is not present in the Southern Willamette subbasin. Layer 6 represents the BCU; it was set to a thickness of 1,000 ft throughout the active model area.

Within the boundaries of a unit extent, where a unit is absent between two adjacent unit layers, it is represented by a 1-ft-thick "pseudo-cell" in order to maintain vertical continuity between model layers. In order for MODFLOW to allow vertical flow across the area of the absent unit, the layer cell must be present and active. Vertical hydraulic conductivity of the pseudo-cell is set several orders of magnitude higher than in neighboring cells so that it does not affect vertical flow between the adjacent upper and lower layers. Horizontal hydraulic conductivity of the pseudo-cell is set several orders of magnitude lower than in neighboring cells to prevent horizontal flow between the layer cells in areas where the unit layer is not actually present (Morgan and Dettinger, 1996).

Regional Boundary Conditions

The boundaries of the regional steady-state model were selected to coincide with hydrologic and geologic boundaries of the system. Three types of boundary conditions were used to represent the groundwater-flow system in the Willamette Basin: no-flow boundaries, constant head boundaries, and specified flux boundaries. Boundaries in the Willamette Basin are divided into two broad categories that describe the boundaries related to the geographic extent of the aquifer systems, and the hydrologic processes active within the model extent.

Geographic Boundaries

No-flow and constant head boundaries represent the geographic boundaries in the Willamette Basin (fig. 4). The northern boundary of the model is defined by the Columbia River, which is simulated as a constant head in layer 2. All other lateral boundaries corresponding to the regional model extent are no-flow boundaries. Additionally, because the Columbia River is assumed to be the regional groundwater sink (McFarland and Morgan, 1996), it is assumed that no horizontal flow crosses this boundary through deeper units. The eastern and southern boundaries of the model follow drainage basin boundaries derived from the PRMS model used to estimate recharge for the Willamette Basin (Lee and Risley, 2001) and were selected to include most of the basin-fill deposits and extend into the low permeability deposits of the western Cascade Range, represented by the BCU. The western boundary of the model coincides with the topographic crest of the Coast Range and was assumed to be a no-flow boundary because a groundwater divide likely occurs as a subdued expression of the surface-water divide caused by the topography of the Coast Range.

The lateral no-flow boundaries extend through all model layers except for the location of the constant-head boundary in layer 2 on the northern boundary associated with the Columbia River (fig. 2). Layers 1 through 5 usually are absent at the edges of the modeled area (except for the northeastern boundary), and were set as no-flow boundaries at their extents. The sedimentary units generally thin and pinch out at their extents; therefore, the edges of the units can be reasonably simulated as no-flow boundaries. An arbitrary thickness of 1,000 ft represents the relatively impermeable layer 6 because the actual thickness of the BCU is not known, and the lower boundary of the model is set as a no-flow boundary.

Hydrologic-Process Boundaries

Hydrologic-process boundaries include recharge, leakage to drains, leakage to and from rivers, and well pumping and are designated as either specified-flux (recharge) or head-dependent-flux (leakage and pumping) boundaries.

Recharge

Recharge is simulated as an areally distributed specified flux to the uppermost active layer in the model. Recharge was estimated using PRMS, which was modified to include the infiltration of precipitation and irrigation water at a hydrologic-response unit (HRU) level, to provide average annual recharge values for water years 1995–96 (Leavesley and others, 1983; Lee and Risley, 2001).

Simulated recharge rates ranged from 7 in/yr in the Willamette lowland areas to 50 in/yr in the upland areas of the Cascade Range foothills, the Coast Range, and other areas of high elevation. Recharge averaged 22 in/yr for water years 1995–96 (Conlon and others, 2005). The simulated pattern of recharge for water years 1995–96 closely follows the pattern of precipitation in the region (fig. 5).

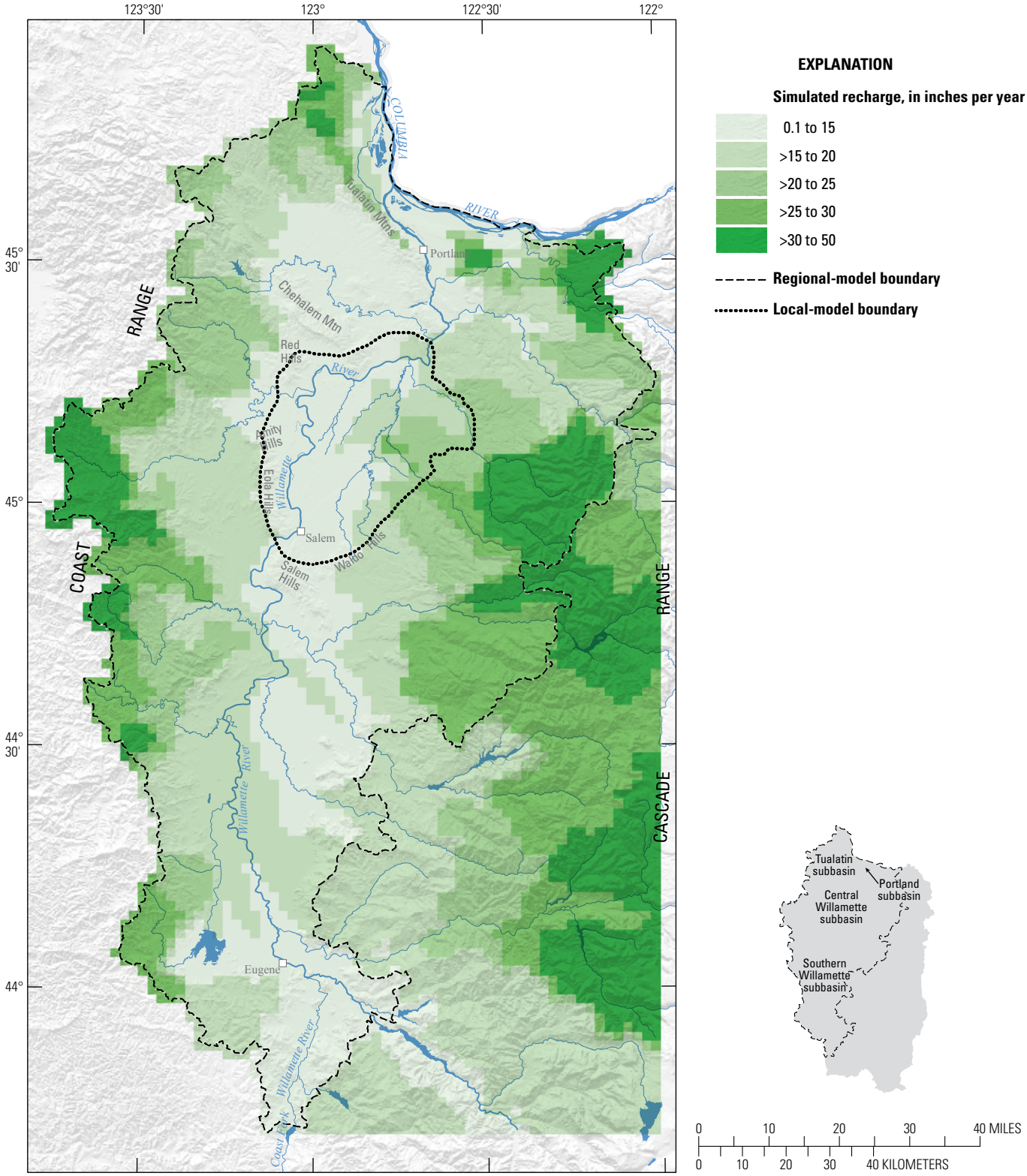

Base map modified from USGS and other digital data sources, various scales. Coordinate system: UTM, Zone 10N, Projection: Transverse Mercator; Datum: North American Datum of 1927.

Figure 5. Simulated mean annual recharge from the Precipitation-Runoff Modeling System (PRMS), Willamette Basin, Oregon, water years 1995–96. Modified from Conlon and others (2005).

River and Drain Leakage

Streams in the regional steady-state model were simulated as head-dependent-flux boundaries using the RIVER and DRAIN packages in MODFLOW, which simulate the movement of water between the aquifer and stream in all cells containing rivers (McDonald and Harbaugh, 1988). Water flows from the aquifer to the river when the head in the aquifer is greater than the head in the river (referred to as a "gaining stream"). Water flows from the river to the aquifer when the head in the aquifer is less than the head in the river (referred to as a "losing stream"). The DRAIN package simulates the drainage of water from the aquifer at a rate proportional to the difference between the head in the aquifer and the head in the drain. Water can flow only from the aquifer to drains, and that occurs when the head in the aquifer is greater than the elevation of the drain.

The regional steady-state model contains 3,856 drains and river reaches (fig. 4*A*). The relatively large number of river cells initially led to model instability; consequently, the DRAIN and RIVER packages were used in conjunction to simulate the streams in the model.

River stage and drain elevation were estimated from the elevation of each model cell in the basin that contained a river reach/drain cell. Stage was estimated as an average of the land surface elevation derived from 1:24,000 digital elevation models (DEMs) at the endpoints of the river segment where it entered and left the model cell or where it intersected another river segment. Each river segment was categorized by size and placed in a particular order; width and depth were assigned based on size category ordered from 1 to 5, with 1 being the relatively smallest river (for example, Zollner Creek), and 5 being the relatively largest river (Willamette River) (table 2). Simulated stage above riverbed (table 2) was used to determine the elevation of the top of the riverbed by subtracting the depth from the stage. The elevation of the bottom of the riverbed was determined by subtracting 5 ft from the elevation of the top of the riverbed. The elevation of the bottom of the riverbed is used by MODFLOW to determine whether the direction of flow is into the river, or into the aquifer. Both river and drain bed conductances are calculated by multiplying the area (width from table 2 times the length of the reach intersecting the model cell) of the river/drain by the hydraulic conductivity of the river or drain bed material (table 3), and dividing this value by the thickness of the river/drain bed material. The river/drain bed material thickness was assumed to equal 1 ft for the conductance calculation.

Table 2. Relation between stream size and values used for simulation of each stream using the RIVER and DRAIN packages in the MODFLOW groundwater-modeling program.

Stream order	Simulated river/drain width (feet)	Simulated stage above river bed (feet)
1	20	2
2	50	5
3	100	10
4	300	20
5	800	30

The rate of exchange between the aquifer and the stream depends on whether or not the hydraulic head in the aquifer is above or below the river bottom because the mechanisms controlling flow differ according to the direction of flow. When aquifer head is above the river bottom, flow is proportional to the difference between the head and the river stage. When head is below the river bottom, the rate of flow is controlled by the head drop across the fine-grained riverbed, so flow is proportional to the difference between the stage and river bottom elevation.

Groundwater flow from the aquifer to the stream results in a gaining stream. Unlike in a losing stream where the flow of water is only within the wetted perimeter of the stream, a gaining stream may have seepage into the stream within the wetted perimeter and from seepage faces and springs above the wetted perimeter. In losing stream reaches, filtration of particles occurs in the streambed as water flows from the stream into the ground, possibly resulting in reduction in streambed permeability over time. However, because particulates generally are low in groundwater, streambed clogging is less likely in gaining stream reaches.

Stream incision is common in the Willamette Basin lowlands and, because of the large amount of fine sediment composing many of the alluvial formations, the processes described in the preceding paragraphs possibly are substantial. Because the MODFLOW RIVER package does not allow for different gaining and losing conductances, the RIVER and DRAIN MODFLOW packages were used in conjunction for this model, using the methods described generally by Zaadnoordijk (2009).

Table 3. Final model parameters and initial values used for the regional model of the Willamette Basin and local model of the Central Willamette subbasin, Oregon.

[Drain and river locations are shown in figure 4. Initial parameter values are in parentheses. Parameters with no parentheses were set during calibration. Bold values were adjusted using parameter estimation. **Kh:** Horizontal hydraulic conductivity. **Kv:** Vertical hydraulic conductivity. **Abbreviations:** ft^{-1}, foot; ft/d, foot per day]

Unit	Layer	Kh (ft/d)	Kv (ft/d)	Kv drain bed (ft/d)	Kv riverbed (ft/d)	Recharge (array multiplier, unitless)	Specific storage (ft^{-1})
Willamette silt unit (WSU)	1	1 (1)	0.01 (0.01)	1.00E-03 (0.1)	1.00E-5	0.58 (1)	1.00E-3
Upper sedimentary unit (USU)	2 and 3	600 (600)	0.6 (0.6)	0.6 (6)	6.00E-3	0.55 (1)	1.00E-4
Portland subbasin-upper sedimentary unit (USUP)	2 and 3	200 (600)	0.6 (0.6)	0.6 (6)	6.00E-3	0.55 (1)	Not determined
Middle sedimentary unit (MSU)	2 and 3	**72 (200)**	0.02 (0.2)	0.2 (2)	2.00E-3	0.55 (1)	1.00E-5
Portland subbasin-middle sedimentary unit (MSUP)	2 and 3	**4 (50)**	0.02 (0.2)	0.2 (2)	2.00 E-3	0.55 (1)	Not determined
Lower sedimentary unit (LSU)	4	**61 (5)**	**0.04 (0.005)**	0.02 (0.5)	2.34E-4	1.14 (1)	1.00E-6
Portland subbasin-lower sedimentary unit (LSUP)	4	1 (10)	0.04 (0.005)	0.02 (0.5)	2.34E-4	1.14 (1)	Not determined
Columbia River basalt unit (CRB)	5 (regional) or 5,6,7 (local)	**1 (2.5)**	**0.03 (0.025)**	1.4 (0.025)	1.40E-2	1. 08 (1)	1.00E-4
Basement confining unit (BCU)	6 (regional) or 8 (local)	**0.8 (1)**	**0.05 (0.01)**	0.14 (0.1)	1.40E-3	0.87 (1)	1.00E-6
Pseudo-cell (USU, MSU, LSU, LSUP, CRB)	Same as unit represented by pseudo-cell	1E-10 (same as unit)	1E+05 (same as unit)	Not determined	Not determined	Not determined	1.00E-10

Altering the DRAIN package and RIVER package notation (McDonald and Harbaugh, 1988, chap. 9) to have the same form, the DRAIN package notation becomes:

$$Q^{drain}_{i,j,k} = -Cond^{drain}_{i,j,k} L^{river}_{i,j,k} \left(h_{i,j,k} - h^{river}_{i,j,k} \right) \quad \text{for } h_{i,j,k} > h^{river}_{i,j,k} \tag{1}$$

$$Q^{drain}_{i,j,k} = 0 \quad \text{for } h_{i,j,k} \le h^{river}_{i,j,k} \tag{2}$$

where

$Q^{drain}_{i,j,k}$ is the groundwater discharge from the cell identified by the triple (i,j,k),

$Cond^{drain}_{i,j,k}$ is the corresponding conductance per unit length of river,

$L^{river}_{i,j,k}$ is the total river length in the cell,

$h_{i,j,k}$ is computed head in the aquifer, and

$h^{river}_{i,j,k}$ is the river stage.

A similar alteration of the RIVER package notation yields:

$$Q^{river}_{i,j,k} = -Cond^{river}_{i,j,k} L^{river}_{i,j,k} \left(h_{i,j,k} - h^{river}_{i,j,k} \right) \quad \text{for } h_{i,j,k} > RBOT \tag{3}$$

$$Q^{river}_{i,j,k} = -Cond^{river}_{i,j,k} L^{river}_{i,j,k} \left(RBOT - h^{river}_{i,j,k} \right) \quad \text{for } h_{i,j,k} \le RBOT \tag{4}$$

where

$Q^{river}_{i,j,k}$ is the flux out of the groundwater in the cell identified by the triple (i,j,k),

$Cond^{river}_{i,j,k}$ is the corresponding conductance per unit length of river, and

$RBOT$ is the elevation of the bottom of the riverbed sediments (McDonald and Harbaugh, 1988, chap. 6).

Defining the total exchange of groundwater with the river [$Q^{total\_river}_{i,j,k}$] as the sum of the water flow simulated in the RIVER and DRAIN packages, the resulting model has the following properties:

- When head in the aquifer is equal to or less than the river surface elevation, all flow is simulated using the RIVER package and the physical processes represented are exchange of water through the wetted area of the channel as represented by $Cond^{river}_{i,j,k}$
- When head in the aquifer is greater than the river surface elevation, flow still passes through the river channel (accounted for with the RIVER package), but the additional processes of streambank seepage, springs, and higher permeability (for example, less plugging due to filtration) gaining reaches bed sediments are accounted for through the DRAIN package as represented by $Cond^{drain}_{i,j,k}$.

Mathematically, the total exchange of water is simulated as:

$$Q^{total\_river}_{i,j,k} = -\left(Cond^{drain}_{i,j,k} + Cond^{river}_{i,j,k} \right) L^{river}_{i,j,k} \left(h_{i,j,k} - h^{river}_{i,j,k} \right) \quad \text{for } h_{i,j,k} > h^{river}_{i,j,k} \tag{5}$$

$$Q^{total\_river}_{i,j,k} = -Cond^{river}_{i,j,k} L^{river}_{i,j,k} \left(h_{i,j,k} - h^{river}_{i,j,k} \right) \quad \text{for } h^{river}_{i,j,k} \ge h_{i,j,k} > RBOT \tag{6}$$

$$Q^{total\_river}_{i,j,k} = -Cond^{river}_{i,j,k} L^{river}_{i,j,k} \left(RBOT - h^{river}_{i,j,k} \right) \quad \text{for } h_{i,j,k} \le RBOT \tag{7}$$

The net result of this formulation is a river that gains water more efficiently than it loses water, which is consistent with all the physical mechanisms described above.

Groundwater Discharge by Wells

Extraction of groundwater through wells, summarized in Conlon and others (2005), is simulated as a specified-flux boundary, and includes industrial, municipal (public supply), and irrigation pumping (fig. 6). Domestic pumping was not included in the simulation because much of the pumped water returns to the aquifer through septic systems and typically takes place in the same model cell. Estimates indicate that less than 1 ft^3/s of water was pumped for domestic use in the Willamette lowland in 1990 (Conlon and others, 2005). Pumping from wells with multiple open intervals or with open intervals spanning several model layers was proportioned according to the percentage of the layer open to the interval. Data for public supply and industrial groundwater use were obtained through OWRD, water suppliers, estimated from previous reports, or estimated from population data (Conlon and others, 2005). Irrigation pumping data were estimated on the basis of OWRD water right records and satellite

imagery (Conlon and others, 2005). For water years 1995–96, mean annual groundwater use was more than 400 ft^3/s (about 300,000 acre-ft/yr), with more than 80 percent of withdrawals used for irrigation, about 14 percent for public supply, and about 5 percent for industrial needs (Conlon and others, 2005).

Evapotranspiration

Conlon and others (2005) calculated maximum evapotranspiration (ET) for areas in the Willamette Basin where the water table is less than 10 ft below land surface, an area representing less than 10 percent of the total basin area, with most of the area located in the Southern Willamette subbasin. Most crops grown in this area generally have shallow root zones of 2–3 ft (Bureau of Reclamation, 2013) that do not extend to the water table; therefore, evapotranspiration from the saturated zone is negligible. Evapotranspiration from the saturated zone was not simulated in the model because it is not considered an important component of groundwater discharge in the Willamette Basin as a whole.

Regional Model Parameters

Hydraulic conductivity values (table 3) used in the regional groundwater model were based on aquifer pumping, slug, and permeameter tests; specific capacity data; core analysis; and geothermal modeling (Conlon and others, 2005). Seven regional hydrologic units defined in Conlon and others (2005) and a summary of previous work and new data and analysis provided a distribution of initial values of horizontal hydraulic conductivity for the Willamette Basin. The units of interest in this study are the WSU, USU, MSU, LSU, CRB, and BCU.

Few wells are open to the WSU, which is considered a confining unit due to its low permeability. Recent slug and permeameter tests by Iverson (2002) (Conlon and others, 2005, table 1) supported previous estimates of low horizontal hydraulic conductivity. A larger number of wells are open to the LSU, which is generally described as fine grained, but has interbeds of coarser grained deposits in the Portland subbasin and stringers of sand and gravel in other areas of the Willamette Basin. The LSU is regionally considered a confining unit, but locally considered an aquifer where these sands and gravels occur (Conlon and others, 2005).

Initially, hydrogeologic units in the study area were zoned according to subbasin distribution in the Willamette Basin (fig. 7*A*–*F*); however, preliminary model results justified that only the USU, MSU, and LSU horizontal hydraulic conductivity values should be differentiated between the Portland subbasin and the Tualatin, Central Willamette, and Southern Willamette subbasins (fig. 7*B*–*D*). The basin-fill sedimentary units in the Portland subbasin have relatively low horizontal hydraulic conductivity values compared to their corresponding units in the other basins in the study area (Morgan and McFarland, 1996; Conlon and others, 2005). Hydraulic conductivity values are assumed uniform throughout a particular zone; however, the value of hydraulic conductivity differs between zones. The spatial distribution of vertical hydraulic conductivity zones follows the same pattern as that of the horizontal hydraulic conductivity zones (fig. 7*A*–*F*).

Regional Model Calibration

The Willamette Basin regional steady-state groundwater model was calibrated to average conditions from water years 1995–96 because conditions during this period were reasonably close to long-term average conditions, and much of the data collection for this phase of the study took place during this time. Calibration parameters included recharge and horizontal and vertical hydraulic conductivity. Well pumping was not adjusted during calibration. Although unconfined flow conditions likely exist in the steady-state flow system in some areas, all model layers were simulated as confined to minimize convergence difficulties and instability commonly observed during simulation of low permeability aquifers. Locations where unconfined flow conditions occurred were generally limited to upland areas or outside the area of primary interest. Layer thicknesses are large compared to water level fluctuations in the Tualatin and Portland subbasins, where the WSU is absent as an upper confining layer; therefore, the implicit assumption of constant transmissivity in cells in the model likely does not cause great errors. Modeling all layers as confined is a typical practice to increase numerical stability, and should yield reasonable estimates of water budget and system response (Gannett and Lite, 2004). The steady-state calibration was completed using a combination of trial-and-error methods and the observation, sensitivity, and parameter-estimation process in MODFLOW-2000 (Hill and others, 2000).

Model Parameters

During steady-state model calibration, 34 parameters were defined (10 horizontal hydraulic conductivity, 7 vertical hydraulic conductivity, 6 drain bed vertical hydraulic conductivity, 6 riverbed vertical hydraulic conductivity, and 5 recharge array multipliers), but only 8 of these parameter values were estimated using computer-assisted parameter estimation (table 3). Initial parameter estimates were obtained from published values for the hydrogeologic units (Conlon, 2005, table 1), and either estimated using parameter estimation procedures in MODFLOW-2000, or adjusted manually to improve model fit and to ensure that the groundwater-flow system and processes were reasonably represented. Drain and riverbed vertical hydraulic conductivity parameters were designated on the basis of mapped geology. The five recharge parameters are array multipliers, one for each hydrogeologic unit exposed at land surface (the USU and MSU are considered one unit for recharge estimates) (table A1).

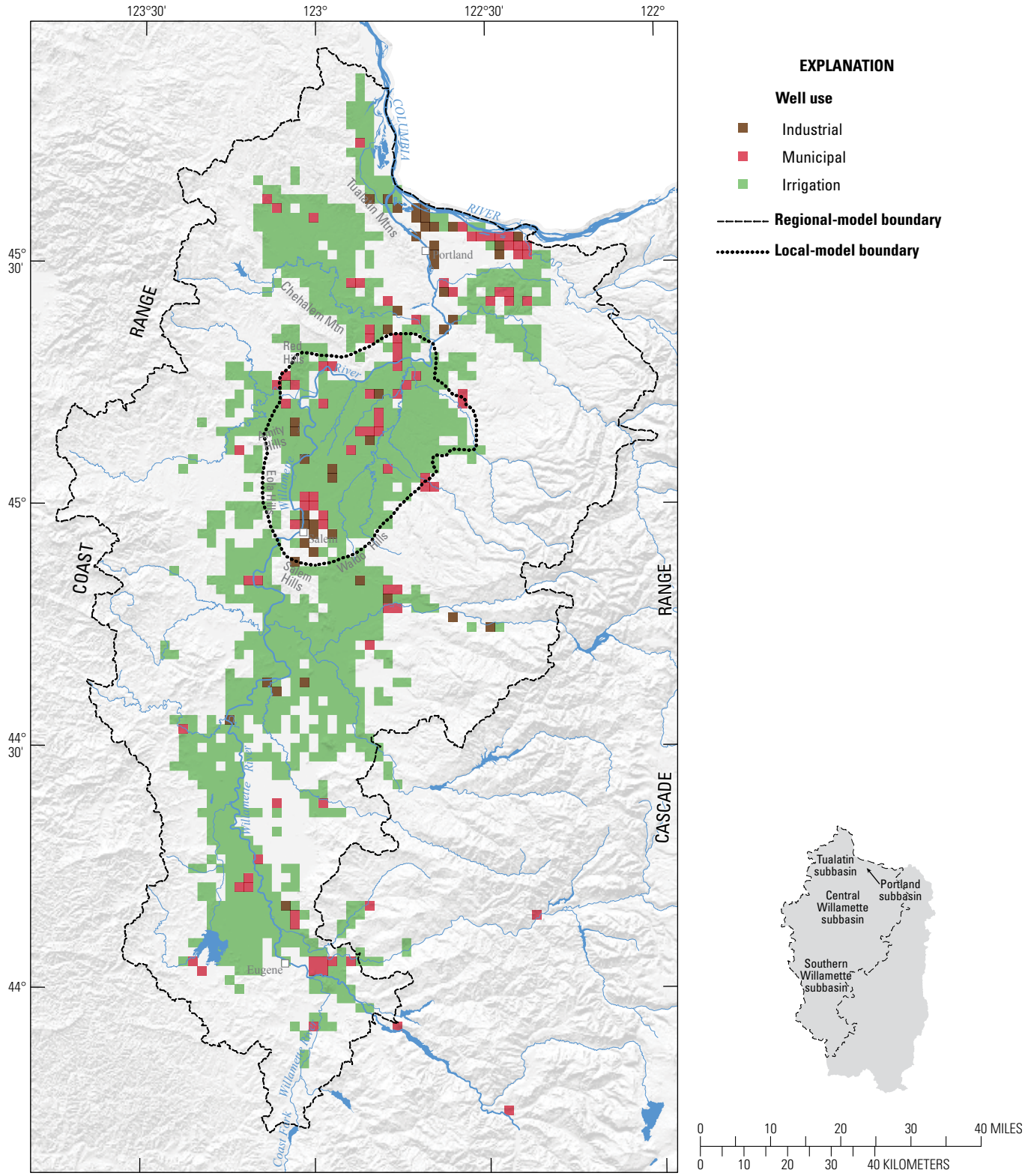

Base map modified from USGS and other digital data sources, various scales. Coordinate system: UTM, Zone 10N, Projection: Transverse Mercator; Datum: North American Datum of 1927.

Figure 6. Regional distribution of average annual industrial, municipal, and irrigation pumping on the model grid, Willamette Basin, Oregon, water years 1995–96.

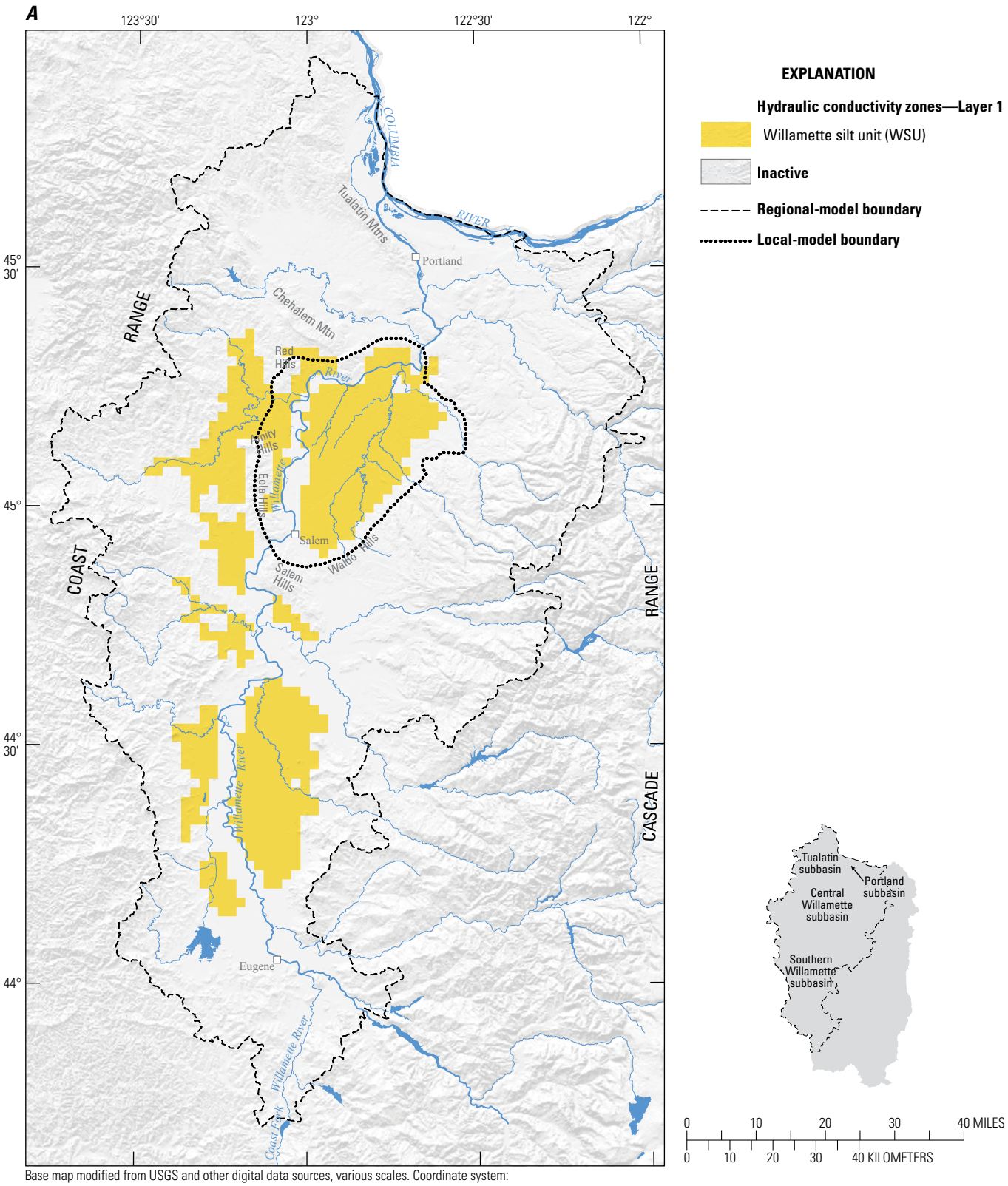

Base map modified from USGS and other digital data sources, various scales. Coordinate system: UTM, Zone 10N, Projection: Transverse Mercator; Datum: North American Datum of 1927.

Figure 7. Hydraulic conductivity zones and extents for all model layers: (*A*) layer 1 (Willamette silt unit), (*B*) layer 2 (upper sedimentary unit/middle sedimentary unit), (*C*) layer 3 (upper sedimentary unit/middle sedimentary unit), (*D*) layer 4 (lower sedimentary unit), (*E*) layer 5 (Columbia River basalt unit), (*F*) layer 6 (basement confining unit), Willamette Basin, Oregon.

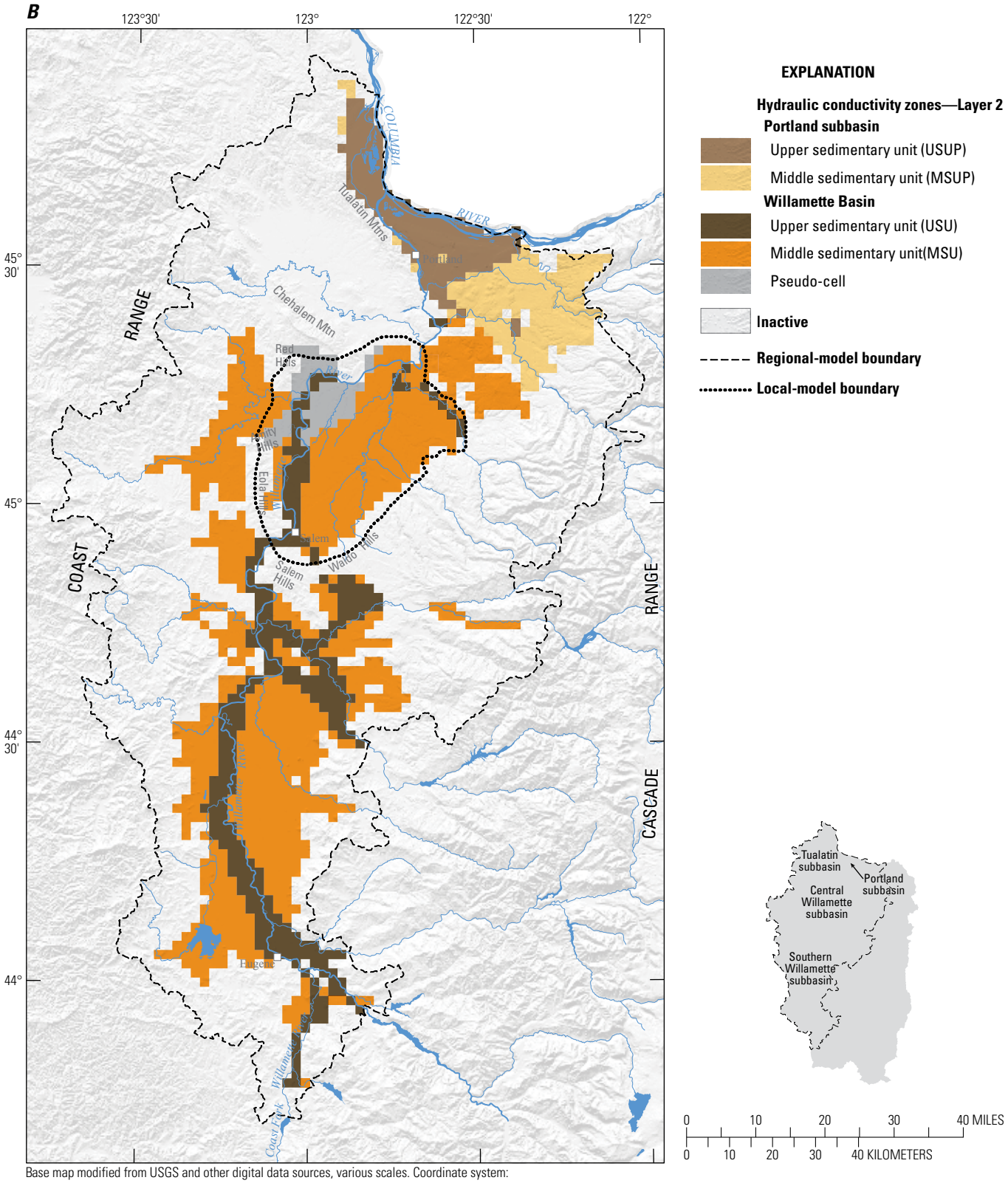

Base map modified from USGS and other digital data sources, various scales. Coordinate system: UTM, Zone 10N, Projection: Transverse Mercator; Datum: North American Datum of 1927.

Figure 7.—Continued

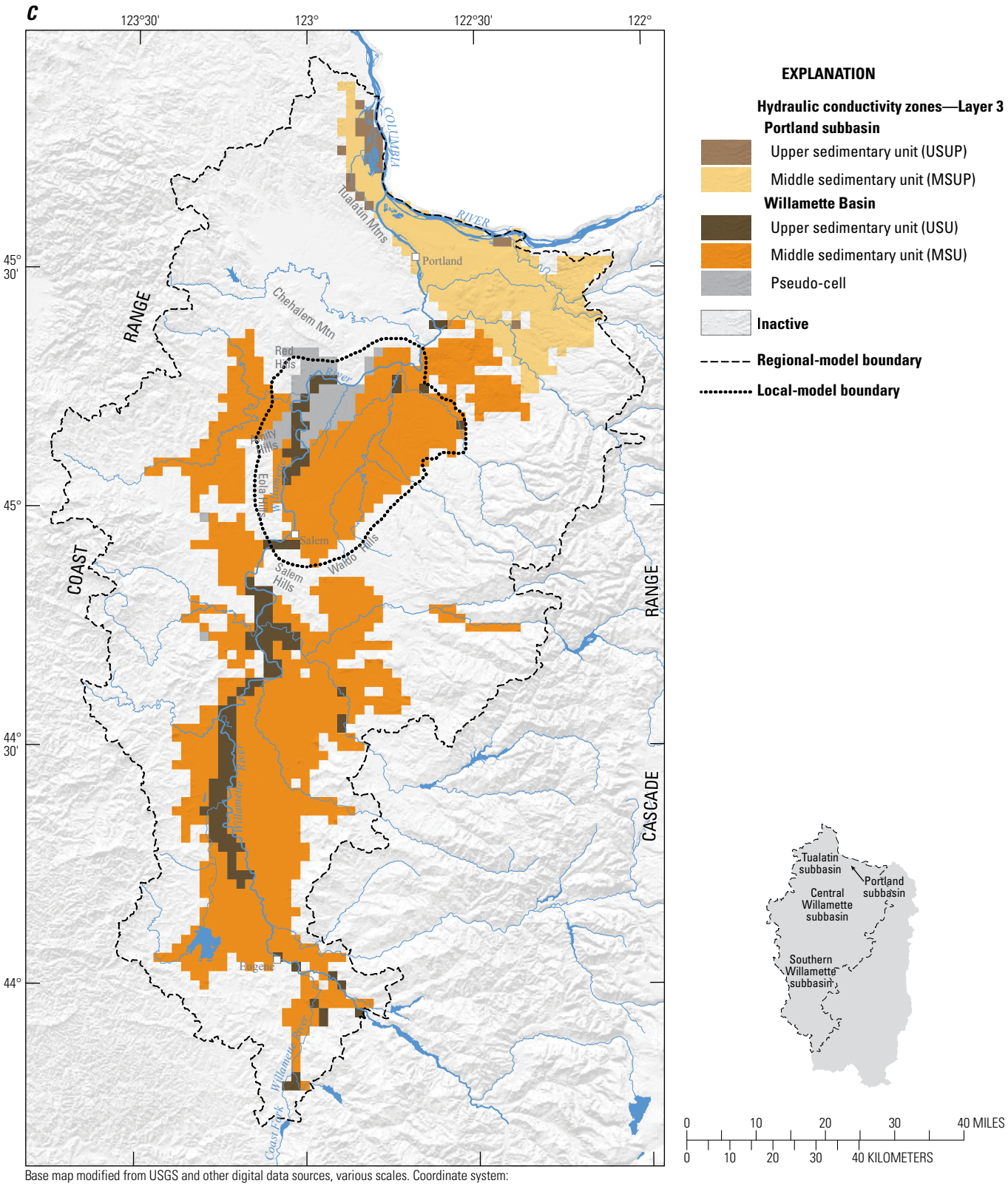

Base map modified from USGS and other digital data sources, various scales. Coordinate system: UTM, Zone 10N, Projection: Transverse Mercator; Datum: North American Datum of 1927.

Figure 7.—Continued

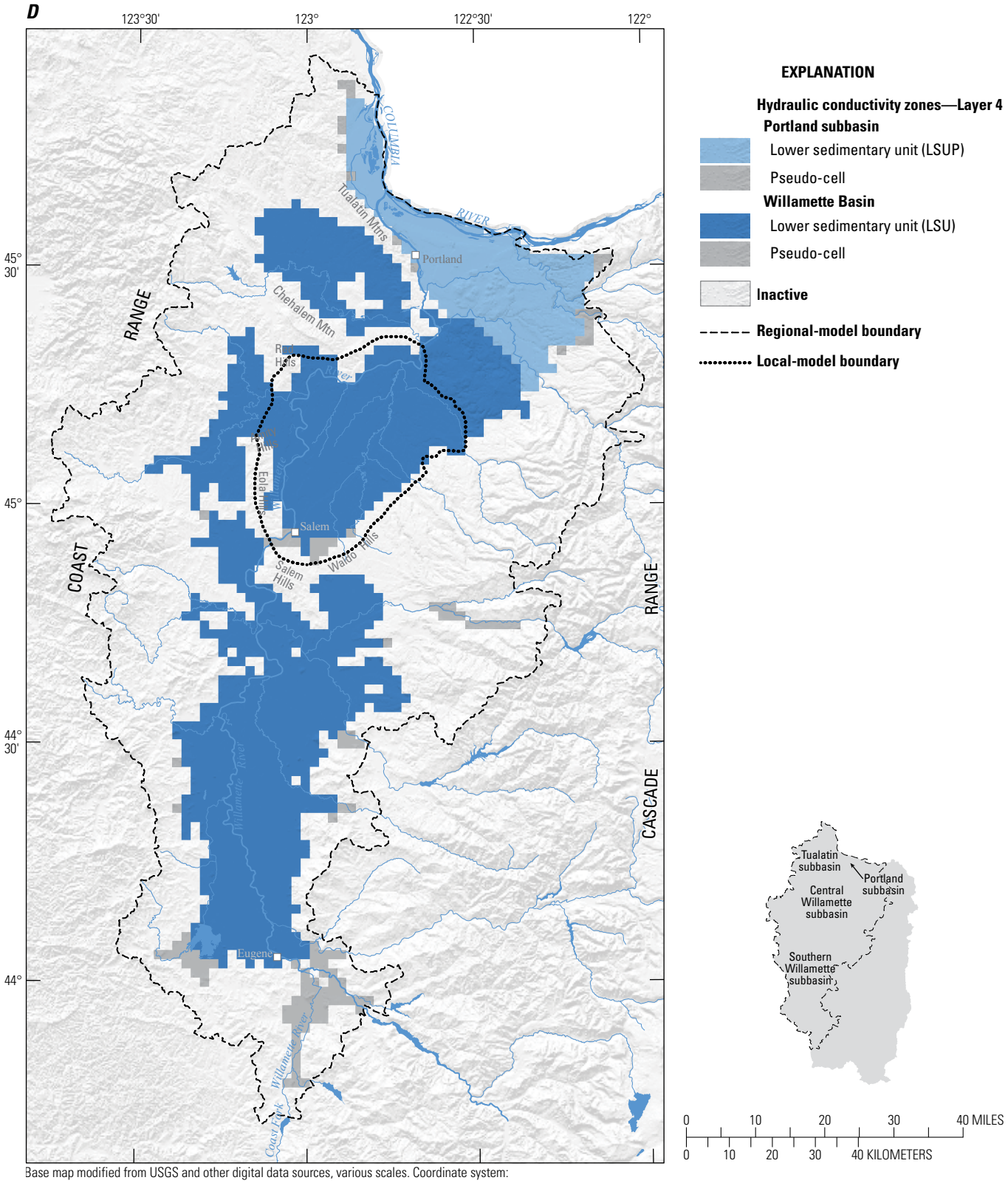

Base map modified from USGS and other digital data sources, various scales. Coordinate system: UTM, Zone 10N, Projection: Transverse Mercator; Datum: North American Datum of 1927.

Figure 7.—Continued

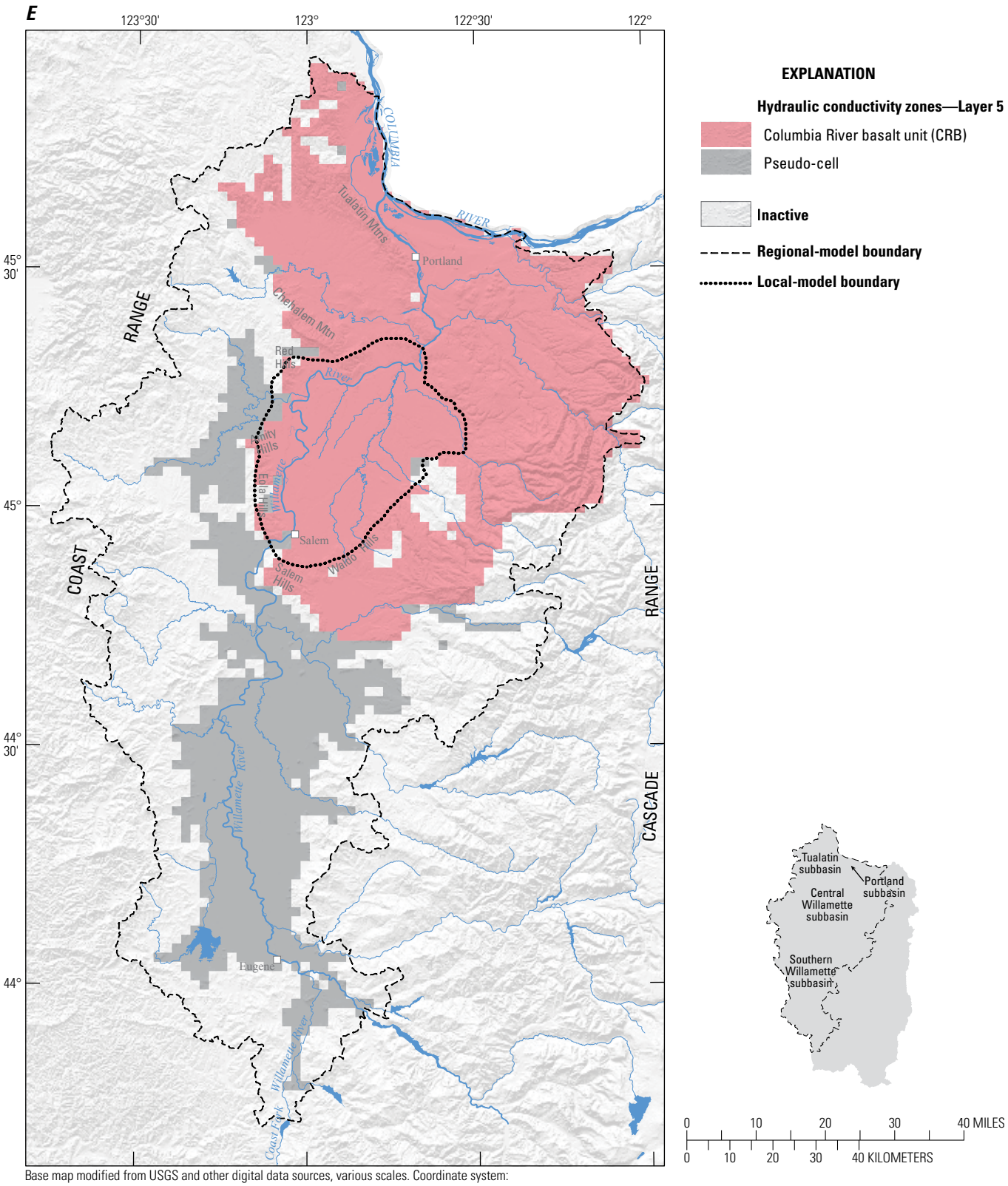

Base map modified from USGS and other digital data sources, various scales. Coordinate system: UTM, Zone 10N, Projection: Transverse Mercator; Datum: North American Datum of 1927.

Figure 7.—Continued

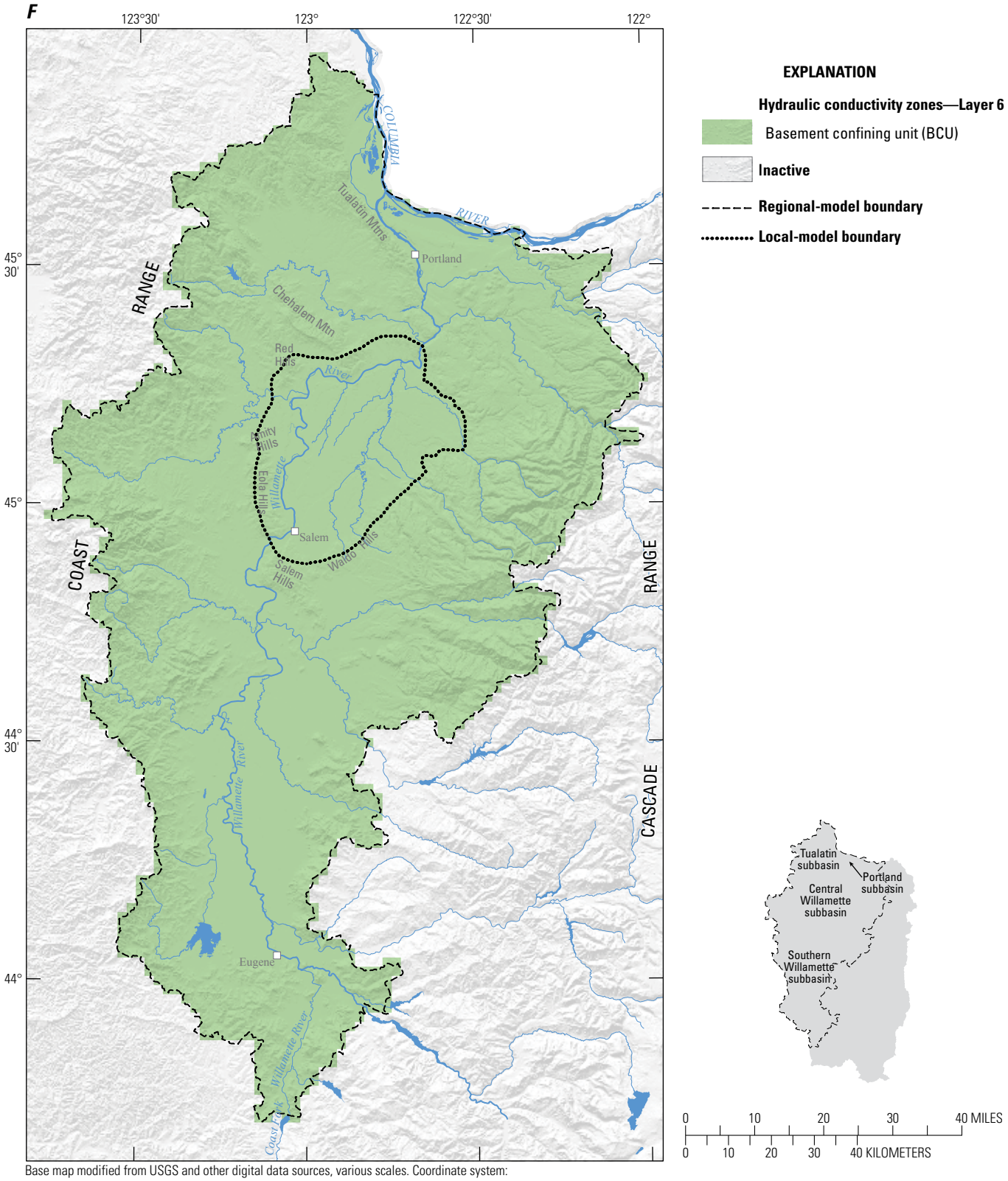

Base map modified from USGS and other digital data sources, various scales. Coordinate system: UTM, Zone 10N, Projection: Transverse Mercator; Datum: North American Datum of 1927.

Figure 7.—Continued

During the initial calibration, horizontal hydraulic conductivity parameters for each hydrogeologic unit were zoned by basin; however, as the calibration progressed, it became evident that some basin-specific hydraulic conductivity parameters were relatively insensitive and could not be determined using parameter estimation. Hydraulic conductivity parameters for each hydrogeologic unit were combined and converted to uniform basinwide values, with the exception of the Portland subbasin. Separate horizontal hydraulic conductivity parameters were designated for the USU, MSU and LSU in the Portland subbasin. Vertical hydraulic conductivity parameters values are uniform basinwide for each hydrogeologic unit. Final estimated parameters included the horizontal and vertical hydraulic conductivity of the LSU, CRB, and BCU, and the horizontal hydraulic conductivity of the MSU and MSUP (fig. 8).

Parameter Sensitivity

The sensitivity process in MODFLOW-2000 was used to calculate composite scaled sensitivities (CSS) for 34 parameters (fig. 8). CSS values are a measure of the amount of information that calibration data provides about the parameter. Parameters with relatively low CSS generally cannot be estimated by regression and are set to reasonable values on the basis of model results and previous studies. Although the CSS of recharge parameters were high relative to the others, the relatively high correlation between recharge and horizontal hydraulic conductivity parameters and inadequate spatial coverage of regional groundwater discharge measurements to act as a constraint for recharge rates precluded the use of the parameter estimation process to estimate recharge parameters. Additionally, recharge values

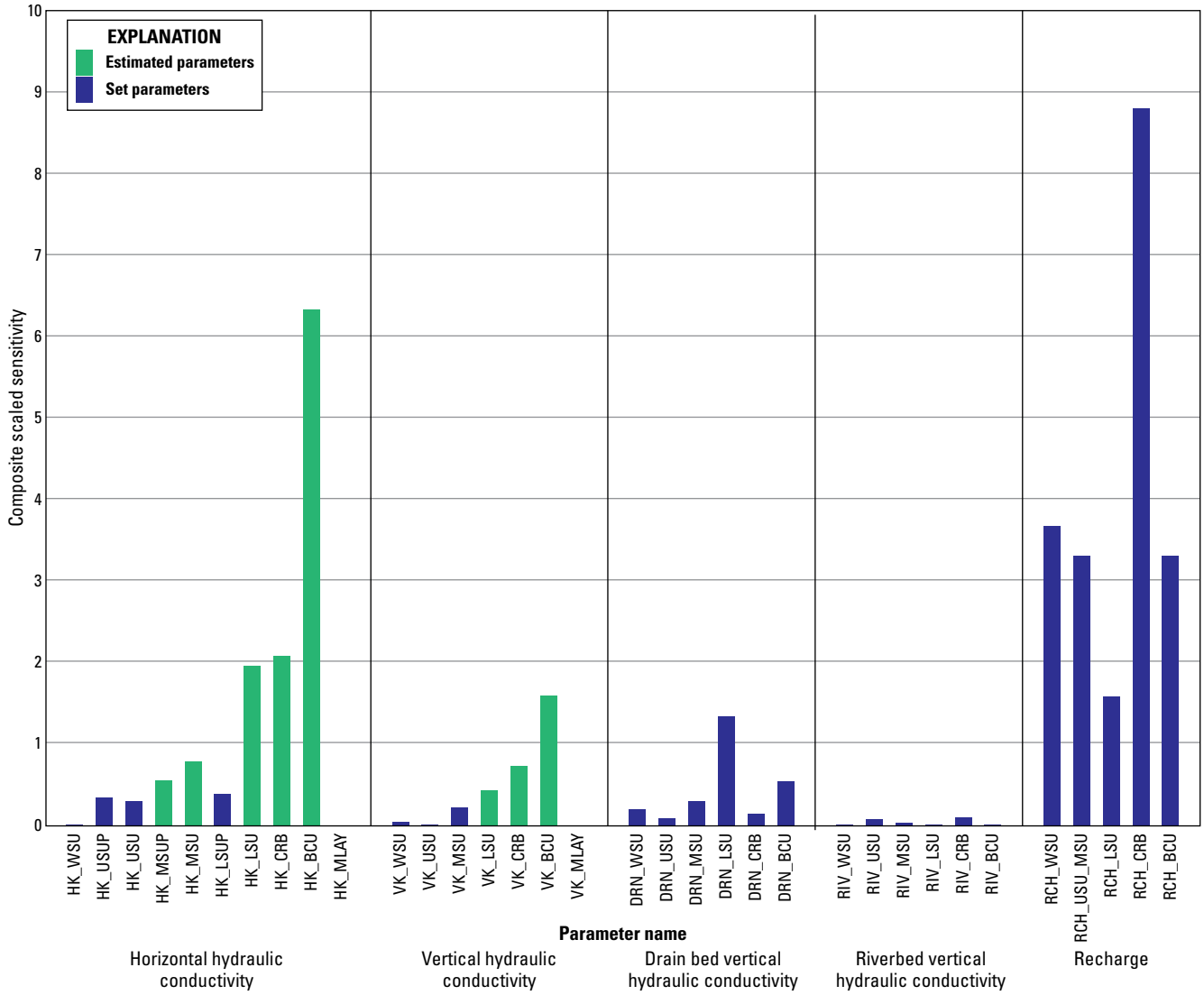

Figure 8. Composite scaled sensitivities of steady-state parameters for the Willamette Basin, Oregon. Parameter names are defined in the section "Abbreviations and Acronyms."

for the Willamette Basin were based on PRMS assumptions, which did not reflect groundwater flow in parts of the model (appendix A). Therefore, the recharge rates were set using the procedure described in appendix A, and only the sensitive horizontal and vertical hydraulic conductivity parameters were calibrated through the inverse (parameter estimation) method.

Measurements Used in Model Calibration and Fit

Water-level measurements from 488 observation wells were used to calibrate the model. Measurement frequencies ranged from once during the study (318 wells) to quarterly (49), bimonthly (84), or hourly (using recorders; 37) (fig. 9; appendix B, table B1). Observation wells are simulated as open to one unit. Model units, except the WSU and the USU, are equally represented. The water-level data are uniformly distributed throughout the study area, excluding the Portland subbasin. Approximately one-third of these measurements are mean annual water levels calculated using data from bimonthly, quarterly, and recorder wells; however, most water-level measurements were made during, or near to, November 1996 to produce a synoptic measurement of water-level conditions throughout the Willamette Basin. November water-level measurements generally provide examples of water levels at the low point of the water year, without the influence of summer pumping and subsequent drawdown, and prior to recharge from autumn rains and recovery from summer pumping.

Because some measurements are assumed to provide a better characterization of mean annual water levels, measurements were weighted based on the accuracy of monitor-well location and water-level elevation, frequency of measurement, amplitude of seasonal fluctuation, and hydrogeologic unit. Water levels from wells measured with recorders, bimonthly, quarterly, or measured once (during the synoptic-measurement period) were assigned different weights, ranging from synoptic-measurement wells with relatively lower weight to recorder wells with relatively higher weight. Water-level measurements were also weighted according to the method of determining elevation, the seasonal fluctuation of the water level, and the unit type in which the well was completed. Wells measured only during the synoptic-measurement period were assigned a standard deviation of 10 ft. An additional 10 ft was added to the calculated or assigned scaled standard deviation for all wells located in the BCU to decrease the influence of these water-level measurements on the regression.

Base-flow estimates from Lee and Risley (2001) at 27 streamflow-gaging stations (fig. 9 and appendix B, table B2) used for calibration were derived by PART (Rutledge, 1998), a "streamflow partitioning" computer program to estimate base flow on unregulated streams. In addition to the spatial bias observed in the PRMS-derived estimates of recharge (see section "Final Parameter Values" and appendix A), PART and PRMS use different methods to calculate base flow, and PART-derived base-flow estimates are systematically higher than PRMS-derived estimates by a factor of 1.9. Base flow and recharge are correlated, which means that using PART base flow and PRMS recharge estimates will result in a water budget shortfall for recharge. To correct for this imbalance, PART base-flow targets were divided by 1.9 to align them with PRMS recharge estimates (appendix A). Base flow targets were weighted by estimating standard deviations of measurement errors on the basis of the mean annual base flow volume, stream regulation, and the status (active or inactive) of the gaging station during water years 1995–96 (table B2). Additional independent estimates of the Willamette River flow upstream of Salem and at Portland derived by base-flow separation methods were used as a check on simulated base-flow estimates (table B2).

Particle tracking using MODPATH (Pollock, 1994) was used as an independent check of estimated model parameter values. Groundwater age estimated from CFC (Conlon and others, 2005, appendix B) compared with groundwater-flow model simulated advective travel times for flow in the Southern Willamette subbasin showed good agreement between the independent methods of estimating groundwater age (table 4).

Because CFC samples generally are collected from wells with screen intervals that are much shorter than the thickness of each groundwater-flow-simulation model cell thickness, the CFC estimate of age should be within the range of advective travel times simulated between the top and bottom of the flow-simulation model cell representing the well sampled. To simulate the range of travel times, the paths of 100 particles between the model cell top and bottom were simulated using reverse particle tracking in MODPATH, a MODFLOW post processor (Pollock, 1994). Two estimates of porosity were used for particle tracking (table 4) to show that a range of reasonable values of porosity (Conlon and others, 2005) yields travel times that agree with CFC ages.

CFC samples were collected from 15 wells in October 1996 (Conlon and others, 2005). Groundwater age estimates from CFC data can be complicated by various factors, including preferential flow of groundwater through heterogeneous geology, mixing of groundwater of different ages in the well borehole, and enhanced vertical flow of groundwater through wells that are open to multiple aquifers. Groundwater age estimates were made for 9 of the 15 samples. Four additional samples had negligible amounts of CFC, indicating that the water was older than 57 years (before the ubiquitous use of CFCs). The age of the two remaining samples could be narrowed only to a range of years.

For 13 samples, the range of predicted travel times using MODPATH spans the CFC age estimate (or part of the estimated range of ages from the CFC data) for one or both estimates of porosity distributions (table 4). One of the remaining samples (443500123105001) has an estimated CFC age that is close to the narrow range predicted by MODPATH,

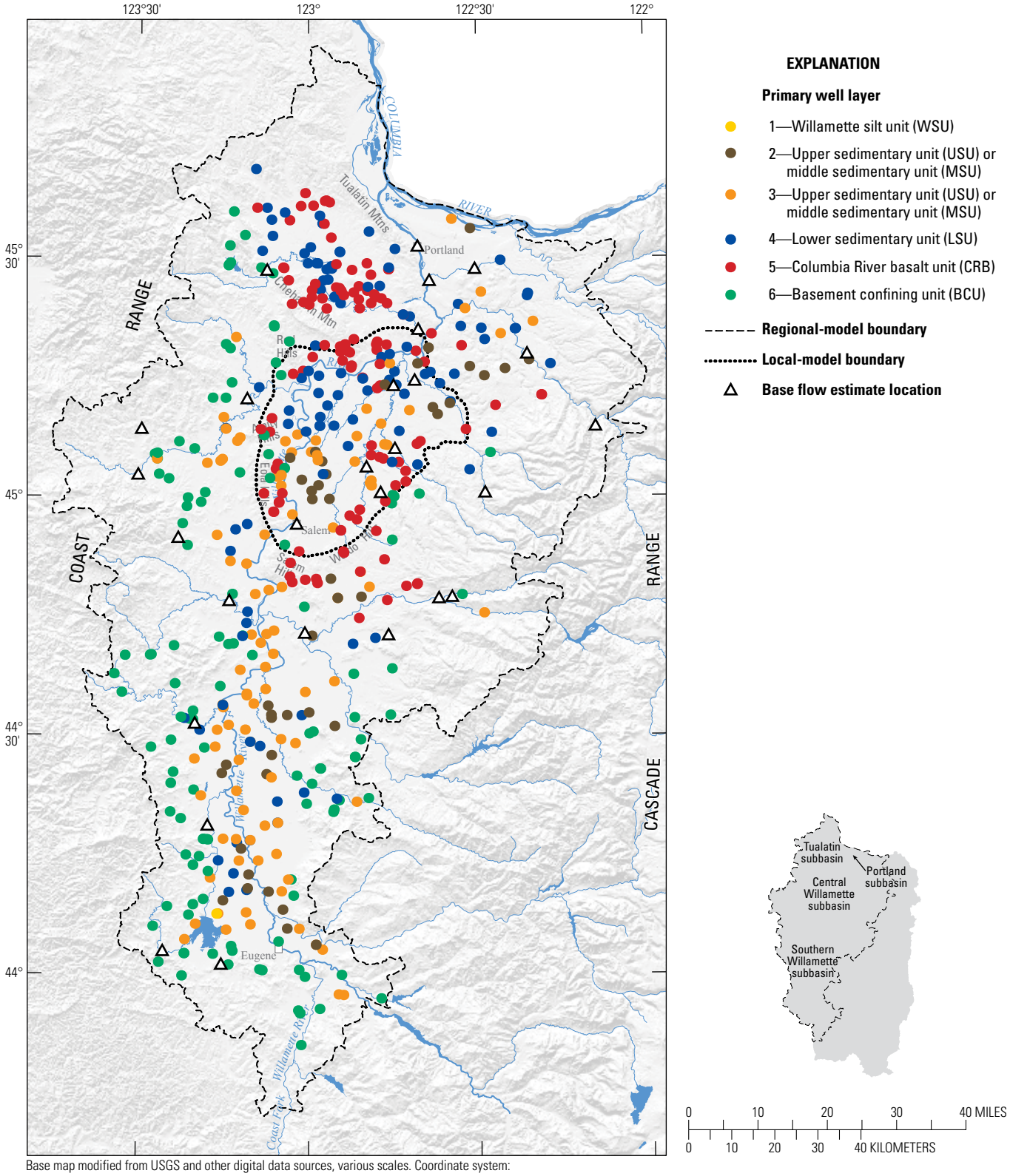

Base map modified from USGS and other digital data sources, various scales. Coordinate system: UTM, Zone 10N, Projection: Transverse Mercator; Datum: North American Datum of 1927.

Figure 9. Observation well and base flow estimate locations used to calibrate the regional steady-state groundwater-flow model of the Willamette Basin, Oregon.

Table 4. Estimated chlorofluorocarbon groundwater age and simulated travel times for flow in the Southern and Central Willamette subbasins of the Willamette Basin, Oregon, from samples collected in October 1996.

[**Abbreviations:** OWRD, Oregon Water Resources Department; USGS, U.S. Geological Survey; CFC, chlorofluorocarbon; GW, groundwater; LSU, lower sedimentary unit; MSU, middle sedimentary unit; WSU, Willamette silt unit; <, less than; >, greater than]

OWRD well log identifier	USGS site identification No.	Unit	Assigned model layer	CFC GW age estimate (years)	Time of travel of particles (years)					
					Porosity = 0.3 for all units			Porosity = 0.5 for WSU and 0.3 for all other units		
					Median	Minimum	Maximum	Median	Minimum	Maximum
LINN 50853	443232123034501	MSU	2	24	30	10	52	36	16	57
LINN 10391	443252122595301	MSU	2	25	28	6	46	33	9	50
LINN 4146	443512123105001	MSU	3	26	19	18	21	26	24	27
LINN 50103	443211123062901	MSU	2	36	33	11	64	40	18	71
LINN 14280	443500123105001	MSU	3	37	26	25	28	33	32	35
LINN 8753	443358123093601	MSU	3	40	39	26	57	45	32	63
LINN 50097	443343123070501	MSU	2	0<Age<57	33	11	88	40	18	95
LINN 50852	443234123063101	MSU	2	16<Age<57	33	11	64	40	18	71
LINN 8756	443352123090401	MSU	3	>57	382	379	386	385	382	389
YAMH 50041	450531123025901	MSU	3	23	16	12	20	19	15	24
MARI 4092	450248122572601	LSU	4	43	461	136	>1,000	476	155	>1,000
MARI 17239	450535122593201	MSU	3	51	56	47	68	78	69	90
MARI 3266	450200122485301	MSU	3	>57	41	28	55	45	33	59
MARI 17263	450432122582001	MSU	2	>57	44	36	57	69	60	81
MARI 3054	450423122514701	MSU	3	>57	126	88	143	148	114	167

indicating that CFC and MODPATH ages are in reasonable agreement and that model grid coarseness or CFC analytic complications might explain the disagreement between the estimates. The final sample (450248122572601) shows poor agreement between CFC and MODPATH estimated ages; however, the disagreement indicates that water is arriving at the well by some preferential fast flow path that is not captured by the flow model, which is possible given the geologic heterogeneity of the system. Overall, agreement of CFC and MODPATH results indicates that the groundwater-flow simulation model parameters are reasonable.

The MODPATH simulations tested the assumption that base-flow estimates from PART should be modified. Vertical flow through the WSU is controlled by the prescribed flux recharge boundary condition. Because travel time through the WSU is long for many of the CFC flow paths, the simulated travel times are sensitive to the estimated WSU porosity. For this reason, a higher silt and clay porosity value for the WSU (porosity = 0.5) was tested (table 4) to evaluate the uncertainty associated with the WSU porosity estimate. This observation was the reason WSU porosity was increased to a reasonable silt and clay porosity of 0.5 for the second MODPATH simulation with all other units held constant at 0.3 (table 4). Core porosity measurements from Price (1967a) and Wilson (1997) indicated that porosities range from 20 to 45 percent for the WSU. Using the porosity values of 0.3 (all sedimentary units), and 0.5 (WSU) and 0.3 (other sedimentary units) values, the calibrated model provided a median and range of values of travel times from particle tracking consistent with most of the isotopic data (table 4). Further, because the MODPATH predicted travel times were sufficiently sensitive to porosity, a reasonable calibration to most estimated travel times could occur by varying only porosities through a range of reasonable values. The general good agreement between CFC and MODPATH travel times for a range of common silt porosity values indicates that recharge estimates also are reasonable, supporting the decision to adjust the PART calibration targets downward rather than increasing recharge (appendix A). If recharge had been increased by the PART correction factor of 1.9, then MODPATH estimated ages would be approximately one-half of the values reported in table 4, indicating that far fewer of the CFC ages would be within the span of predicted MODPATH travel times.

Final Parameter Values

The final values for horizontal and vertical hydraulic conductivity, drain and riverbed vertical hydraulic conductivity, and recharge parameters in the steady-state calibration are shown in table 3. Parameter values not estimated during regression were fixed using trial-and-error and data from previous studies (Freeze and Cherry, 1979; Conlon and others, 2005, table 1) that were reasonable prior to the final estimation of other parameters. Expected ranges presented in figure 10 were determined from previous studies and summarized in Conlon and others (2005, table 1). To test model linearity, 95-percent linear confidence intervals were calculated using MODFLOW-2000 output and

post-processing program BEALE-2000. Linear confidence intervals reflect the reasonableness of the parameter values (Hill, 1998). A relatively small confidence interval range indicates that available data constrained parameter estimates. The similarity between estimated parameter values, linear confidence intervals, and range of expected values indicates how well parameter values reflect independent hydrogeologic information.

Horizontal hydraulic conductivity for the fine-grained WSU was set to 1 ft/d, which is within the range of hydraulic conductivity values in Freeze and Cherry (1979) and Bureau of Reclamation (1985) for silt to silty sand. Horizontal hydraulic conductivity for the unconsolidated sands and gravels of the USU was set to 600 ft/d, which is within the range of hydraulic conductivity values in Freeze and Cherry (1979), and Fetter (1994) for clean sand to gravel. The ratio of horizontal to vertical hydraulic conductivity (vertical anisotropy) was set to 100 for the WSU and to 1,000 for the USU. Limited water-level measurements collected in the WSU and USU resulted in relatively low sensitivity values (fig. 8) and the inability of the model to estimate WSU and USU parameter values. Parameter values were estimated for horizontal hydraulic conductivity for the MSU; and, a horizontal to vertical hydraulic conductivity ratio of 3,600 was set for the MSU in areas outside of the Portland subbasin because the unit typically becomes more compacted and cemented with depth (Conlon and others, 2005).

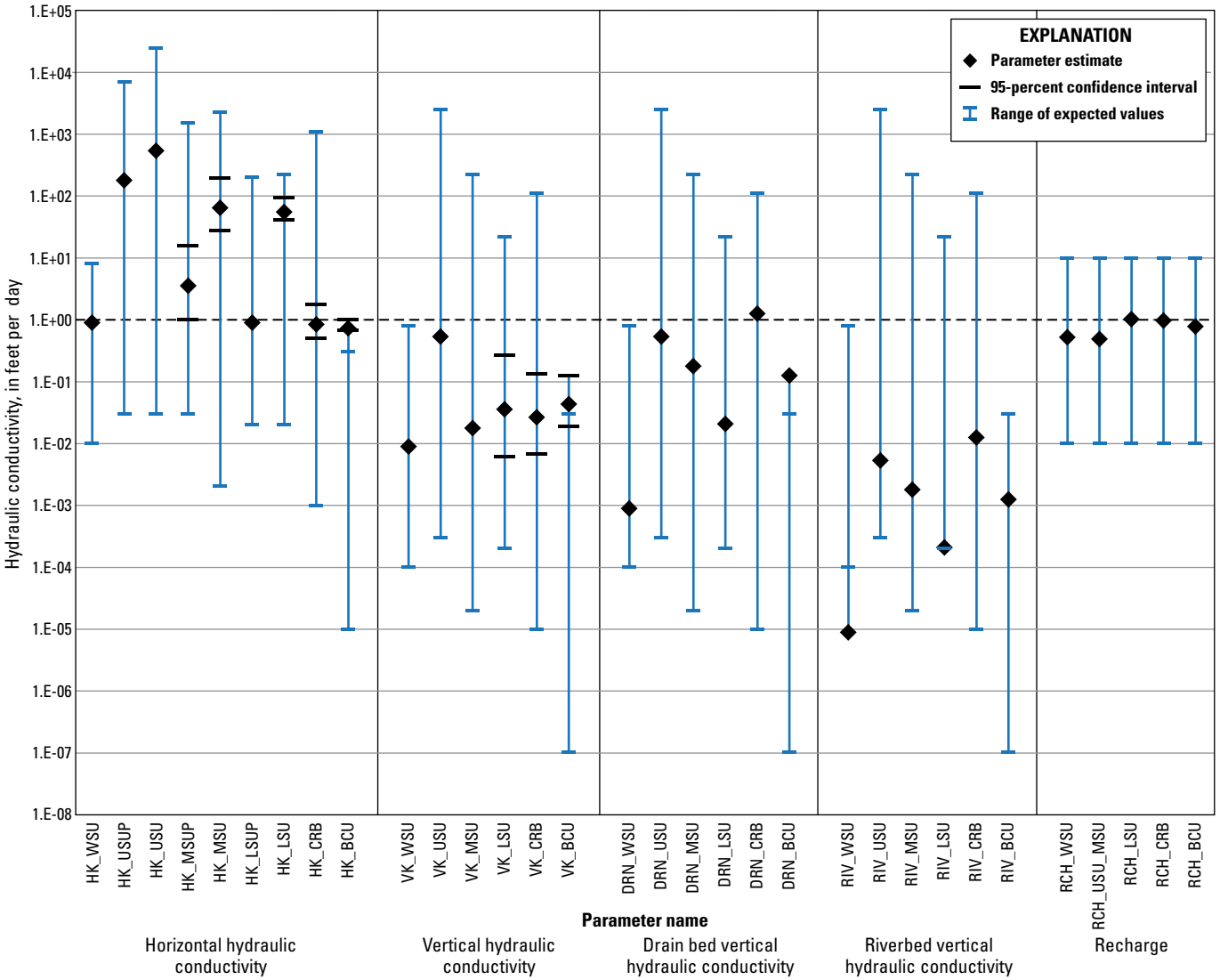

Figure 10. Final estimated parameter values for the regional steady-state model of the Willamette Basin, Oregon. The range of expected values is based on previously published estimates of each parameter (Conlon and others, 2005). Linear confidence intervals were computed only for those parameters that were estimated using computer-assisted calibration methods. Parameter names are defined in the section "Abbreviations and Acronyms."

Additionally, the relatively small number of water-level measurements from wells in the Portland subbasin resulted in low sensitivity values (fig. 8), so parameter values for the upper and lower sedimentary units in the Portland subbasin (USUP and LSUP, respectively) could not be estimated uniquely using computer-assisted methods. These horizontal hydraulic conductivity values were set to 200 and 1 ft/d, respectively (table 3). Relatively lower parameter values for the Portland subbasin than for the rest of the Willamette Basin were based on hydraulic conductivity values from an earlier Portland subbasin study (McFarland and Morgan, 1996, and Morgan and McFarland, 1996). The vertical hydraulic conductivity values for the upper, middle, and lower sedimentary units are generally uniform in the Portland subbasin and the Willamette Basin and result in horizontal to vertical hydraulic conductivity ratios of about 350, 200, and 25, respectively.

Although the LSU often is described as clay, it primarily has a fluvial origin, and wells completed in this unit generally are completed in coarser river channel deposits. Variations in horizontal hydraulic conductivity can range more than two or three orders of magnitude in fluvial depositional areas (Freeze and Cherry, 1979); however, the size and scale of the model cells in the regional model and the lack of location data on the coarse grained deposits preclude separating the LSU into separate hydraulic conductivity zones associated with the relatively fine and coarse grained materials. As a result, the estimated horizontal hydraulic conductivity represents an average for the LSU. In an aquifer with deposits of significantly differing hydraulic conductivity values, the presence of relatively high and low permeability materials can affect groundwater-flow subsystems in a regional basin. The more permeable materials act as the primary conduit for groundwater flow (Freeze and Witherspoon, 1967) and produce a relatively high hydraulic conductivity value.

Horizontal and vertical hydraulic conductivity values for the CRB were estimated to be 1 and 0.03 ft/d (table 3). These values are within the expected range of values from Conlon and others (2005, table 1), and are reasonable values for the CRB. Horizontal and vertical hydraulic conductivity values for the BCU were estimated to be 0.8 and 0.05 ft/d. These values are slightly higher than the expected range of values from Conlon and others (2005, table 1); however, previous studies on the BCU represent limited areas and methods of analysis. The estimated horizontal hydraulic conductivity is within the same order of magnitude as reported in Gonthier (1983), and is a reasonable value for the BCU.

All final parameter values and confidence intervals were within the range of expected values for each parameter except parameters for the BCU. Few data are available for the BCU (Conlon and others, 2005); however, the upper end of the range of expected values for the unit is within, or overlaps, the same order of magnitude as the final parameter value and confidence interval.

Model Fit

The ability of the model to simulate measured conditions, model "fit," is evaluated by using residuals. Residuals are the difference between the measurements and the simulated equivalents. Weighted residuals are residuals weighted for measurement error. Measurements expected to be more accurate have higher weights, whereas measurements expected to be less accurate have lower weights. Weighted residuals should be independent, random, and normally distributed; the independence and randomness can be assessed by plotting them against weighted simulated values (Hill and Tiedeman, 2007). The weighted residuals ideally will be evenly distributed about zero, with no discernible pattern or trend in the data. In a normal distribution of residuals, about 68 percent of the residuals are within one standard deviation of the mean, and 95 percent are within two standard deviations of the mean. Weighted residuals shown in figure 11 meet these criteria. Outliers are (1) generally representative of layers 5 and 6, where a wide range of groundwater level measurement values are difficult for the computer model to simulate or (2) heavily weighted measurements in the sedimentary units with relatively small unweighted residuals and relatively large weighted residuals (fig. 11). Weighted residuals also can provide a means to determine model error and can be more reliable than unweighted residuals in indicating a poor model fit (Hill and Tiedeman, 2007).

Smaller values of calculated error variance (the sum of squared residuals divided by the number of measurements minus the number of parameters) and standard error of the regression (the square root of the error variance) also indicate a better fit to the measurements. Although the calculated error variance and standard error should be near or equal to 1.0, they are normally greater than 1.0. The Willamette Basin regional steady-state model has a calculated error variance equal to 60.7 and a standard error equal to 7.8 (fig. 11). Error measures are significantly affected by measured groundwater-level values in layers 5 and 6 (CRB and BCU). In the upland areas, steep horizontal gradients resulting from wells that are completed at different depths and open to different interflow zones (more indicative of a large vertical gradient) present a wide range of water-level values over relatively small areas, which are difficult for the computer model to simulate. Another measure of model fit is the fitted standard deviation, which is the product of the standard deviation and the standard error of the regression. For example, the standard deviation for most groundwater-level

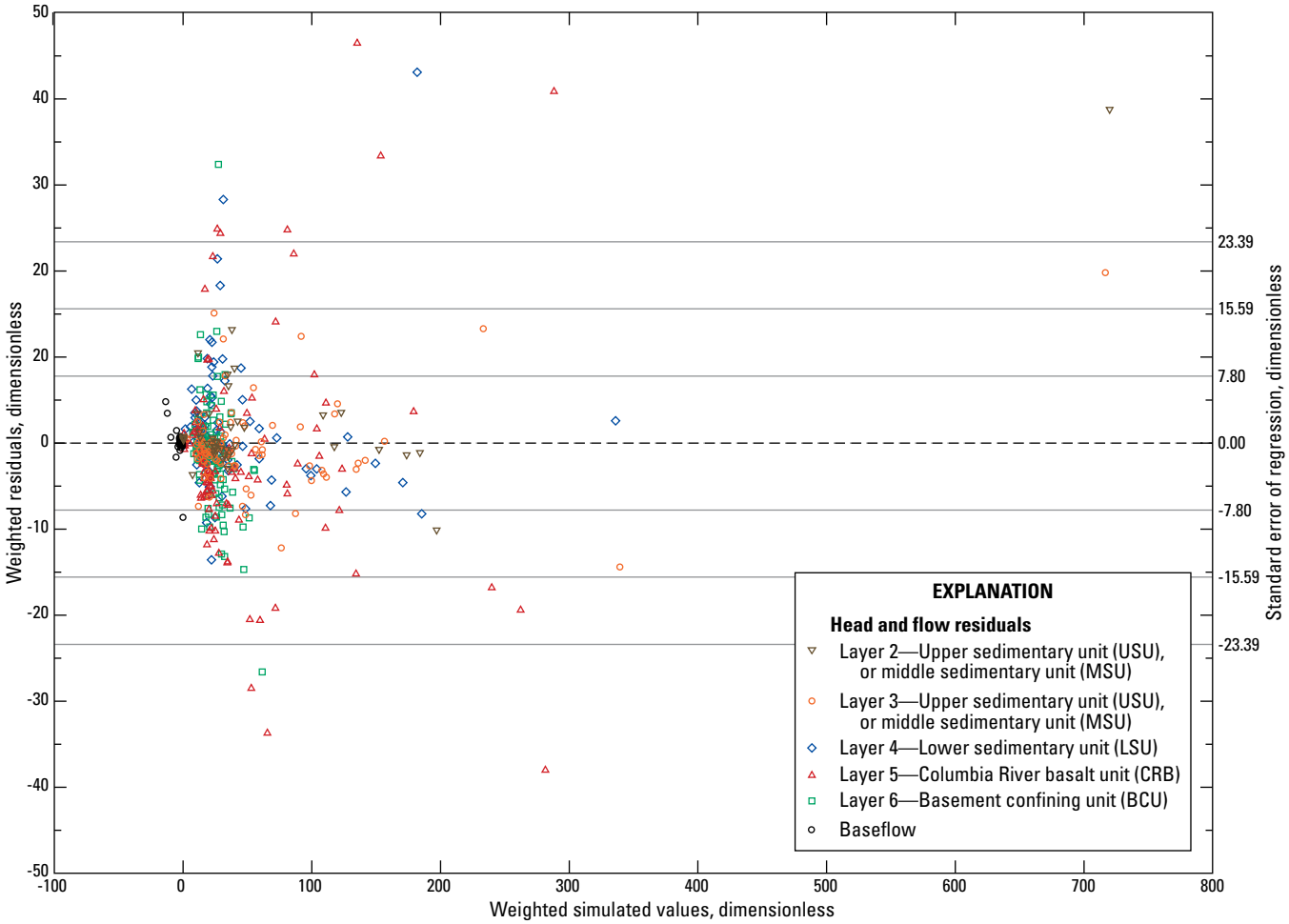

Figure 11. Weighted steady-state residuals as a function of weighted simulated values in the regional model of the Willamette Basin, Oregon.

measurements made during the synoptic measurement is 10 ft because most of these wells were measured only once, and data were not available to assign error on the basis of seasonal groundwater-level fluctuations; therefore a fitted standard deviation for the synoptic-measurement wells is approximately equal to 78 ft and represents the overall fit of the groundwater-level measurements (Hill and Tiedeman, 2007).

Comparison of Simulated and Measured Regional Steady-State Model Hydraulic Heads

A simple method of assessing overall model fit is shown in figure 12. The simulated steady-state hydraulic head values are plotted against the measured water levels to show fit by comparison to a 1:1 line. Hydraulic head values in layers 2, 3, and 4 (USU, MSU, and LSU) generally closely match and cluster around the 1:1 line at relatively low water levels. Hydraulic head values in layers 5 and 6 (CRB and BCU) generally have an increasingly wide scatter as measured water levels and simulated hydraulic heads increase in value. The scatter shows the difficulty of simulating hydraulic heads in a single hydrogeologic unit where water level measurements are from wells completed at different depths and open to different interflow zones. Decreasing head with depth results in large vertical gradients in upland areas in a regional model that has large cell sizes. The regional model may not accurately simulate head variation over short distances because of the large cell sizes in the regional model. Because pumping effects can be localized, they might not be evident in a regional model.

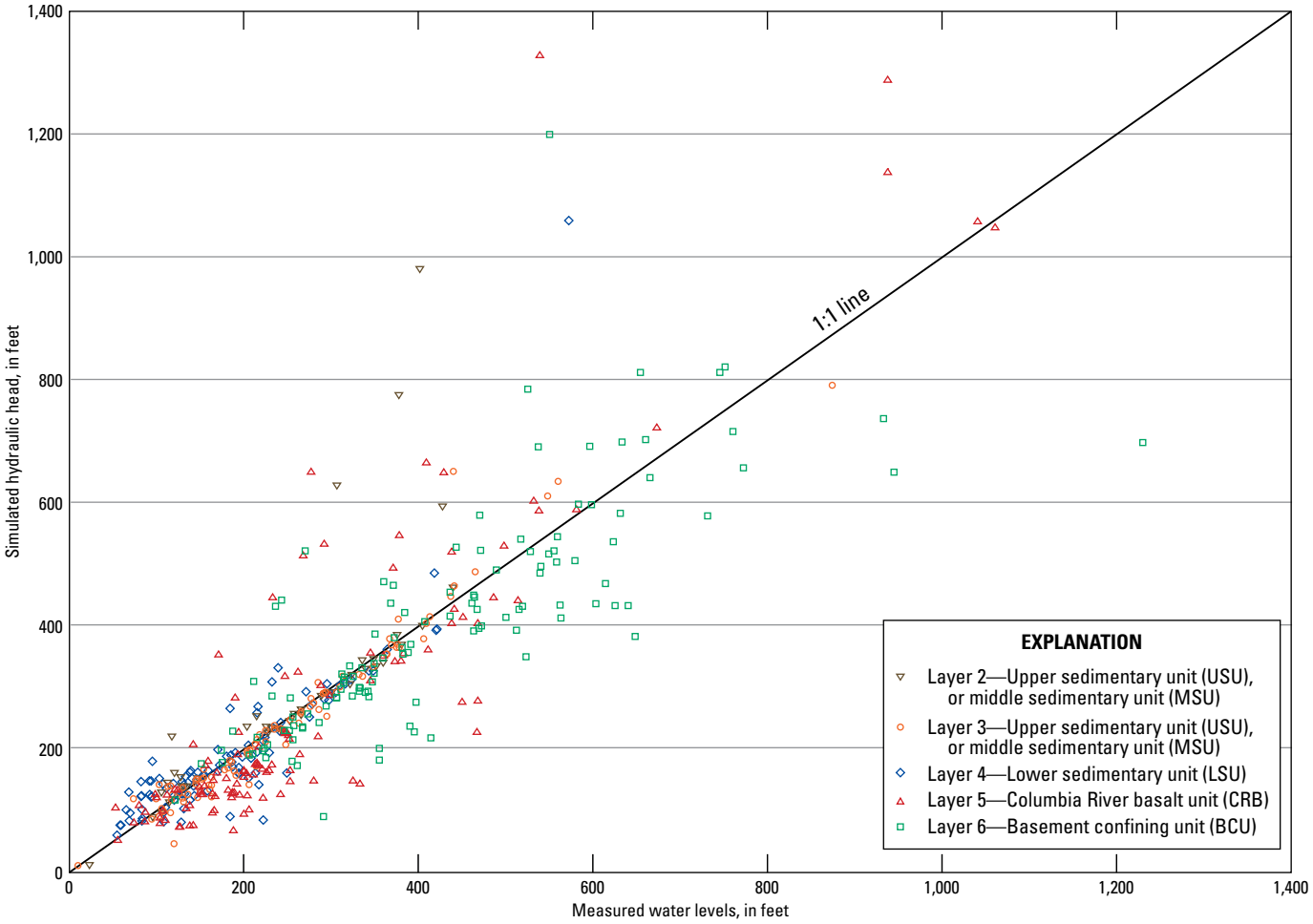

Figure 12. Comparison of simulated hydraulic head values with measured water levels for the regional steady-state model of the Willamette Basin, Oregon.

Model fit was evaluated using maps that show residuals at observation well locations, by assessing the simulated flow direction using maps of simulated hydraulic head in each layer (fig. 13*A*–*F*), and using a generalized water-table map for the Willamette Basin from Conlon and others (2005, pl. 1) (fig. 14) to visually evaluate the simulated heads for the uppermost basin-fill sedimentary units (WSU, USU, MSU, and LSU) relative to the mapped water-table elevation. Simulated groundwater levels for the sedimentary units generally are visually consistent with the contours from the water table map.

No observation-well measurements were available for comparison in the WSU because few wells are completed in this low permeability silt unit. In the Southern and Central Willamette subbasins, simulated heads in the WSU are consistent with the expected direction of groundwater flow and with water levels in local streams (figs. 13*A* and 14). Groundwater flow is south to north in the Southern Willamette subbasin, and from the outer margins toward streams in the Central Willamette subbasin.

Simulated hydraulic head in layers 2 and 3 (USU and MSU) (figs. 13*B* and 13*C*) show directions of flow similar to those in the WSU and LSU (figs. 13*A* and 13*D*). Simulated heads are consistent with the water table map for the Southern Willamette subbasin (fig. 14). However, simulated hydraulic heads are about 20 ft lower than water levels on the water table map in the Central Willamette subbasin. This is expected due to the thickness and low permeability of the WSU, which provides a resistance to flow and results in a downward vertical gradient in the unit. Although the details of contours near streams on the water table map are not reproducible in the regional simulation due to large model cells, the general trends of the simulated heads match the trends in measured water levels shown in the water table map. Simulated hydraulic heads in layer 3 show decreased effects from streams. In both layers 2 and 3, direction of flow is generally from south to north and from upland areas to lowland areas to discharge to local streams.

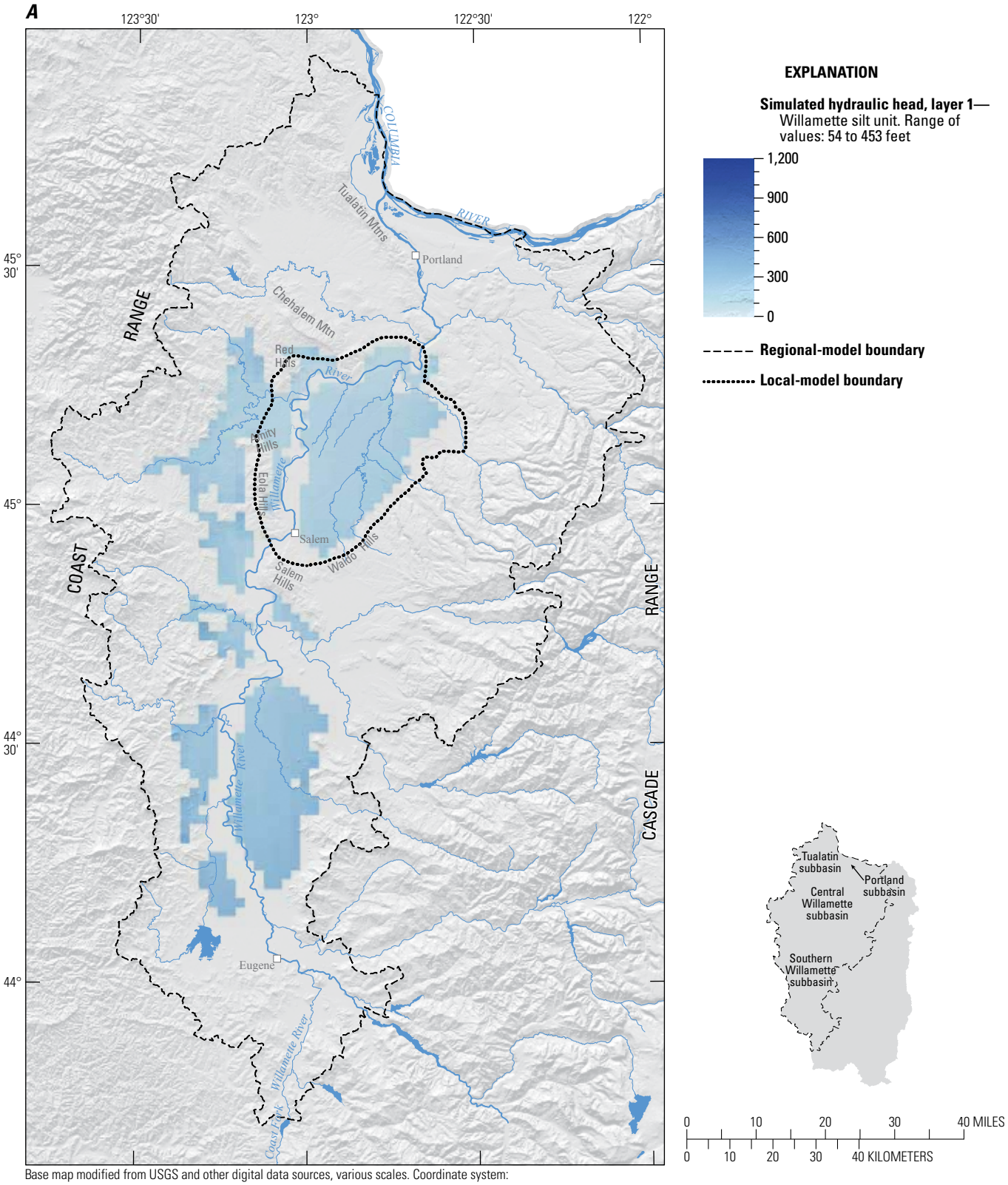

Base map modified from USGS and other digital data sources, various scales. Coordinate system: UTM, Zone 10N, Projection: Transverse Mercator; Datum: North American Datum of 1927.

Figure 13. Simulated hydraulic heads and weighted residuals for all model layers: (*A*) layer 1 (Willamette silt unit), (*B*) layer 2 (upper sedimentary unit/middle sedimentary unit), (*C*) layer 3 (upper sedimentary unit/middle sedimentary unit), (*D*) layer 4 (lower sedimentary unit), (*E*) layer 5 (Columbia River basalt unit), (*F*) layer 6 (basement confining unit), Willamette Basin, Oregon. Histogram represents residuals for indicated model layer.

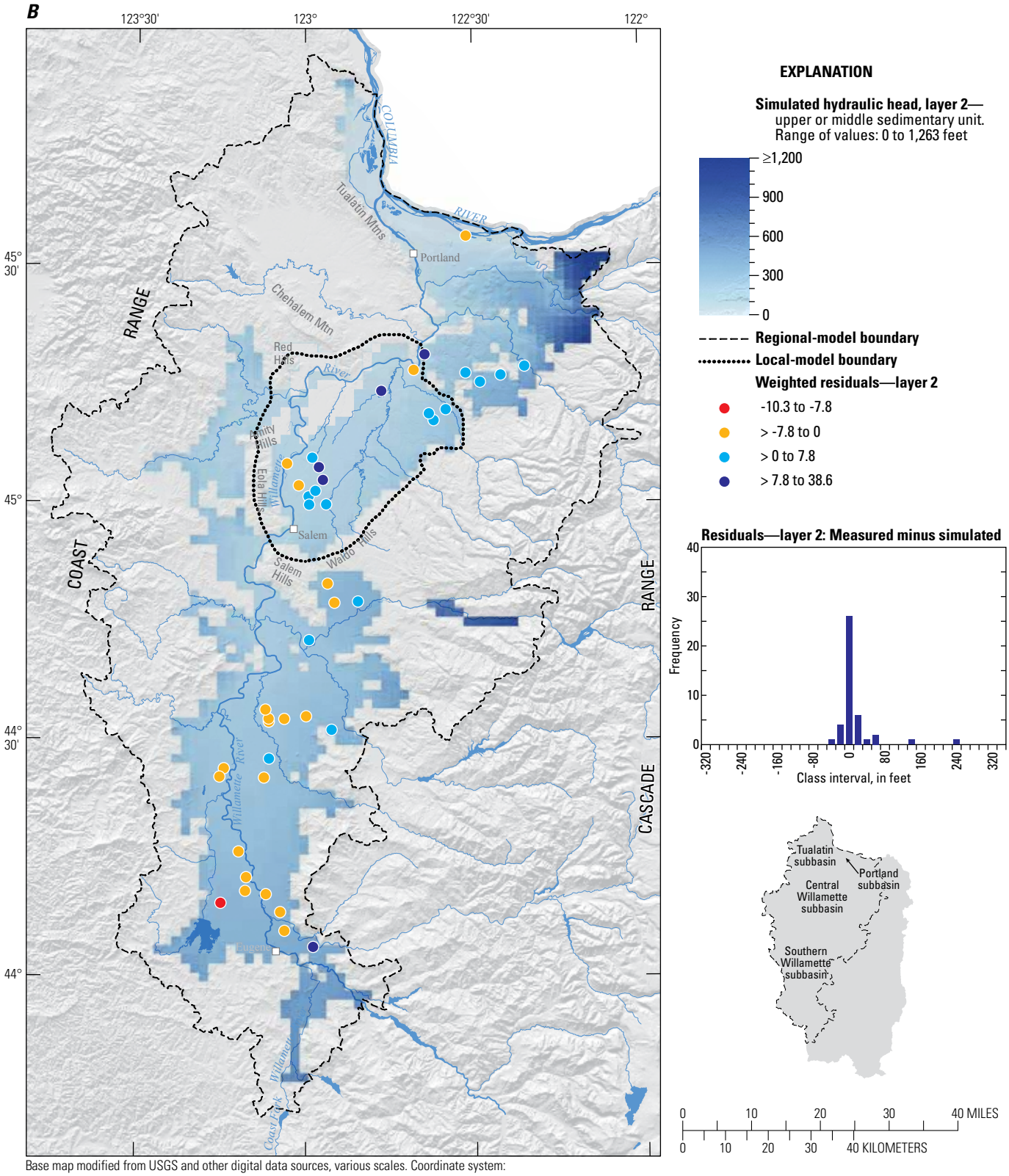

Base map modified from USGS and other digital data sources, various scales. Coordinate system: UTM, Zone 10N, Projection: Transverse Mercator; Datum: North American Datum of 1927.

Figure 13.—Continued

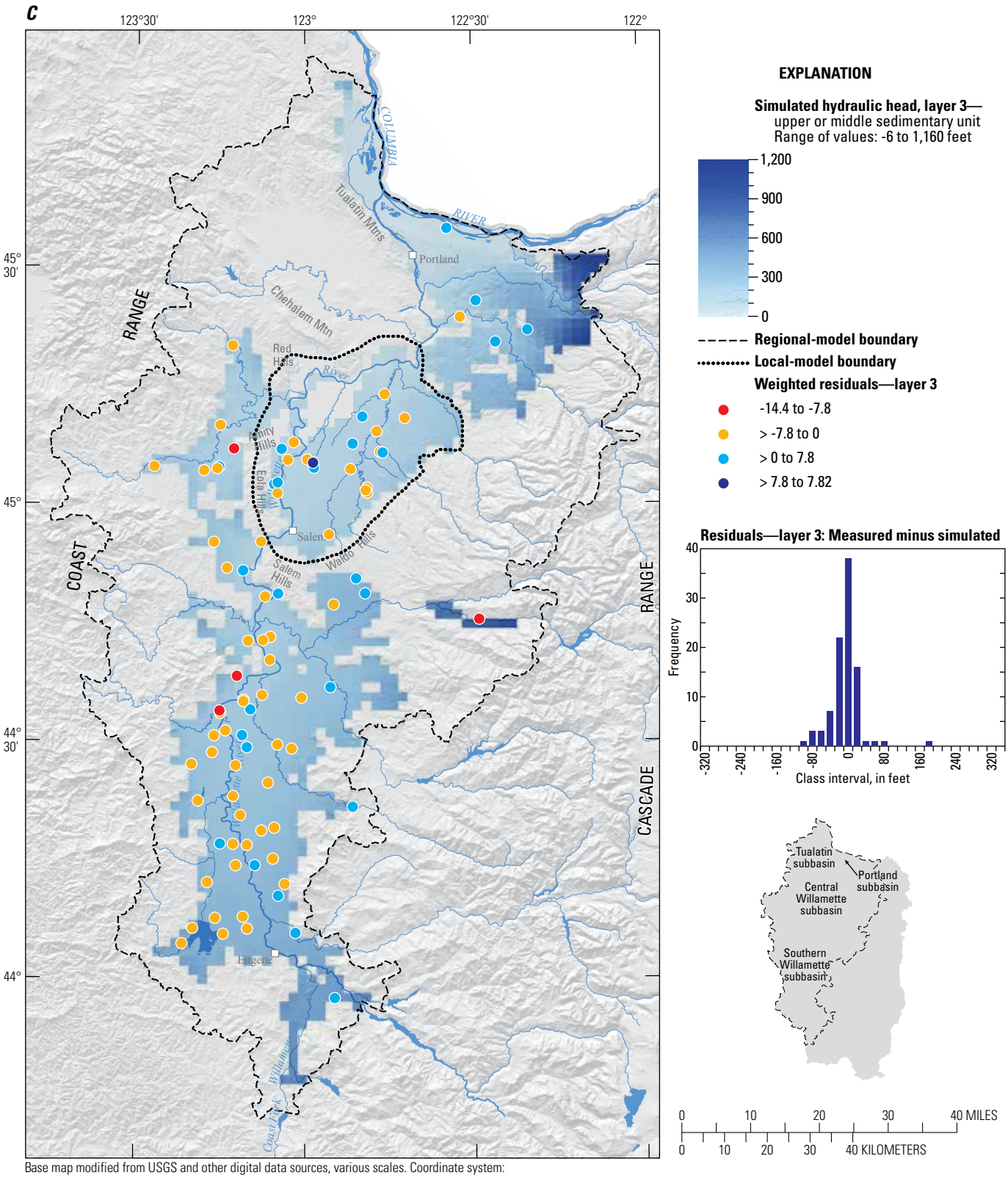

Base map modified from USGS and other digital data sources, various scales. Coordinate system: UTM, Zone 10N, Projection: Transverse Mercator; Datum: North American Datum of 1927.

Figure 13.—Continued

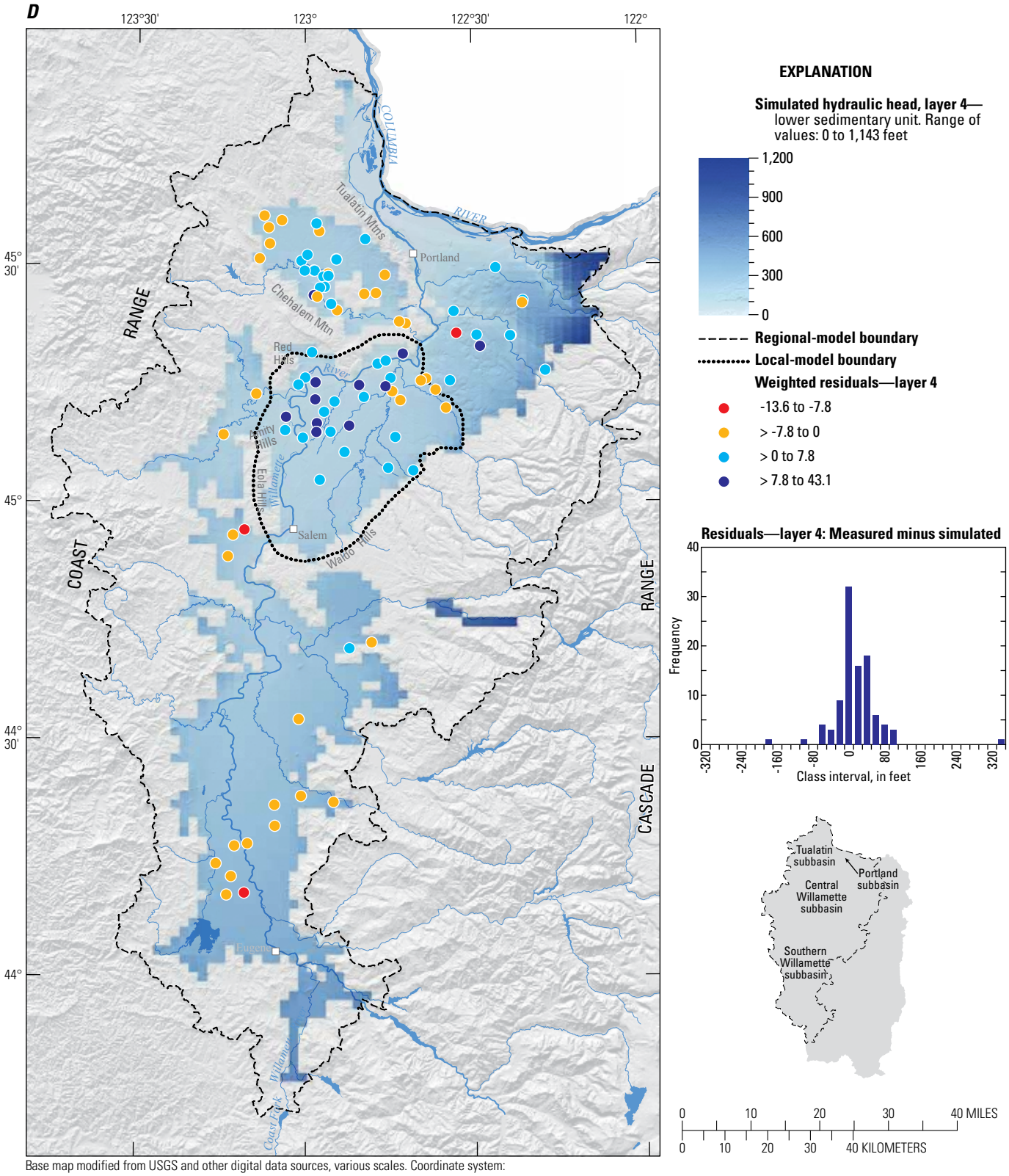

Base map modified from USGS and other digital data sources, various scales. Coordinate system: UTM, Zone 10N, Projection: Transverse Mercator; Datum: North American Datum of 1927.

Figure 13.—Continued

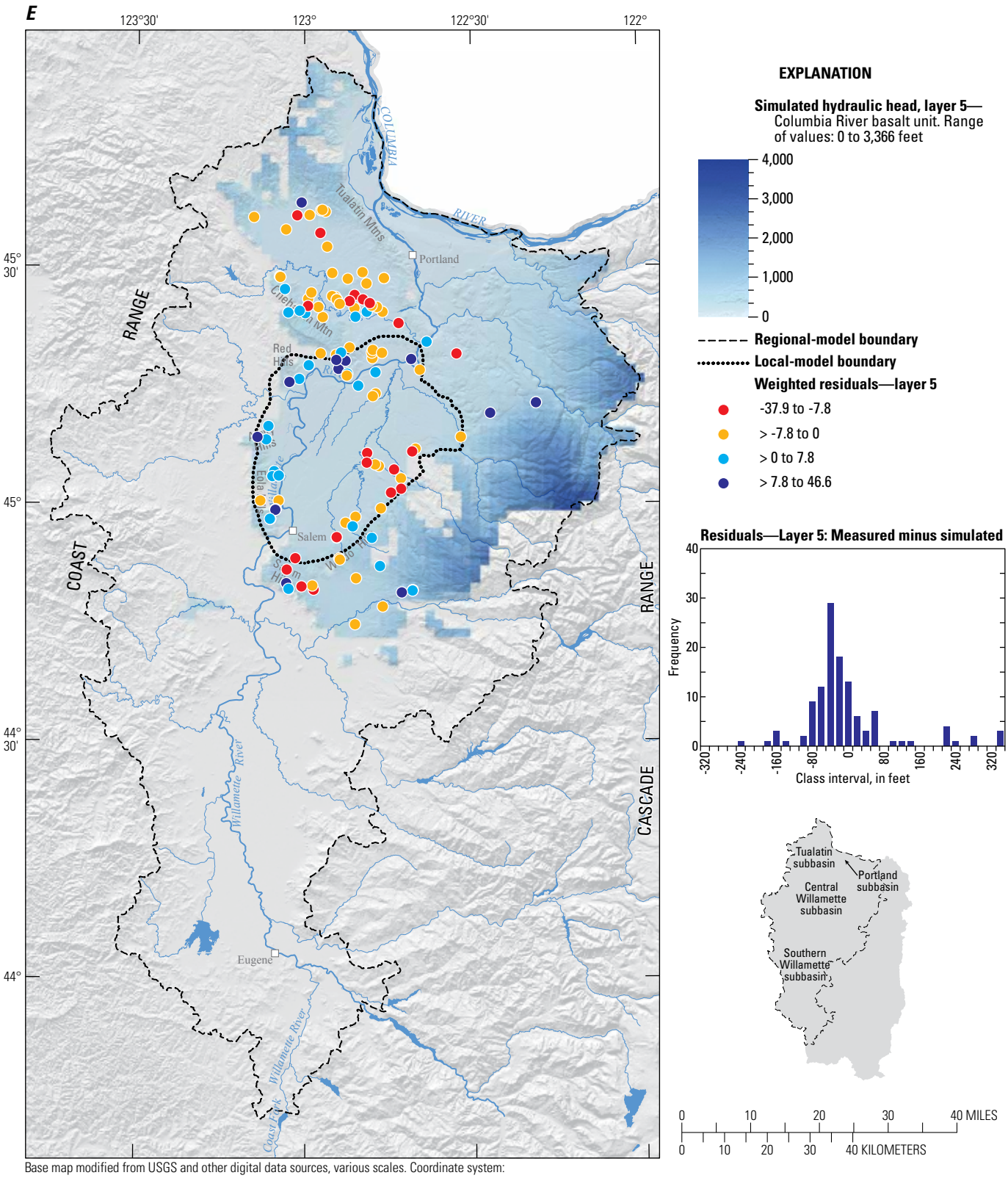

Base map modified from USGS and other digital data sources, various scales. Coordinate system: UTM, Zone 10N, Projection: Transverse Mercator; Datum: North American Datum of 1927.

Figure 13.—Continued

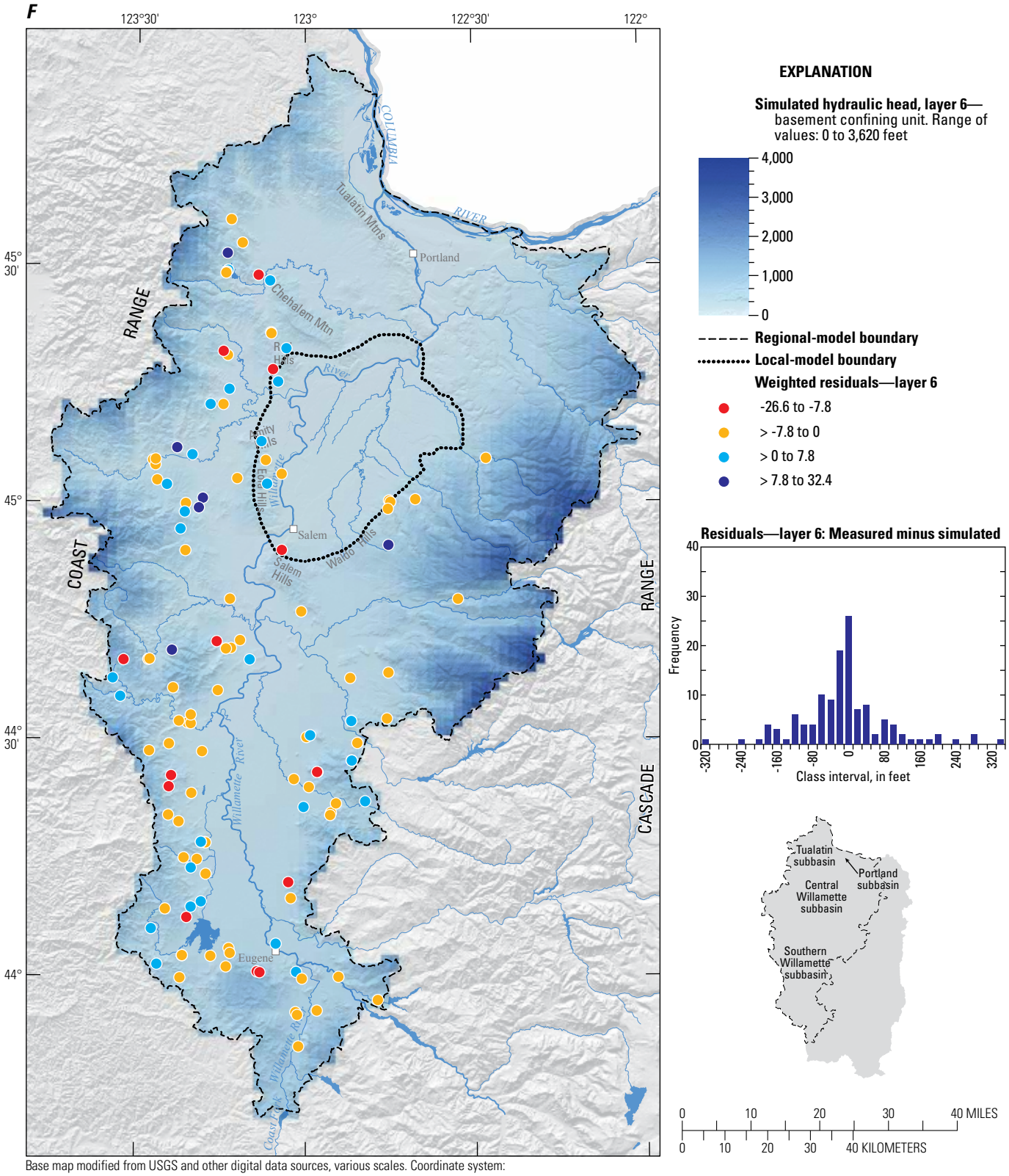

Base map modified from USGS and other digital data sources, various scales. Coordinate system: UTM, Zone 10N, Projection: Transverse Mercator; Datum: North American Datum of 1927.

Figure 13.—Continued

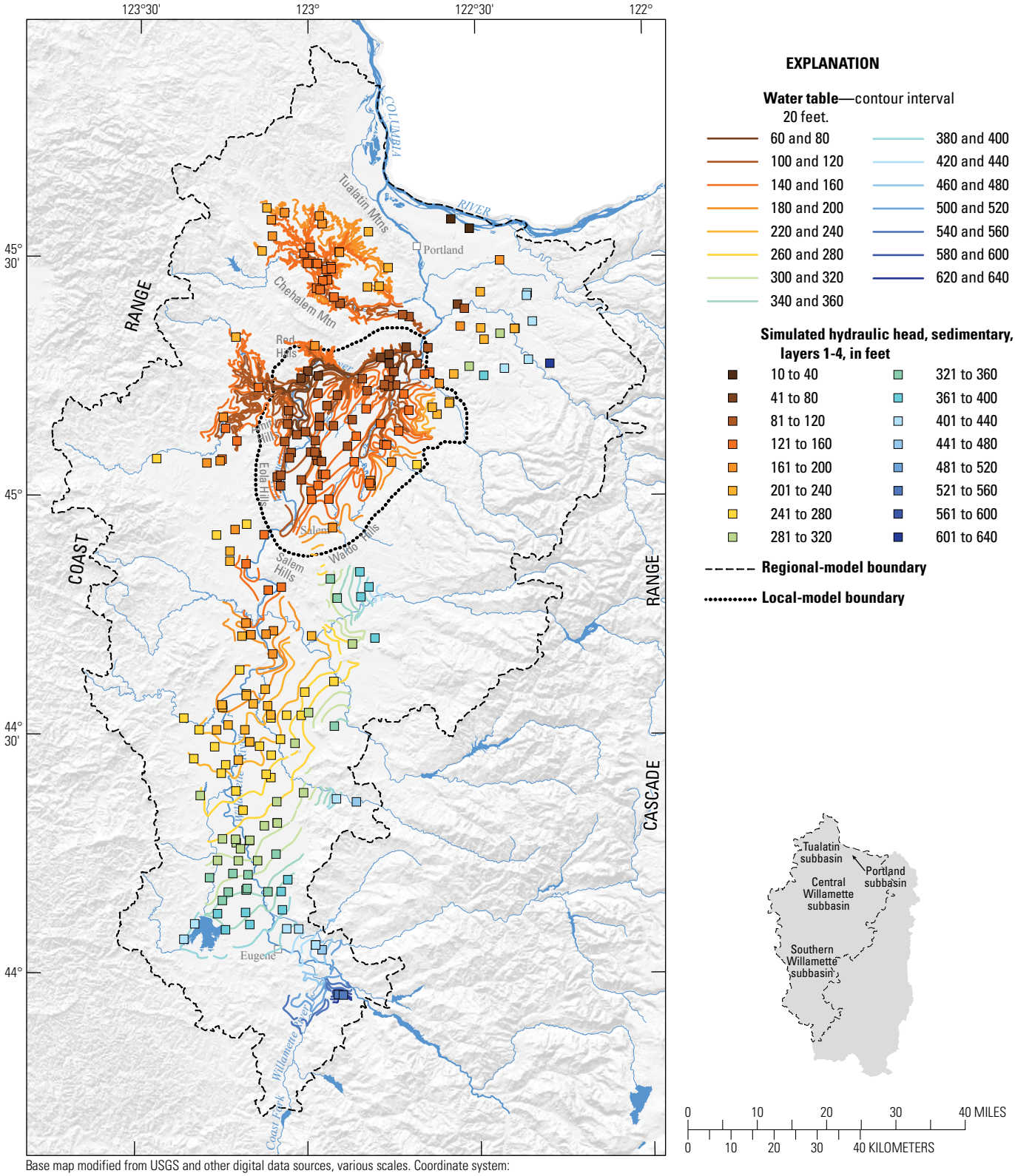

Base map modified from USGS and other digital data sources, various scales. Coordinate system: UTM, Zone 10N, Projection: Transverse Mercator; Datum: North American Datum of 1927.

Figure 14. Simulated hydraulic heads for basin-fill sedimentary layers 1–4 compared with water table map, Willamette Basin, Oregon. Water table contours modified from Conlon and others (2005), pl. 1.

Simulated heads in layer 4 (LSU) were consistent with measured groundwater flow directions (fig. 13*D*). Flow is generally south to north in the Southern Willamette subbasin and from the boundaries of the LSU toward the Willamette River. In the Tualatin subbasin, where the LSU is exposed at land surface, and in the Southern Willamette subbasin, where the WSU and MSU are thin, the LSU simulation fits measured groundwater levels. In the Tualatin subbasin, simulated heads match measured groundwater-levels well, but miss some details of the water table map (fig. 14). Simulated heads are primarily controlled by the total thickness of the LSU and are an average value for the unit. The water table map contours (fig. 14) represent groundwater levels in the uppermost part of the unit and are constrained by stream stage and incision.

In the northwest corner of the Central Willamette subbasin, simulated heads are lower than measured groundwater levels in the LSU (fig. 13*D*). The LSU is generally considered a fine-grained unit, but the bulk hydraulic conductivity of the unit reflects areas of high hydraulic conductivity values rather than the more predominate areas of "blue clay" (low hydraulic conductivity) for which the unit is known. Discrepancies between measured groundwater levels in the northwest corner of the Central Willamette subbasin result from representing the bulk hydraulic conductivity of the unit, rather than the fine-grained matrix, in the simulation. The cell size of the model, the proximity of the measurements to model cells that contain the Willamette River, and the simulation of the Willamette River in layer 4 (the same layer in which the observation wells are located) result in a simulated connection between the Willamette River and hydraulic head in the lower sedimentary unit that is likely greater than measured. The measured groundwater levels in the LSU are more similar to river stage in nearby tributary streams than river stage in the Willamette River.

Simulated heads in layer 5 (representing the CRB) are consistent with measured gradients in the CRB from Conlon and others (2005) (fig. 13*E*). The frequency histogram for the CRB shows residuals are slightly skewed, with simulated hydraulic heads generally greater than measured groundwater levels. Most observation wells are at the margins of the basalt, and few wells are within the interior of the basins (where the unit is deepest). Because the CRB is modeled as one aquifer, rather than a series of isolated aquifers associated with individual flows, the model simulates the general distribution of hydraulic heads in the unit as a whole. Simulated heads in layer 6 (representing the BCU) indicate a reasonable and evenly distributed match to numerous observation wells over the extent of the layer (fig. 13*F*).

Comparison of Simulated and Measured Regional Steady-State Groundwater Flux

As described in the section "Measurements Used in Model Calibration and Fit," 25 PART-derived annual base flow observations from water years 1995 and 1996 (Lee and Risley, 2001) were used to calibrate the regional steady-state model (table B2). Weights for the base-flow flux measurements were assigned based on whether the discharge record is from a regulated or unregulated stream, with or without an active gaging station. The assumption is a 90 percent confidence that actual base flow values are within 10 percent of the calculated estimate. For example, an unregulated stream with an active gaging station is assumed to have a base flow estimate within one standard deviation of the average of the annual base flow measurements for water years 1995–96 in order to reach a 90 percent confidence interval. A regulated stream with an active gaging station is assumed to have a base flow value within two standard deviations of the average annual base flow measurement. Comparisons of measured and simulated flows and locations of the measurements are shown in figures 15 and 16.

Generally good agreement between measured and simulated base flow values (fig. 15) and between simulated gaining and losing stream reaches (fig. 16) and estimates of stream reach gain and loss from Lee and Risley (2001) indicate that the model is simulating base flow reasonably well. Simulated fluxes indicated that most lowland streams are gaining. Lowland reaches simulated as losing are sometimes in the same cell as one or more other reaches and can lose a small amount of flow to those reaches. Most often, losing reaches in the lowlands are associated with effects of pumping on local water-level elevations, and the permeability of river/drain bed materials or the underlying hydrogeologic unit.

The regional steady-state simulation provides a generalized overview of the flow system. Flow is simulated primarily downward in the WSU and upper elevations of the CRB, where most recharge happens. Simulated vertical gradients are variable in the MSU, which also has a horizontal component of flow that generally increases in proximity to streams. The USU includes the younger flood plain deposits adjacent to streams and generally has an upward or short horizontal component of flow discharging to those streams. Discharge to streams also is simulated in areas where upward flow into the LSU is from the underlying CRB and BCU.

Regional Steady-State Groundwater Budget

The simulated regional steady-state water budget is summarized in table 5. The regional model shows that the Willamette Basin receives most of its recharge from precipitation and infiltration from applied irrigation water, with a small amount of seepage from streams and the Columbia River. Groundwater leaves the basin predominantly through discharge to streams, to the Columbia River, and to wells. Total simulated seepage from and discharge to streams includes all streams simulated with the DRAIN and RIVER packages. The Columbia River is simulated as a constant head boundary.

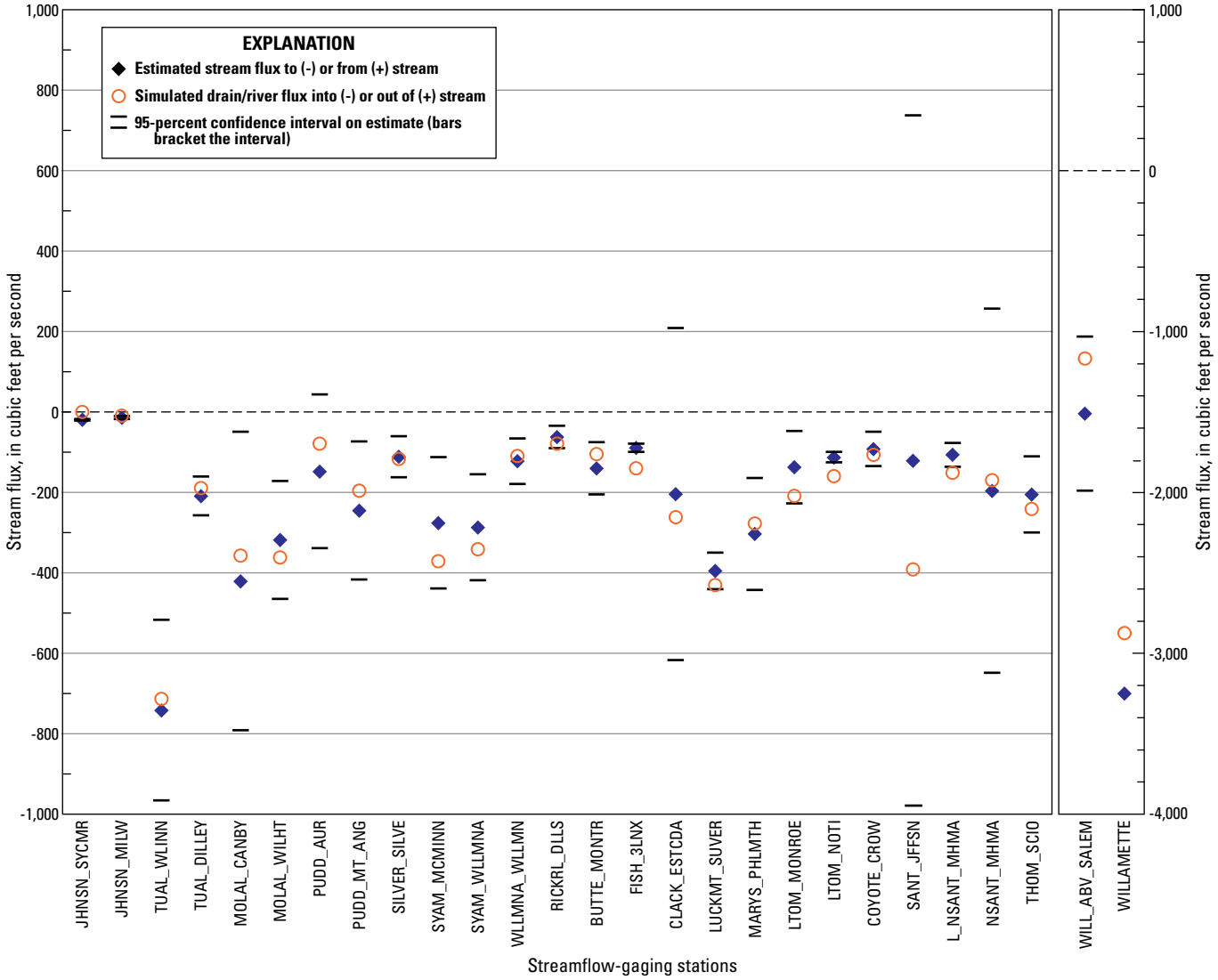

Figure 15. Estimated steady-state stream fluxes, 95-percent confidence intervals on estimated stream fluxes, and simulated steady-state stream fluxes for the Willamette Basin, Oregon, regional steady-state model. Streamflow-gaging station names are defined in section "Abbreviations and Acronyms." Estimated fluxes from Lee and Risley (2001).

Accounting for differences in area (conceptual model area at 11,111 mi^2 and numerical model area at 6,700 mi^2), the simulated budget (table 5) compared well with the calculated budget from the Willamette Basin conceptual groundwater model (table 1; Conlon and others, 2005). Recharge is generally proportional to area, with minor differences explained by the recharge corrections summarized in table A1. Discharge to stream seepage in both numerical and conceptual models consumes approximately 95 percent of recharge in the Willamette Basin. Because the areas of the conceptual and numerical models are different, but almost all pumping is encompassed within both areas, pumping values are nearly identical. Percentages are different, however, because recharge is different.

Local Groundwater Model

Because a transient model of groundwater flow over the entire Willamette Basin was beyond the scope of this study, more detailed steady-state and subsequent transient-flow models were developed for analysis of the groundwater-flow system and seasonal interactions with surface water in the Central Willamette subbasin, where there is increasing demand for water for agricultural and other uses. Summer streamflow is already fully allocated in the subbasin, and additional groundwater development is being considered to augment surface water sources.

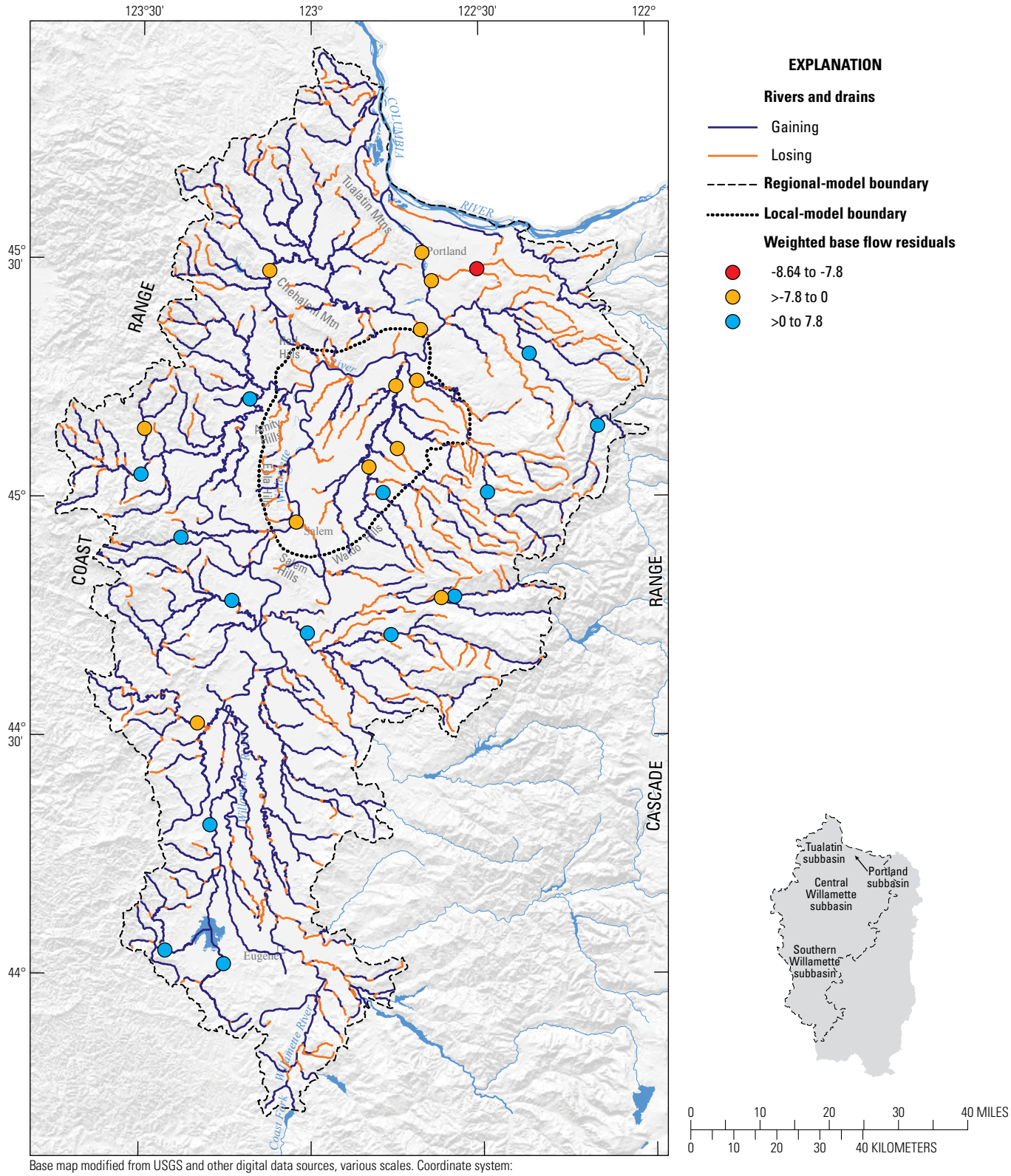

Base map modified from USGS and other digital data sources, various scales. Coordinate system: UTM, Zone 10N, Projection: Transverse Mercator; Datum: North American Datum of 1927.

Figure 16. Distribution of weighted base flow residuals and simulated locations of losing and gaining stream reaches for the Willamette Basin, Oregon, regional steady-state model.

Table 5. Simulated water budget from regional and local steady-state groundwater models, Willamette Basin, Oregon.

[**Abbreviations**: ft^3/s, cubic foot per second; M acre-ft/yr, million acre-feet per year; mi^2, square mile; NA, not applicable]

Budget component	Calibrated regional model (6,700 mi^2)			Calibrated local model (674 mi^2)		
	(M acre-ft/yr)	(ft^3/s)	(percentage of total)	(M acre-ft/yr)	(ft^3/s)	(percentage of total)
In						
Seepage from Columbia River	0.00	2	0.0		NA	
Seepage from streams	0.04	58	0.7	0.00	2	0.3
Boundary flux		NA		0.11	158	27.7
Recharge from irrigation and precipitation	6.30	8,702	99.3	0.30	411	72.0
Total inflow	6.34	8,762	100.0	0.41	571	100.0
Out						
Seepage to Columbia River	0.03	35	0.4		NA	
Withdrawals from wells	0.29	406	4.6	0.12	162	28.3
Seepage to streams	6.02	8,321	95.0	0.29	402	70.5
Boundary flux		NA		0.00	7	1.2
Total outflow	6.34	8,762	100.0	0.41	571	100.0

Local Discretization

The Central Willamette subbasin model area consists of 1,000- by 1,000-ft cells (about 23 acres) (fig.17*A*). The model grid has 177 rows, 164 columns, and 8 layers, with a maximum of 18,807 cells active in any one layer. Lateral boundaries, simulated as no flow boundaries, coincide with the location of groundwater divides to the northeast along the crest of the Boring Lava and sedimentary highlands east of Oregon City, the topographic crest of Parrett Mountain to the north, the Red Hills of Dundee and Eola Hills to the west, and the Salem and Waldo Hills to the south and southeast. Flow into and out of the lateral boundaries of the local model is specified for 1,921 cells using the WELL package from MODFLOW in layers 1 through 8, with a maximum of 506 cells (the entire local model perimeter) in any one layer. This boundary flux was calculated using results from the regional model (appendix B).

The eight layers represent the six hydrogeologic units in the Central Willamette subbasin (fig. 17*B*). Layers 1 through 4 are the same as in the regional model and represent the WSU, USU or MSU, and LSU, respectively; layers 5, 6, and 7 represent the CRB, and layer 8 represents the BCU. Each layer varies in thickness throughout the model, except for layer 8. Layer 1 (WSU) ranges from about 0 to 120 ft thick in the central part of the basin. Layers 2 and 3 (USU/MSU) range in thickness from 0 to approximately 250 ft thick where alluvial fans are present to the east. Layer 4 (LSU) ranges from 0 to 1,600 ft thick in the central part of the basin. Layer 8 (BCU) is set to a thickness of 1,000 ft throughout the active model area. "Pseudo-cells" (as described in the section "Regional Groundwater Model") are used where a unit is absent between two adjacent layers in order to maintain the continuity of the model layer.

The CRB is divided into three layers in the local model (from one layer in the regional model). The intent was to simulate vertical gradients in the basalts on a local scale. Total CRB thickness is greater than 300 ft in all areas of the Central Willamette subbasin, except near the edge of the CRB extent. The top two basalt layers range from 40 to 100 ft thick where the total basalt thickness is greater than 300 ft. In the Central Willamette subbasin, individual Columbia River basalt flows have a minimum thickness of 40 ft and an average thickness of 100 ft (Conlon and others, 2005). If the actual total basalt thickness is less than 200 ft, the top basalt layer is not present in the model and the middle CRB layer thins as total thickness decreases until it is less than 40 ft thick, after which only the bottom model layer is used.

Temporal Discretization

Changes in water levels from wells and streamflows in the Central Willamette subbasin are most often influenced by seasonal responses to changes in recharge and changes in groundwater withdrawals from municipal, industrial, and irrigation wells. In the sedimentary and basalt aquifers, the water table rises and falls in response to recharge and pumping. Generally, water levels are highest during winter and spring, and lowest during the summer and autumn. Because pumping and recharge can change from month to month, the two simulated water years (1999-2000) were divided into 24 stress periods to simulate monthly changes in recharge and discharge. Specified fluxes are constant within each stress period; however, stresses vary from one stress period to the next. Each of the 24 stress periods were divided into 10 time steps using a 1.5 time step multiplier, so that the 2-year calibration period included 240 time steps.

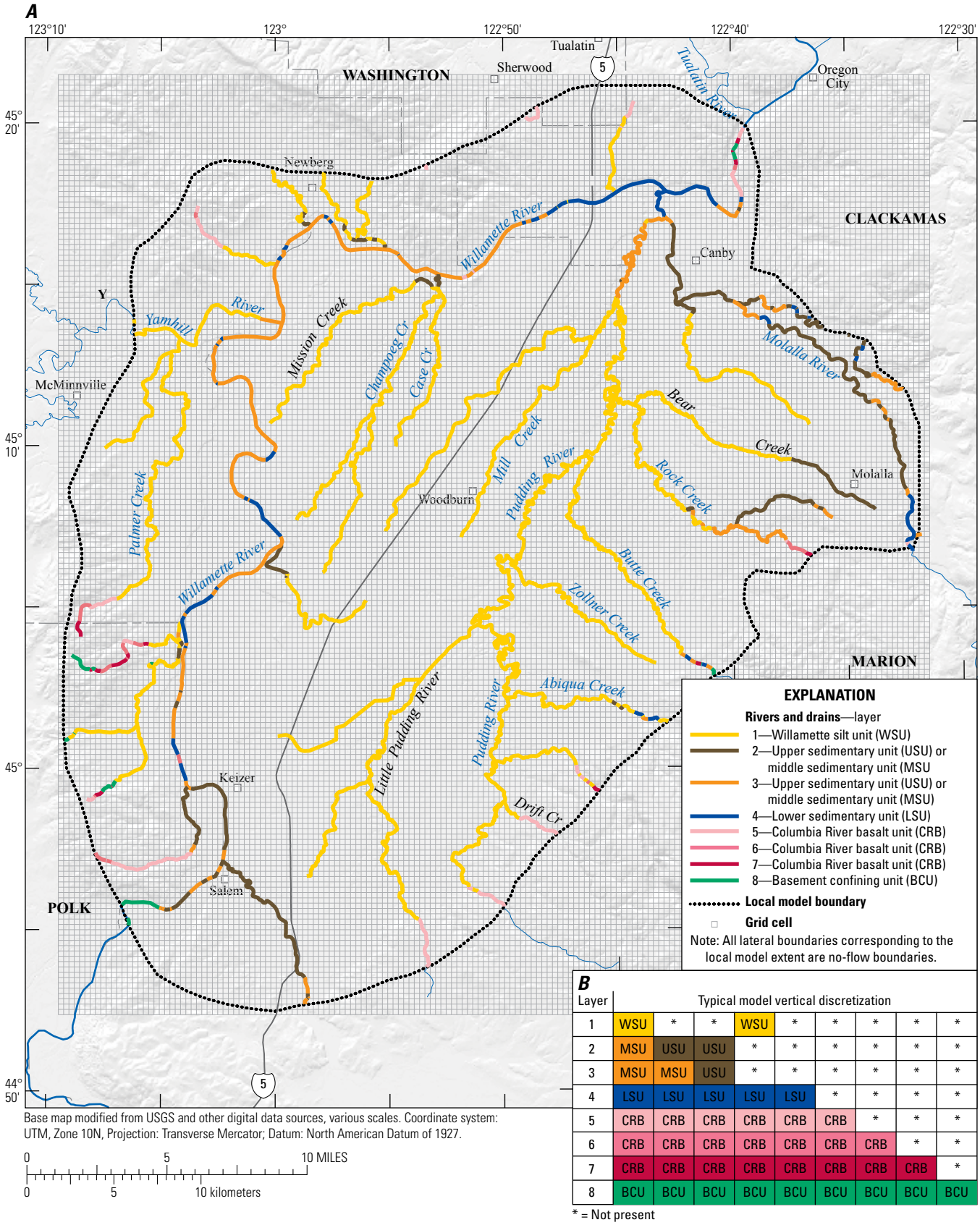

B

Layer	Typical model vertical discretization								
1	WSU	*	*	WSU	*	*	*	*	*
2	MSU	USU	USU	*	*	*	*	*	*
3	MSU	MSU	USU	*	*	*	*	*	*
4	LSU	LSU	LSU	LSU	LSU	*	*	*	*
5	CRB	CRB	CRB	CRB	CRB	CRB	*	*	*
6	CRB	CRB	CRB	CRB	CRB	CRB	CRB	*	*
7	CRB	CRB	CRB	CRB	CRB	CRB	CRB	CRB	*
8	BCU	BCU	BCU	BCU	BCU	BCU	BCU	BCU	BCU

* = Not present

Figure 17. (*A*) Local model grid, locations of river and drain cells, boundary conditions, and (*B*) typical configurations of local hydrogeologic units in model layers, Central Willamette subbasin, Willamette Basin, Oregon. Stream reaches, simulated using river and drain cells, are color coded by layer and hydrogeologic unit. Gaps in the vertical configuration are simulated using thin pseudo-cells that easily transmit water in the vertical direction.

Local-Model Boundary Conditions

The boundaries of the model were selected to encompass the areas of interest within the Central Willamette subbasin, as well as to coincide with hydrologic and geologic boundaries of the system. Three types of boundary conditions were used to define the groundwater-flow system in the Central Willamette subbasin: no-flow boundaries, head-dependent-flux boundaries and specified-flux boundaries. Boundaries in the Central Willamette subbasin were divided into two broad categories that describe the boundaries related to the geographic extent of the aquifer systems: a specified boundary flux and the hydrologic processes active within the model extent.

Specified Boundary Fluxes

Lateral boundaries are represented as no-flow and specified-flux boundaries in the local model. A general no-flow boundary defines the model area and was selected to coincide with the location of groundwater divides and topographic highs. This boundary was augmented with prescribed fluxes (table 6) based on results of the regional model that were assigned to the lateral boundaries of the Central Willamette subbasin using the WELL package to represent nonnegligible regional flux across layers that are present inside and outside the local model boundary. The lower boundary of the model is also a no-flow boundary and is arbitrarily set to a value of 1,000 ft below the top of the BCU. The sedimentary layers in the basin are generally thin and pinch out within the model area; therefore, the lateral boundaries of these units can be simulated as no-flow boundaries.

Table 6. Prescribed annual fluxes for local model boundary of the Central Willamette subbasin, Willamette Basin, Oregon.

[All values are in cubic feet per second. Values are rounded. Fluxes from the regional model were proportionally divided across the finer local model cells]

Layer	Flux out of local model	Flux into local model	Net flux into local model
1	0.0	0.1	0.1
2	0.3	4.2	3.9
3	0.4	3.7	3.3
4	0.8	100.4	99.6
5	0.2	1.9	1.7
6	0.2	2.3	2.1
7	1.4	7.5	6.1
8	3.3	38.0	34.7
Total boundary flux	6.8	158.2	151.4

Hydrologic-Process Boundaries

Hydrologic process boundaries include recharge, leakage to drains, leakage to and from rivers, and well pumping. These processes are either head-dependent- or specified-flux boundaries.

Recharge

Monthly values of recharge for the transient groundwater model were extracted from PRMS simulation results (Lee and Risley, 2001) by upscaling daily simulated values and correcting recharge using the recharge array multipliers derived in appendix A (table A1). Average annual recharge rates ranged from about 5 in/yr in the lowland areas to about 24 in/yr in the upland areas. Average monthly recharge rates for the Central Willamette subbasin vary from 0 during summer to about 3 in. (more than 1,700 ft^3/s) during winter (fig. 18).

River and Drain Leakage

For consistency, gains to and losses from streams were simulated using river and drain processes as described for the regional model. The local model contains 3,217 drain and river reaches (fig. 17*A*). Simulated river stage was varied in the transient model to account for seasonal changes in streamflow. To estimate the amount of variation, average monthly stream stage fluctuations were calculated for a minimum of one stream from each order category (table 7). These estimates of stream stage fluctuation were applied to the average annual stream stage (table 2) on a monthly basis during each water year to simulate the effects of varying stage in streams and rivers. The decrease in monthly fluctuations from water year 1999 to 2000 reflects the downward trend of the cumulative departure from average precipitation curve shown in figure 3. In the transient model, all rivers within the same order (except for Case Creek) have the same monthly fluctuations from average annual stream stage applied (table 7). Order category 5 has two sets of values for the Willamette River upstream of the Newberg Pool, and for the Willamette River downstream of the Newberg Pool.

Groundwater Discharge to Wells

Well pumping for the Central Willamette subbasin is summarized in Conlon and others (2005) and is simulated as a specified-flux boundary (figs. 19 and 20). Multiple LANDSAT images, field inspections, and digital water right maps and associated well logs were used during 1999–2000 to evaluate uncertainties and produce a more refined estimate of irrigation water use for the Central Willamette subbasin (Conlon and others, 2005). Total simulated annual well pumping is about

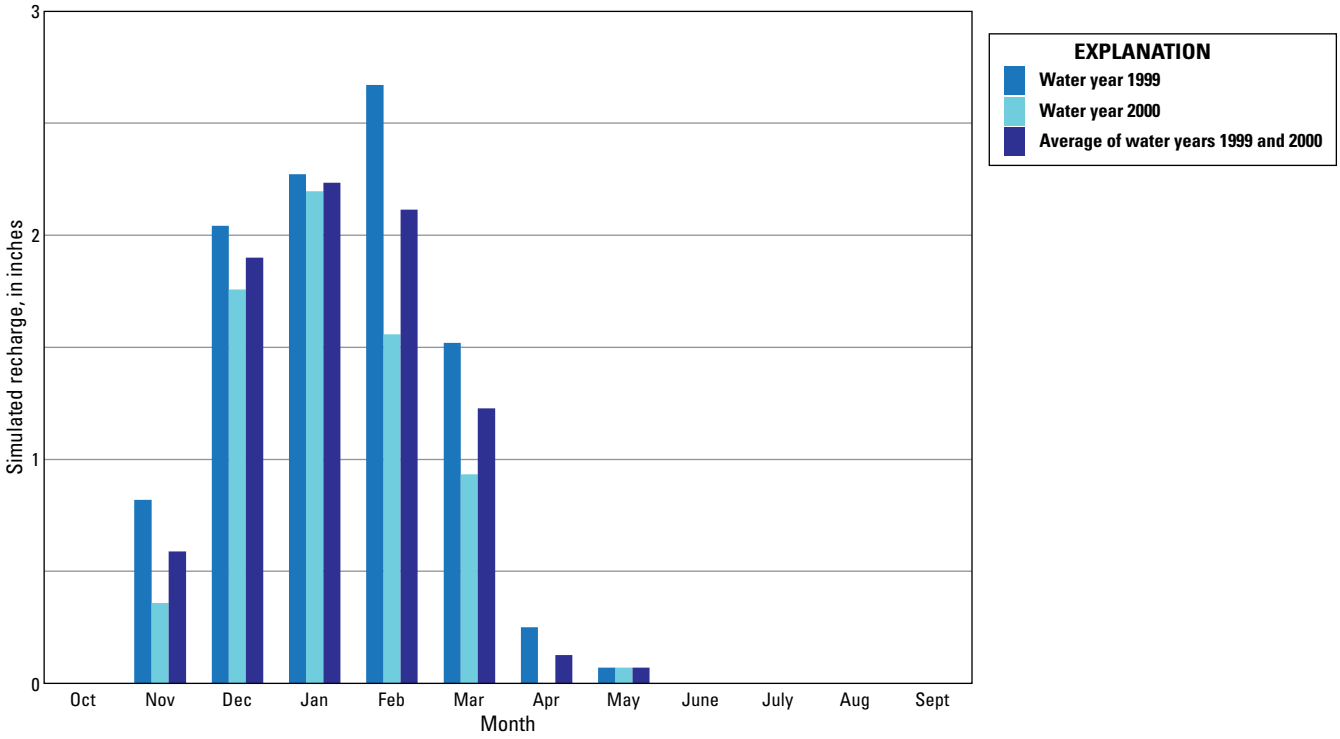

Figure 18. Simulated average monthly recharge, Central Willamette subbasin, Willamette Basin, Oregon, water years 1999–2000.

120,000 acre-ft/yr (162 ft^3/s) (table 5), with approximately 85 percent of the withdrawals pumped from the sedimentary units (Conlon and others, 2005). The well pumping in the Central Willamette subbasin represents about 40 percent of the pumping in the regional model.

Initial Conditions

A long history of development and irrigation and a lack of historical water levels and flow data in the study area precluded a true steady-state simulation of the complete post-development period in order to establish initial conditions for the local transient model. Instead, a steady-state model was developed and calibrated using average annual data from water years 1999–2000. Because groundwater levels vary seasonally, and water level records do not show widespread long-term declines, initial heads for the transient model were set to the heads obtained from the local steady-state simulation. The transient model was developed and calibrated using the local model in transient mode and simulating monthly data from water years 1999–2000 (24 stress periods). To reach dynamic steady-state conditions, the simulation was extended for a period of 50 years (600 stress periods) using and repeating monthly average data from water years 1999-2000, to ensure that water levels would represent a dynamic equilibrium, with no net change in storage. Recharge, discharge, and aquifer properties used in the modeled area, and the final simulated (September) heads were used to represent the initial (October) heads for subsequent transient simulations. Water level changes stabilized within 10 years, and simulated heads were reasonably close to measured September heads where available. The largest differences between the September heads after 50 years and the initial values assigned from the local steady state model generally occurred in model cells with significant pumping because of the varying effects of seasonal pumping compared to constant effects of steady-state pumping, or near the perimeter of the modeled area.

Local Model Parameters

Horizontal and Vertical Hydraulic Conductivity

Initial horizontal and vertical hydraulic conductivity values used in the local groundwater model were from the regional steady-state model (table 3), and no additional zones were delineated. All three basalt layers in the local model have the same hydraulic conductivity values.

Table 7. Average monthly stream stage fluctuations relative to average annual stream stage, Central Willamette subbasin, Willamette Basin, Oregon, water years 1999–2000.

[All values are in feet. Fluctuations were added to mean annual stream stage to simulate the effects of seasonal changes in streamflow]

Stress period	Calendar year	Month	River or drain stage						Case Creek
			Order 1	Order 2	Order 3	Order 4	Order 5		
							Willamette River downstream of the Newberg Pool	Willamette River upstream of the Newberg Pool	
Water year 1999									
1	1998	October	-0.48	-1.55	-3.94	0.25	-0.38	-2.24	-0.48
2		November	0.73	-0.17	3.35	5.98	1.54	2.64	0.73
3		December	1.38	2.18	10.86	5.03	3.79	8.46	1.38
4	1999	January	1.13	-0.25	10.85	13.61	4.11	9.41	1.13
5		February	1.58	0.50	10.82	9.67	3.16	5.66	1.58
6		March	0.51	-0.10	7.23	6.17	1.48	3.10	0.51
7		April	-0.23	0.30	0.59	-0.04	-0.36	0.14	-0.23
8		May	-0.45	-0.52	-0.07	-1.80	-0.03	1.47	-0.14
9		June	-0.66	-0.08	-3.34	-4.14	-1.20	-0.55	-0.28
10		July	-0.75	-1.11	-4.77	-5.98	-2.16	-2.79	-0.22
11		August	-0.80	-1.49	-5.26	-6.74	-1.05	-3.37	-0.58
12		September	-0.84	-1.42	-5.52	-6.75	-0.86	-2.97	-0.57
Water year 2000									
13	1999	October	-0.71	-1.55	-5.16	-6.46	-0.56	-2.44	-0.18
14		November	0.21	-0.17	1.18	4.20	0.98	0.81	0.38
15		December	0.49	2.18	6.90	10.97	2.67	6.13	1.03
16	2000	January	0.63	-0.25	6.12	9.11	2.31	5.63	0.38
17		February	0.78	0.50	6.34	6.58	1.23	2.70	0.17
18		March	0.24	-0.10	3.08	3.33	0.48	1.21	0.05
19		April	-0.38	0.30	-2.04	-2.43	-0.78	-0.44	0.10
20		May	-0.41	-0.52	-0.90	-2.08	-0.76	-0.34	-0.54
21		June	-0.60	-0.08	-3.00	-3.46	-1.75	-2.02	-0.85
22		July	-0.73	-1.11	-5.03	-5.92	-1.46	-3.83	-0.74
23		August	-0.83	-1.49	-5.66	-6.74	-1.38	-3.95	-0.83
24		September	-0.74	-1.42	-5.47	-6.62	-1.04	-3.41	-0.74

Specific Storage

Specific storage is the amount of water per unit volume of a saturated aquifer or confining unit that is stored or expelled from storage due to compressibility of the matrix and the fluid, per unit change in head. Storativity is the volume of water that a unit will store or expel from storage per unit surface area, per unit change in head. Storativity is the product of the specific storage and the aquifer thickness (Fetter, 1994). To simulate variation in water levels from changes in storage, specific storage is used in the transient groundwater model. Specific storage values were obtained from previous studies, core analysis, and specific capacity and aquifer tests (Conlon and others, 2005). The spatial distribution of specific storage values is uniform in each unit. The value of specific storage for pseudo-cells was set to 1×10^{-10} to minimize storage in areas where a layer is absent. All layers were simulated as confined, which assumes a constant saturated thickness in the model layers. The specific storage value of 1×10^{-3} assigned to the upper most unit (WSU) translates to storage coefficient values between 0.06 and 0.36, which compares well to the storativity of unconfined aquifers (0.02–0.30; Fetter, 1994). Because all layers were simulated as confined, specific storage values were assigned to each unit though unconfined flow conditions likely exist in the flow system in some areas. Adjustments to specific storage values were the primary method of calibration for the transient model.

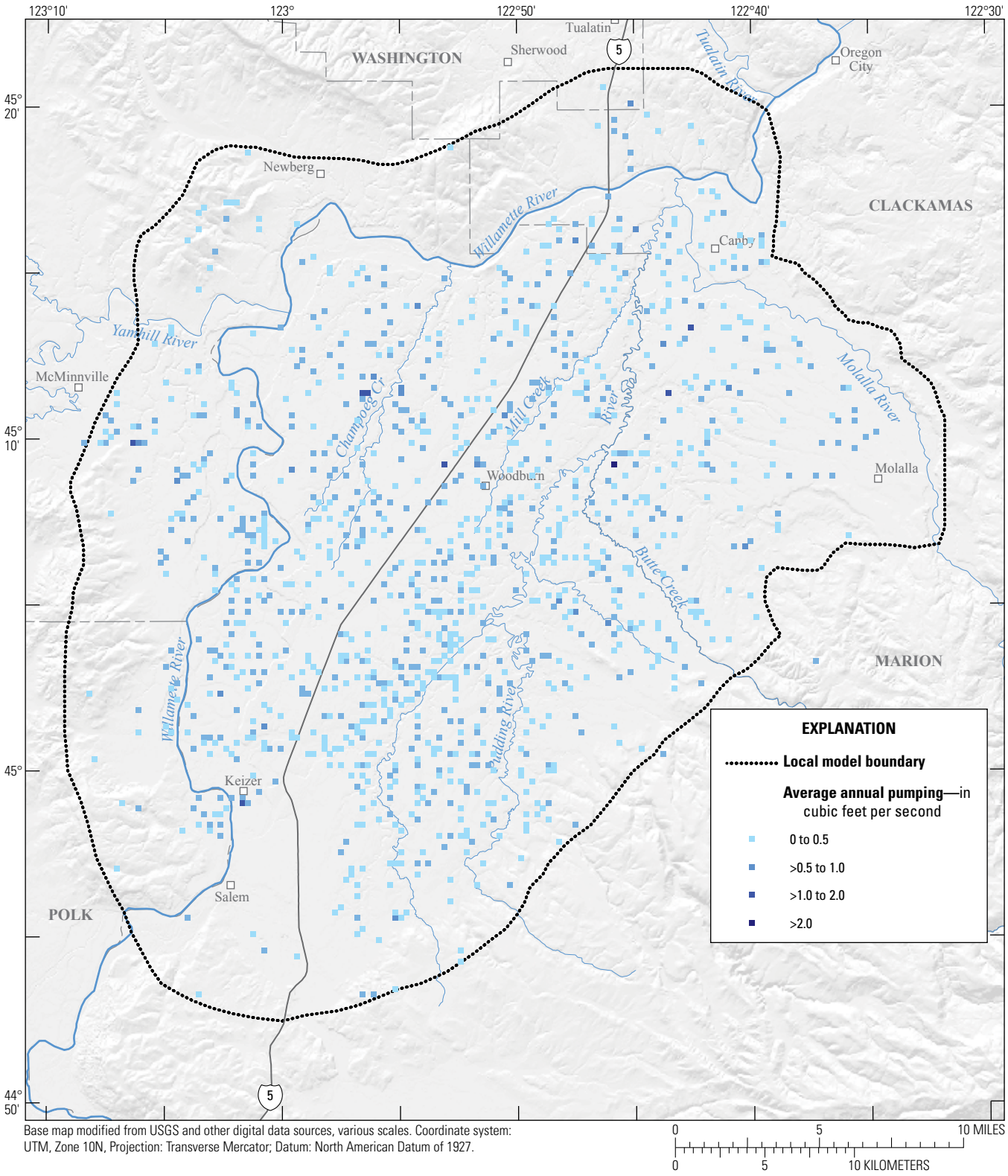

Figure 19. Local distribution of average annual pumping on the model grid of the Central Willamette subbasin, Willamette Basin, Oregon, water years 1999–2000.

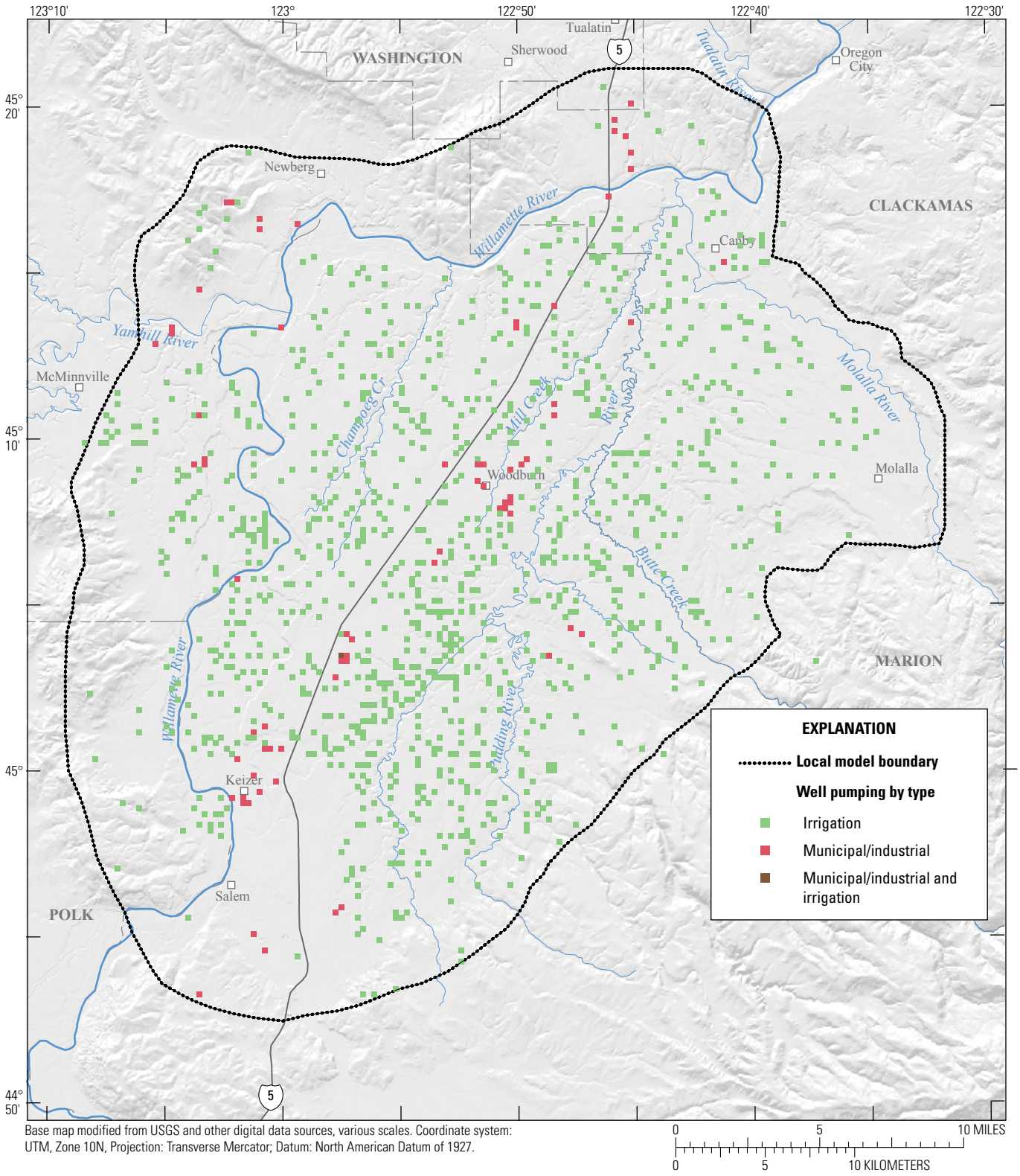

Figure 20. Local distribution of municipal and industrial, and irrigation, pumping on the model grid of the Central Willamette subbasin, Willamette Basin, Oregon, water years 1999–2000.

Local Model Calibration

The Central Willamette subbasin steady-state groundwater model was calibrated to mean annual conditions to test parameter assignment and provide initial conditions for the transient model. The transient groundwater model was calibrated to average monthly conditions for water years 1999–2000 because that was a period of intensive data collection in the subbasin, and average conditions were reasonably close to long-term average conditions. Calibration primarily was based on river and drain bed hydraulic conductivity for the steady-state model and specific storage terms for the transient model. Boundary flux was simulated as a specified flux in the transient model. Well pumping was not adjusted during calibration. Recharge parameters (array multipliers; table 3) were set on the basis of calibration results from the regional steady-state model. Drain losses and river gains and losses were simulated by the model. All model layers were simulated as confined for numerical stability. Independent streamflow measurements were not available in the Central Willamette subbasin for use in model calibration because base flow estimates include a significant amount of streamflow from outside the model boundary. The calibration strategy for the steady-state and transient local models was to approximate water levels for general conditions and verify that the calculated drain and river flows were reasonable compared to the calculated values from the regional model (table 8). Simulated flow values from the regional and local model are within the same order of magnitude (except for the Yamhill River), and 10 of the 12 comparable flows are within 8 ft^3/s of each other. Differences are attributable to limitations on the accuracy of flow estimates for basins with some flow originating from outside model boundaries, errors introduced by different cell sizes, and slightly different comparable areas between the regional and local model.

Table 8. Simulated river and drain flow from the local model and comparable simulated river/drain flow from the regional model for drainage basins in the Central Willamette subbasin, Willamette Basin, Oregon.

[All values in cubic feet per second]

Local stream basin	Simulated flow		Difference
	Regional model	Local model	
Lower Willamette River	160.0	117.6	42.4
Middle Willamette River	94.5	91.8	2.7
Upper Willamette River	67.4	75.4	-8.0
Molalla River	51.9	45.6	6.3
Upper Pudding River	26.5	15.3	11.2
Rock Creek	25.4	20.3	5.1
Yamhill River	12.1	6.9	5.2
Pudding River	11.9	14.3	-2.4
Butte Creek	7.3	4.6	2.7
Little Pudding River	5.0	7.5	-2.5
Mill Creek	2.2	1.5	0.7
Zollner Creek	0.1	0.5	-0.4

Steady-State Calibration

Data and Procedure

Model parameters for the local steady-state model were mostly identical to those for the regional steady-state model; 34 parameters were defined. Initial parameter estimates came directly from the regional calibration process. Calibration was attained by retaining the values of the estimated parameters from the regional model, except for the values of drain and riverbed hydraulic conductivity. The conductance of flow through drain or riverbeds is dependent on the area of the bed in each cell; therefore, the vertical conductance of a cell is adjusted to maintain comparable flows through a different cell size. Recharge parameters were the same as in the regional model (table 3).

The Sensitivity Process in MODFLOW-2000 (Hill and others, 2000) was used to calculate sensitivities for hydraulic head throughout the model. The composite scaled sensitivities for the calibrated local steady-state model are shown in figure 21. Similar to the regional steady-state model, recharge parameters and the horizontal hydraulic conductivity of the BCU are the most sensitive parameters; however, there is an increase in the relative sensitivity of parameters for the basin-fill sediments compared to the corresponding regional model parameters (fig. 8). Although parameter estimation was attempted during the calibration process, the parameters could not be estimated uniquely using automated methods; therefore, calibration was completed manually by adjusting the drain and riverbed hydraulic conductivity values.

Comparison of Simulated and Measured Local Steady-State Heads

Mean annual groundwater-level observations for the local steady-state model were derived from water-level measurements at 52 wells during water years 1999–2000 (fig. 22). These mean annual water levels were derived from bimonthly, quarterly, or continuous records, with most data covering both water years. Measurements were weighted using the same method as for the regional model.

The simulated steady-state hydraulic head values are plotted against the mean annual groundwater levels to show fit along a 1:1 line (fig. 23). Groundwater levels generally fit well about this line; however, because of well proximity to the Willamette River, some simulated hydraulic head

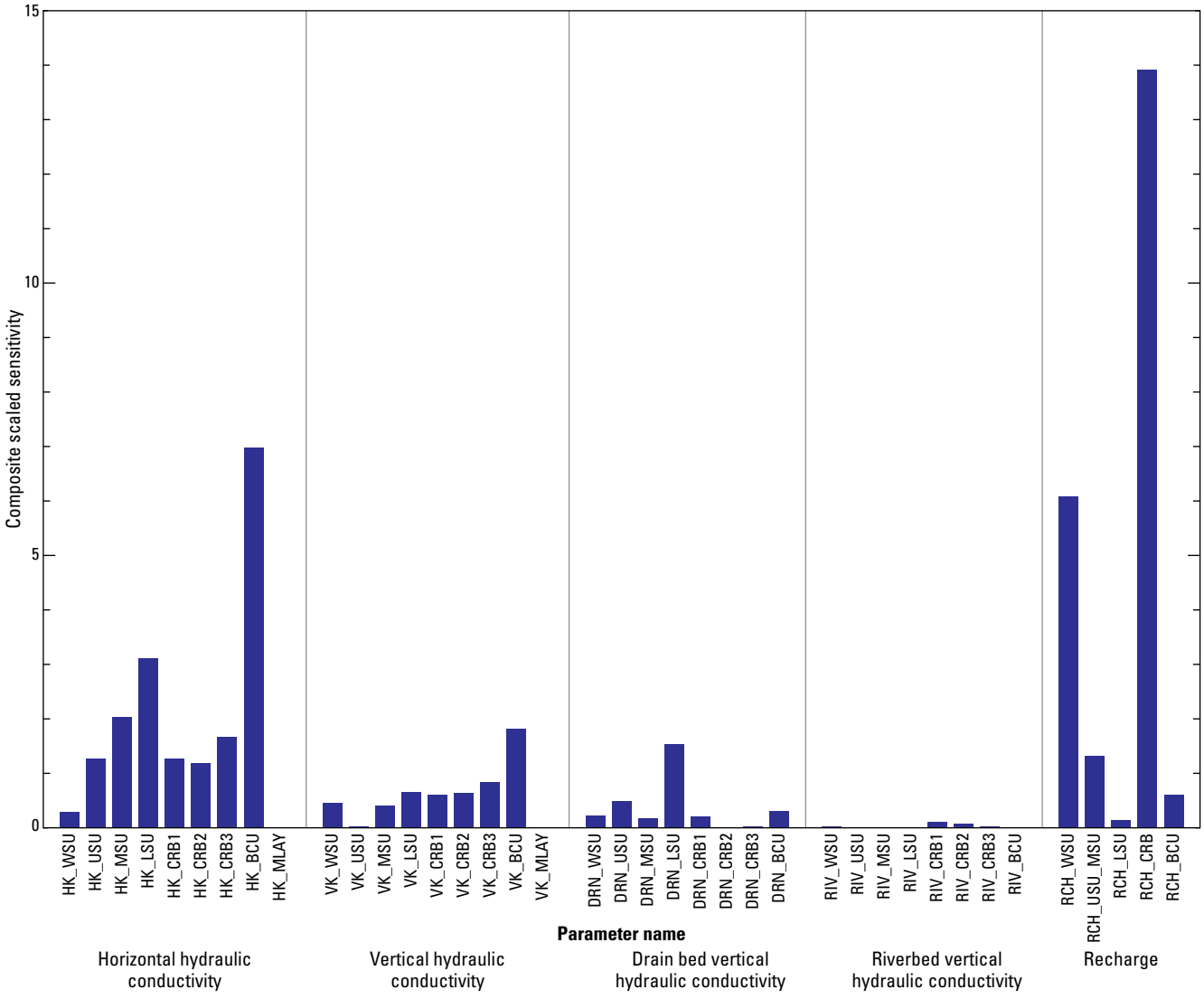

Figure 21. Composite scaled sensitivities of parameters for the local steady-state model of the Central Willamette subbasin, Willamette Basin, Oregon. Parameter names are defined in the section "Abbreviations and Acronyms."

values for the USU/MSU and LSU are 15–50 ft lower than measured levels (fig. 23). Simulated heads in these cells are controlled by the stage of a river and by model layers that are hydrologically well-connected to a river, whereas observation wells can be open to and representative of a relatively small part of a heterogeneous unit that is hydrologically poorly-connected to a river. Some measurement locations also coincide with model cells that have relatively large volumes of pumping, which can locally lower simulated heads. Similar to regional results, local CRB heads show a wide scatter in layer 7 (the third and thickest CRB layer), which reflects the difficulty of simulating mean annual groundwater levels in a complex hydrogeologic unit where groundwater level measurements are from wells completed at different depths and open to different interflow zones.

Local Steady-state Groundwater Flux and Budget

Because no independent data for groundwater discharge to streams were available for calibration of the local model, simulated fluxes from the local steady-state model for drainage basins within the modeled area (fig. 24) were compared with simulated flows from representative areas from the regional model (table 8). The purpose of the comparison was to confirm that the local model could produce similar discharge fluxes over a comparable area of the regional model. All simulated fluxes from the local model (except the Yamhill River) were within the same order of magnitude as the simulated fluxes from the regional model. Most local simulated fluxes were within 5 ft^3/s of regional simulated fluxes for comparable stream reaches. The largest discrepancy between local and regional simulated flux is in the lower Willamette Basin, where regional model results were 160.0 ft^3/s and local model results were 117.6 ft^3/s.

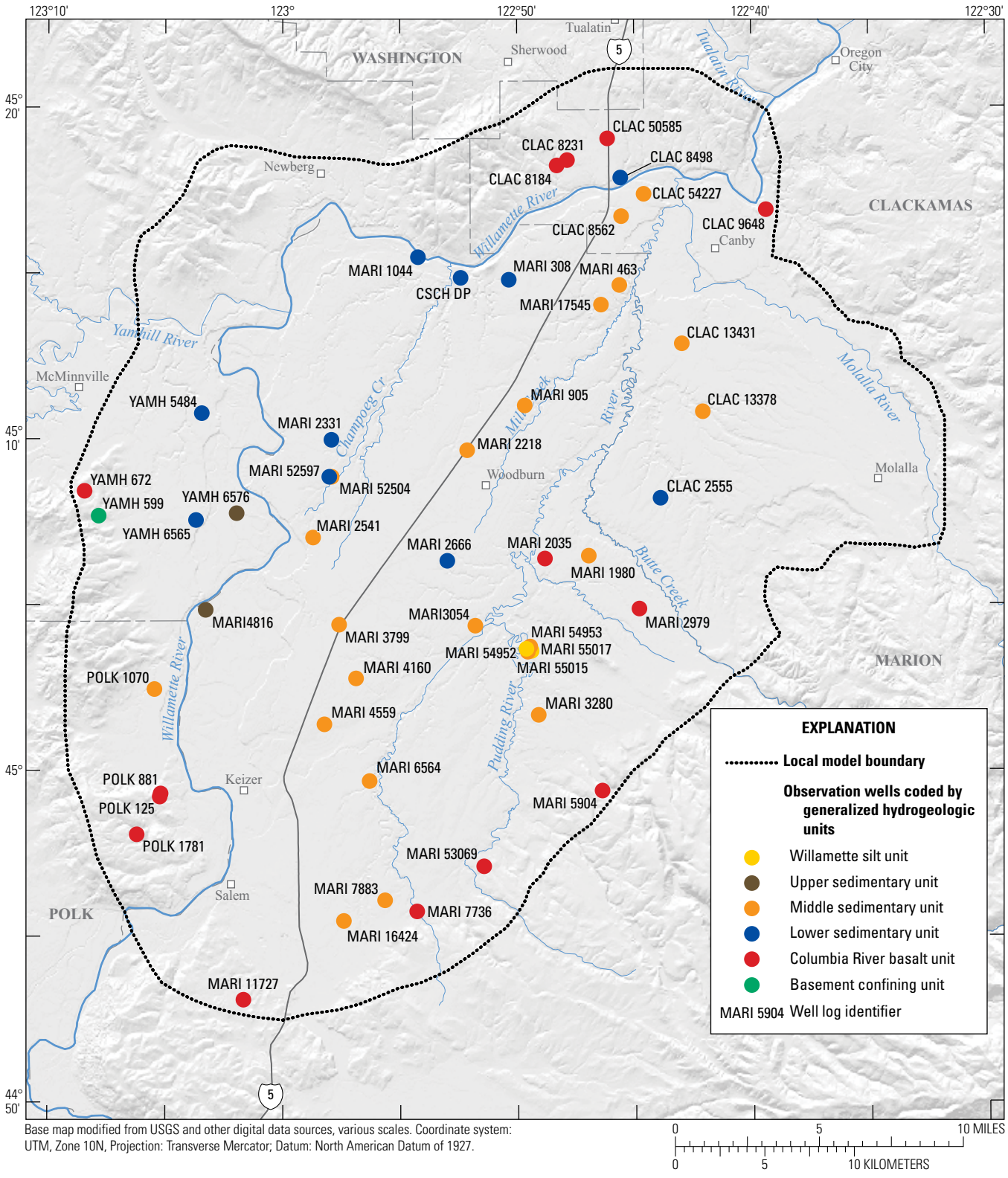

Figure 22. Distribution of observation wells used for calibration of the local steady-state model of the Central Willamette subbasin, Willamette Basin, Oregon, water years 1999–2000.

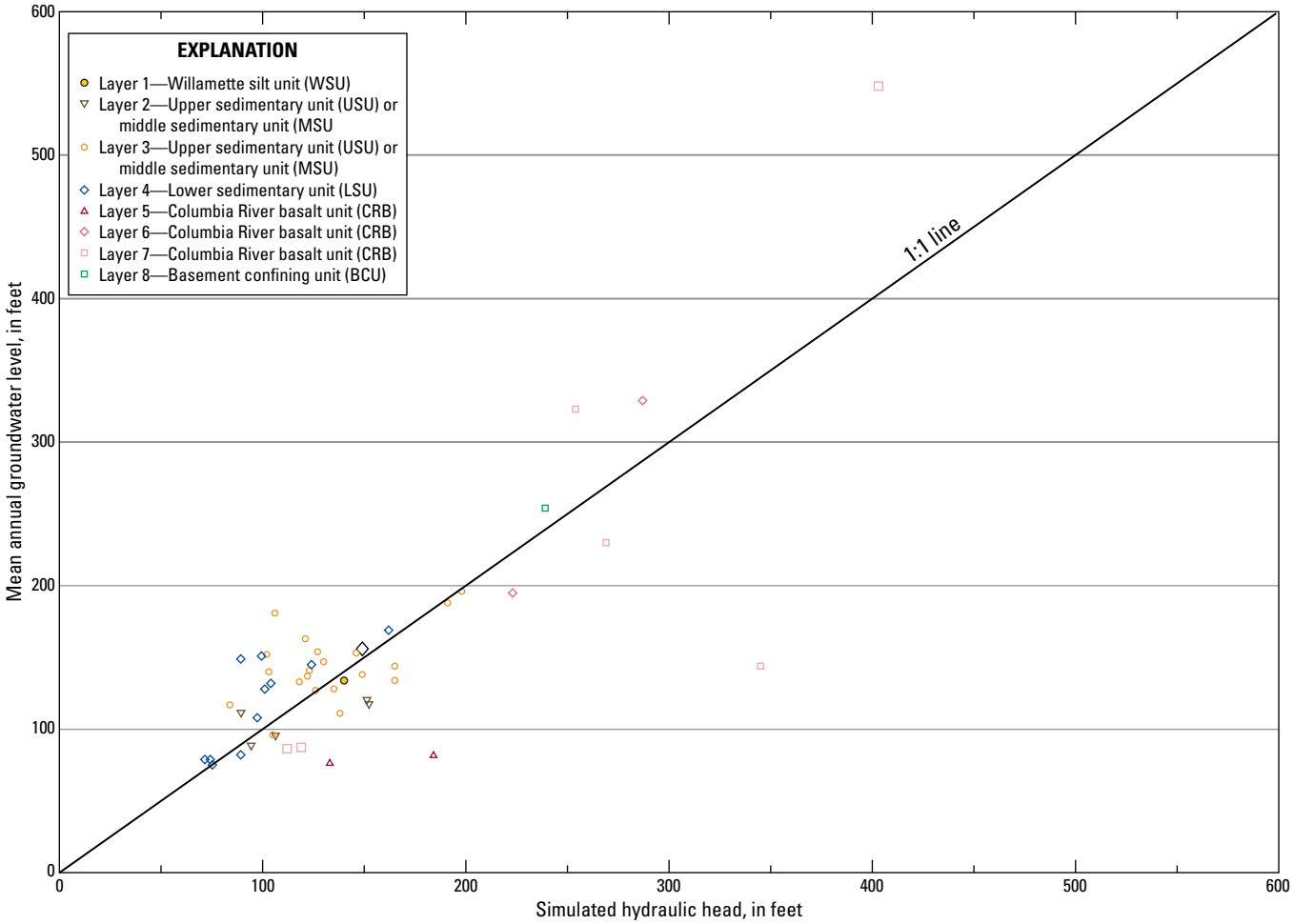

Figure 23. Simulated hydraulic head compared with mean annual groundwater levels for the local steady-state model, Central Willamette subbasin, Willamette Basin, Oregon.

The local steady-state model simulated water budget is summarized in table 5. The Central Willamette subbasin receives 72 percent of total recharge from precipitation and applied irrigation water, 27.7 percent from flux across the lateral model boundaries, and a small amount of seepage from streams. Groundwater leaves the basin predominantly through discharge to streams and wells, and a small amount to boundary flux (70.5, 28.3, and 1.2 percent, respectively). The high percentage of withdrawals from wells in the Central Willamette subbasin compared to withdrawals from wells in the entire Willamette Basin results from a higher concentration of population and irrigation relying on groundwater in this area than in the rest of the Willamette Basin.

The water budget values from the calibrated local steady-state numerical groundwater model (table 5) compares well with the budget values for the Central Willamette subbasin (table 1) from Conlon and others (2005). These values are comparable because the numerical and conceptual models are coincident in this subbasin. Well withdrawal and stream seepage values and percent of budget are similar in both models; differences are due to modifications to initial recharge calculations in the conceptual model.

Transient Calibration

Data and Procedure

The Central Willamette subbasin transient model calibration was done by adjusting storage terms for each hydrologic unit. The objective was to minimize differences between measured and simulated water levels for monthly stress periods during water years 1999–2000. The purpose of the calibration was to match short-term and seasonal water fluctuations over a 2-year period rather than long-term trends over many years or decades; hence, the relatively short (in years) calibration period. Water-level data inputs to the model were either point measurements for a particular day during a month or a monthly average of daily recorder well data. MODFLOW can interpolate the water level value at a relative location of a well within the cell and at a relative time during the simulation.

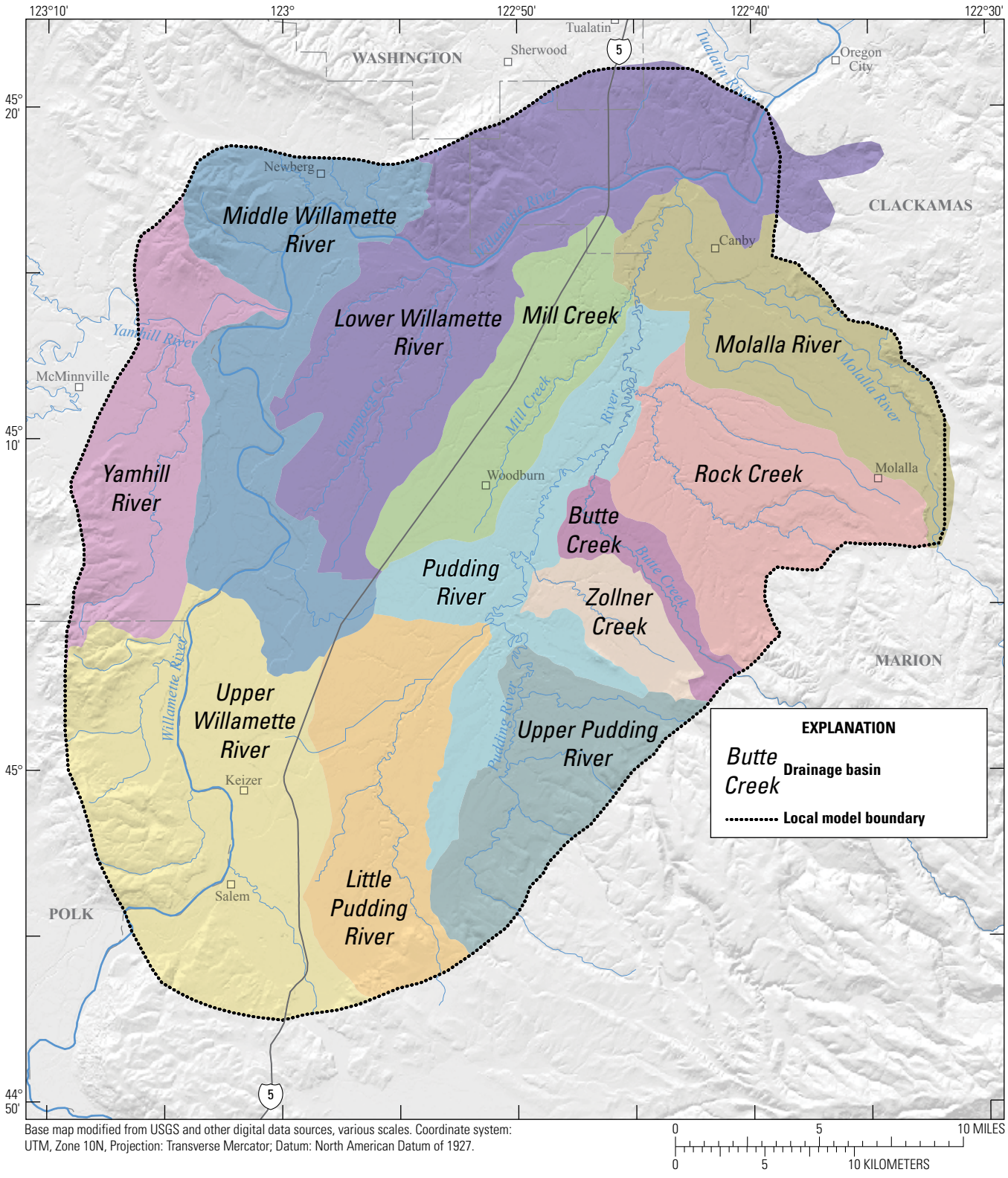

Figure 24. Drainage basins used in the simulation of groundwater-discharge fluxes in the local model of the Central Willamette subbasin, Willamette Basin, Oregon.

Transient model parameters are identical to the calibrated steady-state regional and local parameters except for the addition of specific-storage values (table 3). The added specific-storage terms for each hydrologic unit in the local transient model apply to the same zones as the hydraulic conductivity zones. Numerous model runs were completed and analyzed with a range of reasonable specific-storage values. Initial estimates were calculated using the average thickness for each hydrologic unit in the Central Willamette subbasin and reasonable values for storativity listed in Conlon and others, (2005, table 1).

The final selection of specific storage values during model calibration was accomplished by matching measured groundwater levels to simulated hydraulic heads. The specific storage value for the CRB was larger than initially anticipated, and was estimated from storage coefficient (storativity) values (4×10^{-4}–1×10^{-3}) from Conlon and others (2005, table 1) divided by average unit thickness. Most water-level measurements from wells in the Columbia River basalt are from upland areas near the boundaries of the Central Willamette subbasin. In the upland areas to the south and west, the Columbia River basalt pinches out and unit thickness decreases to zero. Because specific storage is uniform within each model unit, areas where the unit is thinner than average have a relatively small storage coefficient. Modeled areas where the unit is thicker than average have a relatively large storage coefficient. Because most CRB observation wells are in areas where the CRB is thin, the storage coefficient is relatively small, and simulated fluctuations in groundwater levels may be greater than measured. Otherwise, specific storage values generally decrease with depth.

The composite scaled sensitivities for the calibrated local transient model are shown in figure 25. Similar to the local steady-state model, recharge multipliers and the horizontal hydraulic conductivity of the BCU are the most sensitive parameters.

Comparison of Simulated and Measured Local Transient Heads

Data from 51 wells were used for calibration (fig. 22). Each hydrologic unit has at least one observation well open only to that unit; most wells are open to the MSU. Weighted residuals ranged from -70.0 to 53.2, with an average weighted residual of -1.4. Largest residuals occurred in the basalt upland areas. With the exception of some CRB wells, weighted residuals for the observation wells are distributed evenly around zero and generally show values that are independent, random, and normally distributed (fig. 26).

Simulated head values are weighted in part to minimize the influence of less accurate measurements. Plotting weighted residuals against weighted simulated values can display model bias in data sets (Hill and Tiedeman, 2007). About 20 percent of the observation wells used for the transient model show an elevation bias where weighted head residuals decrease (or become more negative) as weighted simulated head values increase. Of the 10 observation wells that show this bias, 1 is a BCU well and 6 are CRB wells near the boundaries of the local model. One well is open to the LSU where layers 2 and 3 are absent, and the two other wells are open to the USU where layers 2 and 3 are thin (about 20 ft or less). The sedimentary-unit observation wells display groundwater levels that do not change much from month to month (stress period to stress period), but are simulated as having greater fluctuations in water levels than measured during the calibration period. Because of this, head residuals increase when simulated water levels rise and decrease when simulated water levels decline. Implementing a uniform specific-storage value in a hydrologic unit can lead to simulated water-level fluctuations that are greater than measured water-level fluctuations where the unit is thinner than the average thickness of the unit. These particular sedimentary-unit observation wells may have a good hydrologic connection to a surface water body resulting in damped water-level fluctuations, which is not simulated in the model.

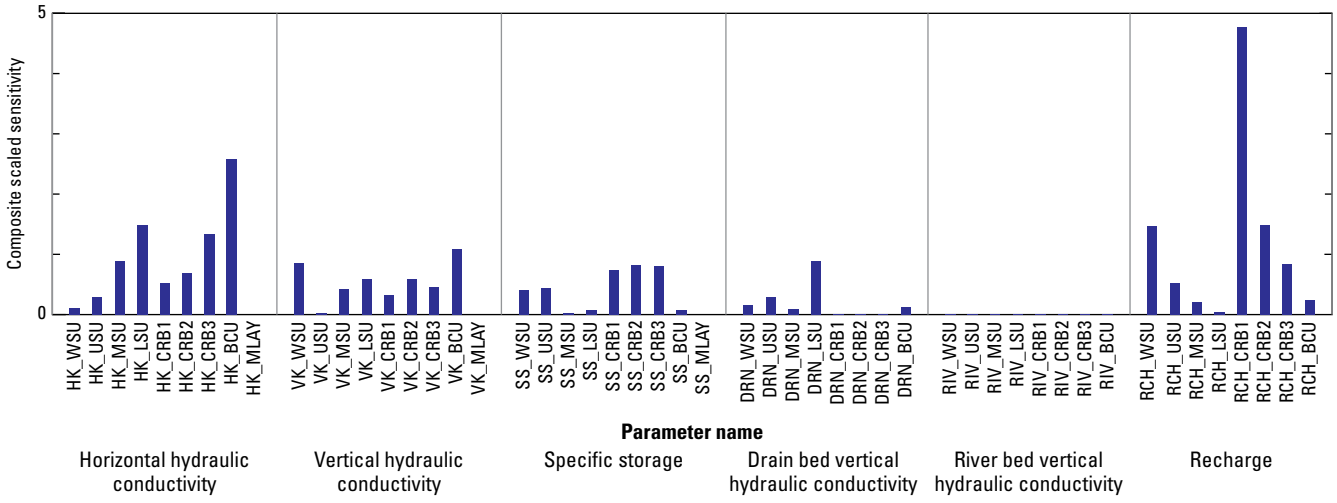

Figure 25. Composite scaled sensitivities of parameters for the local transient model of the Central Willamette subbasin, Willamette Basin, Oregon. Parameter names are defined in the section "Abbreviations and Acronyms."

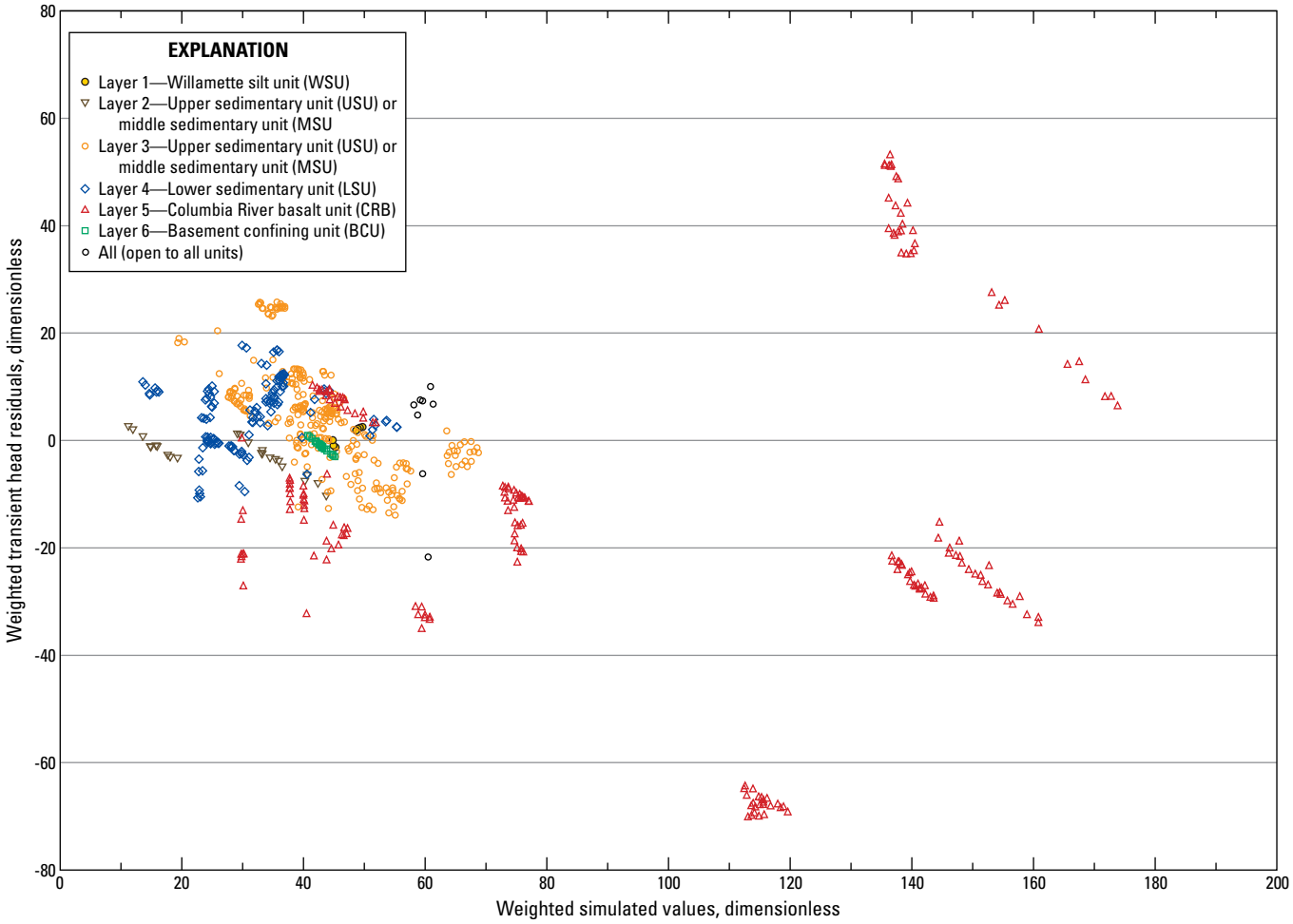

Figure 26. Weighted transient head residuals as a function of weighted simulated values for the local model of the Central Willamette subbasin, Willamette Basin, Oregon.

Fluctuations in water levels in the Central Willamette subbasin may be attributable to long-term climate cycles. The slight decline in measured and simulated water levels from water year 1999 to water year 2000 reflects the decrease in precipitation represented in the downward trend of the cumulative departure from average precipitation curve shown in figure 3.

Minimal data were available for wells in the WSU (layer 1). Two wells (06S/01W-08DAD04 and 06S/01W-08DAD06) provided short-term data for groundwater levels at the end of the calibration period, and simulated heads were within 8 ft or less of measured water levels. Well 06S/01W-08DAD04 (MARI 54953) (fig. 27*A*) is a representative observation well open to the WSU; simulated heads in this well display minimal seasonal variation in this location in the Central Willamette subbasin. Two wells (05S/03W-22AAA and 06S/03W-04ACD) provide data for groundwater levels in the USU, where the unit is relatively thin (32 ft thick or less, both layers 2 and 3 combined). Simulated heads for well 05S/03W-22AAA (YAMH 6576) (fig. 27*B*) are similar to measured water levels. However, the larger fluctuations in simulated heads relative to measured water levels likely are due to the assumption of a confined aquifer and a relatively small simulated storage coefficient in an area where unconfined flow conditions exist.

In layers 2 and 3, 22 observation wells represented groundwater levels in the MSU. Elevation of groundwater levels and the timing, and magnitude of water-level fluctuations of simulated heads and measured groundwater levels match well (9 of the 22 MSU wells are shown in fig. 27*C*). Only two wells show significant differences between the observation well hydrograph and the simulated hydrograph. Well 03S/01W-24DDD01 (CLAC 54227) appears to be an anomaly and might be influenced by nearby pumping or irrigation. Other nearby wells do not show the same pattern. Simulated heads for well 03S/01W-25CBD (CLAC 8562) decline by about 50 ft during August–September compared to measured declines of 1–4 ft; however, measured groundwater levels are point measurements made quarterly to bimonthly and normally at a time when the groundwater levels in the well are static. Because a well with significant pumping during the summer is in the same cell as the observation well, the simulation captured the seasonality of groundwater levels that was not captured by a quarterly or bimonthly well measurement.

Observation wells 05S/02W-01DDA, 04S/01W-32ADB, and 06S/01W-21CDC01 (MARI 2218, MARI 905, and MARI 3280) were assigned to the MSU, and display groundwater levels that likely are a composite of both the MSU and the top of the LSU. Simulated head and measured water levels are similar, although the amplitude of the measured water-level fluctuations is greater. The difference in amplitude is more evident for observation well 06S/01W-21CDC01, which is in an area simulated with less intensive irrigation pumping than the other two observation wells. This disparity indicates that the model does not include all pumping that was occurring during the calibration period.

Ten observation wells were available to calibrate water levels in the LSU, and simulated fluctuations match measured fluctuations well in both timing and magnitude for most of these wells (4 of the 10 LSU wells are shown in fig. 27*D*). Simulated heads in the LSU often reflect a composite water level for the entire unit rather than water levels measured at a specific depth interval, which are directly influenced by pumping during the irrigation season and the limited open interval of the observation well.

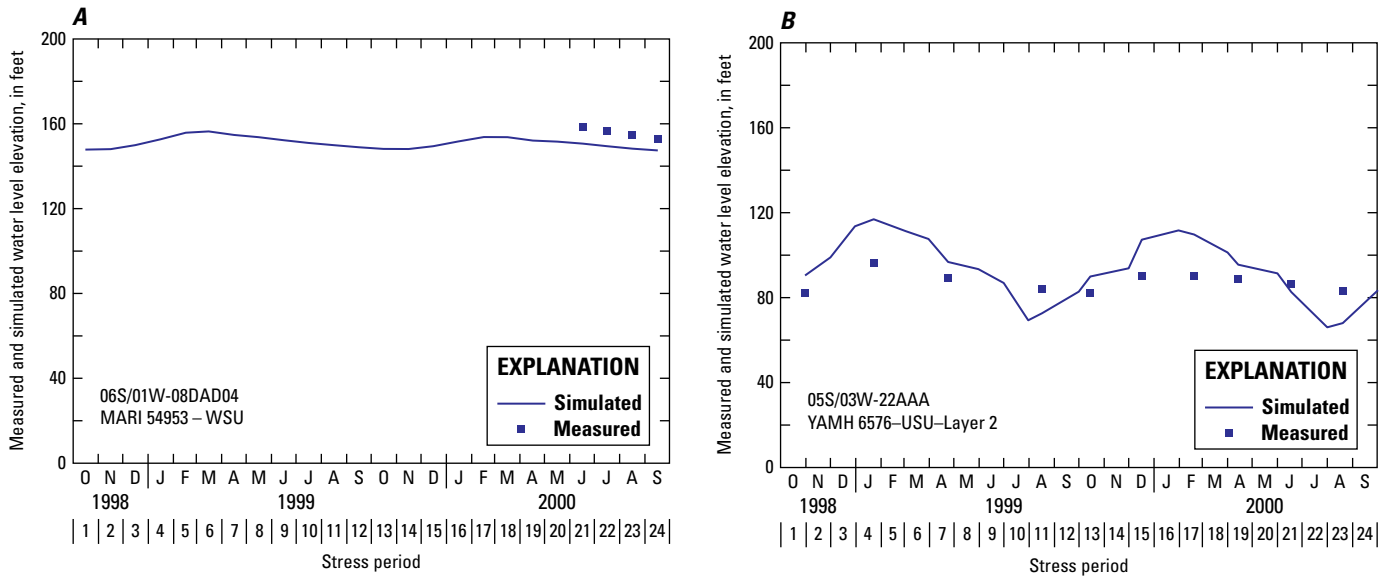

Figure 27. Simulated heads and measured groundwater-level fluctuations in (*A*) Willamette silt unit, (*B*) upper sedimentary unit, (*C*) middle sedimentary unit, (*D*) lower sedimentary unit, (*E*) Columbia River basalt unit, and (*F*) basement confining unit for the Central Willamette subbasin, Willamette Basin, Oregon.

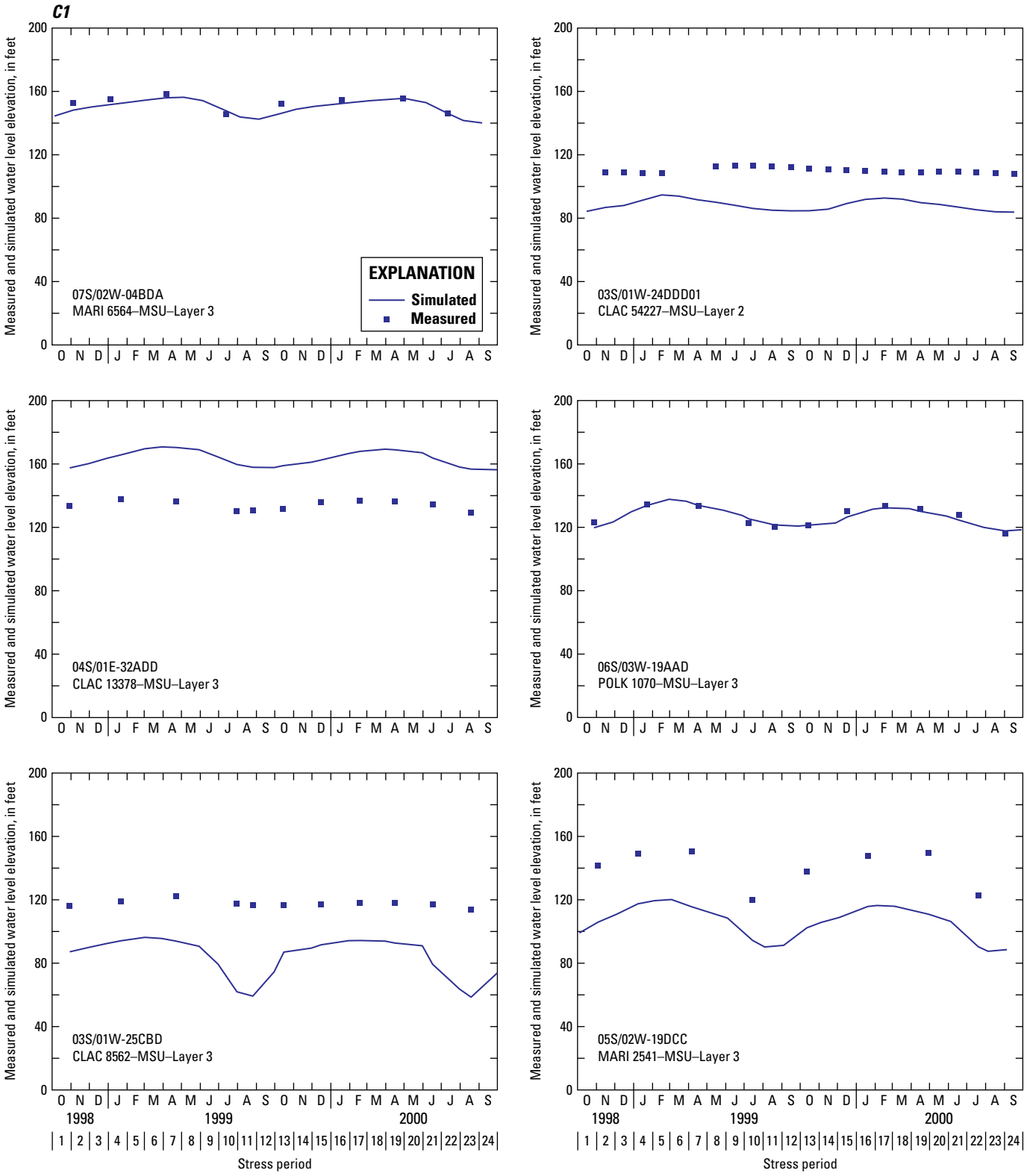

Figure 27.—Continued

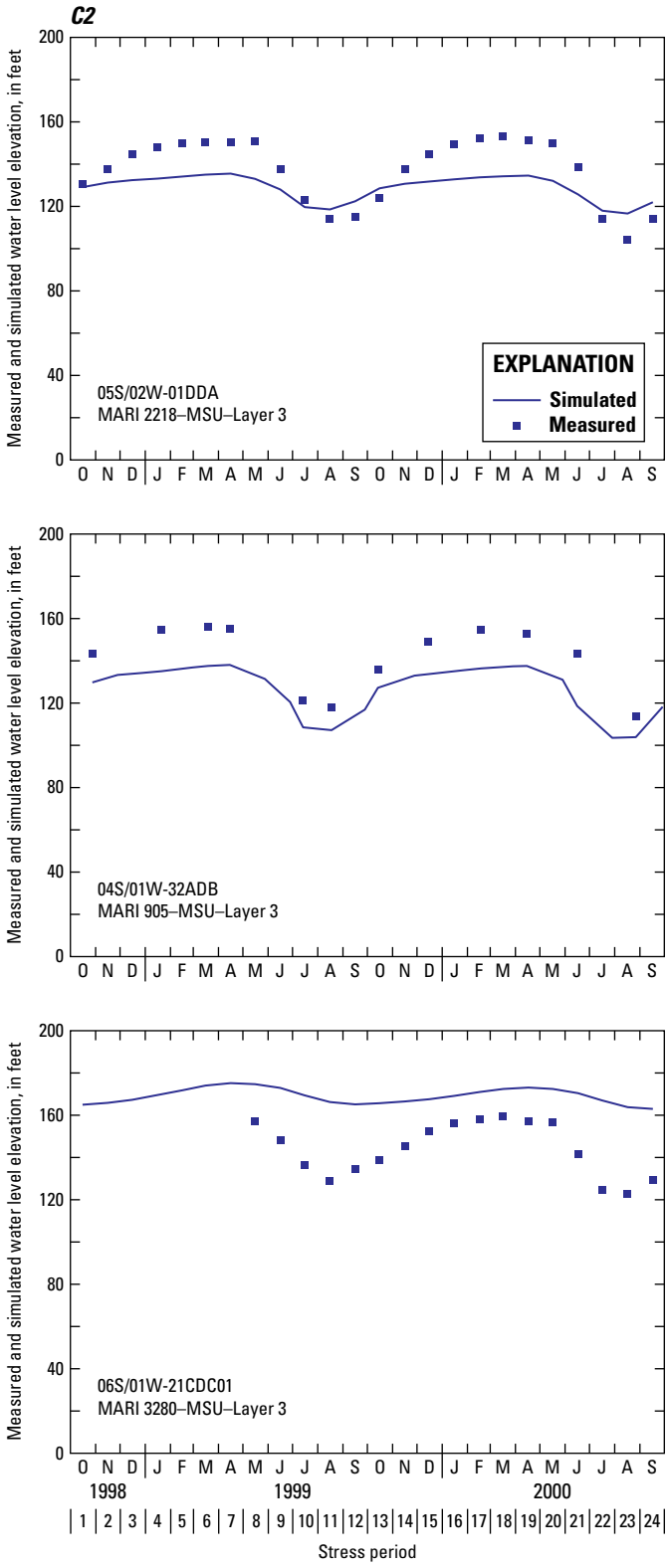

Figure 27.—Continued

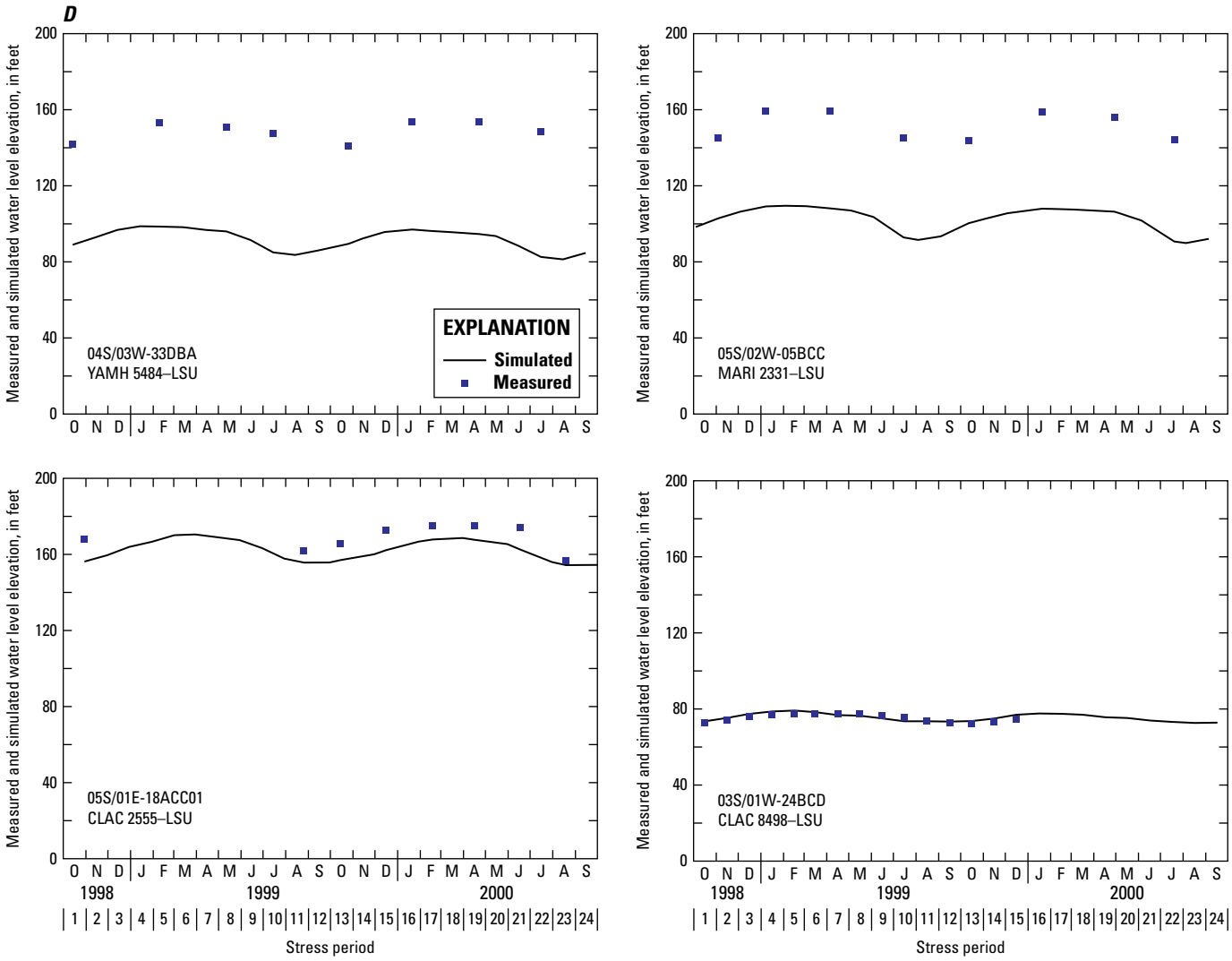

Figure 27.—Continued

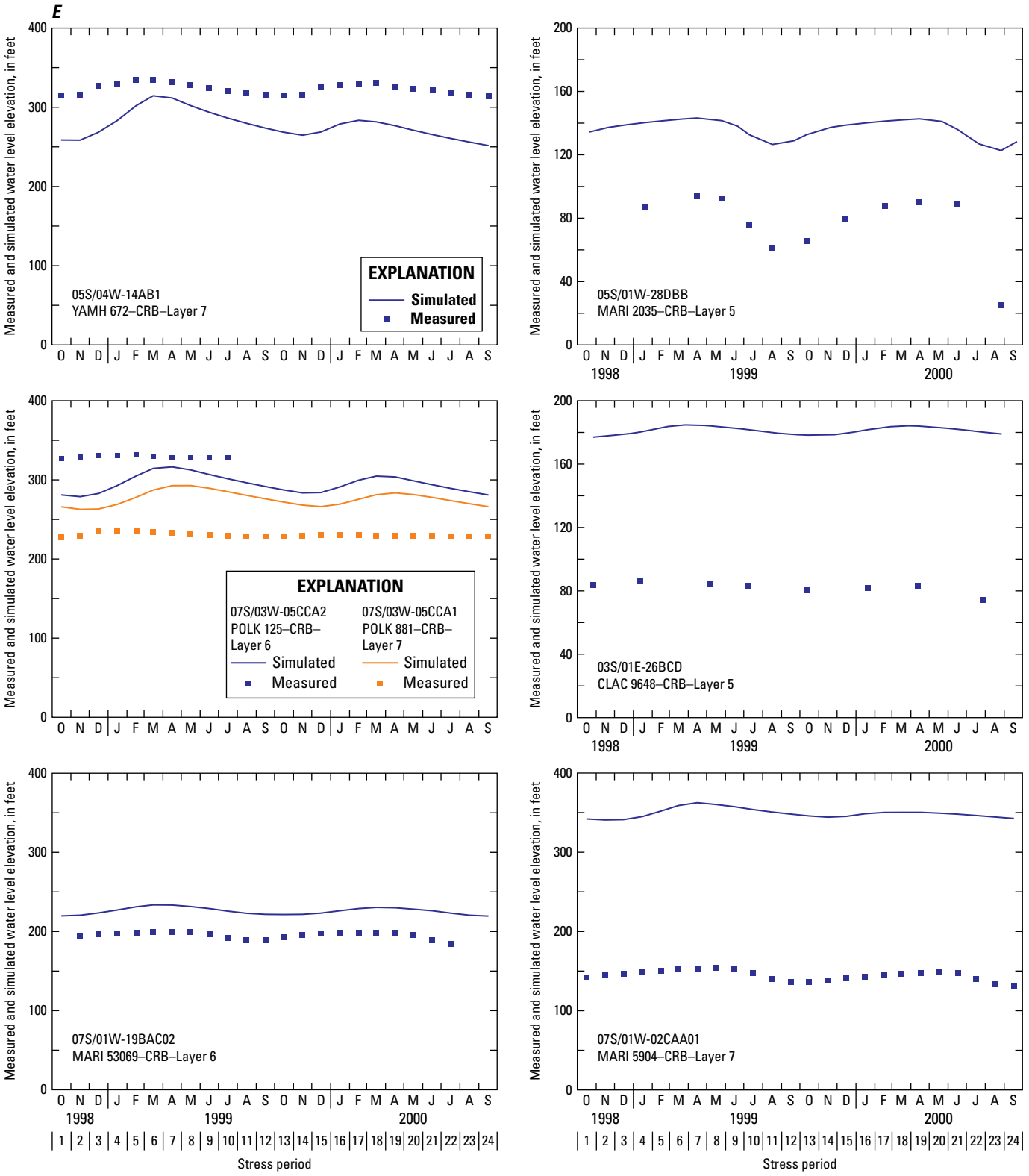

Figure 27.—Continued

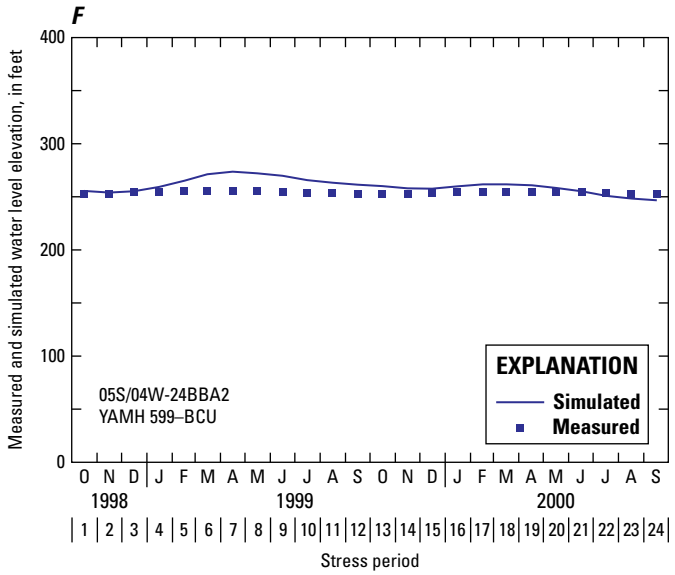

Figure 27.—Continued

Layers 5, 6, and 7 represent the CRB. Thirteen observation wells provided data for the three modeled layers. Three wells are open to multiple basalt layers, two are open only to layer 5, two are open only to layer 6, and six are open only to layer 7. Six of the 13 wells are shown in figure 27E. Simulation results in areas where basalt layers are thin display hydraulic heads that are affected by the assignment of an average specific storage value. This can be seen in an observation well open to layer 7, 05S/04W-14AB1 (YAMH 672), where measured groundwater levels and simulated heads are similar; however, simulated fluctuations in head are greater than the measured value.

The model provides good matches to measured water-level patterns in the upper CRB in layer 5 in an area of shallow horizontal gradients in the lowland. Wells, 05S/01W-28DBB (MARI 2035) and 03S/01E-26BCD (CLAC 9648) show the effects of seasonal pumping (water-level decline). Simulated heads for wells 07S/01W-19BAC02 (MARI 53069, layer 6) and 07S/01W-02CAA01 (MARI 5904, layer 7) show similar seasonal fluctuations; however, measured water levels indicate influence from summer pumping (minimum water levels during summer), whereas simulated heads reflect seasonal effects (minimum water levels during late autumn). This difference indicates a local pumping signature not captured by the simulation and is an example of the inability of the model to simulate local conditions, though general trends in the study area are well simulated. Magnitude and direction of gradient are compared with simulated data where two wells are in close proximity in an upland area: CRB wells 07S/03W-05CCA2 (POLK 125, layer 6) and 07S/03W-05CCA1 (POLK 881, layer 7). Measurements indicate a downward gradient in the CRB, with a difference in water levels of about 100 ft. The simulation indicates a downward gradient between layer 6 and 7 with a difference of about 20 ft in hydraulic heads. The difference in simulated heads and measured groundwater levels and gradients may reveal natural variability in horizontal and vertical conductivity in the CRB. Simulated hydraulic heads for observation well 05S/04W-24BBA2 (YAMH 599), completed in the BCU, are nearly identical to measured groundwater levels (fig. 27*F*); however, simulated fluctuation magnitudes are greater than measured and can be attributed to the influence of a nearby irrigation well open to the BCU.

Local Transient Model Groundwater Flux and Budget

Groundwater discharge to streams (base flow) was simulated for 12 stream groupings in the Central Willamette subbasin (table 9). Although independent measurements were not available for comparisons, the simulated temporal variations and volume in groundwater discharge to streams in the basin appeared reasonable. Conlon and others (2005) described the discharge to streams flowing on the WSU as small relative to streamflow due to the low hydraulic conductivity of the WSU. Simulated transient flow to streams supports this conclusion. Groundwater discharge to streams for stream groupings flowing entirely on the WSU (Pudding River, Zollner Creek, and Mill Creek) is substantially less than stream groupings primarily flowing on other hydrogeologic units (Molalla River, upper Willamette River, and middle Willamette River) (table 9). Additionally, a comparison of simulated groundwater discharge (base flow) to Zollner Creek and measured streamflow in the creek shows that discharge to streams is small relative to streamflow, except during summer, when streamflow is small and groundwater discharge is the primary source of streamflow (fig. 28). Simulated and measured flows decreased during the second year, which reflects the decrease in recharge during that time.

Seasonal variations in flow are apparent in a comparison of simulated head gradients in typical summer and winter stress periods (fig. 29). During summer, discharge is restricted to areas near streams, whereas during winter the contribution area of discharge to streams is more widespread. In winter, groundwater mainly flows downward through the sedimentary units and the top of the CRB, signifying recharge; however, locally, groundwater in the WSU, USU, and MSU discharges to streams flowing on those units. During summer, a downward head gradient occurs in the WSU and MSU, except near streams, where the direction of flow is primarily upward from lower units to the MSU and LSU, and the lower Pudding and Willamette Rivers. The gradient is also reversed where there is substantial pumping in the lower MSU. In other areas, the downward gradient between the MSU and LSU is maintained throughout the summer. Model simulation results show that small streams flowing on the WSU are hydrologically disconnected from the MSU and LSU because there is little discharge from underlying units to these streams in any season.

Table 9. Simulated transient groundwater flow to streams in the Central Willamette subbasin, Willamette Basin, Oregon, water years 1999–2000.

[Streams are simulated as drains and rivers; drainage areas in parentheses. All values are in cubic feet per second. Highlighted stream groupings flow entirely on the Willamette silt unit. **Abbreviation**: mi^2, square mile]

Stress period	Calendar year	Month	Upper Willamette River ($103\ mi^2$)	Middle Willamette River ($78\ mi^2$)	Lower Willamette River ($119\ mi^2$)	Upper Pudding River ($43\ mi^2$)	Pudding River ($51\ mi^2$)	Little Pudding River ($55\ mi^2$)	Zollner Creek ($15\ mi^2$)	Butte Creek ($13\ mi^2$)	Rock Creek ($57\ mi^2$)	Mill Creek ($41\ mi^2$)	Molalla River ($57\ mi^2$)	Yamhill River ($49\ mi^2$)
Water year 1999														
1	1998	October	63	96	104	11	10	5.3	0.2	2.2	13	1.0	35	3.8
2		November	71	100	106	12	0.7	6.3	0.3	4.0	17	0.9	36	3.6
3		December	97	119	111	16	0.4	9.7	0.6	7.5	23	0.4	32	8.5
4	1999	January	114	126	122	20	1.6	15	1.2	9.4	26	2.0	43	5.7
5		February	145	152	132	25	8.6	17	1.8	11	29	2.5	55	13
6		March	120	137	132	25	20	16	1.8	9.9	28	3.0	54	12
7		April	95	119	126	22	24	11	1.5	6.5	23	2.6	52	11
8		May	79	103	119	18	17	10	1.1	6.2	22	2.3	48	11
9		June	70	90	115	17	19	9.0	0.8	4.1	19	1.9	44	10
10		July	54	70	111	16	16	8.2	0.5	3.2	17	1.6	38	9.2
11		August	52	69	105	14	14	6.9	0.3	2.6	15	1.3	36	8.7
12		September	58	81	105	13	13	6.0	0.3	2.3	14	1.1	37	8.6
Water year 2000														
13	1999	October	66	97	106	13	13	5.9	0.3	2.4	14	1.1	39	8.6
14		November	65	97	104	11	0.6	5.4	0.3	3.5	17	0.7	34	3.6
15		December	90	115	115	15	0.7	8.6	0.6	5.9	21	1.1	42	4.0
16	2000	January	111	129	127	19	8.4	14	1.1	9.2	26	2.5	52	5.8
17		February	122	131	128	21	16	14	1.3	8.9	26	2.4	53	6.8
18		March	101	120	126	22	21	12	1.4	7.9	25	2.7	54	7.9
19		April	84	110	120	18	22	9.7	1.0	4.8	20	2.3	50	8.9
20		May	75	100	116	16	15	9.0	0.9	4.8	20	2.0	45	8.0
21		June	62	83	112	15	17	7.7	0.6	3.3	17	1.6	41	7.6
22		July	48	65	106	14	16	7.0	0.4	2.7	15	1.5	37	7.4
23		August	45	63	104	13	14	5.8	0.3	2.1	14	1.2	35	7.1
24		September	54	78	104	12	12	4.9	0.2	1.9	13	1.1	36	7.1

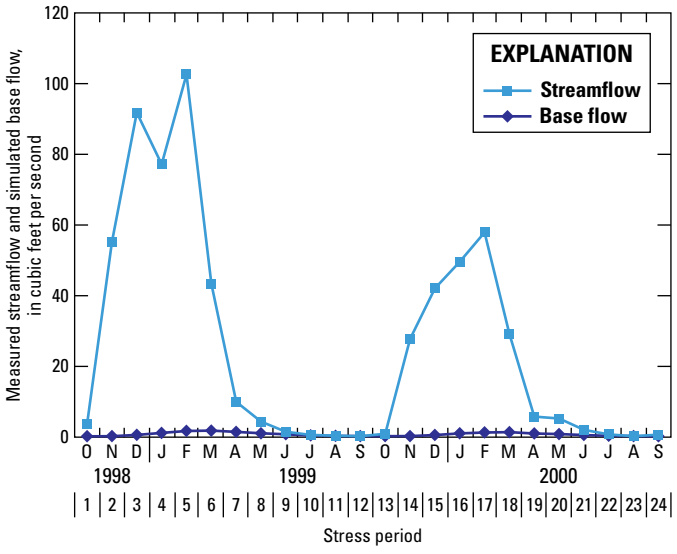

Figure 28. Monthly mean measured streamflow and simulated groundwater discharge (base flow) to Zollner Creek, Central Willamette subbasin, Oregon.

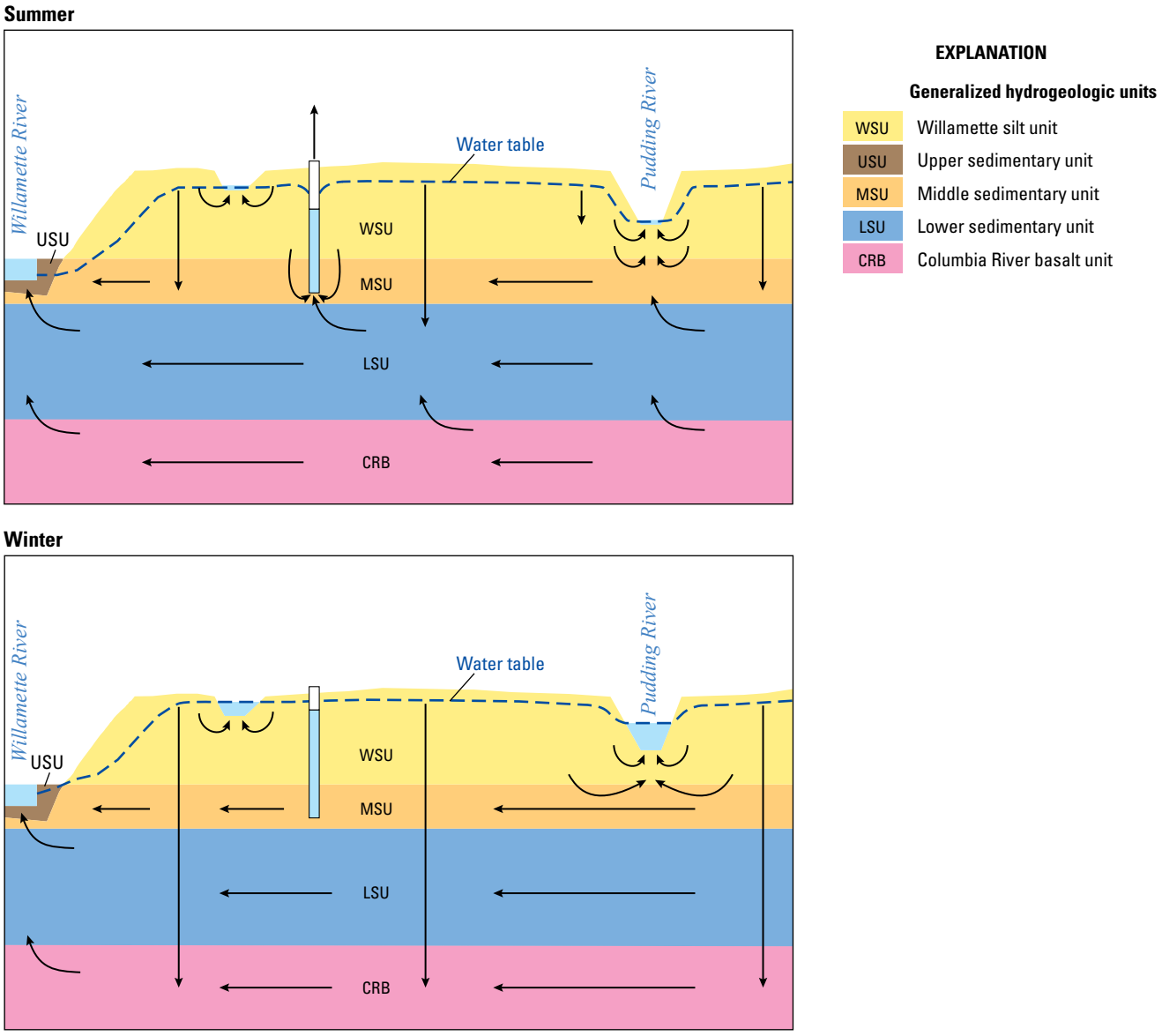

Figure 29. Simulated seasonal change in groundwater flow in the Central Willamette subbasin, Willamette Basin, Oregon.

Seasonal variations in budget terms for water years 1999–2000 are shown in figure 30 and table 10. Base flow during late autumn markedly decreases in streams that flow primarily on the WSU (table 9), as most recharge replenishes groundwater storage. Because average monthly recharge decreased (by 143 ft^3/s) and average monthly pumping increased (by 5 ft^3/s) from water year 1999 to water year 2000 during the 2-year calibration period, there was a net decrease in storage. The decrease manifests as a reduction in water levels and a decrease in streamflow primarily in the upper and middle Willamette River stream groupings (table 9). Average monthly discharge to drains and rivers for the Central Willamette subbasin decreased by about 22 ft^3/s from water year 1999 to water year 2000 (table 10; fig. 31*A*–*B*).

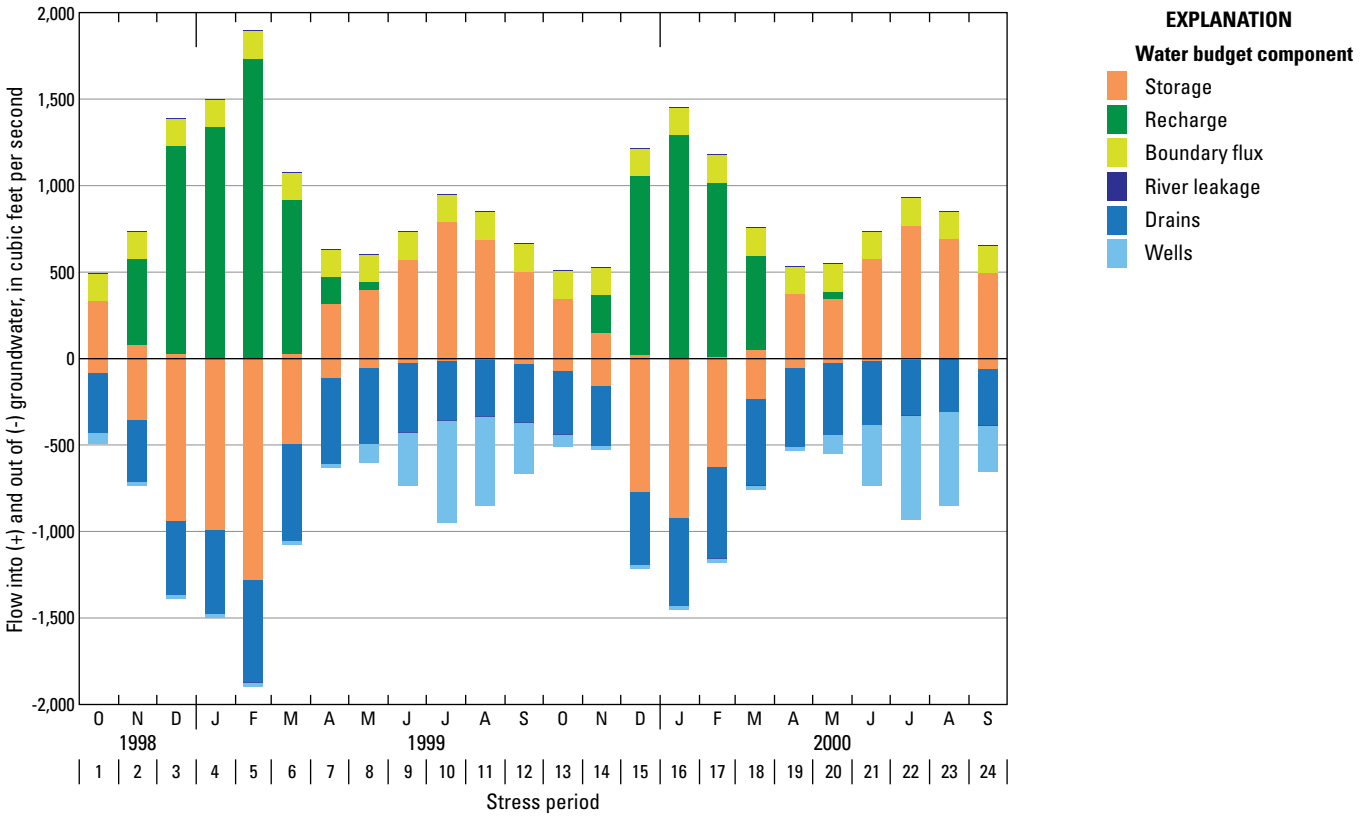

Figure 30. Simulated local model water budget by stress period and budget components for the Central Willamette subbasin, Willamette Basin, Oregon, water years 1999–2000.

Model Limitations

The regional and local models simulate groundwater levels and flows within the boundaries of the Willamette Basin and Central Willamette basin, respectively. The models primarily are intended to provide information for water management decisions and not necessarily to replicate water levels and flows at a specific location. Modeled areas were divided into cells either 7,000 ft (regional) or 1,000 ft (local) on a side, and the properties within each cell are assumed uniform and homogeneous over an area of about 1,125 acres (1.76 mi^2) for the regional model and about 23 acres (0.04 mi^2) for the local model. Evapotranspiration from the saturated zone was assumed not to be an important component of groundwater discharge in the Willamette Basin and was not simulated. Additionally, land subsidence due to primary and secondary consolidation is not included in the model, nor are the potential effects on land surface infrastructure and hydraulic response of the sedimentary units (Bear, 1979). The model simulations presented herein are only approximations to actual occurrences within the study area. Overall, the models replicate groundwater levels, flow, and gradients regionally, in the Willamette Basin, and locally, in the Central Willamette subbasin.

The regional Willamette Basin model simulation uses time-averaged data from water years 1995 and 1996. Pre-development information was not available to establish a true steady-state model; therefore, a dynamic average steady-state condition, where recharge and discharge are balanced and head varies spatially, was simulated for the regional model. This same protocol was used to simulate a dynamic average steady-state condition for the local model, using water-level data from water years 1999 and 2000 and boundary flux data from the regional model. The heads

Table 10. Simulated transient model water budget for each stress period for the Central Willamette subbasin, Willamette Basin, Oregon, water years 1999–2000.

[All values are in cubic feet per second]

Stress period	Calendar year	Month	Storage			Recharge	Boundary flux			Stream leakage				Wells
			Into model from storage	Out of model to storage	Net change in storage	In	Into model from boundary flux	Out of model to boundary flux	Net boundary flux into model	Into model from river	Out of model to river	Out of model to drains	Net out of model	Out
Water year 1999														
1	1998	October	333	83	250	0	159	7	152	2	2	347	347	55
2		November	78	356	-279	497	159	7	152	2	2	358	358	12
3		December	30	942	-911	1,198	159	7	152	2	2	425	426	13
4	1999	January	6	991	-985	1,333	159	7	152	2	3	487	488	12
5		February	1	1,280	-1,279	1,734	159	7	152	2	3	594	595	13
6		March	26	497	-471	891	159	7	152	2	3	559	560	13
7		April	319	113	206	152	159	7	152	1	3	495	497	13
8		May	401	58	344	41	159	7	152	1	3	437	438	99
9		June	573	28	545	0	159	7	152	1	2	401	402	295
10		July	789	13	776	0	159	7	152	2	2	346	346	582
11		August	688	8	680	0	159	7	152	2	2	328	328	504
12		September	502	29	473	0	159	7	152	1	2	342	342	283
Water year 2000														
13	1999	October	348	71	277	0	159	7	152	2	2	369	369	60
14		November	151	163	-12	217	159	7	152	2	2	344	344	13
15		December	23	775	-752	1,031	159	7	152	2	2	418	419	12
16	2000	January	5	925	-919	1,288	159	7	152	2	3	508	509	12
17		February	6	625	-619	1,011	159	7	152	2	3	531	532	12
18		March	49	232	-184	547	159	7	152	2	3	502	503	12
19		April	374	60	314	0	159	7	152	1	3	452	453	14
20		May	348	29	318	41	159	7	152	2	3	414	415	97
21		June	575	14	561	0	159	7	152	2	2	370	370	342
22		July	770	7	762	0	159	7	152	2	2	322	323	592
23		August	692	5	686	0	159	7	152	2	2	304	305	534
24		September	494	61	433	0	159	7	152	2	2	326	327	258

from the local model steady-state simulation were used to provide starting heads for the local transient model. Any discrepancies resulting from the propagation of transient effects of the specified initial conditions were mitigated by extending the period of the model run to 50 years before it was used to simulate prescribed management scenarios. Monthly water-level data from water years 1999 and 2000 were time averaged to construct a 50-year transient simulation with monthly stress periods to evaluate management scenarios.

Division of the model into distinct layers defining deposits of differing hydraulic properties is a simplification of the characteristics of the deposits. Transitions between the sedimentary deposits probably are more gradual and depend on the depositional environment at the time the deposit was emplaced. Water levels in the model area likely reflect hydraulic properties of coarse-grained material because most wells tend to be screened in more permeable deposits, as discussed in particular in sections "Hydrogeologic Units" and "Final Parameter Values" pertaining to the LSU. Basalt in the Willamette Basin consists of stacked basalt flows, generally 40–100 ft thick with dense flow interiors between more permeable interflow zones. The CRB was generalized to a single unit layer in the regional model and partitioned into three layers in the local model.

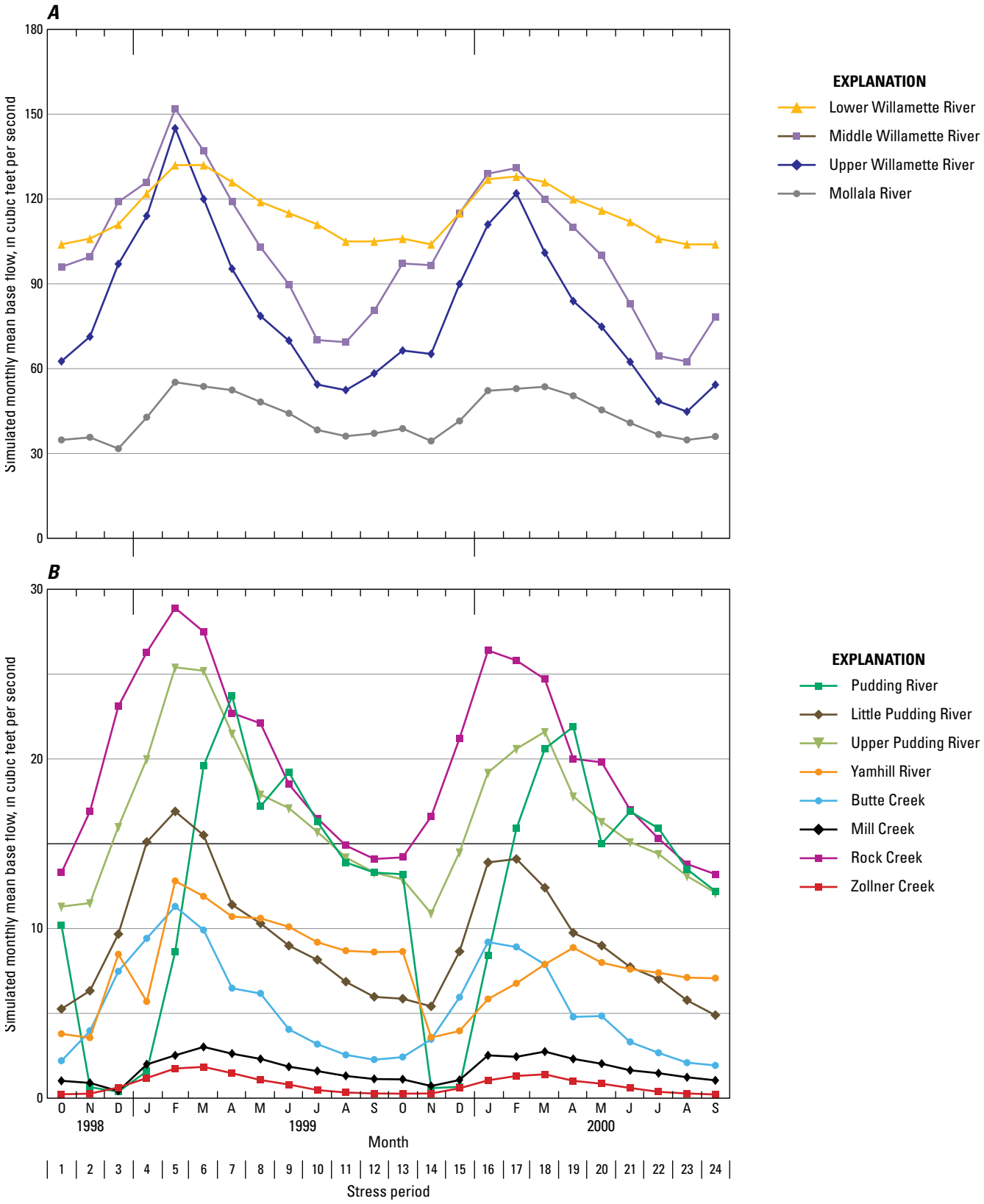

Figure 31. Simulated monthly mean base flow by stress period for (*A*) large and (*B*) small stream basins in the Central Willamette subbasin, Willamette Basin, Oregon, water years 1999–2000.

Simulations reflect general responses to stresses. The simulations are estimates and do not necessarily accurately represent measured conditions at a specific location. For example, in the northwest area of the Central Willamette subbasin, wells 05S/02W-08CCA2 (MARI 52504, MSU, layer 3) and 05S/02W-08CCB1 (MARI 52597, LSU, layer 4) (fig. 32) are located in an area of simulated upward flow during summer that is in close proximity to an area with simulated downward flow. The measured water levels indicate a downward gradient from the MSU to the LSU in all seasons, whereas the simulation indicates an upward gradient from the LSU to the MSU during summer, induced by pumping in the MSU. Because water-level measurements usually are made when water levels are static, measured monthly water levels might not capture the instantaneous effects of pumping during summer and the simulation may more closely resemble actual water levels in the aquifers. Simulated unit thicknesses are a thin layer of MSU (14 ft) and a thick layer of LSU (1,200 ft) in this area. Additionally, a review of well logs for wells 05S/02W-08CCA2 and 05S/02W-08CCB1 indicated the presence of permeable sands and gravels that allow for high well yield, which occur in locations where a gradational unit boundary between the MSU and LSU is present in the Central Willamette subbasin. Measured water levels in these wells may be more representative of hydrologic conditions at this gradational unit boundary rather than either the MSU and LSU individually, and are an example of downward flow known to occur in basin-fill sediments (Conlon and others, 2005).

Because simulated specific storage values do not change as the thickness of the units change in the local model, the storage coefficient will vary as the thickness of the unit varies. This limitation affects model simulation results primarily where sedimentary units pinch out and around the perimeter of the study area, where CRB thickness decreases abruptly at flow margins. The result is a relatively small storage coefficient and greater water-level fluctuations during the simulation than is indicated by measured groundwater levels. Additionally, large vertical head gradients and the complex geometry of the basalt limit characterization of groundwater flow in upland areas of the basalt aquifer system.

The lateral boundary for the local model was generally specified as a no-flow boundary because the boundary is at the topographic crest of surrounding upland areas or where sedimentary units pinch out in the basin. In areas where lateral flux across the model boundary was simulated in the regional steady-state model, the flux was specified as a constant flux using the WELL package. These assumptions were considered valid for conditions in the basin during the simulation period (water years 1999–2000); however, each assumption should be reviewed if simulating conditions that differ from an average water year.

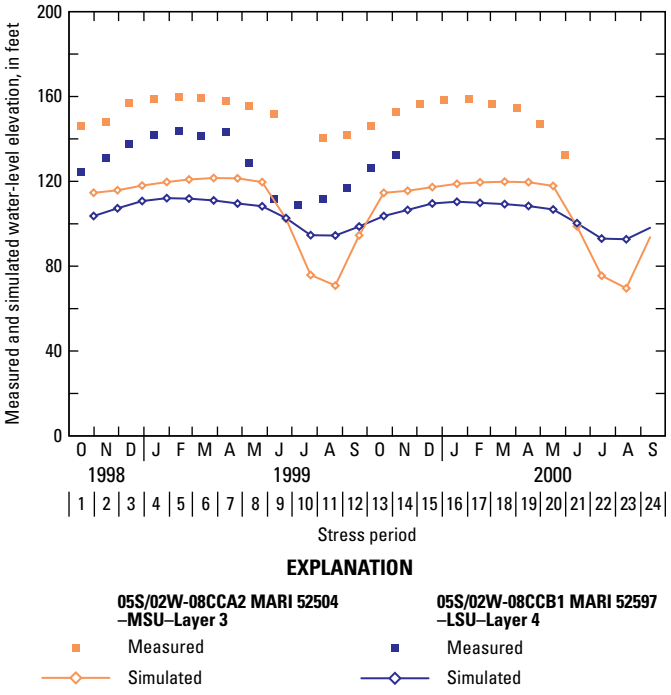

Figure 32. Measured water levels and simulated heads showing seasonal head gradients in wells 05S/02W-08CCA2 (MARI 52504, MSU—layer 3) and 05S/02W-08CCB1 (MARI 52597, LSU—layer 4), Central Willamette subbasin of the Willamette Basin, Oregon, water years 1999–2000.

Scenario Simulations

Four scenarios for the regional steady-state model (referred to as RSS1–4) were simulated to estimate long-term effects of pumping on groundwater levels and streamflows in the basin-fill sedimentary units and the CRB. For each scenario, pumping was either increased or decreased from current conditions. To evaluate the effects of changes in pumping, groundwater levels in wells and groundwater discharge to streams (base flow) were compared with the baseline (calibrated) steady-state simulation. With the exception of altered pumping rates, all hydraulic properties and boundary conditions were the same as in the baseline model. The first two scenarios consider regional effects of ceasing all pumping and doubling all pumping (scenarios RSS1 and RSS2, respectively). These scenarios correspond to pre-development conditions and the full utilization of currently permitted groundwater rights, respectively. Scenarios RSS3a,b,c and RSS4a,b evaluate the effects of geology and river proximity on groundwater and streamflow in two subbasins with rapidly growing populations: the Southern Willamette subbasin and the Tualatin subbasin. These two subbasins are not included in the local, Central Willamette subbasin model.

The groundwater-flow model can simulate the effect of well discharge on base flow for any particular stream reach. The sum of the reduction in groundwater discharge to and the increase in seepage from the stream due to groundwater pumping is referred to as capture (Lohman and others, 1972). By simulating pumping at many spatially distributed well locations, maps can be created that show the proportion of capture from any stream reach (Leake and others, 2010).

Numerous steady-state and transient scenarios using the local model were simulated to estimate the long-term and seasonal effects of pumping in the Central Willamette subbasin on groundwater levels and streamflows in the basin-fill sedimentary units. In each scenario, pumping was increased from current conditions. “Capture maps” were developed to show the effects of pumping throughout the Central Willamette subbasin to the Willamette River, Pudding River, and other streams. Steady-state capture transects and maps show long-term effects of pumping on groundwater levels and streamflows. Graphs of transient groundwater levels and stream base flow show the long-term and seasonal effects of pumping. Finally, transient capture cross sections show how geology, location, and seasonal pumping affect groundwater and stream capture over the short and long term.

Regional Steady-State Simulations

Pre-Development Conditions—Scenario RSS1

The calibrated regional steady-state model was used to simulate pre-development conditions in the Willamette Basin to determine whether the model was able to produce a reasonable match between measured and simulated heads during a different time period (scenario RSS1) and to estimate pre-development conditions throughout the basin. Pre-development conditions are defined as the conditions that existed in the region prior to significant human effects on the hydrologic system and are simulated by removing all groundwater pumping (table 11). No other model conditions or parameters were modified. Available data on which to base comparisons are limited to the 1935 water-table map (Piper, 1942). Pre-development conditions were accomplished by assuming that all prior boundary conditions were similar to annual average water year 1995–96 conditions, a period during which precipitation compared well to average annual precipitation. Changes to streamflows and groundwater levels in Willamette Basin wells were calculated based on the difference between the calibrated steady-state model and the simulated pre-development base flow and hydraulic heads. Maps of simulated base flow and changes in hydraulic heads for the WSU, USU/MSU, LSU, and CRB are shown in figures 33–34.

Table 11. Simulated regional steady-state groundwater budget compared with scenarios for pre-development (RSS1) and full use of groundwater rights (RSS2), Willamette Basin, Oregon.

[**Abbreviations:** M acre-ft/yr, million acre-feet per year; ft^3/s, cubic foot per second]

Component	Water years 1995–96 (baseline) simulation			Pre-development (RSS1)				Full use of groundwater rights (RSS2)			
	M acre-ft/yr	ft^3/s	Percentage of total	M acre-ft/yr	ft^3/s	Percentage of total	Change from baseline	M acre-ft/yr	ft^3/s	Percentage of total	Change from baseline
In											
Seepage from Columbia River	0.00	2	0.0	0.00	0	0.0	-2	0.00	4	0.0	2
Seepage from streams	0.04	58	0.7	0.04	54	0.6	-4	0.05	68	0.8	10
Recharge	6.30	8,702	99.3	6.30	8,702	99.4	0	6.30	8,702	99.2	0
Total inflow[1]	6.34	8,762	100.0	6.34	8,757	100.0	5	6.35	8,774	100.0	12
Out											
Seepage to Columbia River	0.03	35	0.4	0.03	38	0.4	3	0.02	31	0.4	-4
Withdrawals from wells	0.29	406	4.6	0.00	0	0.0	-406	0.59	811	9.2	405
Seepage to streams	6.02	8,321	95.0	6.31	8,719	99.6	398	5.74	7,932	90.4	-389
Total outflow[1]	6.34	8,762	100.0	6.34	8,757	100.0	5	6.35	8,774	100.0	12

[1]Differences due to rounding.

Pre-development conditions compared to current conditions show that about 406 ft^3/s of simulated base flow is captured by pumping in the Willamette Basin, including the Columbia River (table 11). Some of the largest simulated decreases in base flow are in the Central Willamette subbasin along the Willamette River (fig. 33). The simulated decrease in base flow in the Willamette River is the result of increases in well pumping since pre-development. Simulated decreases in base flow in some small stream segments may result from a combination of increases in well pumping and the scale of discretization at the regional level. In some areas, small stream reaches are simulated as cutting through the WSU to the underlying USU or MSU. Because the hydraulic conductivity is higher in the USU and MSU than in the WSU, there is preferential flow associated with the USU and MSU stream segments. Overall, large-scale patterns of diminished base flow are more meaningful when reviewing results than small-scale patterns due to limitations on model discretization.

Model simulation results indicate that pumping has caused declines in mean annual hydraulic head of less than 10 ft throughout most of the study area (fig. 34). Simulated water-level declines in the sedimentary layers generally result from irrigation pumping, and in the basalt layer generally result from municipal pumping. Areas of greater change are located in the Central Willamette subbasin and are primarily the effect of pumping. Although groundwater levels in the basin-fill sedimentary units generally return to previous seasonal high water levels in winter due to recharge (Conlon and others, 2005), an increase in summer pumping can cause an increase in the magnitude of the range of seasonal groundwater levels and lower the mean annual hydraulic head over time. When the seasonal low groundwater level is lowered and the seasonal high groundwater level remains the same, the mean annual head will be lowered to a new average of those heads (fig. 34*A*–*E*).

Simulated groundwater-level declines due to pumping in the Southern Willamette subbasin are minimal and generally less than 2 ft (fig. 34*A*–*D*). Most wells in this area are irrigation wells screened in the USU near the Willamette River, with most other wells screened in the MSU. Groundwater pumping in the Southern Willamette subbasin accounts for 75 percent of total pumping from the USU and 28 percent of total pumping from the MSU in the Willamette Basin (Conlon and others, 2005). The proximity to, and hydraulic connection between, the USU and the Willamette River increases the effects of pumping on the river and minimizes the effects of pumping on hydraulic heads—pumping from wells in the USU in the Southern Willamette subbasin causes less drawdown in groundwater levels and more capture from the Willamette River. Pre-development conditions compared to current conditions show that about 130 ft^3/s of simulated base flow in the Southern Willamette subbasin is captured by pumping that otherwise would discharge to streams, and ultimately to the Willamette River, upstream of Salem (fig. 33).

Simulated mean annual hydraulic heads in the CRB and LSU in the Tualatin subbasin show minimal changes (less than 10 ft) from pre-development conditions (fig. 34*D*–*E*), and little change is evident in base flows (fig. 33). Only 5 percent of total groundwater withdrawals in the Willamette Basin occur in the Tualatin subbasin (Conlon and others, 2005). Base flows in the Portland subbasin are little affected by changes since pre-development, although some areas to the south and east show moderate declines (as much as 40 ft) in mean annual hydraulic head (fig. 34*B*–*E*).

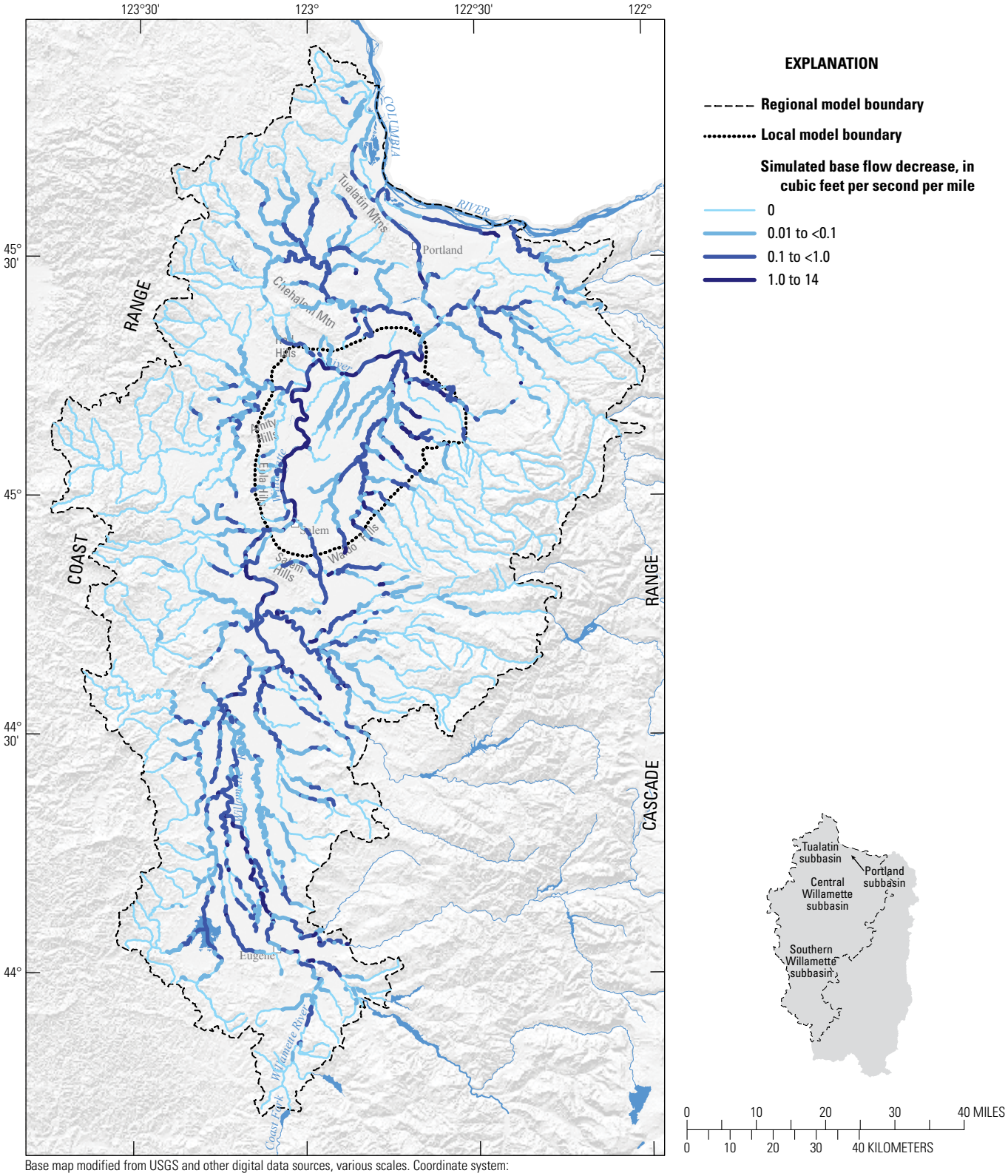

Base map modified from USGS and other digital data sources, various scales. Coordinate system: UTM, Zone 10N, Projection: Transverse Mercator; Datum: North American Datum of 1927.

Figure 33. Simulated average annual decrease in base flow since pre-development conditions (scenario RSS1) using the regional groundwater-flow model of the Willamette Basin, Oregon.

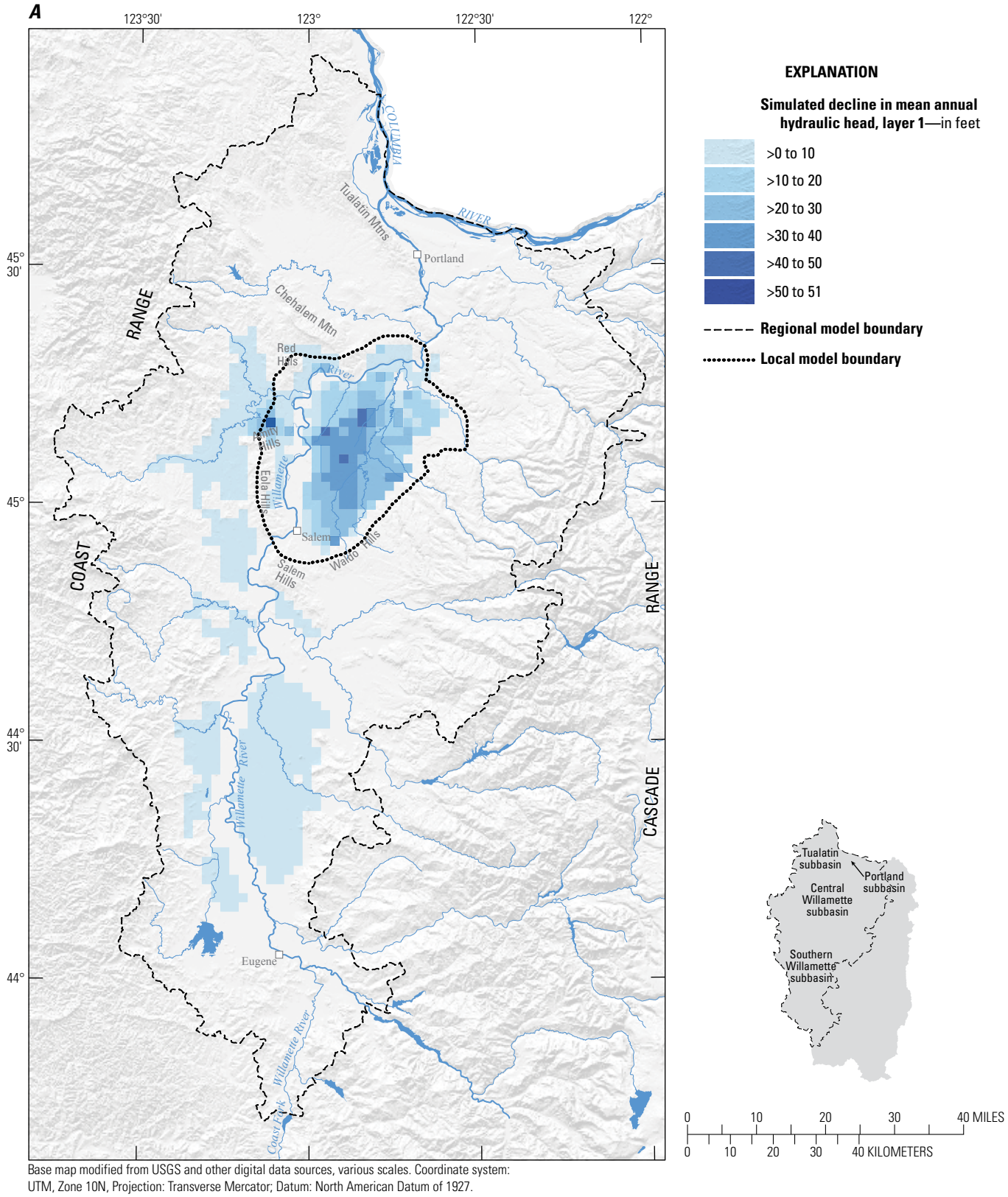

Base map modified from USGS and other digital data sources, various scales. Coordinate system: UTM, Zone 10N, Projection: Transverse Mercator; Datum: North American Datum of 1927.

Figure 34. Simulated decline in mean annual hydraulic head since pre-development conditions (scenario RSS1) for (*A*) model layer 1 (Willamette silt unit), (*B*) model layer 2 (upper sedimentary unit/middle sedimentary unit), (*C*) model layer 3 (upper sedimentary unit/middle sedimentary unit), (*D*) model layer 4 (lower sedimentary unit), and (*E*) model layer 5 (Columbia River basalt unit) using the regional groundwater-flow model of the Willamette Basin, Oregon.

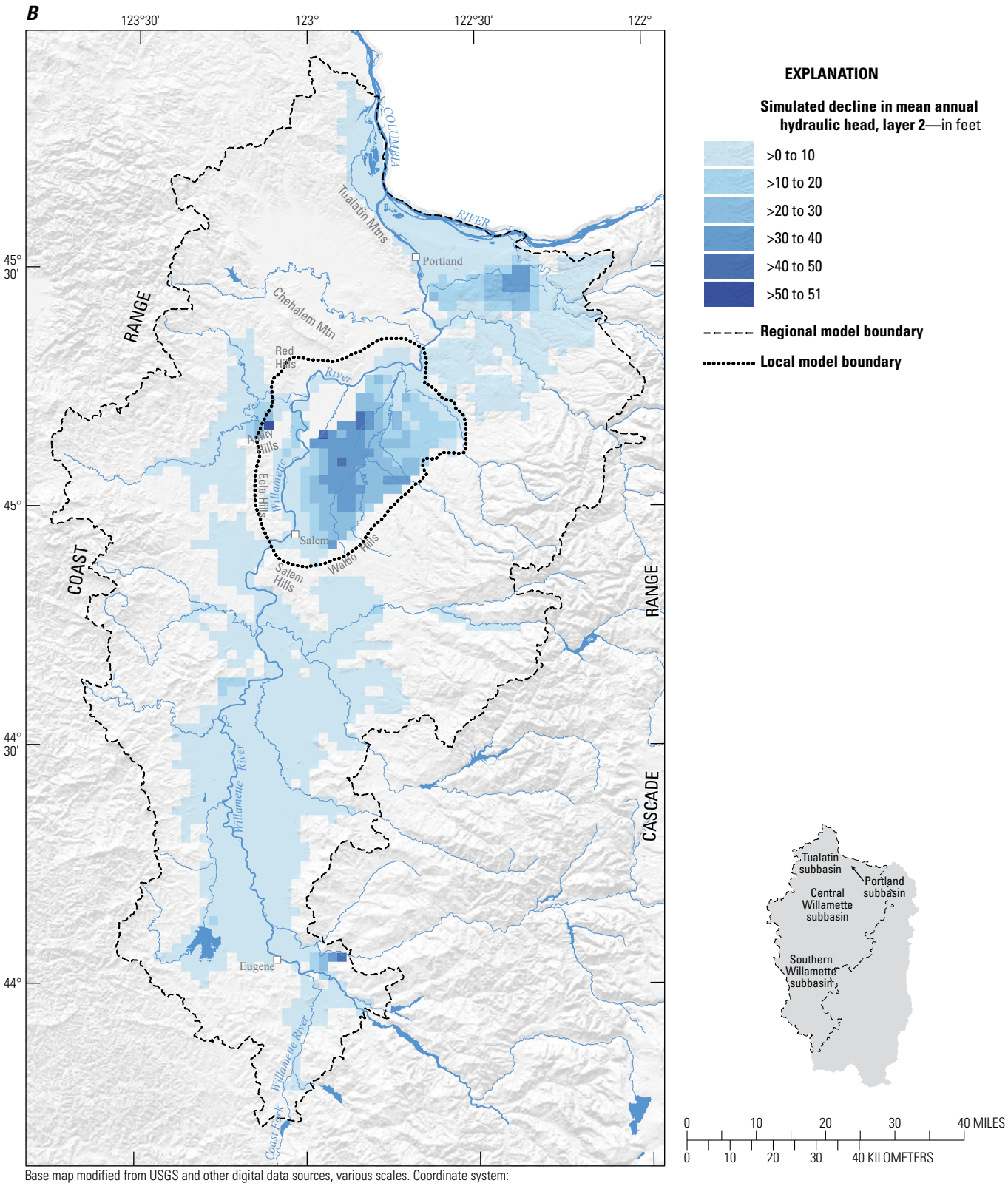

Base map modified from USGS and other digital data sources, various scales. Coordinate system: UTM, Zone 10N, Projection: Transverse Mercator; Datum: North American Datum of 1927.

Figure 34.—Continued

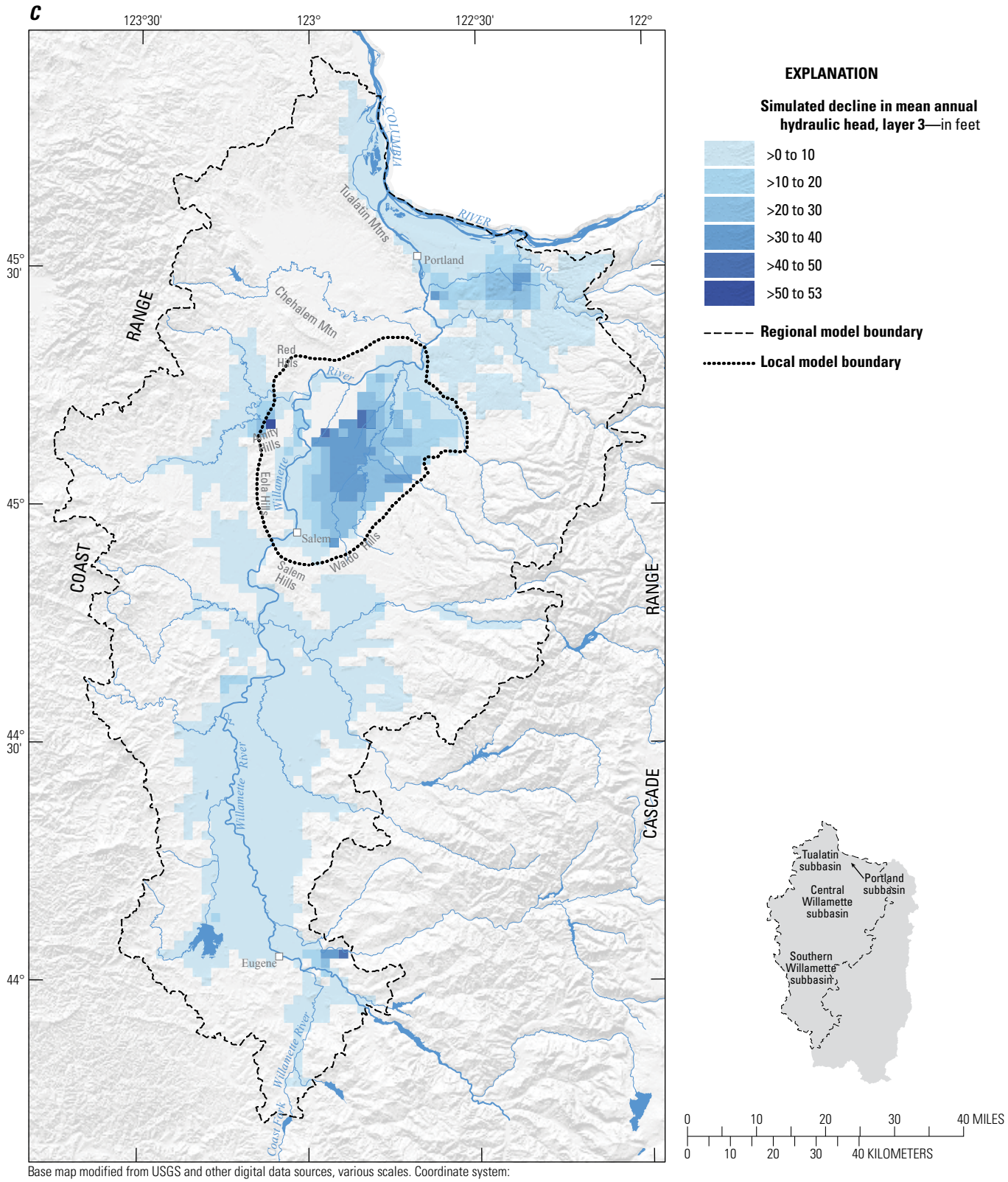

Base map modified from USGS and other digital data sources, various scales. Coordinate system: UTM, Zone 10N, Projection: Transverse Mercator; Datum: North American Datum of 1927.

Figure 34.—Continued

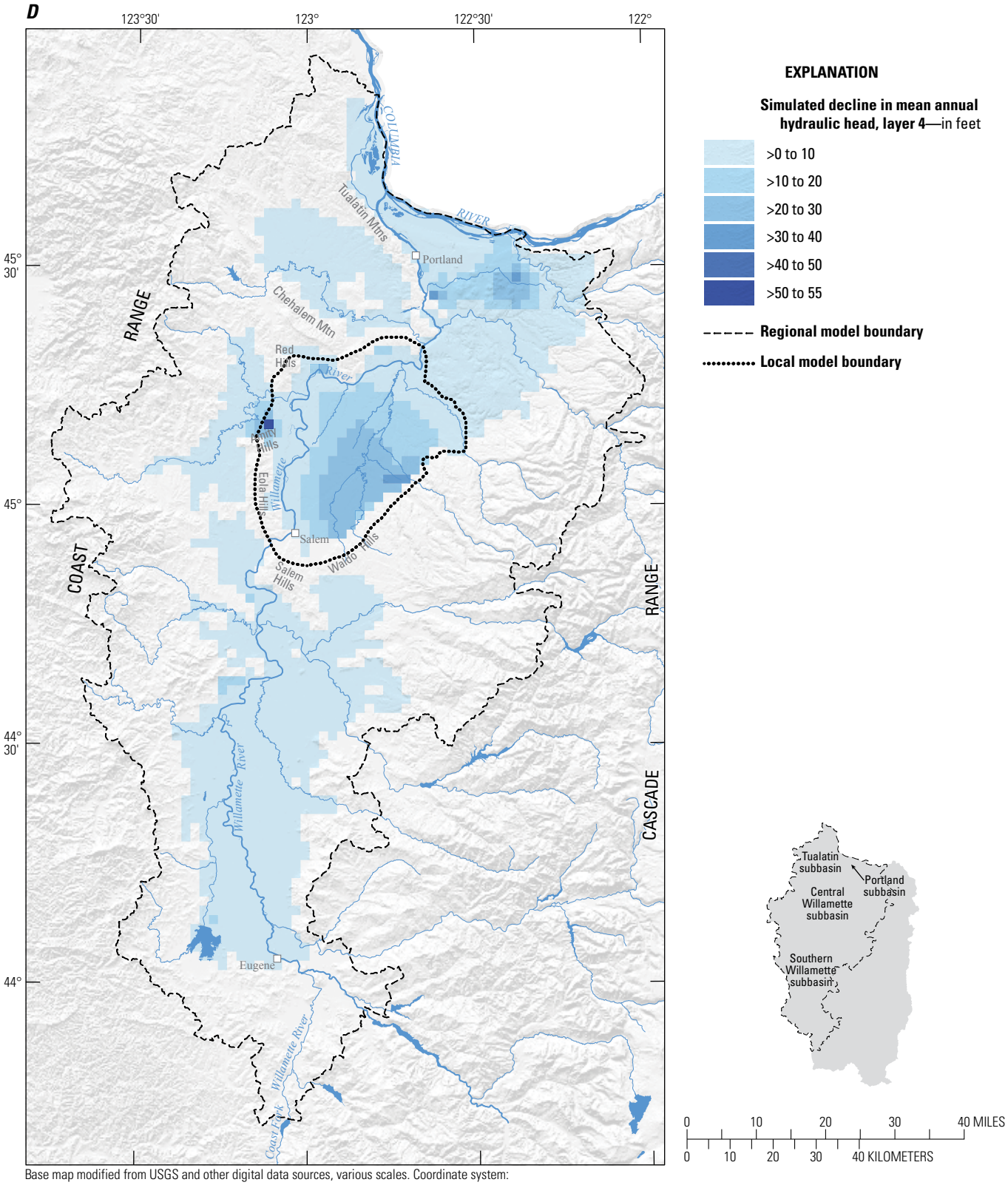

Base map modified from USGS and other digital data sources, various scales. Coordinate system: UTM, Zone 10N, Projection: Transverse Mercator; Datum: North American Datum of 1927.

Figure 34.—Continued

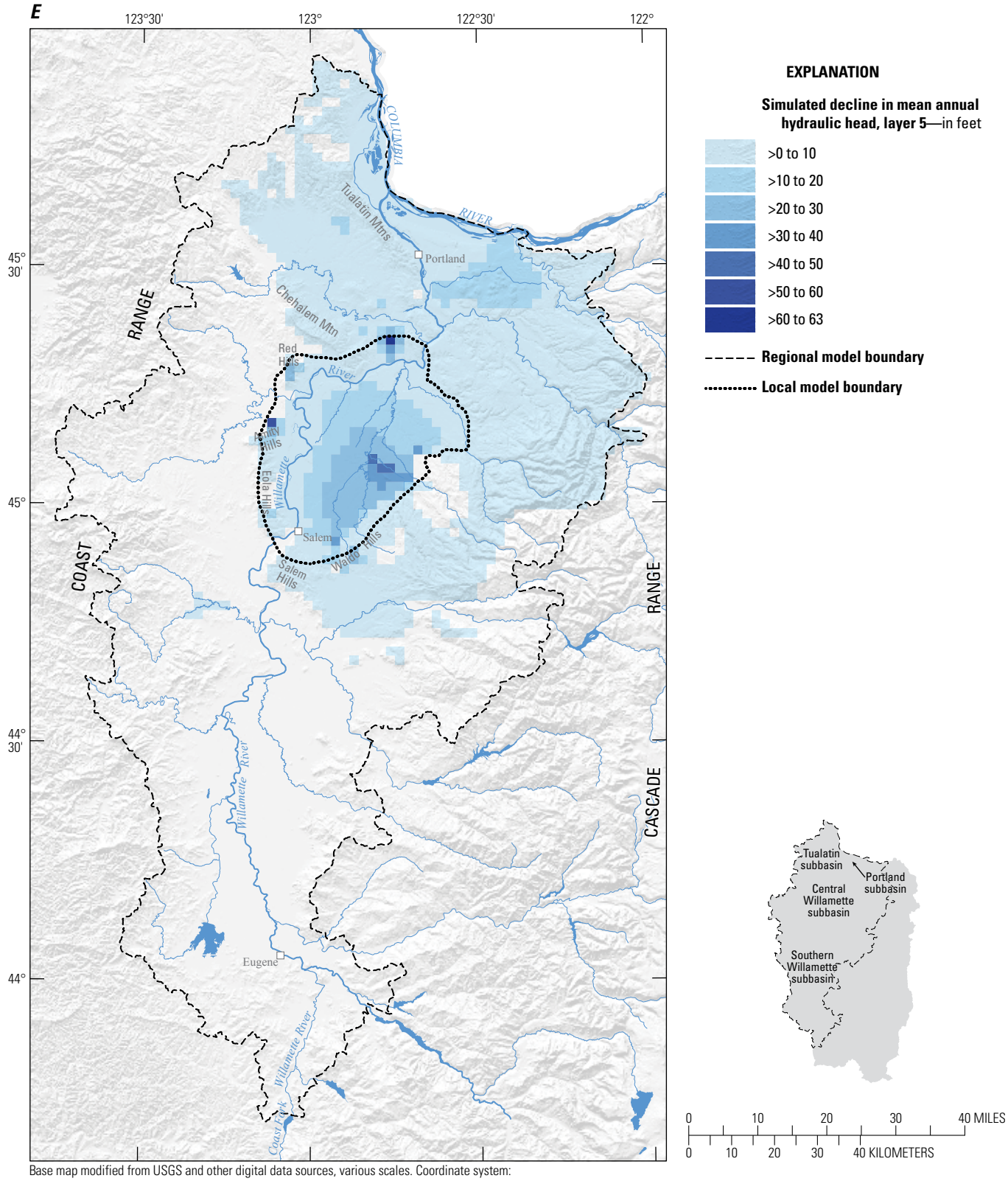

Base map modified from USGS and other digital data sources, various scales. Coordinate system: UTM, Zone 10N, Projection: Transverse Mercator; Datum: North American Datum of 1927.

Figure 34.—Continued

Comparison of simulated pre-development groundwater-level elevations from the uppermost unit at land surface with the 1935 water-table map (Piper, 1942) shows that water-level elevations and directions of groundwater flow are similar (fig. 35). In the Southern Willamette subbasin (fig. 2), simulated groundwater levels are nearly identical to Piper's water-table map. In the Central Willamette subbasin, simulated pre-development groundwater levels are similar to those in the 1935 water-table map, but detail around the streams is limited due to the relatively coarse scale of the regional model grid. In the Central and Southern Willamette subbasins, simulated pre-development groundwater levels in the sedimentary units are within 10–20 ft of 1995–96 average annual groundwater levels in the sedimentary units.

Pumping during simulated water years 1995–96 results in less groundwater discharge to streams compared with pre-development conditions, with a net decrease of seepage to streams (398 ft^3/s) and the Columbia River (3 ft^3/s) from aquifers and a net increase of seepage from streams (4 ft^3/s) and the Columbia River (2 ft^3/s) to aquifers (table 11). Decreasing hydraulic head results in streams receiving less or no groundwater discharge or becoming a source of recharge for an aquifer. Simulated 1995–96 conditions generally show vertical groundwater flows through adjacent layers to ultimately discharge to streams. This is a nearly identical direction of vertical flow compared with simulated pre-development conditions, with slightly less groundwater moving downward through the WSU into underlying sedimentary layers and ultimately discharging to the Willamette River (the regional sink).

Full Use of Groundwater Rights—Scenario RSS2

During most water years, the amount of groundwater pumped is far less than the total currently permitted groundwater rights, which are approximately equal to twice the 1995–96 estimated actual pumping (Karl Wozniak, Oregon Department of Water Resources, oral commun., 2007). To simulate the long-term effect of sustained pumping for full use of groundwater rights, the current distribution of permitted groundwater rights was assumed similar to the distribution of simulated wells, and the pumping rates in the steady-state model were doubled. Total withdrawals in the Willamette Basin were increased by 405 ft^3/s, a 100 percent increase from 1995–96 average annual conditions. Relative pumping percentages were unchanged across the hydrogeologic units. No other model conditions or parameters were modified. Changes to base flow and groundwater levels in the Willamette Basin were calculated based on the difference between the calibrated steady-state model and the fully utilized groundwater rights scenario flows and water levels. Maps of simulated reduction in base flow in streams and hydraulic head declines for the WSU, USU/MSU, LSU, and CRB are shown in figures 36 and 37*A*–*E*; the groundwater budget is summarized in table 11.

The simulated groundwater budget indicates that at steady-state conditions, an increase in seepage from the Columbia River (2 ft^3/s) and other streams (10 ft^3/s) of 12 ft^3/s and a decrease in discharge to the Columbia River (4 ft^3/s) and other streams (389 ft^3/s) of 393 ft^3/s would supply the additional pumping requirements for full use of permitted groundwater rights in the Willamette Basin (table 11). Pumping conditions had little effect on streams in the upland areas, but a reduction in base flow was evident in the Willamette and Pudding Rivers and other tributaries in the lowlands. The largest change in simulated base flow was in the Central Willamette subbasin (fig. 36). Discharge to streams in the Willamette Basin was decreased by about 5 percent (table 11).

Simulated full use of groundwater rights show declining mean annual hydraulic heads in the Willamette Basin (figs. 37*A*–*E*). Whereas average annual heads in the basin-fill sediments in the Portland subbasin, Tualatin subbasin and Southern Willamette subbasin (fig. 2) generally show declines of less than 5 ft in the simulation, average annual heads decline by about 20–50 ft in the Central Willamette subbasin (fig. 37*A*–*D*), as much as about 60 ft near Springfield in the Southern Willamette subbasin (fig. 37*A*–*B*), and 20–40 ft in some areas on the eastern side of the Portland subbasin (fig. 37*B*–*D*). Declines in the CRB follow the same general patterns (fig. 37*E*). Similar to results discussed in the section "Pre-Development Conditions—Scenario RSS1," maximum head declines in the sedimentary layers generally result from irrigation pumping, and in the basalt layer generally result from municipal pumping. Declines in simulated average annual hydraulic head caused approximately 100 river cells to convert from gaining to losing conditions. Most of these streams are near the Willamette River and the Pudding River in the Central Willamette subbasin. These declines are due to increased pumping and changes in vertical gradients.

At the regional scale, the vertical component of flow in the WSU is downward into the underlying layers, and full use of groundwater rights has little effect on the magnitude and direction of groundwater flow between the WSU and underlying units except for areas near the Pudding River, where the magnitude of the downward vertical gradient increases substantially. Between the upper and lower parts of the USU and MSU (represented by layers 2 and 3) there is little change in the direction of vertical flow between the baseline model and the full-use model, but there is a general decrease in the magnitude of the gradient. Vertical flow between the USU, MSU, and LSU shows a large decrease in magnitude and a gradient reversal in areas closely associated with increased groundwater withdrawals from the MSU in the Central Willamette subbasin. Direction and magnitude of vertical gradients between the LSU and CRB and between the CRB and BCU are similar in the baseline and full use of groundwater rights scenarios.

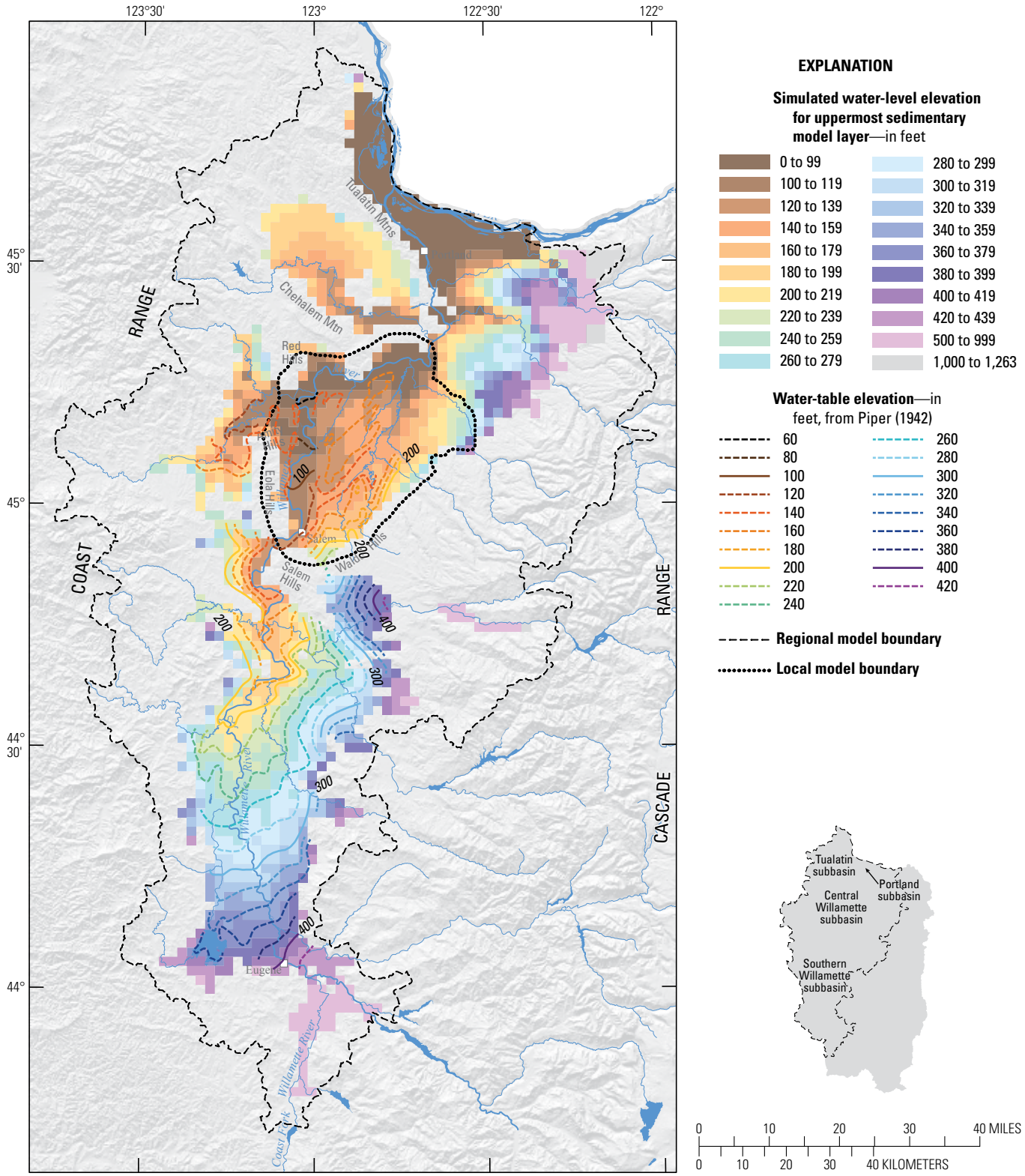

Base map modified from USGS and other digital data sources, various scales. Coordinate system: UTM, Zone 10N, Projection: Transverse Mercator; Datum: North American Datum of 1927.

Figure 35. Simulated pre-development (scenario RSS1) water-level elevation for the uppermost sedimentary model layer (Willamette silt unit, upper sedimentary unit, middle sedimentary unit, or lower sedimentary unit) compared with 1935 pre-development water-table elevations of Piper (1942), Willamette Basin, Oregon.

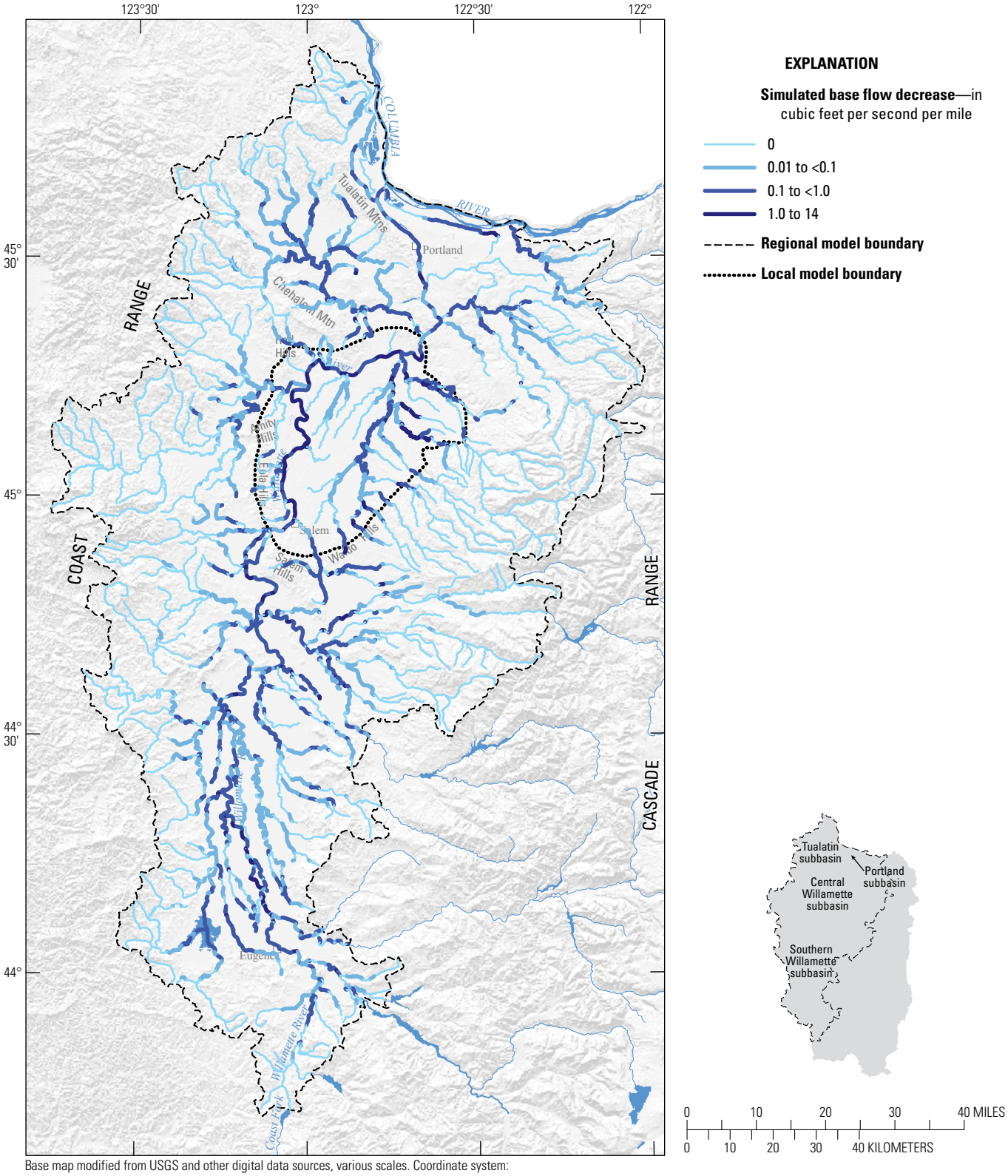

Base map modified from USGS and other digital data sources, various scales. Coordinate system: UTM, Zone 10N, Projection: Transverse Mercator; Datum: North American Datum of 1927.

Figure 36. Simulated average annual decrease in base flow with the full use of groundwater rights model scenario RSS2, Willamette Basin, Oregon.

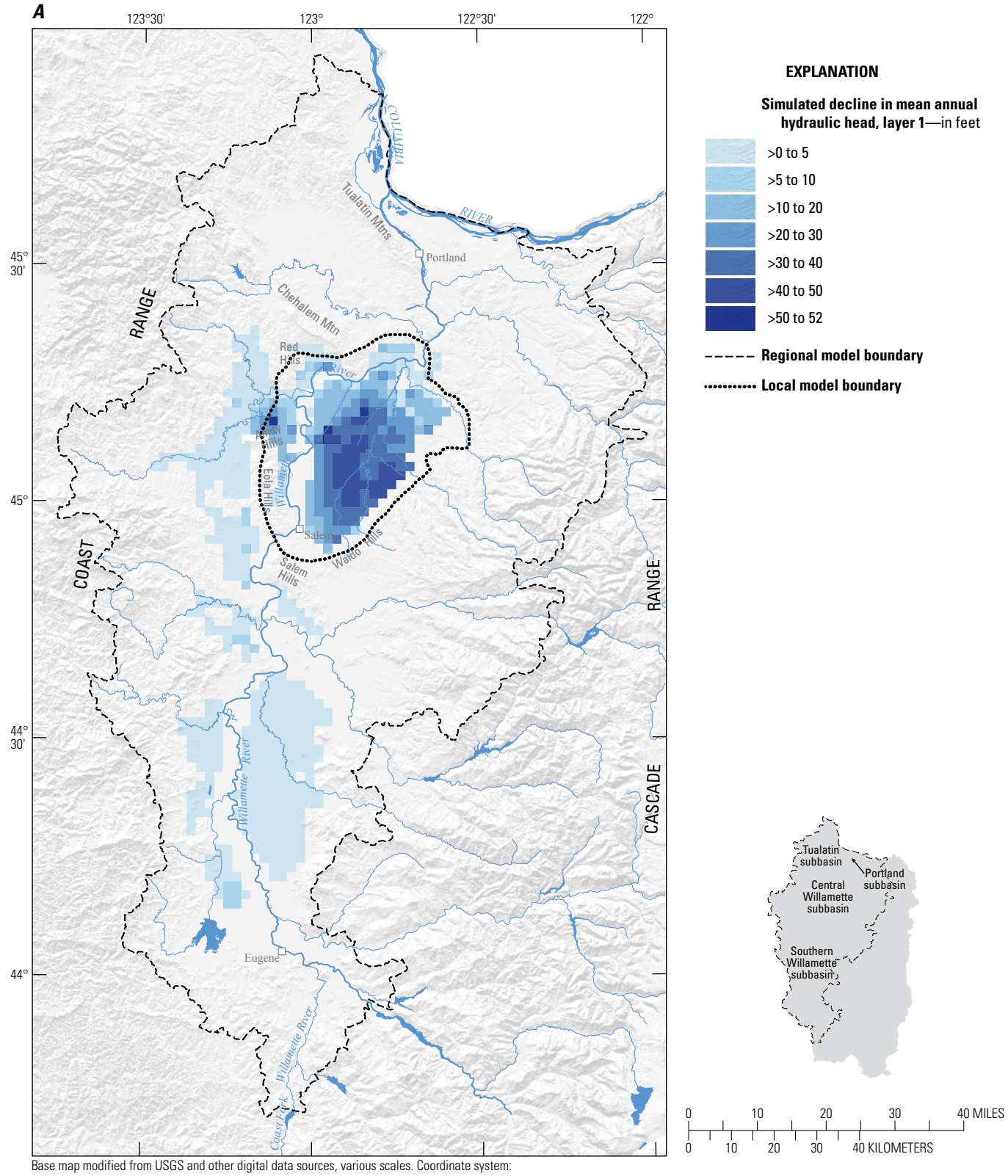

Base map modified from USGS and other digital data sources, various scales. Coordinate system: UTM, Zone 10N, Projection: Transverse Mercator; Datum: North American Datum of 1927.

Figure 37. Simulated decline in mean annual hydraulic head in (*A*) model layer 1 (Willamette silt unit), (*B*) model layer 2 (upper sedimentary unit/middle sedimentary unit), (*C*) model layer 3 (upper sedimentary unit/middle sedimentary unit), (*D*) model layer 4 (lower sedimentary unit), and (*E*) model layer 5 (Columbia River basalt unit), with full use of groundwater rights scenario RSS2, Willamette Basin, Oregon.

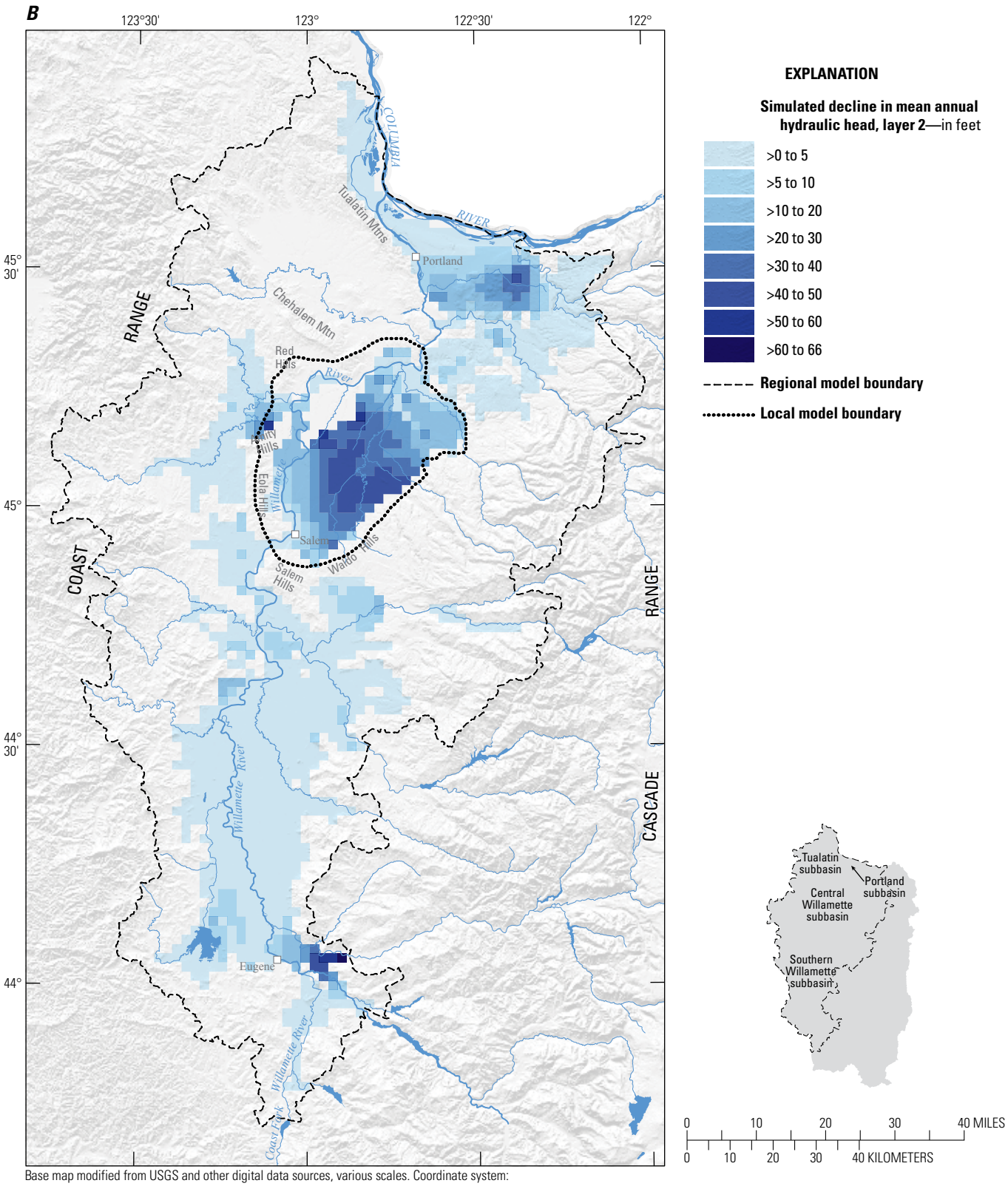

Base map modified from USGS and other digital data sources, various scales. Coordinate system: UTM, Zone 10N, Projection: Transverse Mercator; Datum: North American Datum of 1927.

Figure 37.—Continued

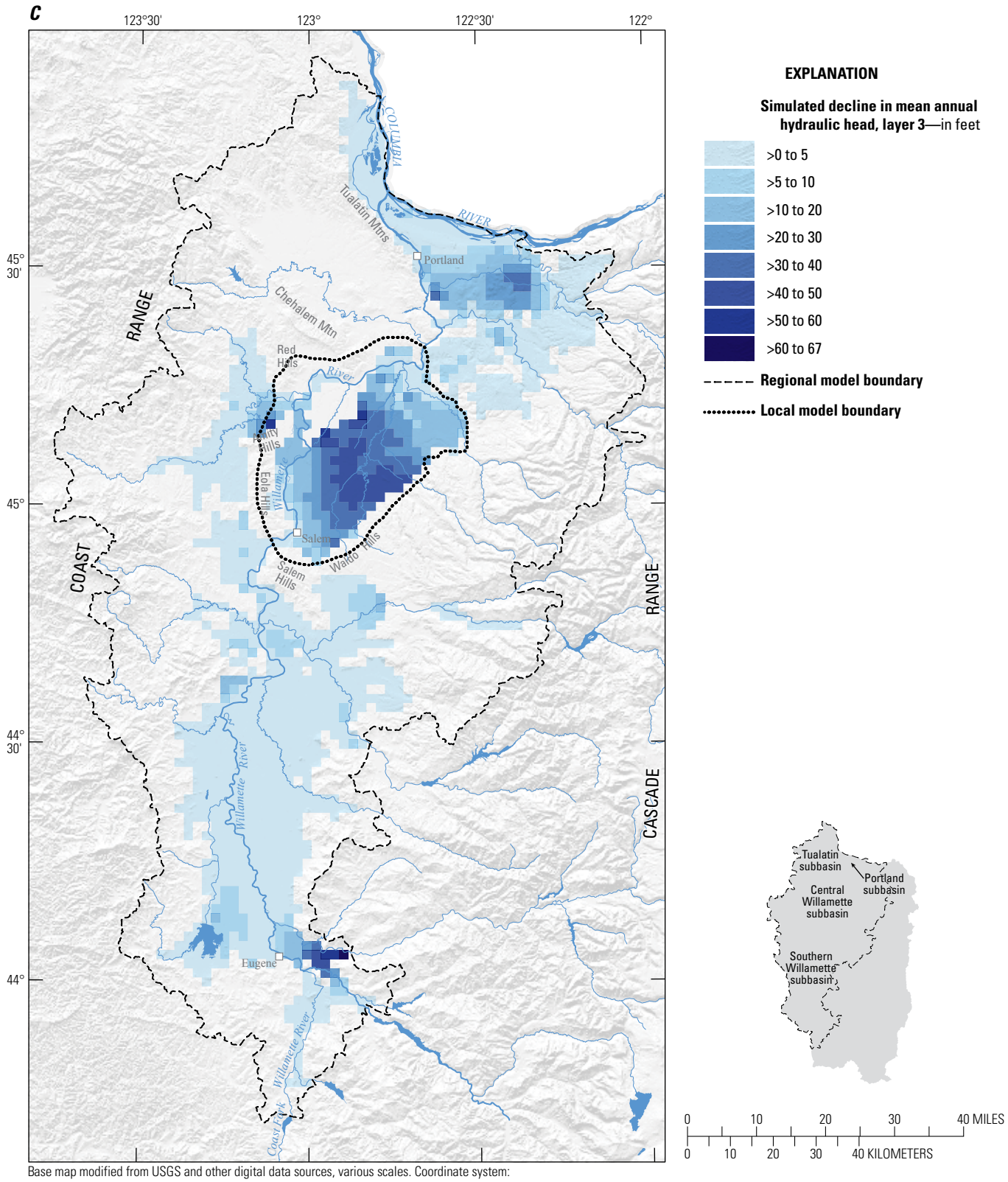

Base map modified from USGS and other digital data sources, various scales. Coordinate system: UTM, Zone 10N, Projection: Transverse Mercator; Datum: North American Datum of 1927.

Figure 37.—Continued

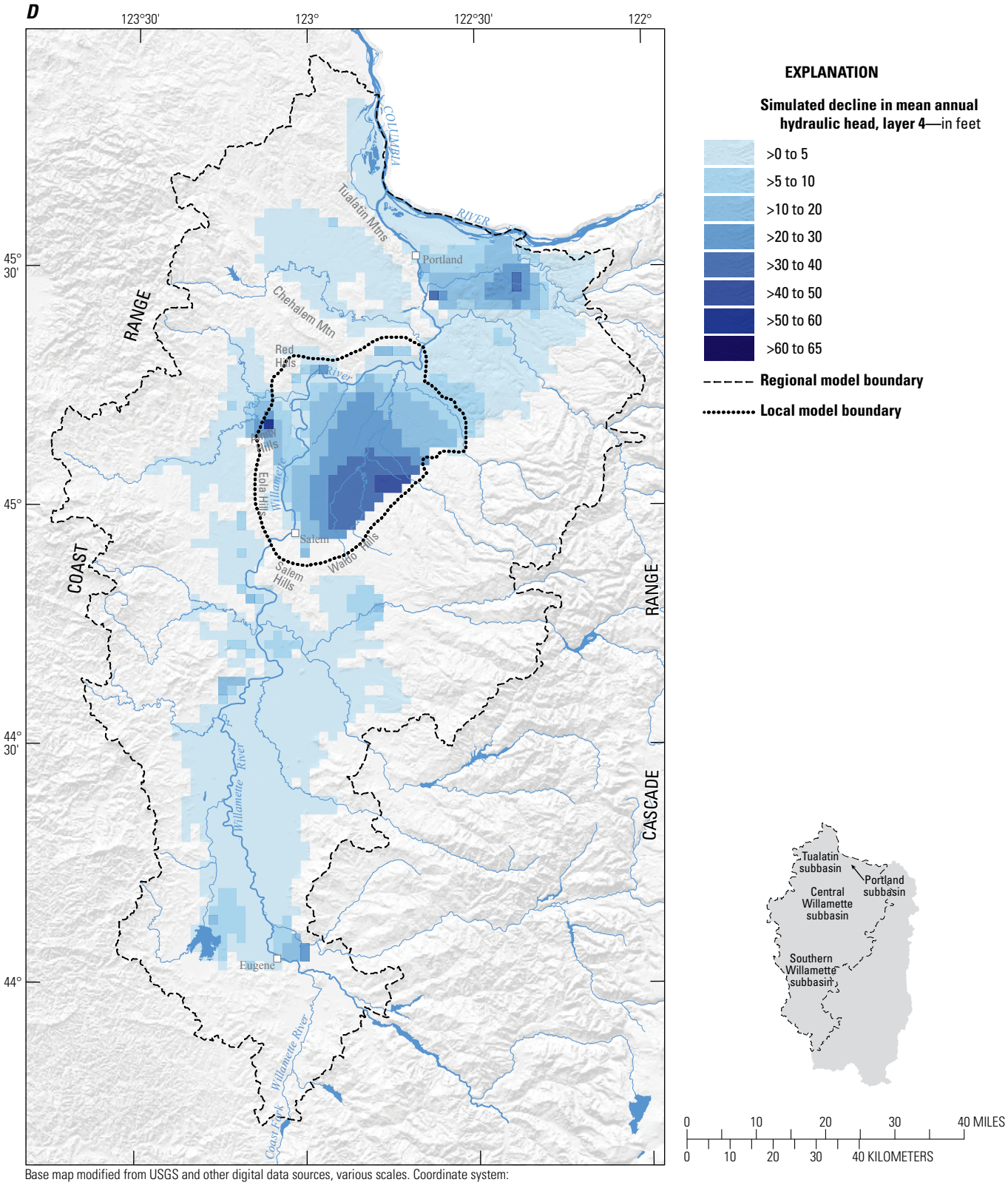

Base map modified from USGS and other digital data sources, various scales. Coordinate system: UTM, Zone 10N, Projection: Transverse Mercator; Datum: North American Datum of 1927.

Figure 37.—Continued

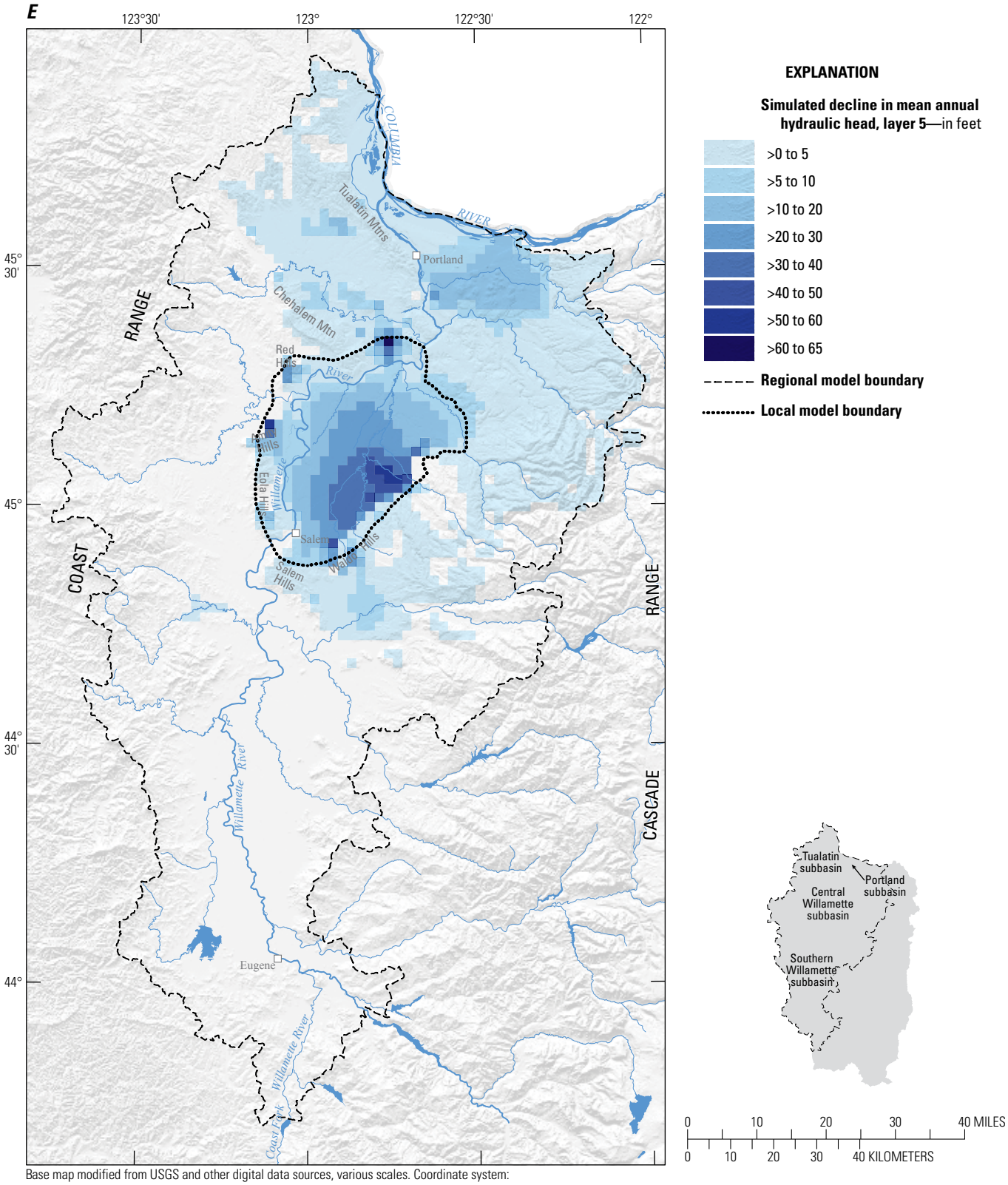

Base map modified from USGS and other digital data sources, various scales. Coordinate system: UTM, Zone 10N, Projection: Transverse Mercator; Datum: North American Datum of 1927.

Figure 37.—Continued

Pumping in Alluvium near the Willamette River in the Southern Willamette Subbasin—Scenarios RSS3a, RSS3b, RSS3c

The effects of variations in pumping depth and distance from the Willamette River in the Southern Willamette subbasin were demonstrated with three steady-state simulations. A steady-state simulation shows the effects of a stress when a new equilibrium is reached. For each simulation, an additional pumping stress of 10 ft^3/s (4,500 gal/min) was assigned either to layer 2 or 3. The first two simulations show the effect of varying the depth of pumping near the Willamette River (fig. 38*A*–*D*). The pumping stress is simulated in the USU, comparing the effects of shallow well completion (in model layer 2; scenario RSS3a), and deeper well completion (in model layer 3; scenario RSS3b). The WSU is not present at the simulated pumping location (fig. 38*A*–*D*). For the third simulation in this grouping (RSS3c), pumping was assigned to layer 3 where the USU is not present and the MSU is overlain by the WSU, about 7 mi east of the Willamette River (fig. 39*A*–*D*).

The first pumping scenario (RSS3a) simulated an additional average annual pumping rate of 10 ft^3/s applied to a cell in the USU in layer 2 near the Willamette River (row 80, column 20) (fig. 38*A*–*D*). The simulated decrease in base flow is greatest in the Willamette River and nearby tributaries incised into the USU (fig. 38*A*–*D*). Streams flowing on the WSU (fig. 4) show substantially less effect than streams flowing on other units. Maximum head decline is about 18 ft in layer 2 and 3 (fig. 38*B*–*C*), with less than 3 ft of decline in layer 1 (fig. 38*A*). Maximum head decline in layer 4 is about 8 ft (fig. 38*D*). Mean annual hydraulic head decline from pumping is apparent on both sides of the Willamette River in all layers, and the area affected increases with depth (fig. 38*A*–*D*). Head decline of as much as 2 ft is evident more than 2 mi away (fig. 38*A*–*D*). Simulated drawdown is minimized because of the high transmissivity in the USU and the hydrologic connection of the unit to the Willamette River. However, the additional pumping stress causes a change in the vertical gradient in the area of the pumping, with flow moving upward from the underlying units to the USU in layer 2.

The second pumping scenario (RSS3b) simulated additional pumping at the same location from a greater depth in the USU. The USU is about 20–40 ft thick in the Southern Willamette subbasin near the Willamette River. Pumping from the lower part of the USU caused nearly identical effects as pumping from the upper USU (scenario RSS3a). These results are not shown.

The third pumping scenario (RSS3c) simulated an additional average annual pumping rate of 10 ft^3/s assigned to a cell in the MSU in layer 3, about 7 mi east of the Willamette River (row 80, column 25) (fig. 39*A*–*D*) where the MSU is overlain by the less permeable WSU layer. Most effects are to nearby streams with channels flowing on the MSU (fig. 4), and evidence of stream capture can be seen in streams 10 mi away (fig. 39*A*–*D*). Capture from nearby streams simulated as flowing on the WSU is about two orders of magnitude less than for stream channels simulated as flowing on other units. The influence of simulated pumping in the MSU propagates farther than simulated pumping near the Willamette River in the USU. Drawdown of as much as 2 ft can be seen 4 mi away (fig. 39*A*–*D*). The distance of pumping influence increases with depth, and is consistent with the behavior of confined aquifers; however, the drawdown effects of pumping do not extend beyond the Willamette River except in the LSU (fig. 39*D*). This results from a decreased hydrologic connection between the LSU and the Willamette River in the Southern Willamette subbasin. Maximum decline in hydraulic head is about 39 ft in layers 1 (fig. 39*A*) and 2 (fig. 39*B*), 45 ft in layer 3 (fig. 39*C*), and 12 ft in layer 4 (fig. 39*D*). Hydraulic head decline increases when simulated pumping is farther away from the Willamette River because of the relatively lower transmissivity in the MSU compared to the USU and the presence of the overlying WSU limiting connection between the MSU and surface water bodies.

Pumping in Basalt and Alluvium near the Tualatin River in the Tualatin Subbasin—Scenarios RSS4a and RSS4b

In the Tualatin subbasin, the LSU (layer 4) is present at land surface and overlies the CRB (layer 5), which is present at depth and forms most of the upland areas in and around the basin. The effects of pumping at different depths in the Tualatin subbasin were demonstrated with two steady-state simulations illustrating variations in pumping depth and distance from the Tualatin River. One scenario (RSS4a) simulated the effect of relatively shallow pumping in the basin-fill sediments (layer 4), and the other scenario (RSS4b) simulated the effect of relatively deeper pumping from the basalt (layer 5). The pumping rate was set to 5 ft^3/s (compared to 10 ft^3/s in the Southern Willamette subbasin) to reflect a realistic rate of pumping for the Tualatin subbasin.

In the first simulation (RSS4a), pumping in layer 4 (LSU, row 25, column 29) (fig. 40*A*–*B*) captures flow from the Tualatin River and nearby tributaries. Capture from streams flowing on layer 5 (CRB) (fig. 40*B*) is minimal because these streams are in upland areas, generally outside the area influenced by the additional pumping. Maximum mean annual head decline is less than 5 ft in layer 4 (fig. 40*A*), and about 2 ft in layer 5 (fig. 40*B*). Declines in hydraulic head in layer 4 extend outward past the Tualatin River to the north and east, where it is limited by the boundaries of the LSU (fig. 40*A*). Declines in hydraulic head in layer 5 follow a similar pattern (fig. 40*B*). Vertical head gradients remain relatively unchanged.

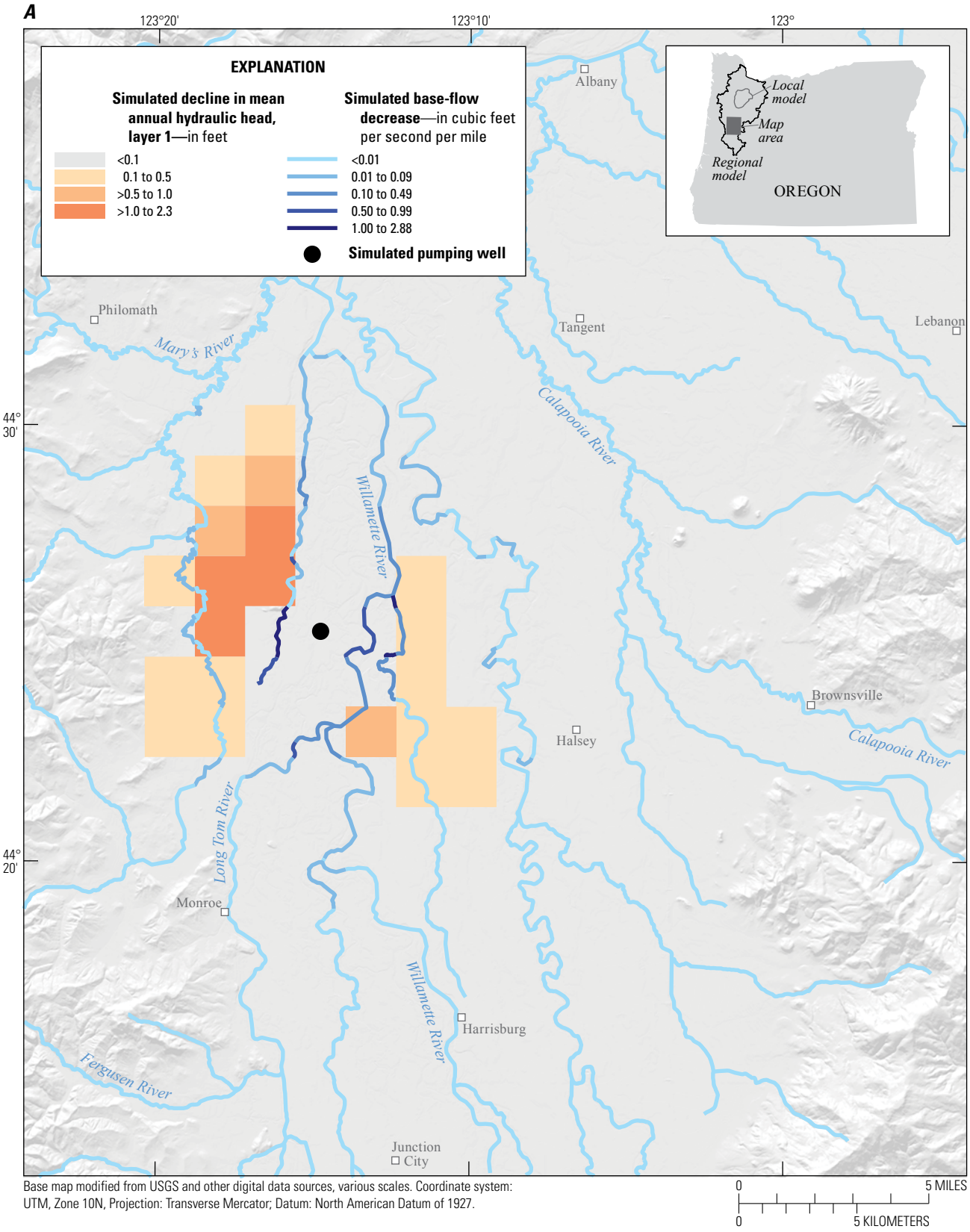

Figure 38. Simulated steady-state decline in mean annual hydraulic head for scenario RSS3a in (*A*) model layer 1 (Willamette silt unit), (*B*) model layer 2 (upper sedimentary unit/middle sedimentary unit), (*C*) model layer 3 (upper sedimentary unit/middle sedimentary unit), and (*D*) model layer 4 (lower sedimentary unit) and decrease in simulated base flow to streams after pumping an additional annual 10 cubic feet per second from the upper sedimentary unit in model layer 2, near the Willamette River in the Southern Willamette subbasin, Willamette Basin, Oregon.

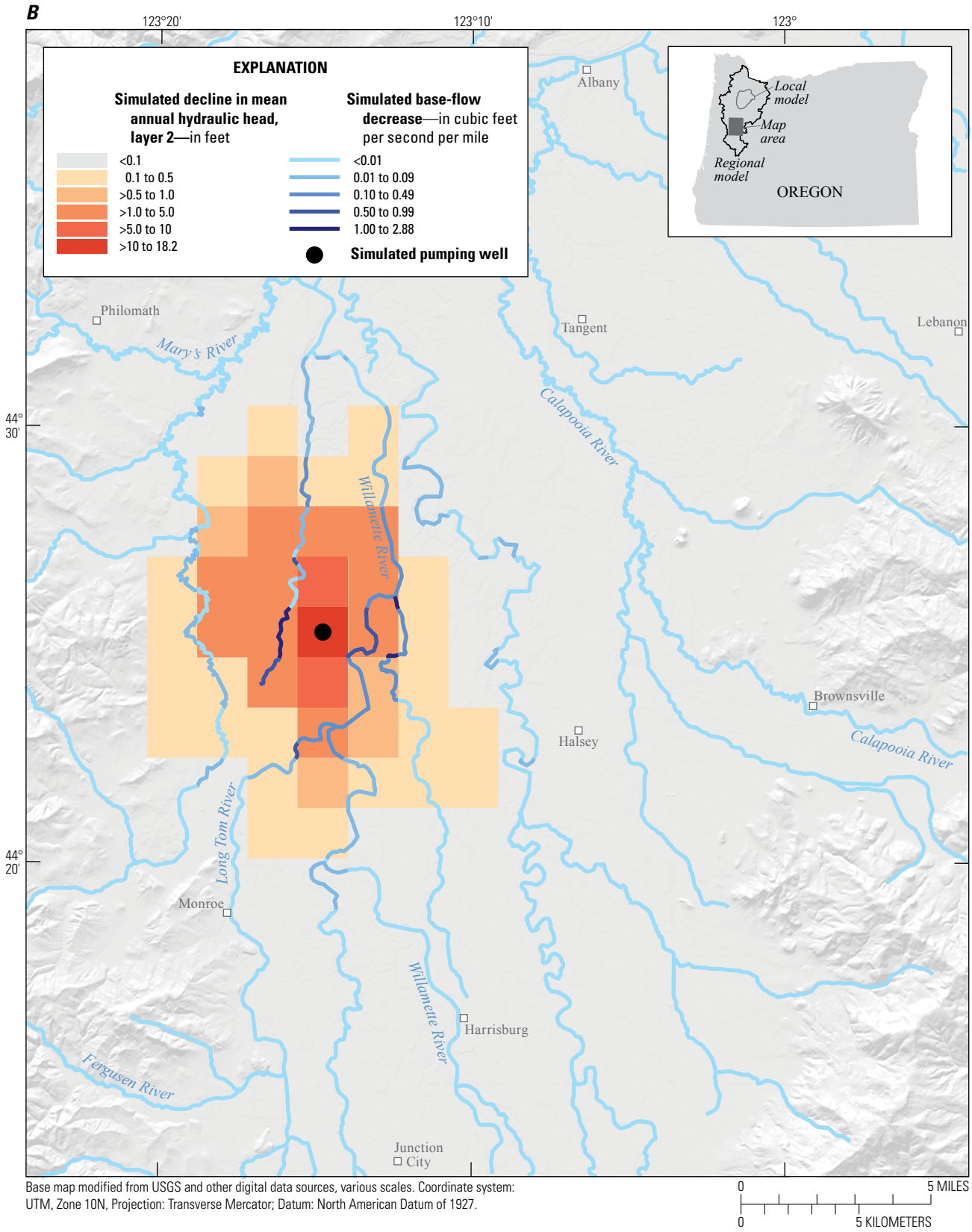

Figure 38.—Continued

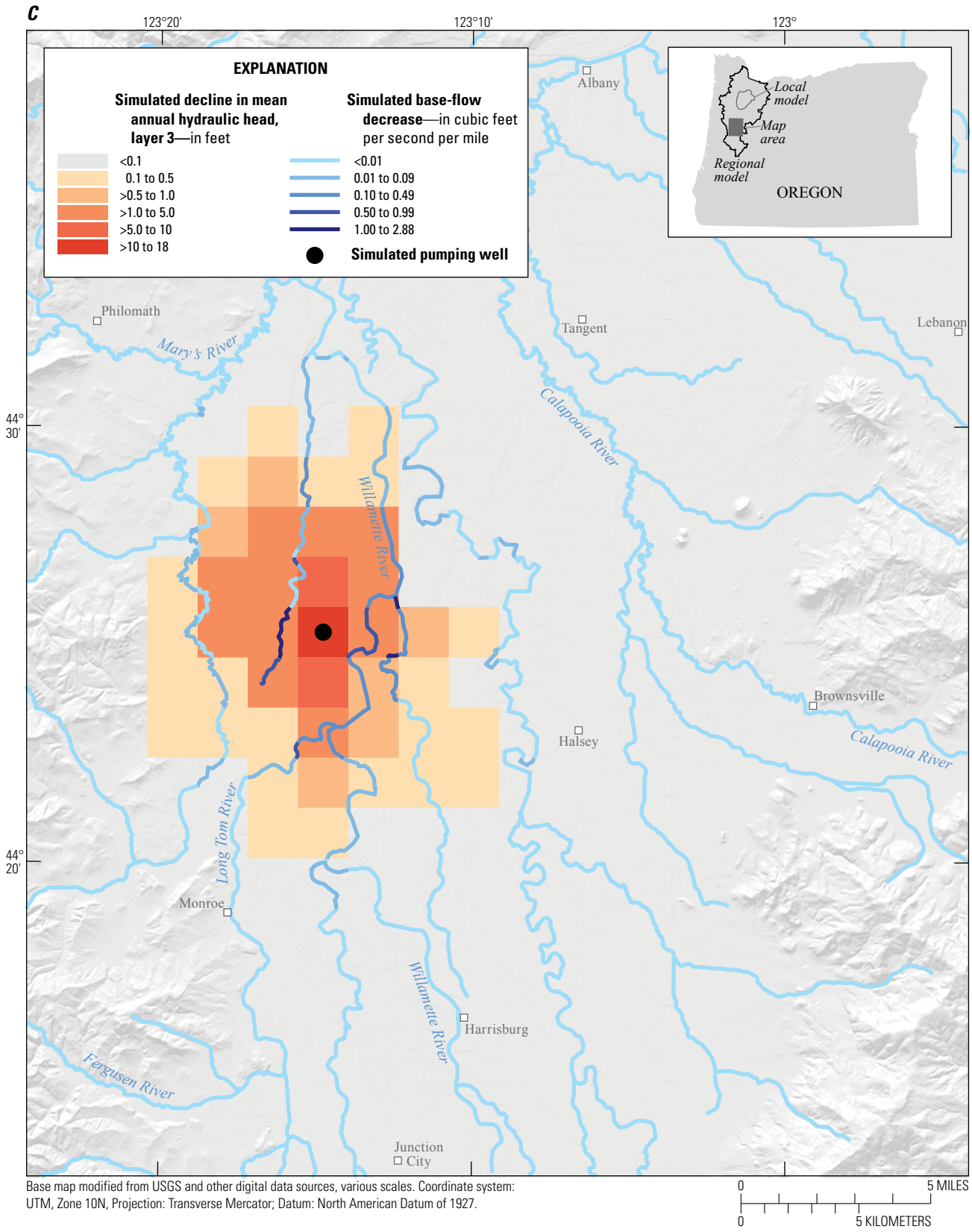

Figure 38.—Continued

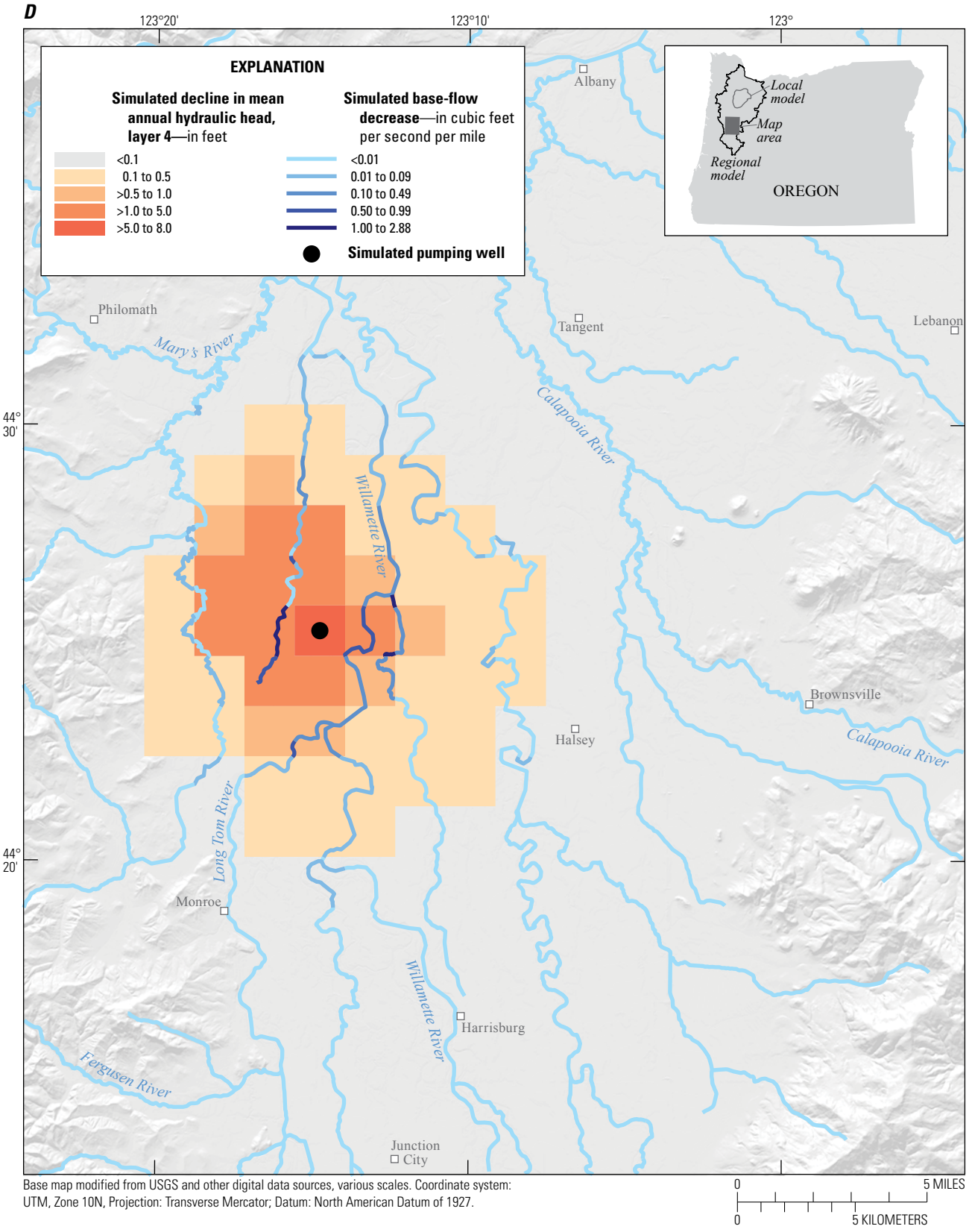

Figure 38.—Continued

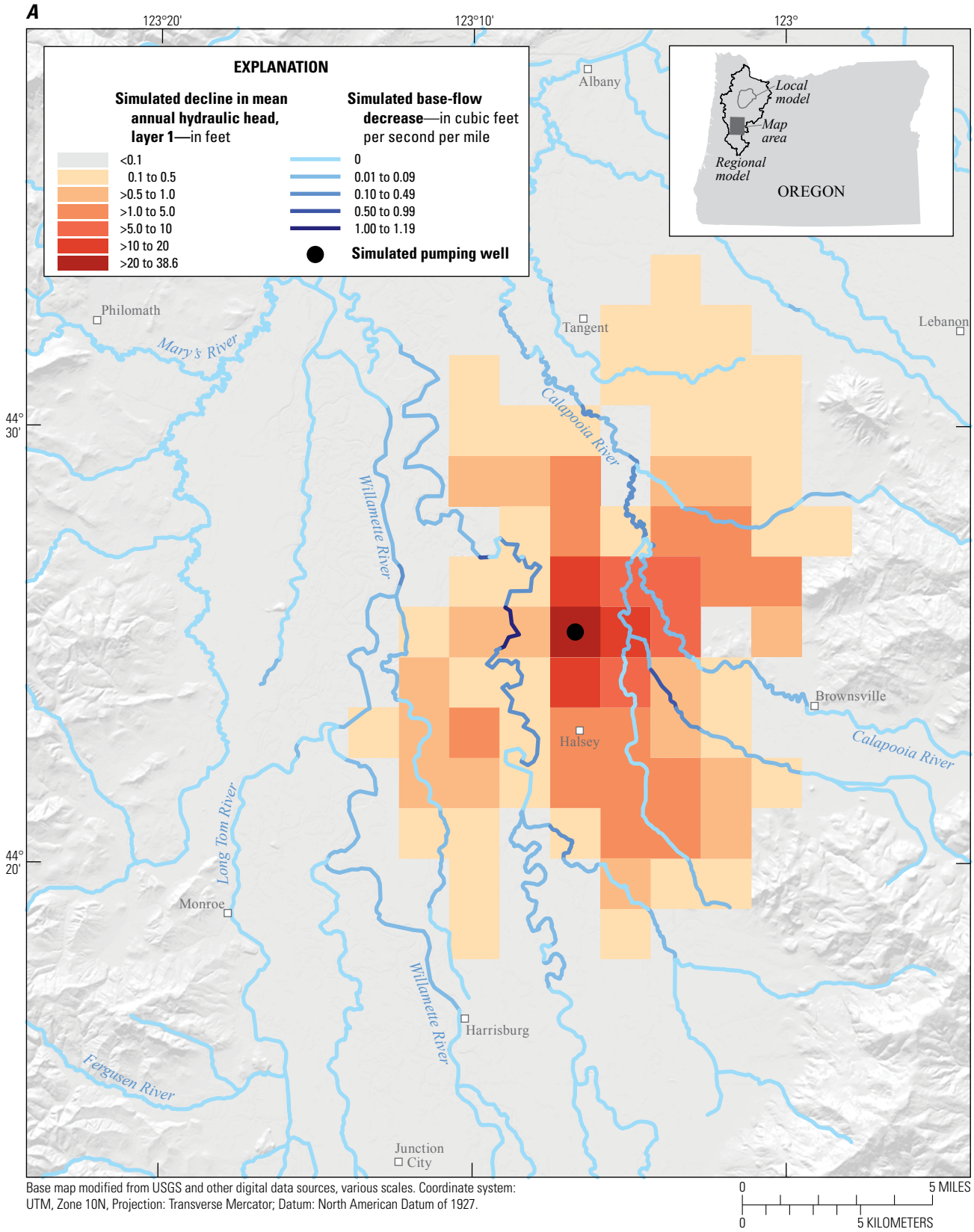

Figure 39. Simulated steady-state decline in mean annual hydraulic head for scenario RSS3c in (*A*) model layer 1 (Willamette silt unit), (*B*) model layer 2 (upper sedimentary unit/middle sedimentary unit), (*C*) model layer 3 (upper sedimentary unit/middle sedimentary unit), and (*D*) model layer 4, (lower sedimentary unit) and decrease in simulated base flow to streams after pumping an additional annual 10 cubic feet per second from the middle sedimentary unit in model layer 3, 7 miles east of the Willamette River in the Southern Willamette subbasin, Willamette Basin, Oregon.

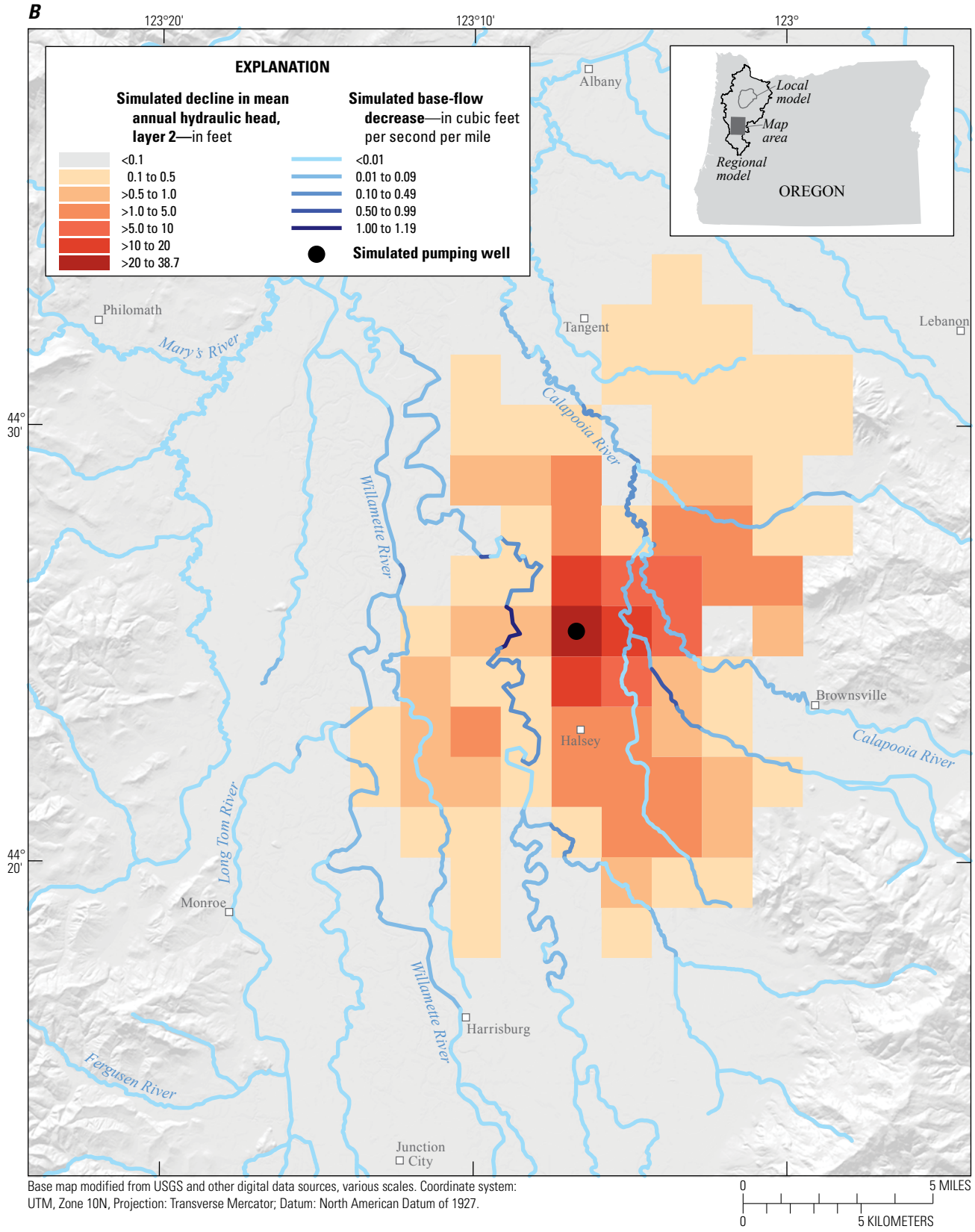

Figure 39.—Continued

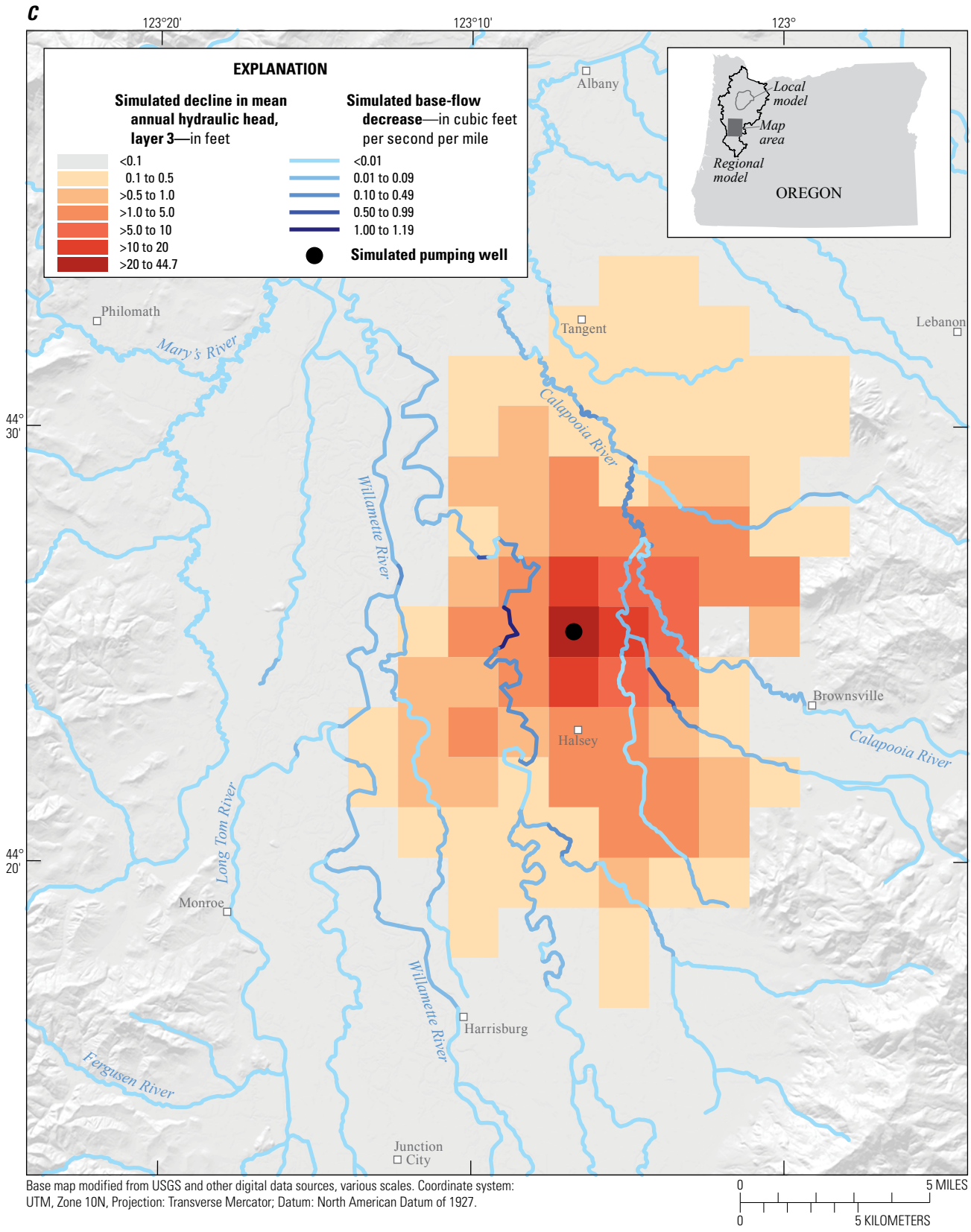

Figure 39.—Continued

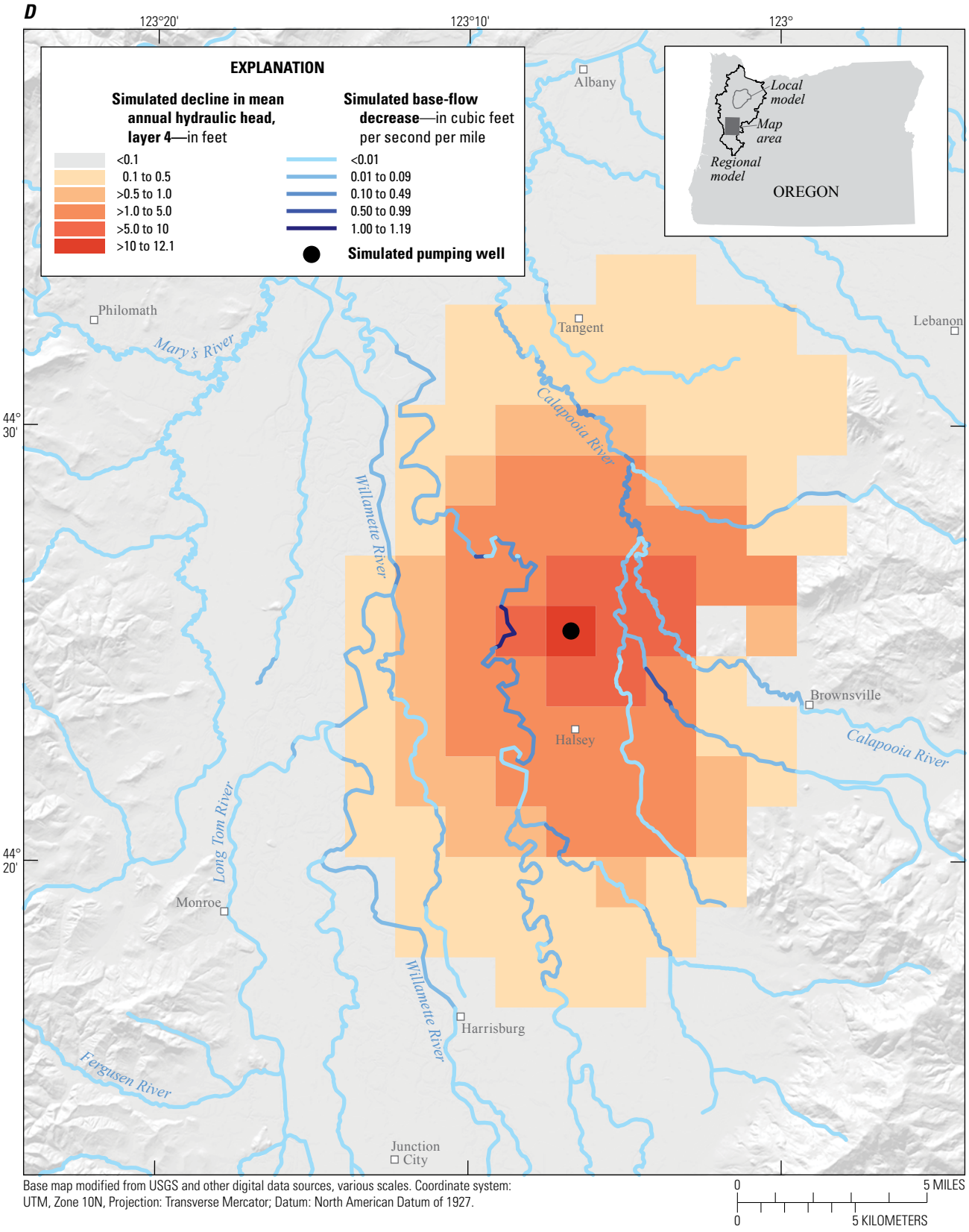

Figure 39.—Continued

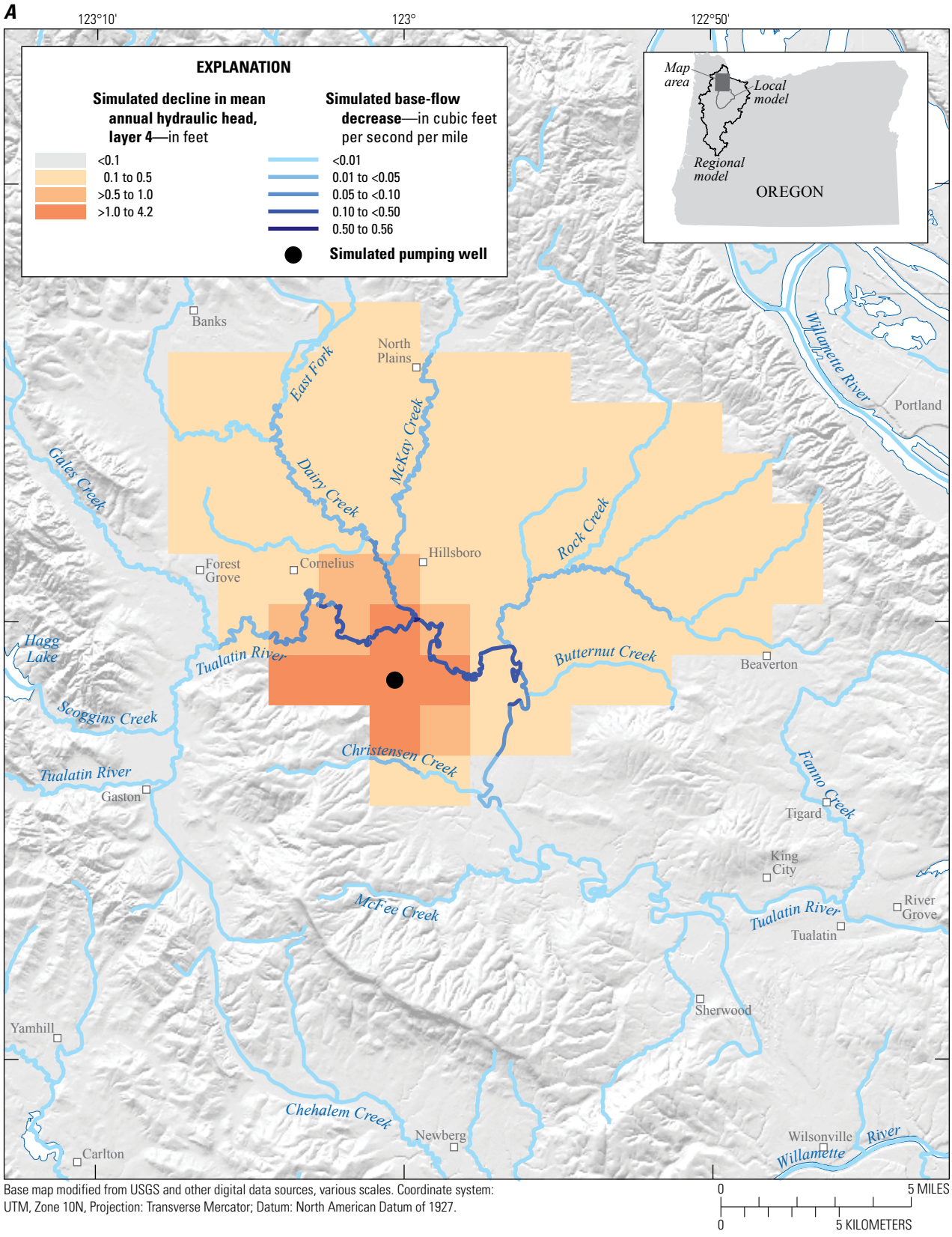

Figure 40. Simulated steady-state decline in mean annual hydraulic head for scenario RSS4a in (*A*) model layer 4 (lower sedimentary unit) and (*B*) model layer 5 (Columbia River basalt unit), and decrease in simulated base flow to streams after pumping an additional annual 5 cubic feet per second from the lower sedimentary unit in model layer 4, near the Tualatin River in the Tualatin subbasin, Willamette Basin, Oregon.

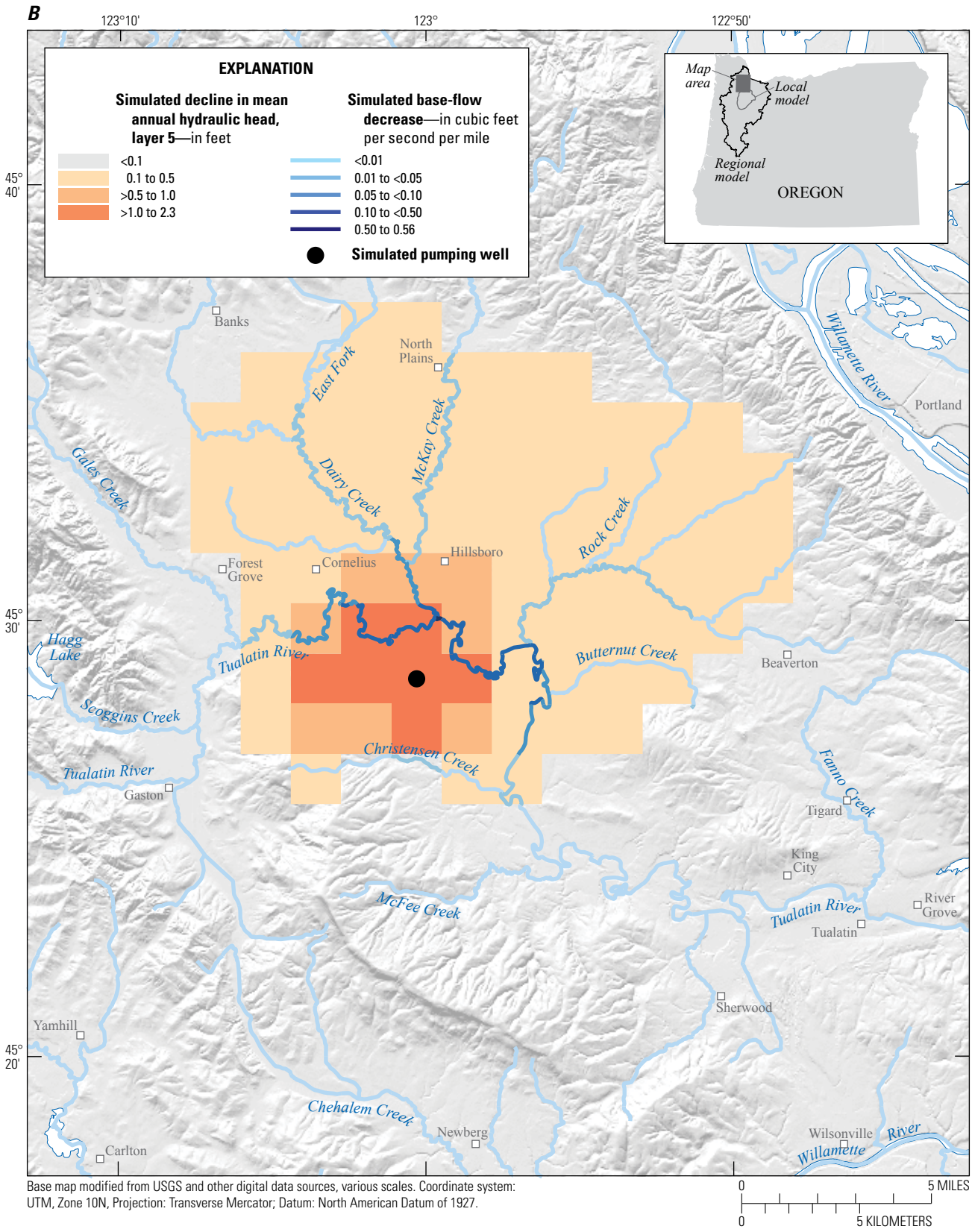

Figure 40.—Continued

In the second Tualatin subbasin scenario (RSS4b), pumping from layer 5 (CRB, row 25, column 29) (fig.41*A*–*B*) affects streamflow in the region in a manner similar to simulation RSS4a, but there is substantially more capture from streams flowing on the CRB compared to streams flowing on the LSU (fig. 4). The maximum rate of reduction in base flow is essentially the same as in the scenario RSS4a in the Tualatin River and nearby tributaries. Maximum decline in hydraulic head is about 80 ft in layer 5 in the cell with the additional pumping (fig. 41*B*). Cells immediately adjacent to that cell show simulated head declines of less than 15 ft (fig. 41*B*), and less than 10 ft in layer 4 (fig. 41*A*). The relatively low horizontal hydraulic conductivity value (table 3) estimated for the CRB in layer 5 results in a smaller calculated transmissivity when compared to values for the LSU in layer 4. Pumping stresses in units with a relatively high horizontal hydraulic conductivity result in smaller declines in hydraulic head when compared to results from pumping stresses in units with similar thickness, but a relatively low horizontal hydraulic conductivity. The area of pumping influence in both layers 4 and 5 is significantly larger in scenario RSS4b relative to scenario RSS4a as the hydraulic head reduction propagates outward across the Tualatin subbasin and southward (fig. 41*A*–*B*). As in scenario RSS4a, vertical head gradients remain relatively unchanged, except for the location near the additional pumping stress, where a downward vertical head gradient is induced in layer 4 due to the substantial reduction in head in layer 5 (fig. 41*B*).

Regional Assessment and Key Findings

Of the subbasins in the Willamette Basin study area, the greatest effect from pumping was in the Central Willamette subbasin. Simulation results indicate that mean average annual hydraulic head and groundwater-supplied base flow have decreased since pre-development in most areas of the Central Willamette subbasin and localized areas of the Portland and Southern Willamette subbasins, and will continue to decrease if full use of permitted groundwater rights occurs. Additionally, increased pumping in the Willamette Basin has resulted in increased stream capture from streams primarily in the lowland areas; the largest effects are predominantly in the Central Willamette subbasin.

Model simulation results indicate that changes to heads and flows have been relatively small in the Portland and Tualatin subbasins since pre-development due to historically less groundwater use in those basins. Although hydraulic head changes have been minor in the Southern Willamette subbasin, model simulation results indicate that substantial decreases in base flow have resulted from the relatively high conductivity of the sedimentary aquifers (USU and MSU), in which most wells are completed, and their proximity to sources of recharge from nearby streams. Both the pre-development and full-use simulations indicate that pumping stresses applied in units hydrologically connected to major streams (for example, a well completed in the USU with a nearby stream channel in the same unit) cause less drawdown in the surrounding area, but capture flow that normally would be present in nearby streams. Vertical gradients throughout the study area remained relatively unchanged from the pre-development to current conditions simulations; however, larger vertical head differences may occur with full use of permitted groundwater rights. In the Central Willamette subbasin, downward vertical gradient reversals occur in units overlain by the MSU when pumping is increased in the MSU.

Results from pumping scenarios provide detailed information for the Southern Willamette and Tualatin subbasins and support regional pumping simulation findings. Scenarios also provide examples of simple case studies that water managers can modify by adjusting hydrologic stresses and use to estimate the effects of those modifications on hydraulic head and base flow in subbasins in the Willamette Basin. One finding specific to simulations in the Southern Willamette subbasin is that pumping in the USU and MSU demonstrate (approximately two orders of magnitude) less effect on base flow in streams flowing on but not fully penetrating the WSU, than streams flowing on the USU or MSU. Thicknesses of USU and MSU in the Southern Willamette subbasin and Central Willamette subbasin are similar, but the WSU thins significantly in the Southern Willamette subbasin. Results from Southern Willamette subbasin scenarios could be extrapolated to apply to the Central Willamette subbasin. The greater thickness of the WSU in the Central Willamette subbasin indicates that pumping from the USU or MSU has relatively less effect on base flow in streams where channels flow on, but do not fully penetrate, the WSU.

Pumping from the USU near the Willamette River generally produces less head reduction in the surrounding aquifer and more Willamette River capture than pumping from the MSU or LSU due to the high transmissivity of the USU. Where aquifer thicknesses are relatively small, pumping from either the upper or the lower part of the USU produces similar results, and differences are negligible when comparing changes in aquifer head and stream base flow values. In scenarios where pumping from both the USU and MSU was simulated, vertical head gradient changes were restricted to the immediate area of the pumping stress and induced upward flow to the pumping wells in areas where vertical flow is normally downward to the LSU. Vertical head gradient changes also occurred in the Tualatin subbasin pumping scenario, where a downward vertical gradient was induced in the LSU by the added CRB pumping stress.

The influence of pumping wells is controlled by the hydrologic properties and spatial distribution of the aquifer in which the pumping is located, as well as by the proximity of streams. The oblong area of influence from pumping from the USU in the Southern Willamette subbasin near the Willamette River is coincident with the spatial distribution of the hydrologic unit and the proximity of the river (fig. 38*B*–*C*). Pumping at a distance from major streams can have a larger area of influence (fig. 39*A*–*D*) than pumping near major

streams that act as a water source (fig. 38*A*–*D*). The area of influence from pumping on both sides of the Willamette River in the USU reflects the hydrologic connection between the river and the aquifer and the close proximity of pumping to the stream channel (fig. 38*B*–*C*). The area of influence from pumping simulated in the MSU 7 mi east of the river does not extend beyond the Willamette River except in the underlying LSU (fig. 39*A*–*D*). This indicates that the Willamette River serves as a water source and limits drawdown from distant pumping for aquifers penetrated by the river (Freeze and Cherry, fig 8.15D). A stream that only partially penetrates an aquifer may not provide water as efficiently for distant wells open to that aquifer, allowing the area of influence to propagate beyond the stream. An increasing size of the area of influence with depth can be an indication of vertically decreasing horizontal hydraulic conductivity. Diminishing thickness of the unit and, consequently, transmissivity also can result in a larger area of influence from pumping.

Scenarios in the Southern Willamette and Tualatin subbasins support regional findings that streams with channels incised into the same aquifer as pumping wells are more susceptible to capture than streams that do not penetrate the aquifer. Streams that do not fully penetrate a fine-grained unit are minimally affected by pumping from underlying units. This is demonstrated in the Tualatin subbasin, where simulated pumping in the CRB induces greater stream capture in streams flowing on the CRB than in streams flowing on the LSU (figs. 2 and 41).

The results of these regional steady-state simulations provide examples of how the model can be used by water-resource managers to evaluate possible long-term effects of current pumping, and changes to current pumping, on water levels from wells and streamflows in the Willamette Basin. The regional model gives managers a means to assess the effects of pumping on hydraulic heads and streamflow on a regional basis and by specific subbasin. The study results also indicate areas where additional data are needed to better understand the groundwater and surface-water interactions in the Willamette Basin, such as groundwater-level measurements for the CRB in lowland areas.

Central Willamette Subbasin Steady-State and Transient Simulations

Regional steady-state simulations indicate that most of the change in the developed groundwater and connected surface-water system has occurred in the Central Willamette subbasin. The simulations and results presented in this section provide information on the current groundwater-flow system and the short- and long-term effects of changes in pumping on the groundwater-flow system in the Central Willamette subbasin.

Capture transects and maps for the basin were created using methods similar to those described in Leake and Pool (2010). “Capture fraction” is defined as the net change in streamflow (river/drain) divided by the additional average annual pumping rate that causes the change. This analysis simulates an additional average annual pumping stress of 10 ft^3/s sequentially assigned to every fifth grid cell in layers 1, 2, 3, or 4 of the Central Willamette subbasin MODFLOW model to provide simulations that evaluate capture on 5,000-ft centers. As the simulation is repeated for each well, the results are subtracted from the baseline model run to determine capture. Only a subset of model simulation results is shown here. Results from layer 1 are not shown in this report because hydraulic properties of the WSU preclude it from being used as a primary source of groundwater. Results from layer 2 are not presented because they are nearly identical to results from layer 3.

Care must be taken when using capture-fraction maps calculated using a certain pumping rate for assessing capture at a higher pumping rate to prevent overestimating the amount of capture of a particular surface-water feature (Leake and others, 2010). Capture-fraction maps are valid where surface and groundwater interactions are linear; that is, where transmissivity values are constant, and the configuration of rivers and drains and the water table (McDonald and Harbaugh, 1988, figs. 36 and 41) allows for linear changes in flow as the relation between the head in rivers and drains and the head in the aquifer changes. Nonlinearities can result when substantially different pumping rates are used to calculate capture fractions. Large pumping rates may cause nonlinearities where, for example, the unit is unconfined and aquifer thickness changes, or when head in the model cell declines below the bottom of a streambed in the same cell.

Steady-State Scenario Pumping—Capture Transects and Maps

The effects of pumping on the Willamette and Pudding Rivers in the Central Willamette subbasin were simulated and are presented as transects and steady-state capture maps in figures 42–45. The transects and maps show the fraction of pumping being supplied by a decrease in discharge to, and an increase in seepage from, a specified stream. Results are presented for layer 3 (USU/MSU) and layer 4 (LSU). A series of transects was oriented from the northwest to southeast in the Central Willamette subbasin (fig. 42). The transect series demonstrates the effects of pumping in different areas in the Central Willamette subbasin. Transects are numbered *N3, N2, N1, S1, S2*, and *S3*, starting from the northeastern-most transect to the southwestern-most transect (fig. 42). Transects to the north are *N1, N2*, and *N3* and to the south are *S1, S2*, and *S3*. Unit thickness and unit designation at transect midpoints, and of associated stream segments for the Willamette and Pudding Rivers at specified locations along transects are shown in table 12.

The net decrease to streamflow and the decline in hydraulic head illustrate effects from pumping at three locations in the Central Willamette subbasin (fig. 43).

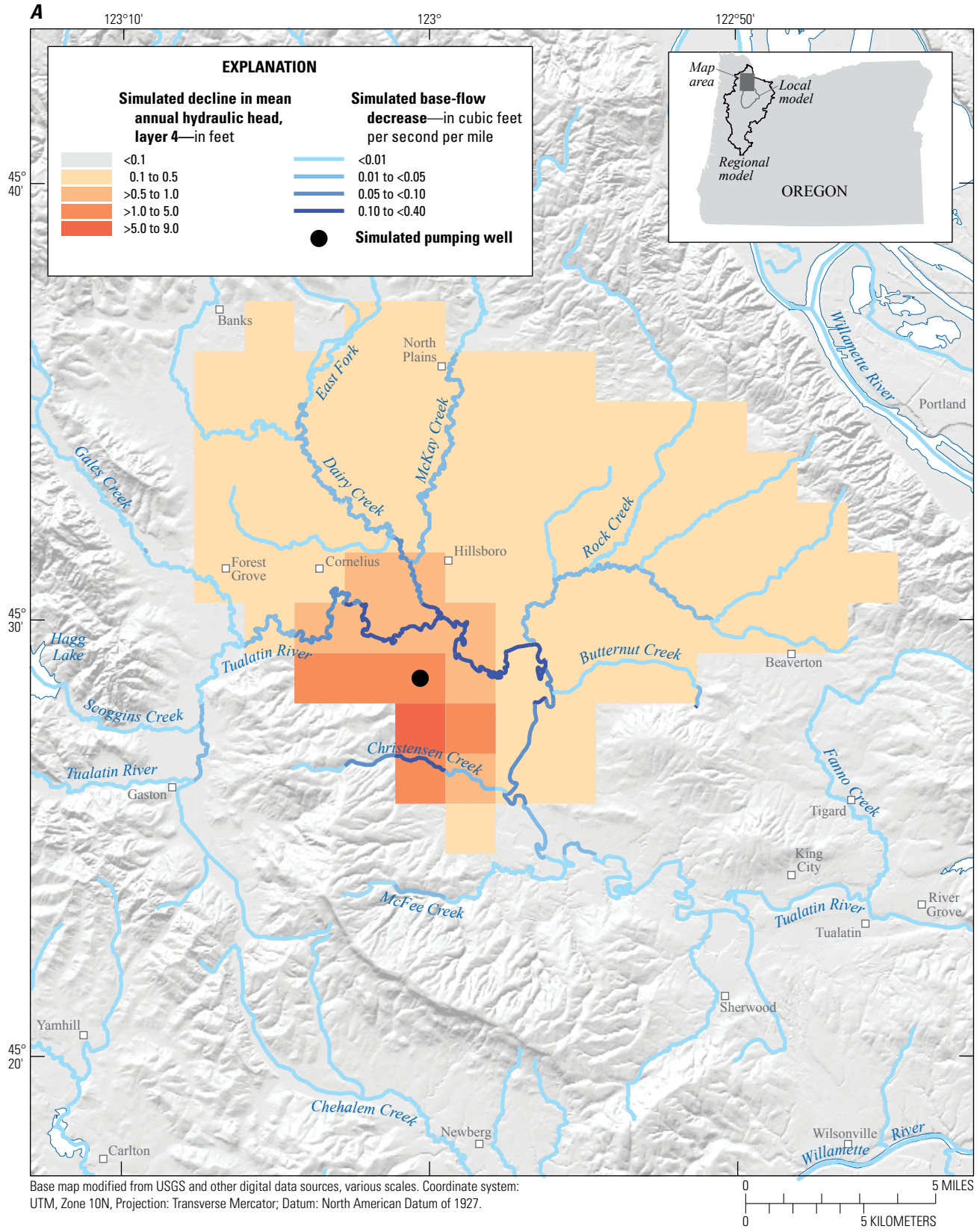

Figure 41. Simulated steady-state decline in mean annual hydraulic head for scenario RSS4b in (*A*) model layer 4 (lower sedimentary unit) and (*B*) model layer 5 (Columbia River basalt unit), and decrease in simulated base flow to streams after pumping an additional 5 cubic feet per second from the Columbia River basalt unit in model layer 5, near the Tualatin River in the Tualatin subbasin, Willamette Basin, Oregon.

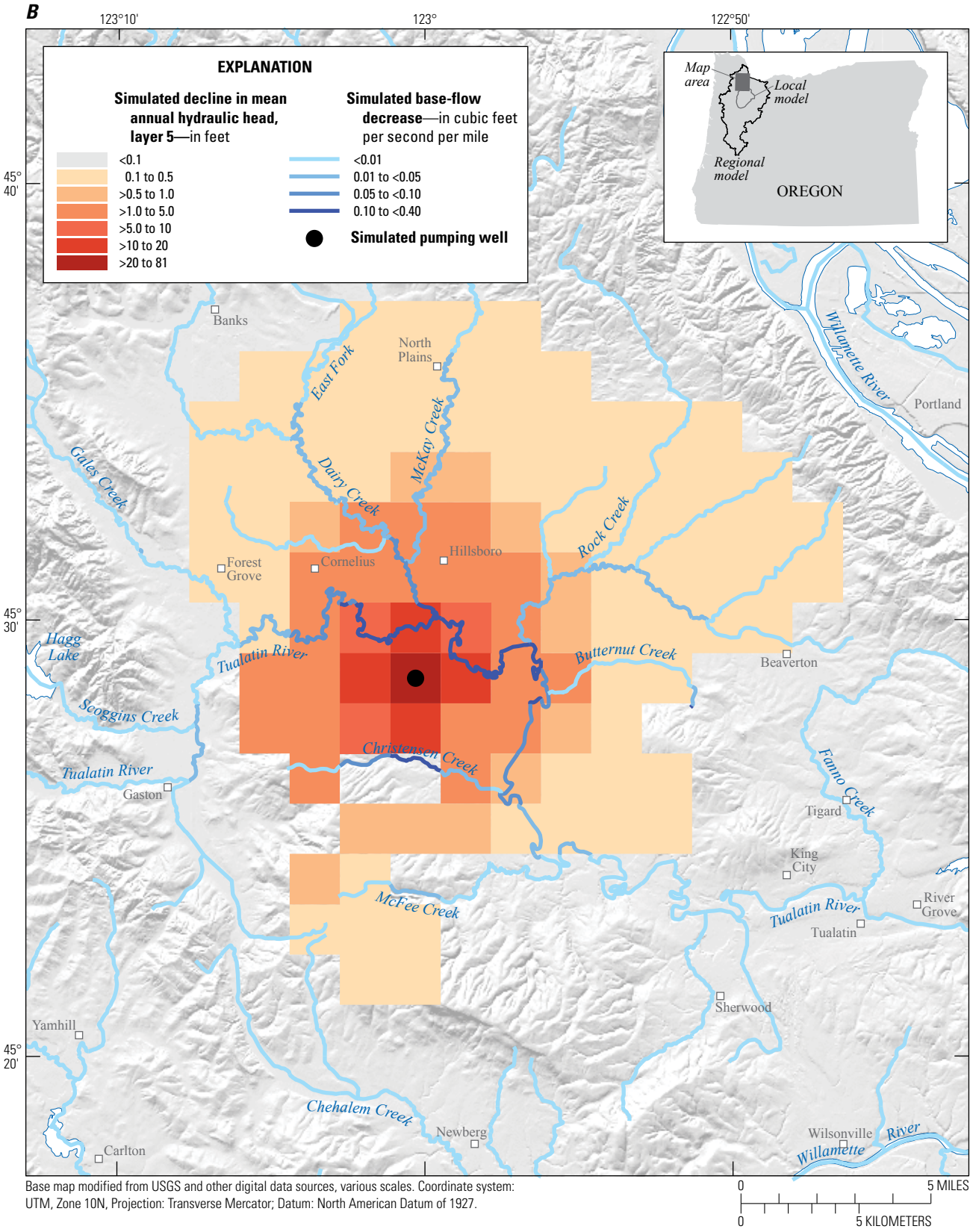

Figure 41.—Continued

The first pumping simulations (fig. 43*A*) are in model layers 3 (MSU) and 4 (LSU) near Woodburn (row 77, column 77). In this area, the MSU is relatively thin (table 12) and is not present to the northwest. The Willamette River channel is in the USU, and the Pudding River is incised into the WSU. Declines in head are large when pumping is from relatively thin areas of the MSU and cause an increase in Pudding River capture in the Central Willamette subbasin. The large declines in head in the MSU compared to declines in the LSU occur because the MSU is thin (30 ft) relative to the LSU (more than 1,000 ft) at that location (table 12). Graphs (fig. 44) represent the series of transects oriented northwest-southeast (fig. 42) in the Central Willamette subbasin. Capture fractions for the Willamette River are about 0.6 when pumping from the LSU compared to a little more than 0.5 when pumping from the MSU (fig. 44, *N1*, col 77). Capture fractions for the Pudding River are small, between 0.1 and 0.2 for pumping from the MSU or LSU (fig. 44, *N1*, col 77). Pumping from the sedimentary units in the Woodburn area captures water primarily from the Willamette River because of the efficient hydrologic connection between the river and the USU, MSU, and LSU. Pudding River capture is larger when pumping from the MSU rather than the LSU because the MSU has a better hydrologic connection with the Pudding River than the LSU due to the closer vertical proximity of the MSU to the stream. Most small streams in the Central Willamette subbasin flow on the WSU and show little effect from MSU and LSU pumping because they are isolated by the less permeable WSU. Contributions from other streams are similar regardless of the layer pumped (fig. 44, *N1*, col 77), with the exception of streams reaches located where the WSU is less thick or absent (for example, Butte and Zollner Creeks, and the upper reaches of Rock Creek) (figs. 42 and 43*A*). Head declines caused by added pumping at this location in the MSU significantly increases leakage from the Pudding River, Butte Creek, and Zollner Creek.

The next pumping simulations (fig. 43*B*) show the effects of pumping in layer 3 (MSU) and layer 4 (LSU) in close proximity to the Pudding River (row 87, column 87). These simulations again demonstrate that pumping from the relatively thin MSU results in greater head declines and Pudding River capture than pumping from the relatively thick LSU (table 12). Capture fractions for the Willamette River are about 0.5 when pumping from the LSU compared to less than 0.4 when pumping from the MSU (fig. 44, *N1*, col 87). The smaller capture fractions for the Pudding River between 0.1 and 0.3 (fig. 44, *N1*, col 87) is consistent with the conceptualization that where the Pudding River is incised into the WSU and does not cut into the underlying hydrogeologic units, there is a poor hydrologic connection between the Pudding River and the underlying MSU and LSU. The MSU has a poor, but better, hydrologic connection to the Pudding River than the LSU because the MSU is contiguous to the WSU in the area of the Pudding River. Pudding River capture is more significant where it is incised into the USU and MSU in the northeastern area of the Central Willamette subbasin. Substantial increases in Pudding River capture or from nearby tributary streams to the east is apparent only in pumping locations in close proximity to the Pudding River or those tributaries (fig. 44, transect N3, col 112).

The final pumping simulations (fig. 43*C*) shown are located midway between the Willamette River and the Pudding River in the area between Salem and Woodburn (row 97, column 57) in layer 3 (MSU) and layer 4 (LSU). Near this area, the Willamette River channel cuts into a thin layer of USU, and the Pudding River is incised into the WSU (table 12). Although the pumping is located approximately midway between the two rivers, Willamette River capture fraction is about 0.7 compared to 0.1 for the Pudding River (fig. 44, *S1*, col 57) when pumping from either the MSU and LSU (layers 3 and 4, respectively). The similarity in capture fractions for layers 3 and 4 indicate that the continuity of the unit has a significant effect on capture. This is evident in simulations where results (figs. 43*A*-*B*, and 44, transect *N1*) are affected by the absence of the USU/MSU in the northwestern area of the Central Willamette subbasin. Differences in capture fractions between pumping from the MSU and pumping from the LSU are minimal; however, differences in head declines are significant.

Graphs of north (*N1, N2, N3*) and south (*S1, S2, S3*) transects show that capture fractions change as layer geometry changes from northeast to southwest in the Central Willamette subbasin. Where the Willamette River has eroded through

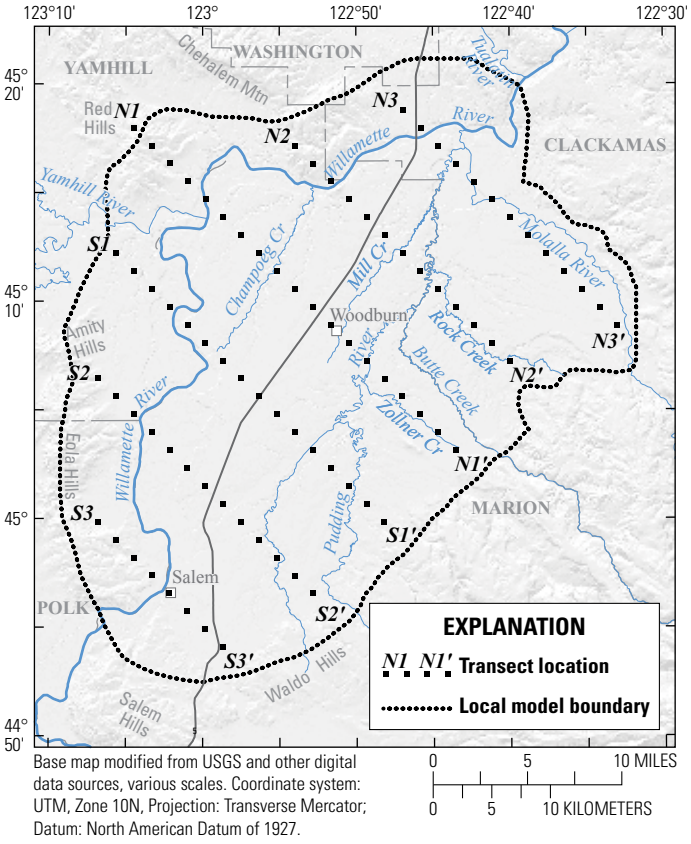

Figure 42. Capture-transect locations in the Central Willamette subbasin, Willamette Basin, Oregon.

Table 12. Thicknesses of hydrologic units measured at specified transect locations in the Central Willamette subbasin, Willamette Basin, Oregon.

[Locations of transects are shown in figure 42. Shading indicates unit that the Willamette or Pudding River is flowing on at that specified location. River can flow on underlying unit when the river has incised through overlying surficial unit(s). **Abbreviations**: CRB, Columbia River basalt unit; LSU, lower sedimentary unit; MSU, middle sedimentary unit; USU, upper sedimentary unit; WSU, Willamette silt unit; NA, not applicable]

Transect	Row	Column	Description of specified location along transect	Unit thickness at location (feet)				
				WSU	USU	MSU	LSU	CRB
N3	24	104	Willamette River	[1]	15	5	600	700
	27	107	Midpoint	90	[1]	20	600	800
	31	111	Pudding River	[1]	20	[1]	600	900
N2	38	78	Willamette River	[1]	40	[1]	10	600
	52	92	Midpoint	100	[1]	20	600	800
	64	104	Pudding River	80	[1]	20	1,000	800
N1	42	42	Willamette River	[1]	40	[1]	300	400
	77	77	Midpoint	120	[1]	30	1,100	600
	87	87	Pudding River	80	[1]	60	800	600
S1	74	34	Willamette River	[1]	40	[1]	900	300
	97	57	Midpoint	110	[1]	50	800	500
	124	84	Pudding River	60	[1]	80	200	500
S2	104	24	Willamette River	[1]	20	[1]	200	300
	117	37	Midpoint	[1]	30	70	300	500
	[2]	[2]	Pudding River	NA	NA	NA	NA	NA
S3	151	31	Willamette River	[1]	30	70	10	60
	157	37	Midpoint	[1]	40	30	10	400
	[2]	[2]	Pudding River	NA	NA	NA	NA	NA

[1]Unit not present at location.

[2]Transect does not intersect river.

the USU and MSU, and has good connection to the LSU, most pumping from the LSU is supplied by Willamette River capture (fig. 44). Tributary capture increases as pumping locations move away from the Willamette River. As pumping moves to the east, away from the Willamette and Pudding Rivers, tributary river (Molalla River and others) capture fractions increase, Pudding River capture remains nearly constant, and Willamette River capture decreases (fig. 44). Willamette River capture decreases relatively linearly in a southeasterly direction between the Willamette and Pudding Rivers (fig. 44, *N1, S1, S2*). Pumping from the LSU in the northern area of the Central Willamette subbasin has little effect on Pudding River capture (fractions are less than 0.2) (fig. 44, *N1, N2, N3*). Pudding River capture fractions are greatest to the northeast (more than 0.4 for pumping from layer 3 in close proximity to the Pudding River) (fig. 44, *N3*) where it has eroded through the WSU, and flows on a thin layer of the USU (table 12). As pumping moves into areas where the Pudding River is incised into the WSU, the poor connection between the underlying aquifers and the Pudding River becomes evident. As WSU thickness increases, Pudding River capture fraction for pumping from the MSU near the river decreases from 0.42 (fig. 44, *N3*, col 112) to 0.36 (fig. 44, *N2*, col 102) to 0.32 (fig. 44, *N1*, col 87). Pumping from the USU and MSU (layer 3) have similar effects on Pudding River capture as pumping from the LSU (layer 4) at locations distant from the river (fig. 44, *N1, N2, N3*).

Capture fractions can be displayed spatially using maps of capture as shown in figure 45. These maps show the relative contribution of streamflow capture to groundwater pumping in layers 3 (USU/MSU) and 4 (LSU) from the Willamette, Pudding, or other tributary rivers in the Central Willamette subbasin. Willamette River capture fractions generally range from 0.4 to 1.0 for pumping in the USU/MSU and LSU in all areas west of the Pudding River, indicating that Willamette River capture ultimately provides a significant amount of the pumping in most areas of the Central Willamette subbasin. Pudding River capture fractions range from 0.2 to 0.4 (as much as 0.6 near the lower reaches of the Pudding River) for pumping in the USU and MSU in areas within 2–3 mi of the Pudding River and diminish rapidly with distance. Pudding River capture fractions are much smaller, and range from zero to 0.2 in most areas in the Central Willamette subbasin for pumping in the LSU. Capture fractions for pumping in the LSU generally decrease uniformly from northwest to southeast between the Willamette and Pudding Rivers. Response to pumping in either the MSU or LSU becomes more similar in the southern part of the Central Willamette subbasin as the thickness of the lower sedimentary layer decreases, and transmissivity in the sedimentary units becomes more uniform.

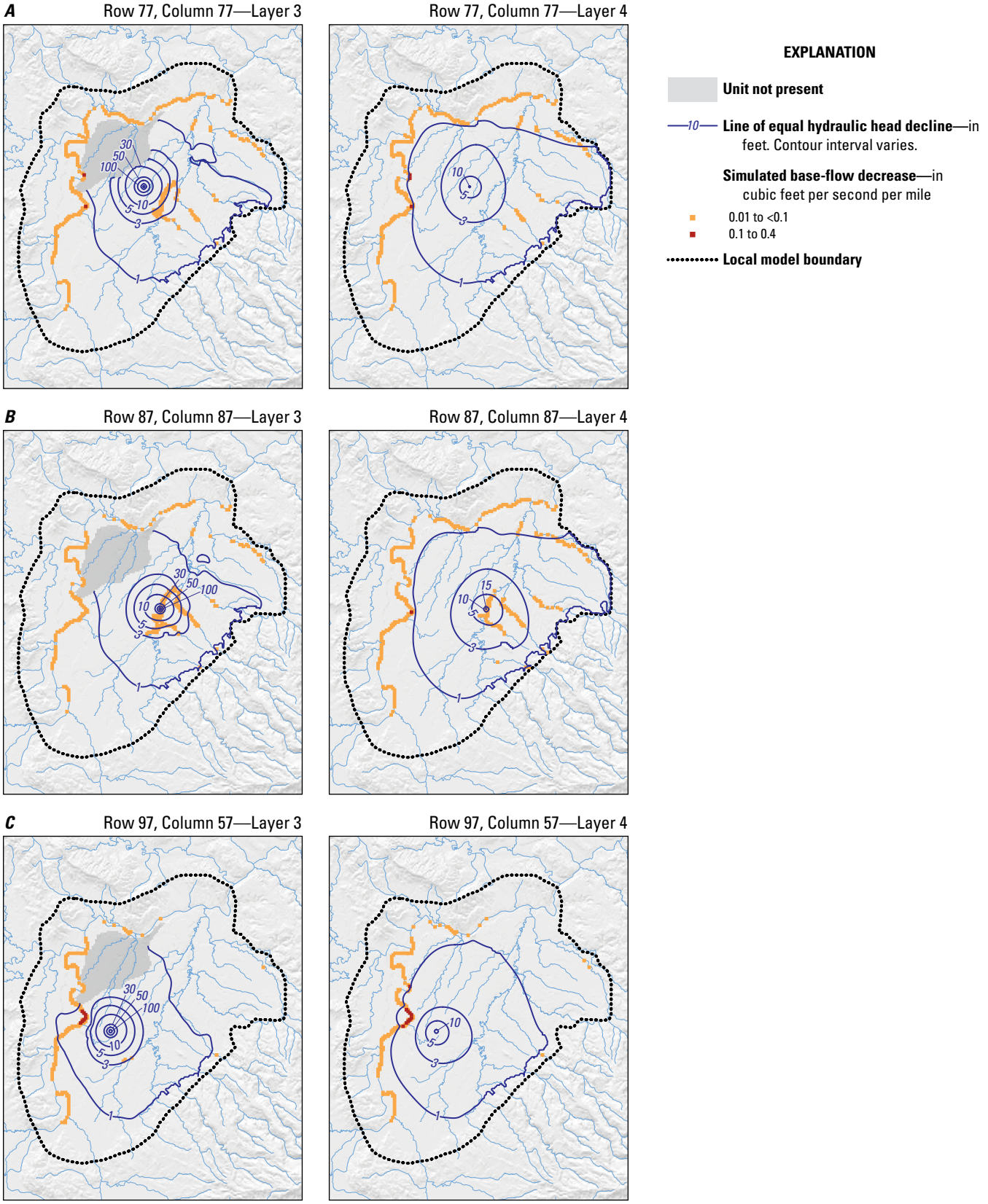

Figure 43. Simulated steady-state hydraulic-head decline in model layers 3 (upper sedimentary unit/middle sedimentary unit) and 4 (lower sedimentary unit) and base-flow decrease from pumping an additional annual 10 cubic feet per second from model layer, (*A*) near Woodburn, (*B*) near the Pudding River, and (*C*) between the Willamette and Pudding Rivers in the Central Willamette subbasin, Willamette Basin, Oregon.

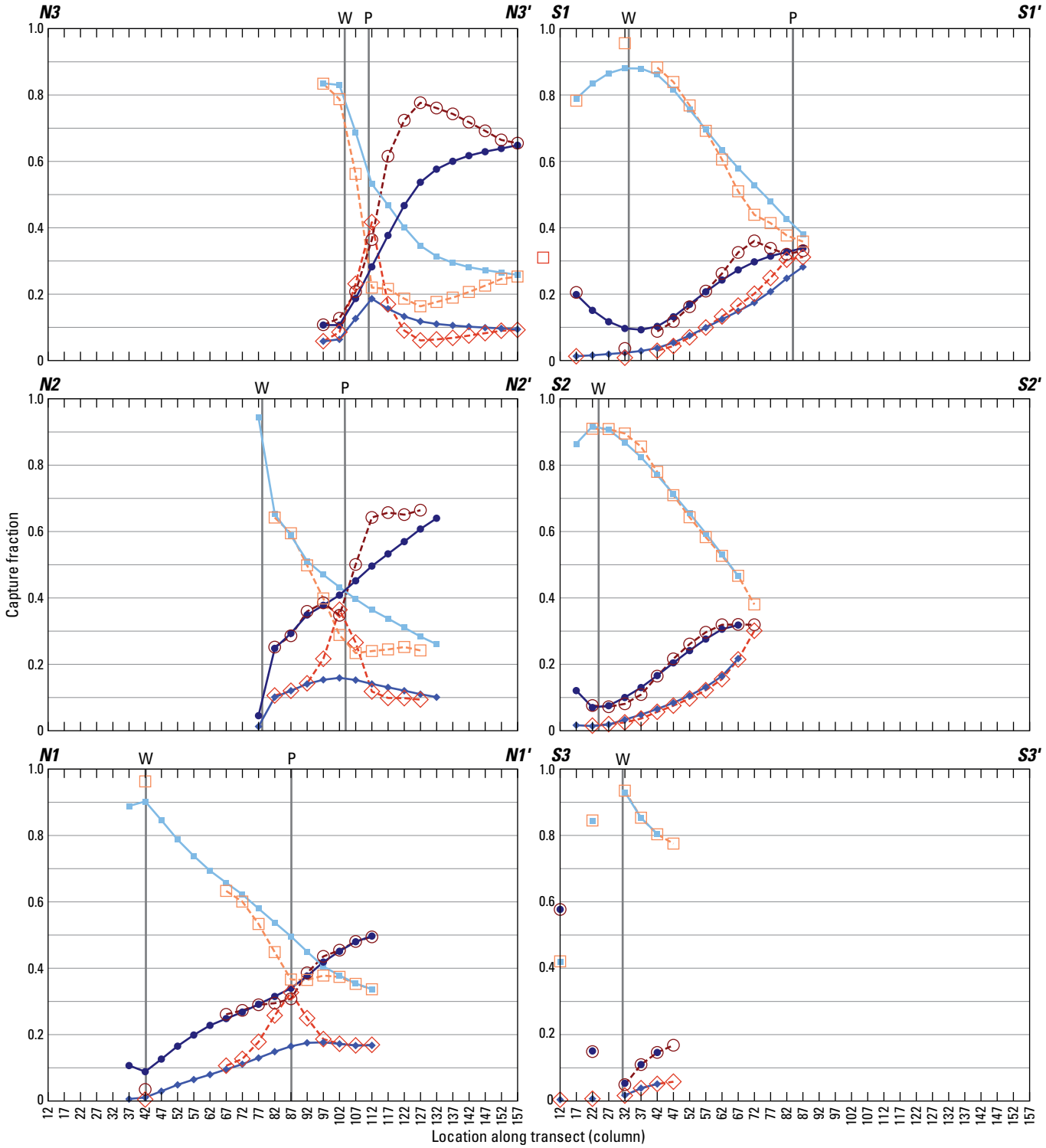

Figure 44. Ultimate capture fraction due to pumping in model layers 3 (upper sedimentary unit/middle sedimentary unit) and 4 (lower sedimentary unit) along north (*N1, N2, N3*) and south (*S1, S2, S3*) transects supplied by the Willamette, Pudding, and other selected rivers in the Central Willamette subbasin, Willamette Basin, Oregon.

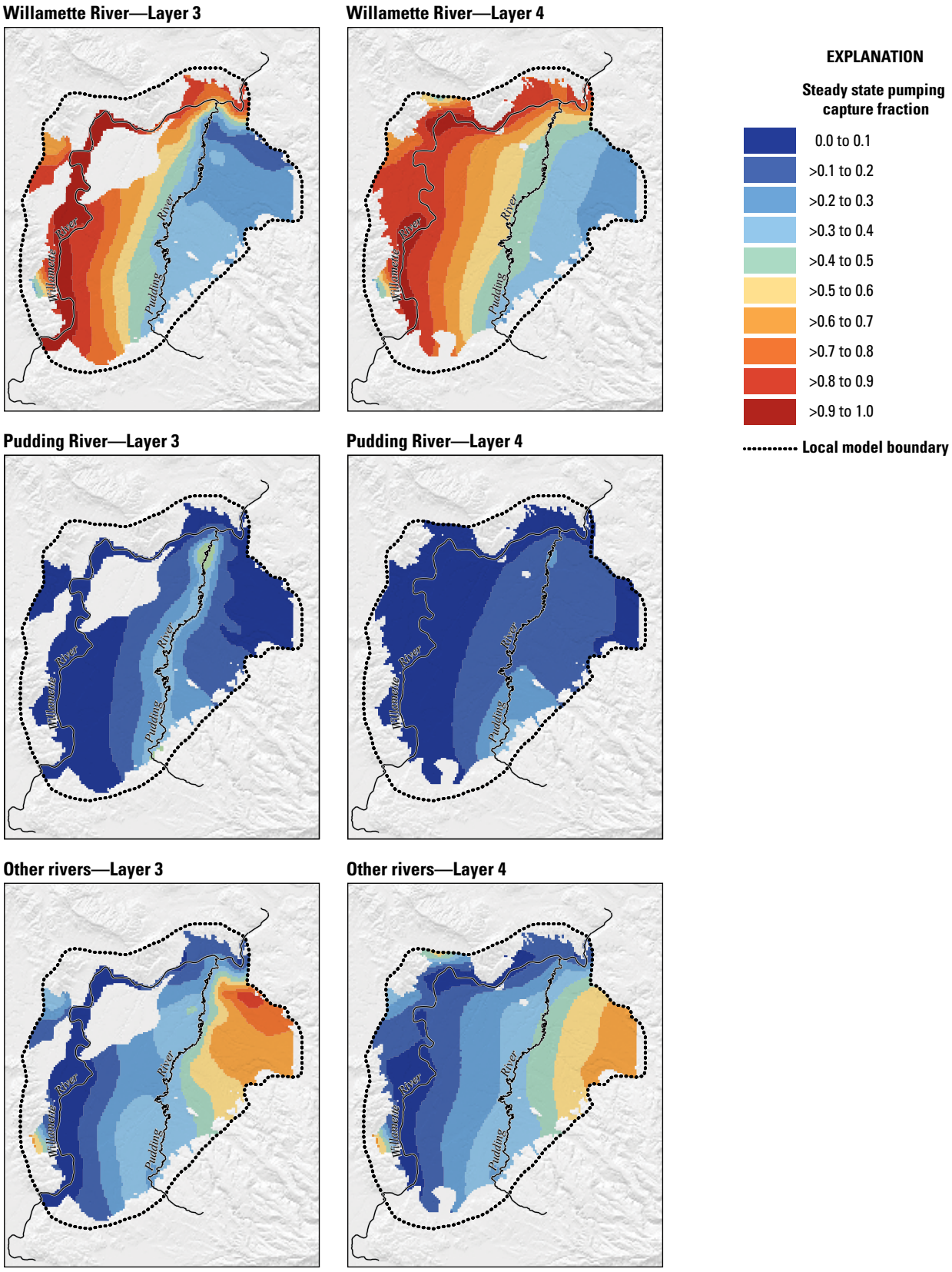

Figure 45. Computed steady-state capture fraction that would result from withdrawal of water from model layer 3 (upper sedimentary unit/middle sedimentary unit) or layer 4 (lower sedimentary unit) at a constant rate in the Willamette, Pudding, and other selected rivers in the Central Willamette subbasin, Willamette Basin, Oregon. The color at any location represents the fraction of the withdrawal rate at that location that can be accounted for as changes in outflow from and inflow to the sedimentary unit at model cells with boundary conditions representing the Willamette, Pudding, or other selected rivers.

Tributary stream ("Other rivers" in figures 44 and 45) capture in the Central Willamette subbasin is greatest east of the Pudding River near the Molalla River, and ranges from 0.3 to 0.7 for pumping in the LSU, and from 0.3 to 0.9 for pumping in the USU/MSU, with capture fractions west of the Pudding River generally less than 0.3. In areas east of the Pudding River, the Molalla River capture is substantial when compared to other streams in the Central Willamette subbasin. The Molalla River is incised into the USU and MSU, and is more responsive to pumping in the MSU and LSU because the river has a better hydrologic connection to the MSU and LSU when compared to streams incised into the WSU.

Seasonal Fluctuations and Trends of Groundwater Levels and Stream Capture Affected by Pumping

Seasonal fluctuations in groundwater levels have increased and groundwater levels have declined since pre-development to reach a new steady state, as groundwater has become a greater component of water use in the Central Willamette subbasin (Conlon and others, 2005). The local transient model that simulates dynamic-steady-state conditions was used to estimate the effects of seasonal pumping on groundwater levels. Pseudo-steady-state is the condition where seasonal effects fluctuate around an essentially constant mean (no significant long-term trends in the simulated values). To simulate monthly groundwater-level fluctuations when no long-term trend in groundwater levels occurs, the final 5 years of a 50-year simulation are used in the analysis and show groundwater levels at a pseudo-steady-state condition. Simulations represent average pumping conditions for water years 1999–2000, pre-development conditions (no pumping stress), and full use of groundwater rights (doubled pumping stress for water years 1999–2000). These simulations will be referred to as the "baseline," "pre-development," and "full-use" simulations in the remainder of this report.

Simulated groundwater levels in layers 3 (MSU) and 4 (LSU) for two locations midway between the Willamette and Pudding Rivers (row 77, column 77, and row 97, column 57; see fig. 43*A* and *C*, respectively for location) in the Central Willamette subbasin are presented in figures 46*A*–*B*. Baseline and full-use simulations show annual trends caused by consistent annual pumping withdrawals in the surrounding area, and the pre-development simulation reflects only seasonal changes in recharge and discharge. Maximum groundwater levels are present in the MSU beginning in March for baseline and pre-development scenarios, and in April for the full-use simulation. In the LSU, maximum groundwater levels begin in February for the baseline and pre-development simulations, and in March for the full-use simulation. The delay in maximum groundwater levels with full-use conditions is the result of groundwater refilling depleted storage in the aquifer. Groundwater levels are at seasonal lows during August in the baseline and full-use simulations in both the MSU and LSU, the result of increases in use during summer. In comparison, under pre-development conditions, minimum groundwater levels occur during autumn in October in both the MSU and LSU, reflecting the lag time between when the rainy season begins and when the groundwater system begins to recharge.

The increase in pumping from pre-development to the baseline condition, and from baseline to the full-use condition increases the magnitude in groundwater-level fluctuations and causes a decline in average annual groundwater levels (fig. 46*A*–*B*). Pre-development conditions show relatively stable groundwater levels, with seasonal changes of about 3–4 ft. In contrast, baseline groundwater levels fluctuate about 14–16 ft annually at the two locations in the Central Willamette subbasin. Full-use conditions fluctuate 30–32 ft annually. Between pre-development and baseline conditions, average annual groundwater levels declined from 25 to 30 ft in the MSU and about 20 ft in the LSU. Between baseline and full-use conditions, average annual groundwater levels declined an additional 30–40 ft in the MSU and 25 ft in the LSU. Simulated groundwater level declines and fluctuations vary across the Central Willamette subbasin due to local pumping and hydrogeologic unit geometry. Simulations indicate that groundwater levels declined and annual groundwater-level fluctuations increased since pre-development in the Central Willamette subbasin. Full-use simulations showed that increased pumping would cause further declines in groundwater levels and increases in annual groundwater-level fluctuations. In some areas, declines in groundwater-levels can be significant enough to cause a reversal in the vertical direction of groundwater flow (fig. 46*A*).

Development of groundwater use in the Central Willamette subbasin influences groundwater discharge to streams within the subbasin. Simulated groundwater discharge to the Willamette and Pudding Rivers from the Central Willamette subbasin is shown in figure 47. Groundwater discharge to the Willamette River for baseline conditions ranges from about 200 ft^3/s (summer) to 360 ft^3/s (winter). A summer-low/winter-high discharge pattern is displayed for the Willamette River under baseline and full-use conditions, and indicates that groundwater discharge is influenced by groundwater-use patterns in the Central Willamette subbasin. An autumn-low/winter-high discharge pattern is shown for the Willamette River pre-development condition, indicating that seasonal changes are the primary control for groundwater discharge under this condition (fig. 47). Groundwater discharge to the Willamette River responds similarly to pumping changes from pre-development to baseline to full-use conditions, except for late spring and summer, when the addition of groundwater pumping under baseline and full-use conditions decreases discharge to the Willamette River.

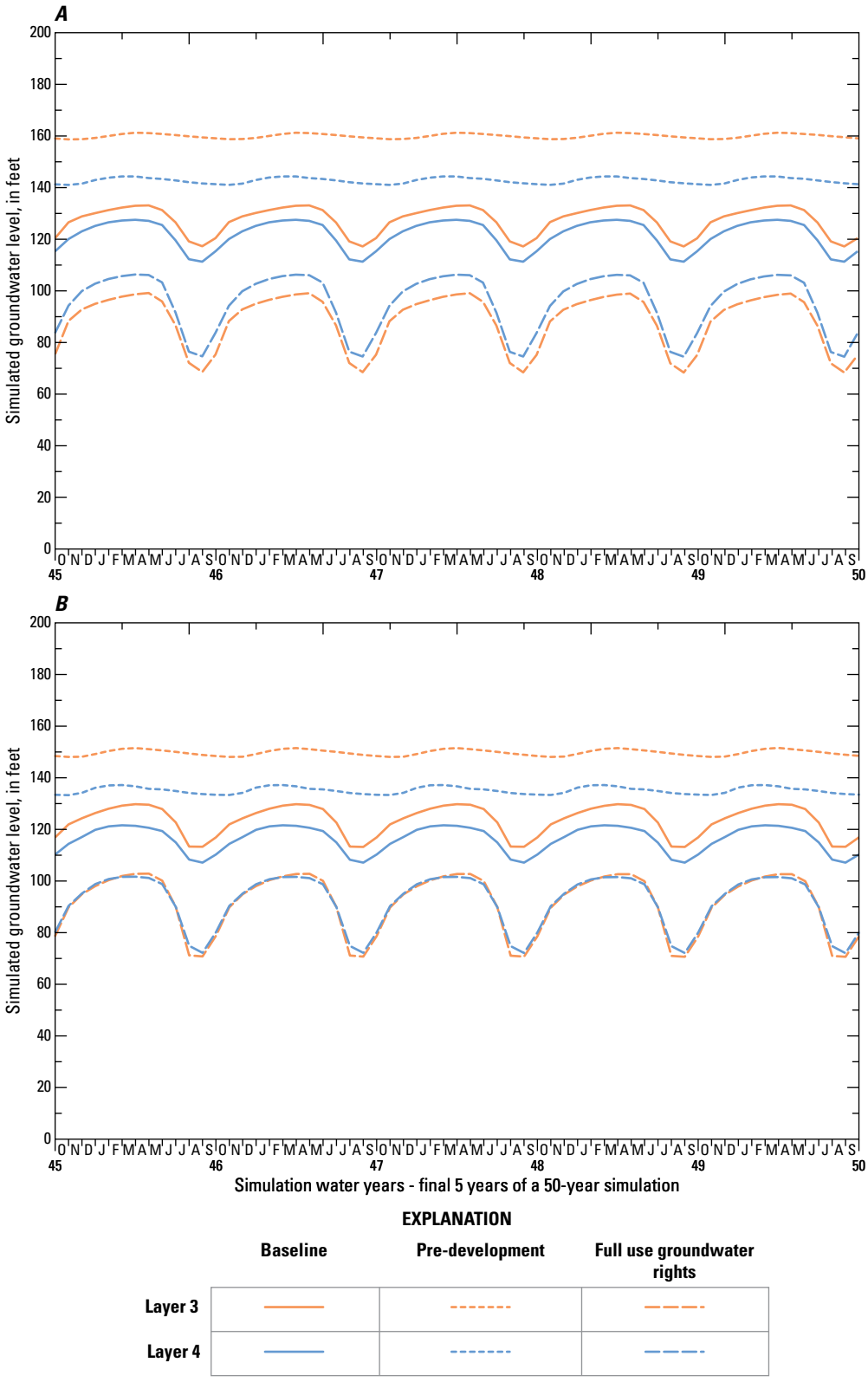

Figure 46. Simulated groundwater levels in model layer 3 (middle sedimentary unit) and layer 4 (lower sedimentary unit) for baseline, pre-development, and full use of groundwater rights conditions, for the final 5 years of a 50-year simulation in the Central Willamette subbasin, Willamette Basin, Oregon. The locations of the simulated water levels are (*A*) model cell (row 77, column 77) and (*B*) model cell (row 97, column 57).

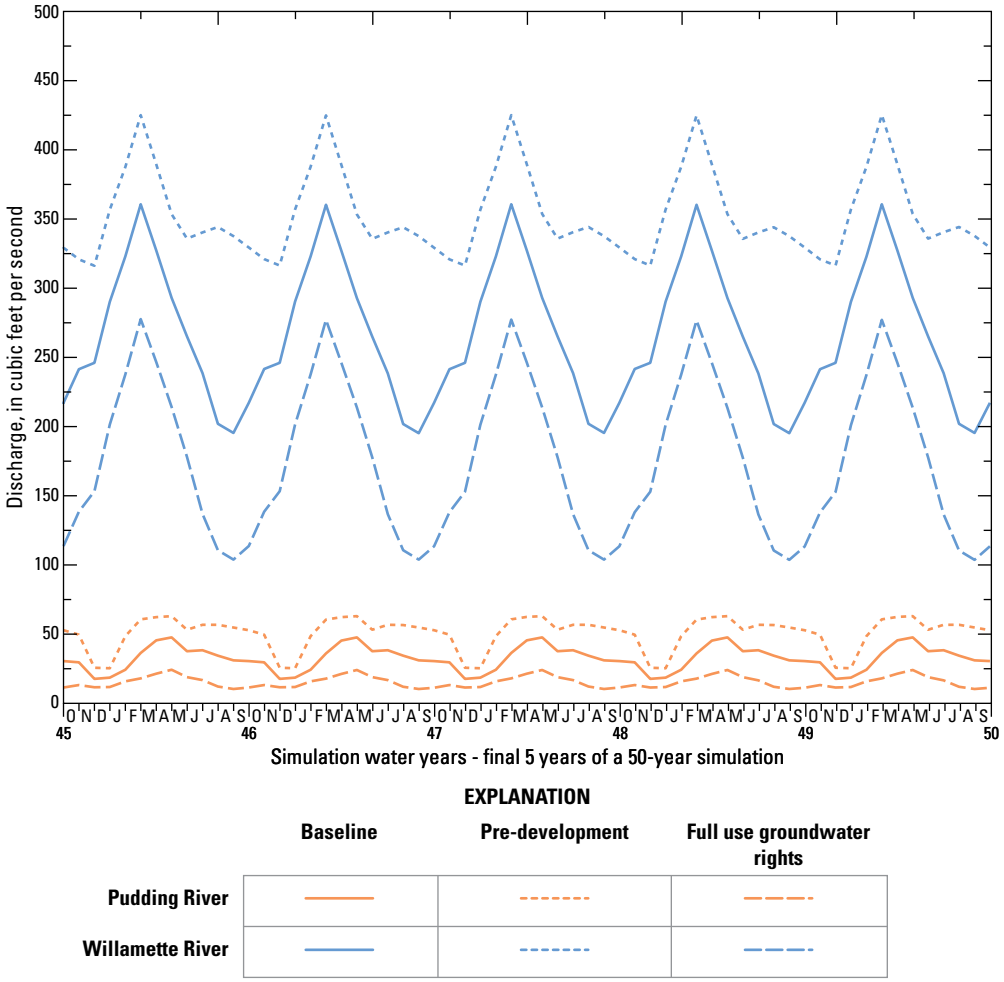

Figure 47. Simulated groundwater discharge for baseline, pre-development, and full use of groundwater rights conditions to Willamette and Pudding Rivers in the Central Willamette subbasin, Willamette Basin, Oregon, for the final 5 years of a 50-year simulation.

Groundwater discharge to the Pudding River from the Central Willamette subbasin for baseline conditions ranges from about 20 ft^3/s (autumn) to 50 ft^3/s (spring). Baseline and pre-development groundwater discharge to the Pudding River in the model area show an autumn-low/spring-high pattern, indicating that discharge to the Pudding River is controlled by seasonal fluctations of recharge and discharge rather than by pumping. Under full-use conditions, the Pudding River transitions to a summer-low/spring-high pattern, which indicates that discharge is influenced by seasonal pumping fluctuations. The discharge pattern for the Pudding River indicates a system less affected by pumping than the Willamette River. Groundwater discharge is at a minimum during November and December, prior to soil moisture field capacity being exceeded and influx of recharge. Groundwater discharge is at a maximum in early spring at the end of the recharge season and gradually tapers off as recharge lessens and the pumping season begins. When pumping is removed, as in the pre-development simulation, groundwater otherwise discharging to wells remains in the groundwater system to maintain relatively higher discharge during summer. Under conditions of increased groundwater pumping, maximum discharge occurs at the end of the recharge season, but flow rapidly decreases to reach lows during summer and late autumn. The increased discharge in October signifies the end of the pumping season and a decrease in discharge to wells in the Central Willamette subbasin.

Evaluation of Geology and Distance from Streams on Groundwater Levels and Stream Capture

Other than the Willamette and Molalla Rivers, most streams in the Central Willamette subbasin (including the Pudding River) flow on or are incised into (but have

not downcut through) the WSU. Groundwater exchange between these streams and the underlying aquifers is limited by the low-permeability WSU. Transient simulations compared the effects of seasonal pumping at a variable rate from May to October equivalent to an annual average pumping rate of 10 ft^3/s (fig. 48) additional to pumping in the baseline simulation on a stream with a bed downcut to permeable sedimentary units (the Willamette River), and on a stream that flows on the WSU (the Pudding River). Figures 49–64 show the capture fractions for the Willamette River, which has an efficient hydrologic connection to the pumped aquifer, and for the Pudding River, which has a less efficient connection to the pumped aquifer because it flows primarily on the low-permeability WSU. Capture fractions show the differences between the "baseline" simulation and simulations that include the additional seasonal pumping along a transect. Capture rates for steady state conditions are commonly calculated as a fraction, which is generally equivalent to a percentage of the additional pumping rate. In transient simulations, the monthly pumping rate can be greater than the average annual pumping rate; therefore, monthly capture fractions can total more than 1, or more than 100 percent of the average annual pumping rate. Because of this distinction, transient capture is discussed in this report in terms of percentage. Layer 3 comprises the MSU, except near the Willamette River where the USU is present, and therefore, layer 3 will be referred to interchangeably as MSU or USU, where applicable. Layer 4 is entirely composed of the LSU and will be referred to as such in this section.

The computed transient capture for the Willamette River along the *N1* transect (fig. 42) during the final 5 years of a 50-year simulation after implementation of additional seasonal pumping (fig. 48) in layer 3 (USU/MSU) is shown in figure 49*A*. A specific pumping location (row 77, column 77, location in fig. 43*A*) is provided as an example in figure 49*B*. Steady-state capture (figs. 44 and 45) indicates that on a long-term average annual basis, about 53 percent (capture fraction equal to 0.53) of the water pumped from this location from the MSU is supplied by Willamette River capture. Transient data indicate that Willamette River capture ranges from less than 52 percent from January through May (during the time when groundwater recharge is needed to replenish storage in the aquifer) to more than 60 percent in August (when pumping demands are high). USU is present in layer 3 where the *N1* transect intersects the Willamette River and is directly connected to the river as indicated by the seasonal pumping signal evident in Willamette River capture where the river is located. The amount of pumped water attributed to Willamette River capture diminishes as distance between the river and the pumping location increases and the hydrologic unit transitions from USU to MSU. Willamette River capture for pumping at row 42, column 42, ranges from 20 to more than 100 percent, whereas at row 102, column 102, the capture is less than 40 percent and is nearly constant over the 5 years shown despite seasonal pumping.

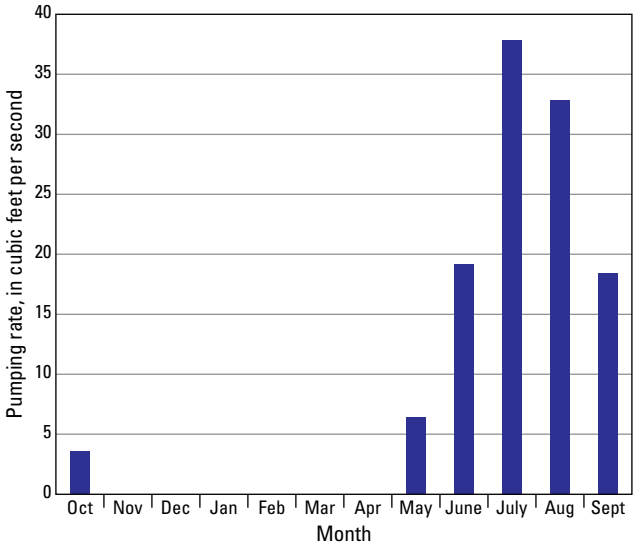

Figure 48. Additional average monthly pumping rates for simulated pumping applied in transient simulations in the Central Willamette subbasin, Willamette Basin, Oregon.

Steady-state results for the Pudding River indicate that nearly 20 percent (capture fraction equal to 0.2) (figs. 44 and 45) of the long-term average annual pumping at the specified pumping location (row 77, column 77, see fig. 43*A* for location) is supplied by Pudding River capture. Transient capture data for the Pudding River (fig. 50*A*) indicate that simulated capture ranges from less than 10 percent from November through January to more than 30 percent in February.

Data for the specific pumping location (row 77, column 77) are shown in more detail in figures 49*B* and 50*B*. The simulated pumping stress shown on the graphs (figs. 48, 49*B*, and 50*B*) is added to the existing pumping in the transient simulations. Capture for the Willamette River (fig. 49*B*) and the Pudding River (fig. 50*B*) are compared with stresses from additional simulated pumping, total simulated change in storage, and total simulated capture, which is the summation of all stream capture, including capture for Willamette and Pudding Rivers. Figures 49*A*–*B* and 50*A*–*B* show that Willamette River capture is significantly greater than Pudding River capture.

The computed transient capture for the Willamette and Pudding Rivers along the *N1* transect (fig. 42) during the final 5 years of a 50-year simulation after implementation of additional seasonal pumping (fig. 48) in layer 4 (LSU) is shown in figures 51*A* and 52*A*, respectively. The same pumping location (row 77, column 77) is shown as an example in figures 51*B* and 52*B*. Steady-state capture (figs. 44 and 45) indicates that nearly 60 percent (capture fraction equals 0.6) of pumping is supplied by Willamette River capture, and less than 15 percent (capture fraction equals 0.15) of pumping is

supplied by Pudding River capture on a long-term average annual basis. Transient capture data indicate that simulated Willamette River capture ranges from less than 50 percent from November through April to nearly 90 percent in July and August. The seasonal pumping signal is stronger in the LSU because the geometry of the unit facilitates a better hydrologic connection between the Willamette River and the LSU than between the Willamette River and the MSU. The seasonal pumping signal diminishes as the distance between the Willamette River and the pumping location increases. Simulated Pudding River capture ranges from less than 1 percent from November through January to about 25 percent in February, which demonstrates the relatively poor hydrologic connection between the Pudding River and the LSU when compared to capture results for the Willamette River.

The computed transient capture for the Willamette and Pudding Rivers along the *S1* transect (fig. 42) during the final 5 years of a 50-year simulation after implementation of additional seasonal pumping (fig. 48) in layer 3 (USU/MSU) is shown in figures 53*A* and 54*A*, respectively. A specific pumping location (row 97, column 57, see fig. 43*C* for location) provided as an example is highlighted in figures 53*B* and 54*B*. Steady-state capture (figs. 44 and 45) indicates that on a long-term average annual basis, nearly 70 percent (capture fraction equals 0.7) of pumping is supplied by Willamette River capture and about 10 percent (capture fraction equals 0.1) of pumping is supplied by Pudding River capture. Transient data indicates that Willamette River capture ranges from less than 60 percent in April to nearly 85 percent in August and September. Pudding River capture ranges from less than 1 percent from November through January to about 20 percent in February.

The computed transient capture for the Willamette and Pudding Rivers along the *S1* transect (fig. 42) during the final 5 years of a 50-year simulation after implementation of additional seasonal pumping (fig. 48) in layer 4 (LSU) is shown in figures 55*A* and 56*A*, respectively. The same pumping location (row 97, column 57) is shown as an example in figures 55*B* and 56*B*. Steady-state capture (figs. 44 and 45) indicates that on a long-term average annual basis, nearly 70 percent (capture fraction equals 0.7) of pumping is supplied by Willamette River capture, and about 10 percent (capture fraction equals 0.1) of pumping is supplied by Pudding River capture. Transient data indicate that simulated Willamette River capture ranges from less than 50 percent from February through April to more than 100 percent in July and August. Capture percentages can be reported in excess of 100 percent because they are expressed as a percentage of the annual average pumping rate (10 ft^3/s), and simulated monthly pumping rates may exceed 10 ft^3/s. Simulated Pudding River capture ranges from less than 1 percent from November through January to about 20 percent in February.

The computed transient capture for the Willamette and Pudding Rivers along the *N1* and *S1* transects (fig. 42) during 50-year simulations after implementation of additional seasonal pumping (fig. 48) in either layer 3 (USU/MSU) or layer 4 (LSU) are shown in figures 57*A*–64*A*. Monthly stress periods reflect seasonal changes from pumping effects. As pumping begins, a larger percentage of discharge is derived from groundwater storage rather than from stream capture, with the percentage from storage diminishing and the percentage from stream capture increasing over time. Although the source of most summer pumping is water released from storage, the average annual change in storage goes to zero as a new equilibrium is reached and total stream capture reaches the annual average pumping value of 10 ft^3/s. The time required to reach a new dynamic equilibrium varies according to distance from the Willamette River. The closer the simulated pumping location is to the Willamette River, the more quickly the system reaches a new equilibrium (generally within 10 years) (figs. 57–64).

Transient capture data shows that less water is released from storage when pumping from the LSU (figs. 59–60 and 63–64) compared to pumping from the USU or MSU (figs. 57–58 and 61–62). Storage decreases with depth (specific storage is set to 1–2 orders of magnitude lower in the LSU than in the USU or MSU) and smaller storage values for the LSU result in less water available for release from aquifer storage. Consequently, more pumping is supplied by stream capture than by aquifer storage because of the diminished availability of water from the LSU, significant pumping during summer, and an increase in stream capture during the winter to replenish storage (figs. 59–60 and 63–64). Initially, pumping from the MSU has greater influence on total stream capture during summer than winter. Over time, the effect diminishes as total stream capture is distributed across the year and continues into winter to replenish aquifer storage depleted by summer pumping (fig. 57–58 and 61–62). The same effect can be seen when pumping from the LSU along the *N1* transect (figs. 59–60), but is not as evident along the *S1* transect (figs. 63–64). Overall, pumping from the LSU results in greater stream capture during summer and less stream capture during winter (figs. 59–60 and 63–64).

The continuous geometry of the LSU across the basin and the resultant hydrologic connection between the LSU and the Willamette River influence stream capture in the Central Willamette subbasin. This connection causes pumping in the LSU to significantly increase Willamette River capture compared with pumping in the MSU. This contrasts with the geometry of the MSU and its absence in part of the study area that produces a barrier to flow in the Central Willamette subbasin between the Willamette River and the MSU. Pudding River capture is more influenced by pumping from the MSU (figs. 58 and 60) because the MSU directly underlies the WSU-incised Pudding River, and LSU pumping effects on Pudding River capture (fig. 60 and 64) are restricted by the relative location of the unit compared to the MSU.

Simulation results indicate that Pudding River capture is small relative to Willamette River capture at nearly all locations in the Central Willamette subbasin (figs. 49–64).

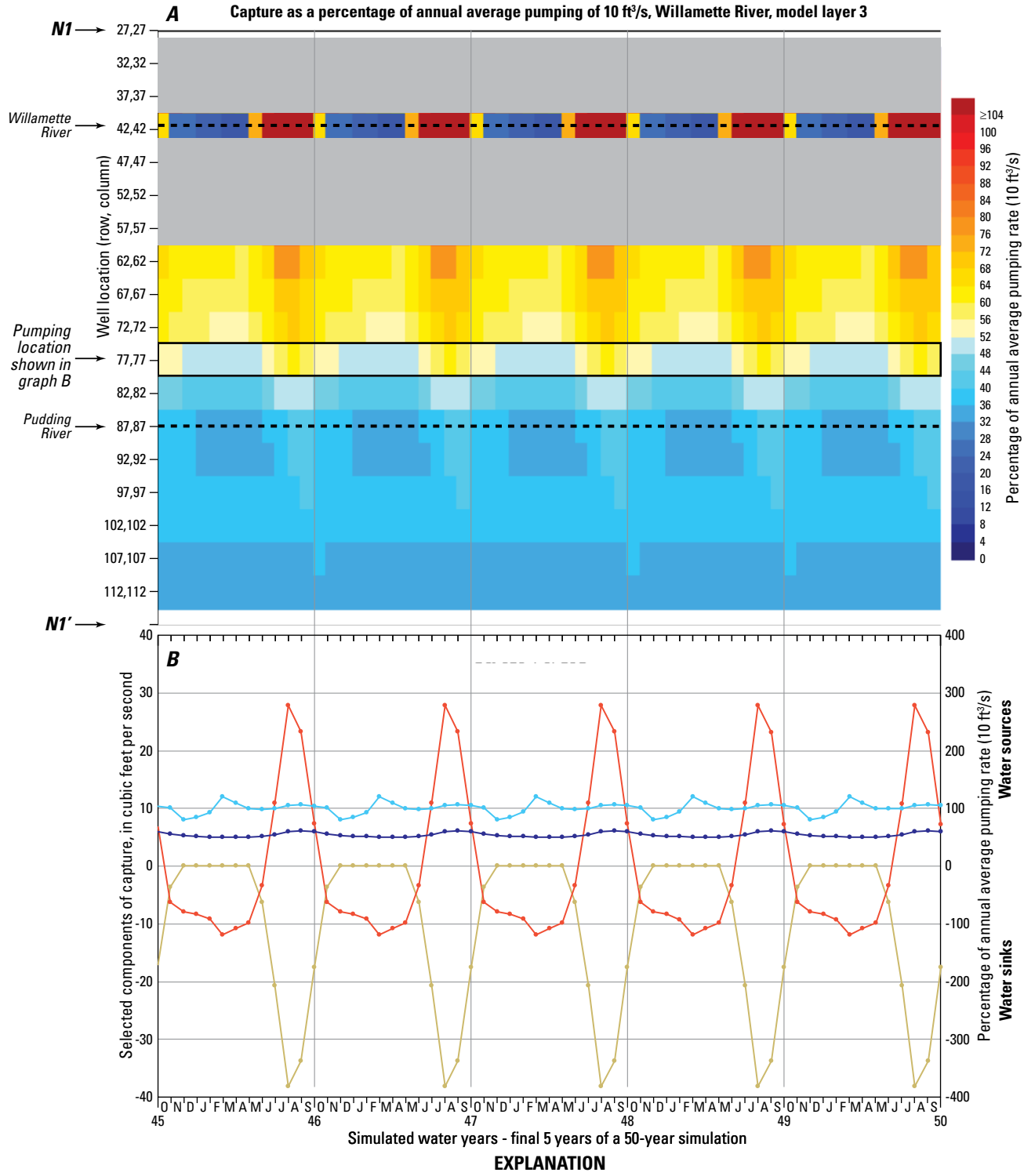

Figure 49. (*A*) Computed transient capture as a percentage of annual average pumping of 10 cubic feet per second (ft³/s) that would result from additional simulated seasonal pumping from model layer 3 and (*B*) variations in the amounts of groundwater from storage and depleted streamflow, and into storage and additional pumping, in response to an annual average increase of 10 ft³/s in pumping from row 77, column 77, model layer 3, along the *N1–N1'* transect, for the Willamette River in the Central Willamette subbasin, Willamette Basin, Oregon, for the final 5 years of a 50-year simulation.

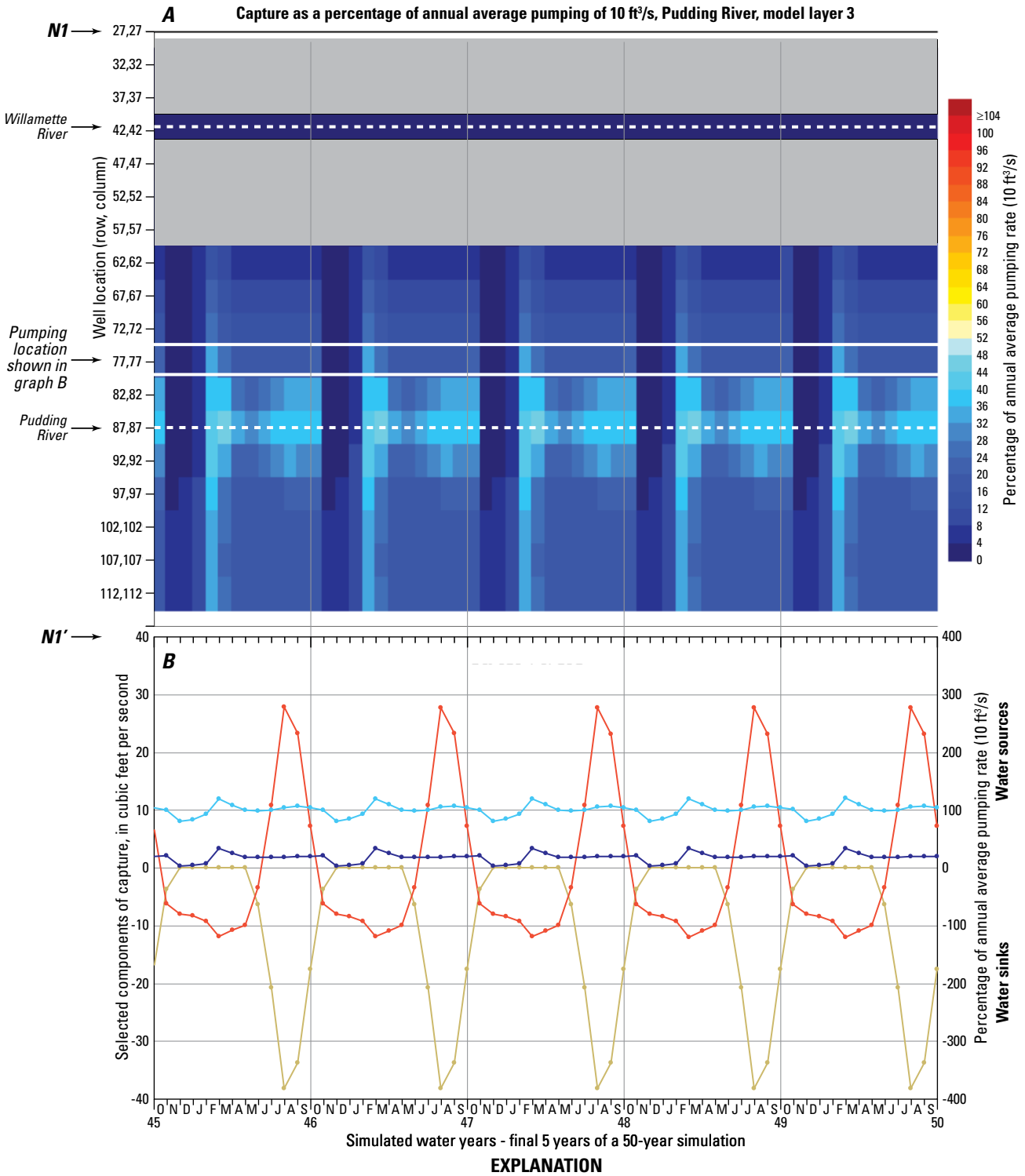

Figure 50. (*A*) Computed transient capture as a percentage of annual average pumping of 10 cubic feet per second (ft^3/s) that would result from additional simulated seasonal pumping from model layer 3 and (*B*) variations in the amounts of groundwater from storage and depleted streamflow, and into storage and additional pumping, in response to an annual average increase of 10 ft^3/s in pumping from row 77, column 77, model layer 3, along the *N1–N1′* transect for the Pudding River in the Central Willamette subbasin, Willamette Basin, Oregon, for the final 5 years of 50-year simulation.

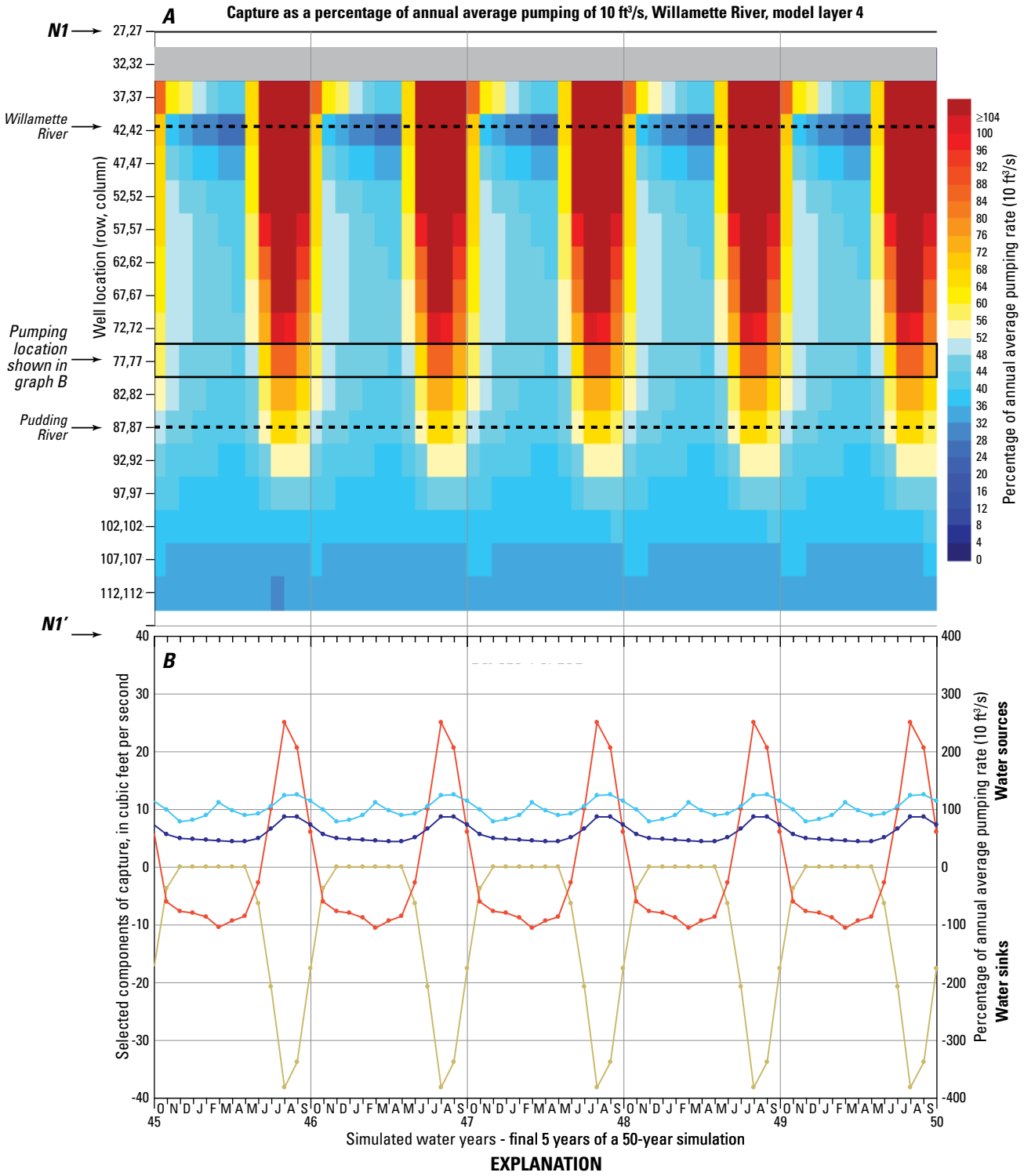

Figure 51. (*A*) Computed transient capture as a percentage of annual average pumping of 10 cubic feet per second (ft^3/s) that would result from additional simulated seasonal pumping from model layer 4 and (*B*) variations in the amounts of groundwater from storage and depleted streamflow, and into storage and additional pumping, in response to an annual average increase of 10 ft^3/s in pumping from row 77, column 77, model layer 4, along the *N1–N1′* transect for the Willamette River in the Central Willamette subbasin, Willamette Basin, Oregon, for the final 5 years of 50-year simulation.

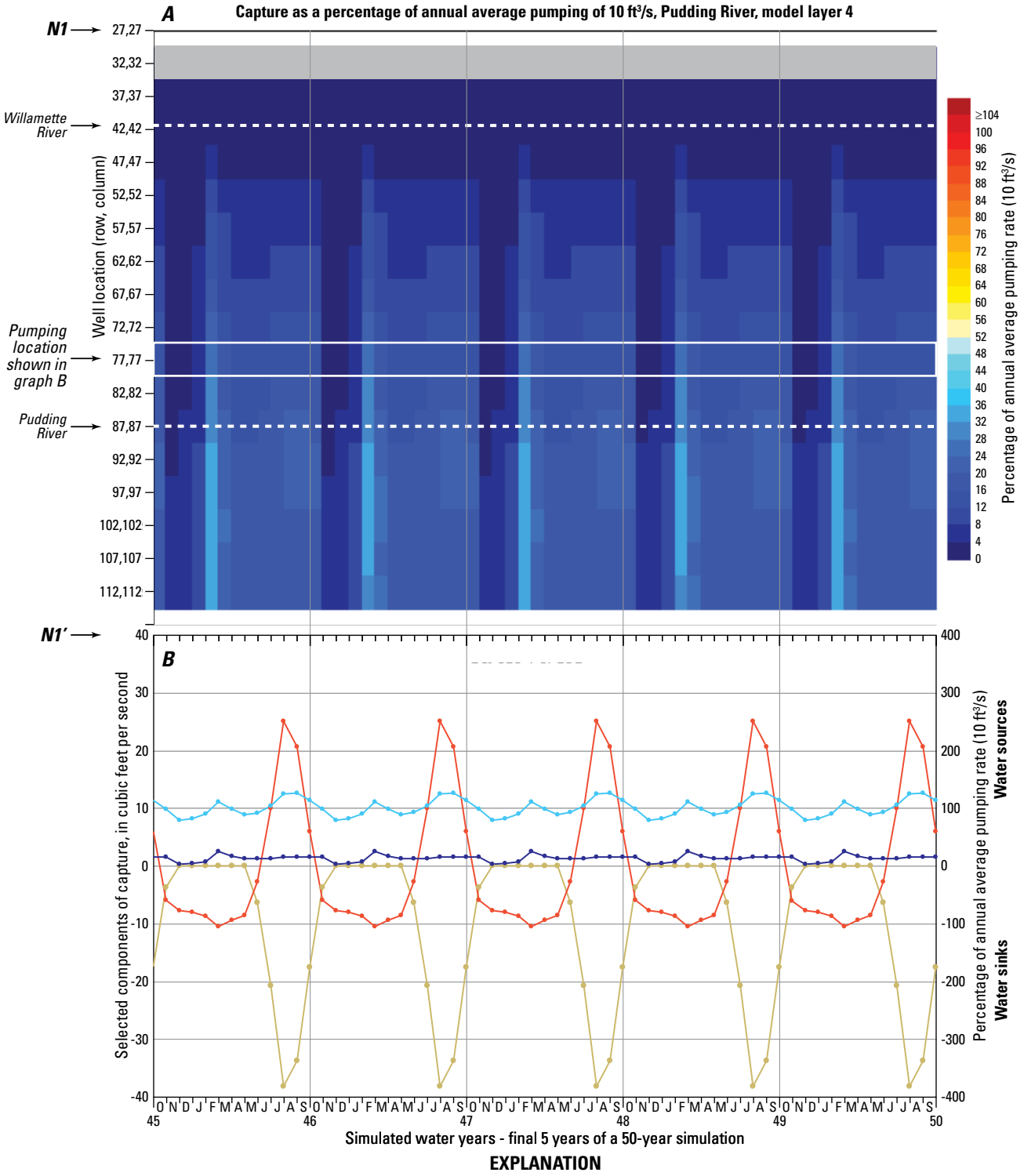

A Solid grey indicates areas where LSU is not present. Y-axis is position along *N1–N1′* line in figure 42. Pudding River capture for the pumping location shown in graph *B*; Willamette and Pudding River locations are noted along transect in white.

B **Selected components of capture for pumping at well location 77,77 in graph *A*—**Total capture is a summation of all stream capture, including Pudding River capture.

Figure 52. (*A*) Computed transient capture as a percentage of annual average pumping of 10 cubic feet per second (ft³/s) that would result from additional simulated seasonal pumping from model layer 4 and (*B*) variations in the amounts of groundwater from storage and depleted streamflow, and into storage and additional pumping, in response to an annual average increase of 10 ft³/s in pumping from row 77, column 77, model layer 4, along the *N1–N1′* transect for the Pudding River in the Central Willamette subbasin, Central Willamette subbasin, of the Willamette Basin, Oregon, for the final 5 years of a 50-year simulation.

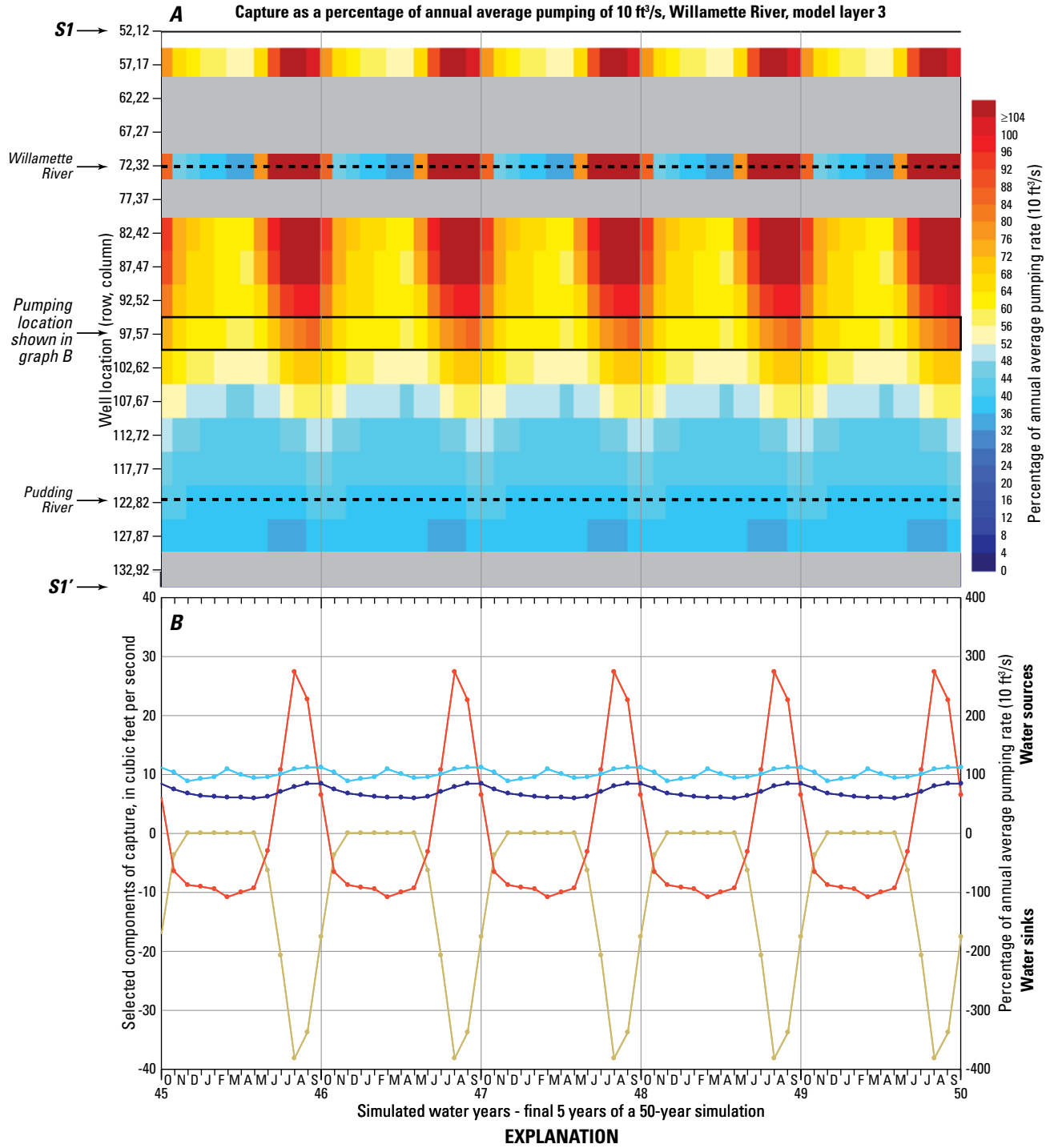

A Solid grey indicates areas where USU/MSU is not present. Y-axis is position along *S1–S1′* line in figure 42. Willamette River capture for the pumping location shown in graph *B*; Willamette and Pudding River locations are noted along transect in black.

Figure 53. (*A*) Computed transient capture as a percentage of annual average pumping of 10 cubic feet per second (ft^3/s) that would result from additional simulated seasonal pumping from model layer 3 and (*B*) variations in the amounts of groundwater from storage and depleted streamflow, and into storage and additional pumping, in response to an annual average increase of 10 ft^3/s in pumping from row 97, column 57, model layer 3, along the *S1–S1′* transect for the Willamette River in the Central Willamette subbasin, Willamette Basin, Oregon, for the final 5 years of 50-year simulation.

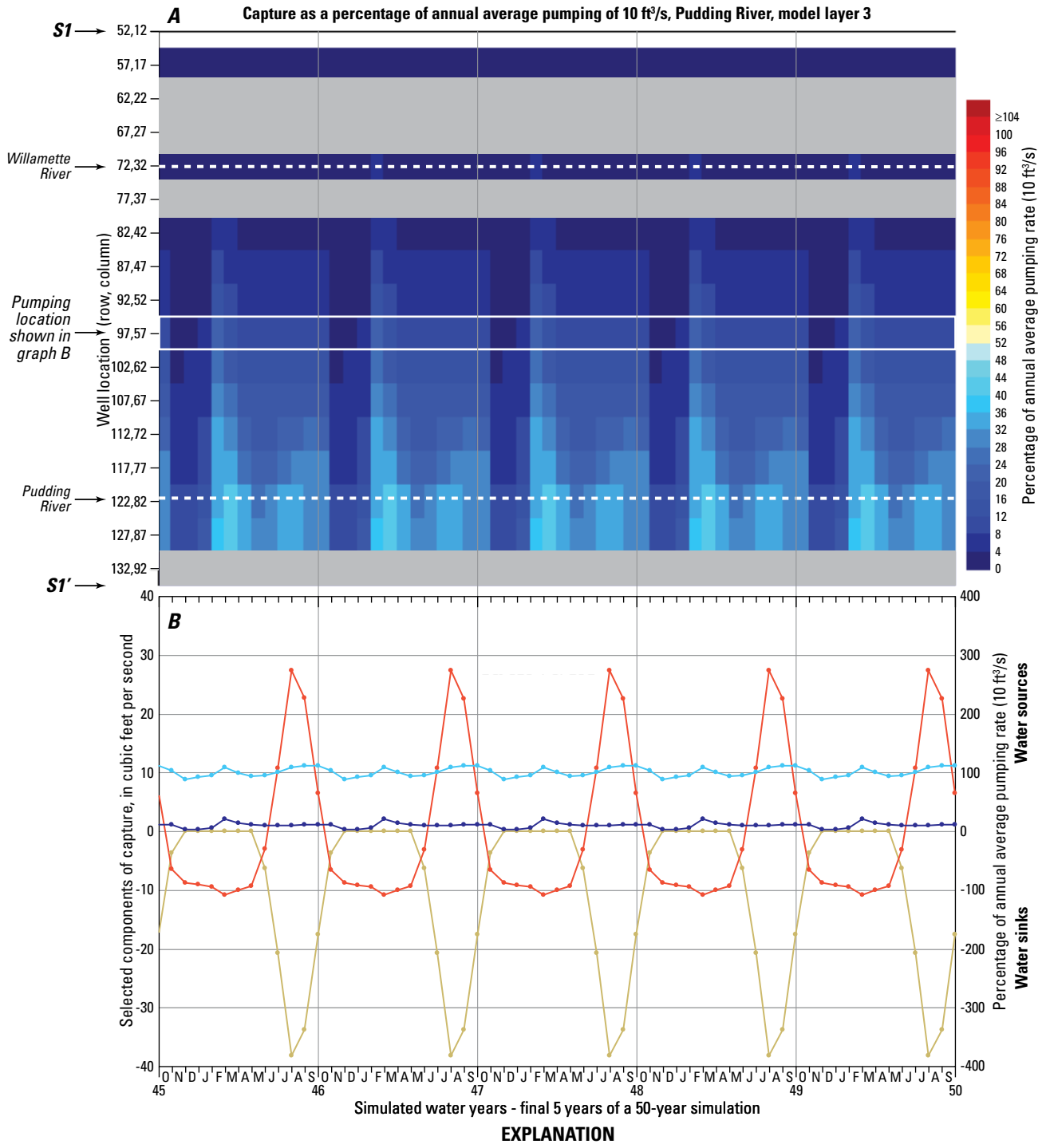

Figure 54. (*A*) Computed transient capture as a percentage of annual average pumping of 10 cubic feet per second (ft^3/s) that would result from additional simulated seasonal pumping from model layer 3 and (*B*) variations in the amounts of groundwater from storage and depleted streamflow, and into storage and additional pumping, in response to an annual average increase of 10 ft^3/s in pumping from row 97, column 57, model layer 3, along the *S1–S1′* transect for the Pudding River in the Central Willamette subbasin, Willamette Basin, Oregon, for the final 5 years of 50-year simulation.

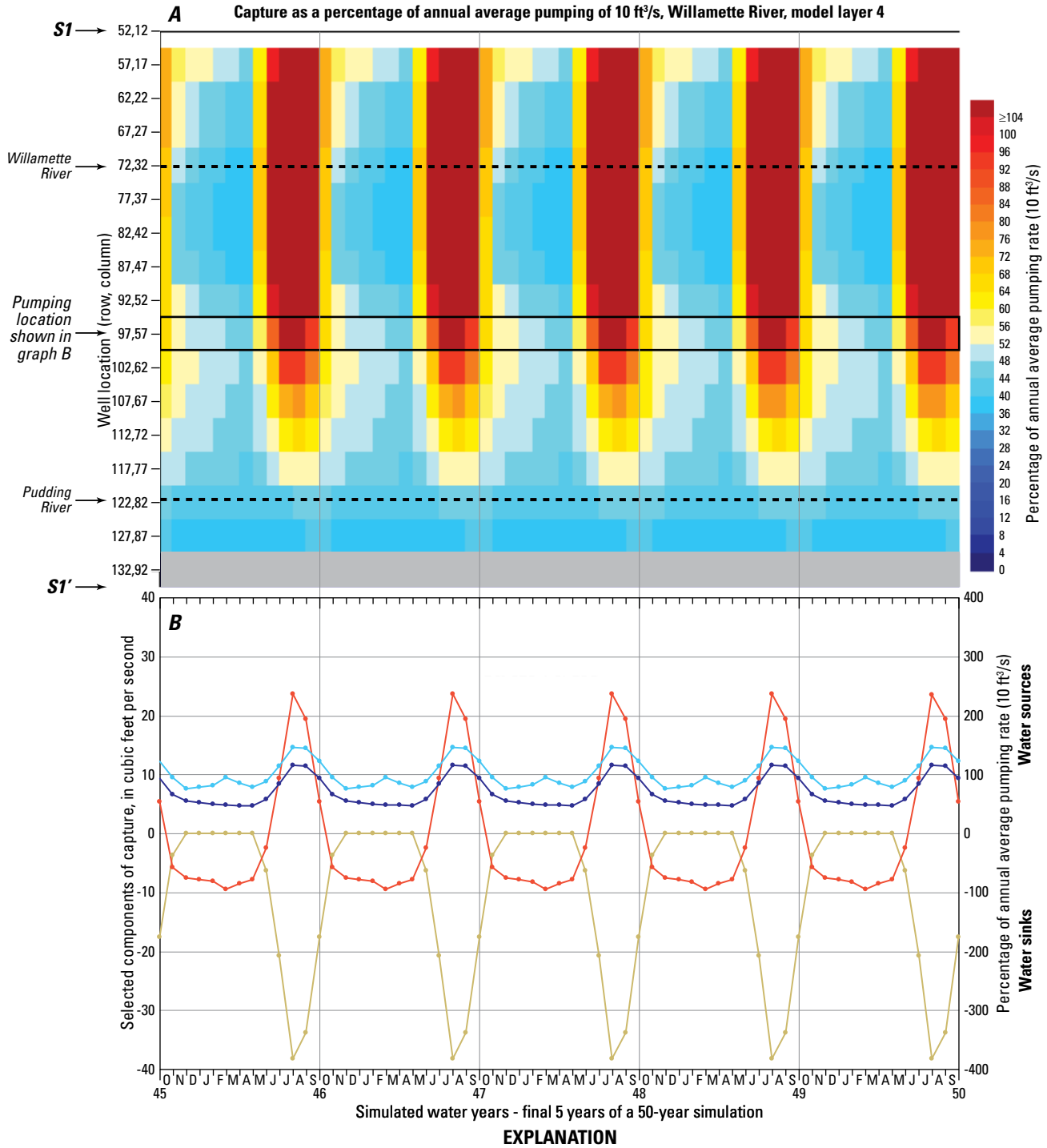

A Solid grey indicates areas where LSU is not present. Y-axis is position along *S1–S1′* line in figure 42. Willamette River capture for the pumping location shown in graph *B*; Willamette and Pudding River locations are noted along transect in black.

B **Selected components of capture for pumping at well location 97,57 in graph *A*—**Total capture is a summation of all stream capture, including Willamette River capture.

Figure 55. (*A*) Computed transient capture as a percentage of annual average pumping of 10 cubic feet per second (ft³/s) that would result from additional simulated seasonal pumping from model layer 4 and (*B*) variations in the amounts of groundwater from storage and depleted streamflow, and into storage and additional pumping, in response to an annual average increase of 10 ft³/s in pumping from row 97, column 57, model layer 4, along the *S1–S1′* transect for the Willamette River in the Central Willamette subbasin, Willamette Basin, Oregon, for the final 5 years of a 50-year simulation.

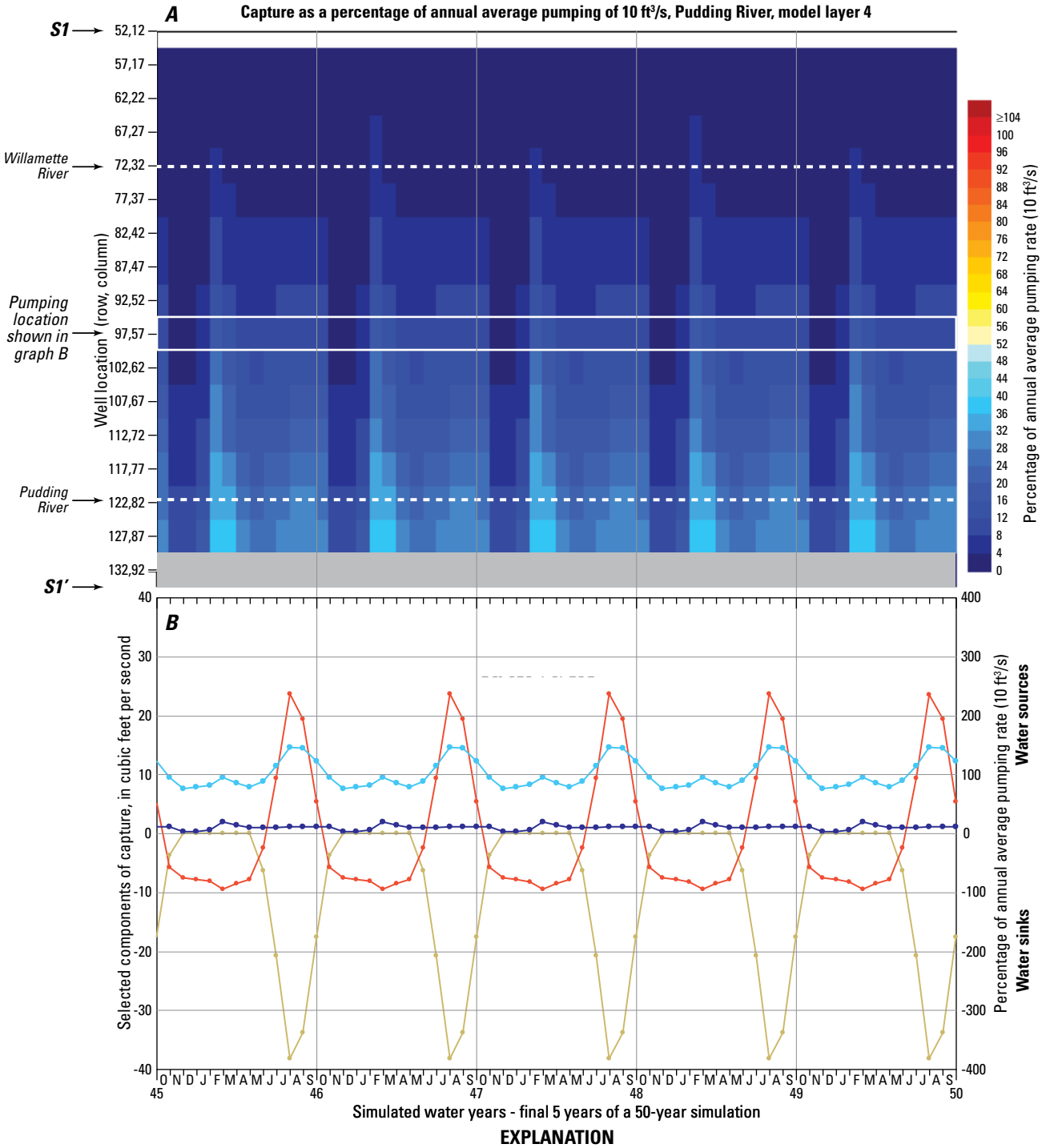

Figure 56. (*A*) Computed transient capture as a percentage of annual average pumping of 10 cubic feet per second (ft³/s) that would result from additional simulated seasonal pumping from model layer 4 and (*B*) variations in the amounts of groundwater from storage and depleted streamflow, and into storage and additional pumping, in response to an annual average increase of 10 ft³/s in pumping from row 97, column 57, model layer 4, along the *S1–S1′* transect for the Pudding River in the Central Willamette subbasin, Willamette Basin, Oregon, for the final 5 years of a 50-year simulation.

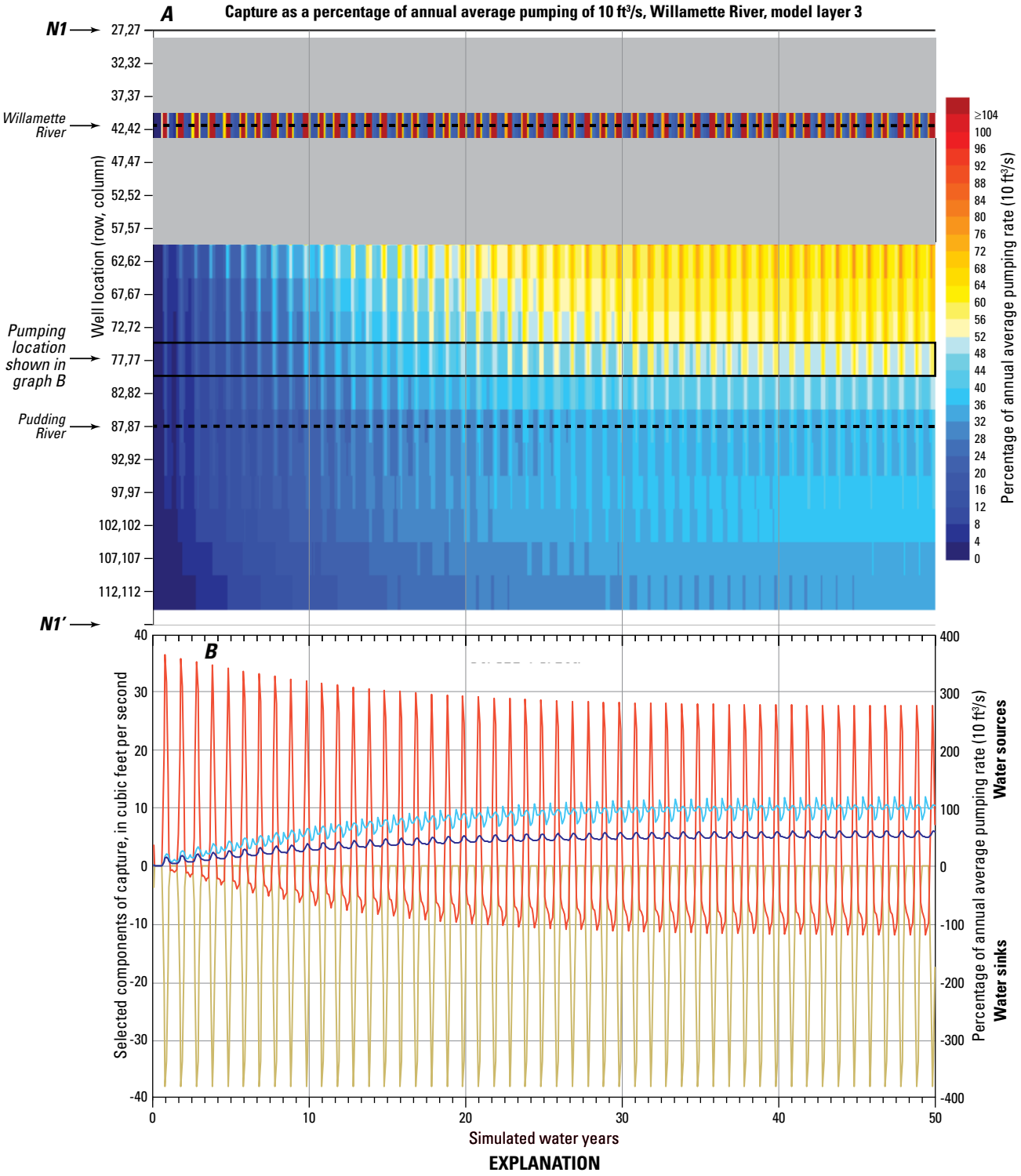

Figure 57. (*A*) Computed transient capture as a percentage of annual average pumping of 10 cubic feet per second (ft^3/s) that would result from additional simulated seasonal pumping from model layer 3 and (*B*) variations in the amounts of groundwater from storage and depleted streamflow, and into storage and additional pumping, in response to an annual average increase of 10 ft^3/s in pumping from row 77, column 77, model layer 3, along the *N1–N1′* transect for the Willamette River in the Central Willamette subbasin, Willamette Basin, Oregon, for a 50-year simulation.

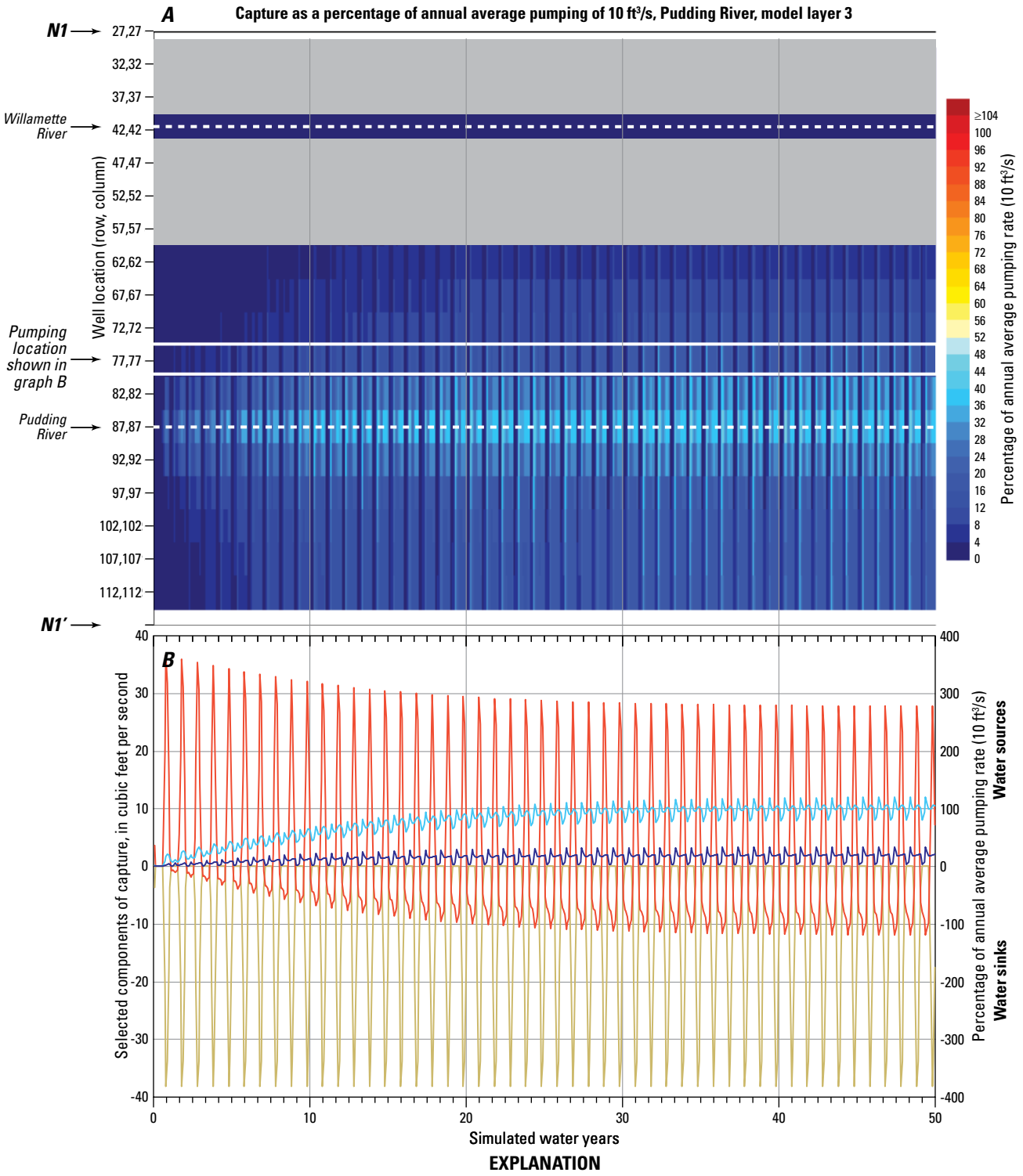

Figure 58. (*A*) Computed transient capture as a percentage of annual average pumping of 10 cubic feet per second (ft^3/s) that would result from additional simulated seasonal pumping from model layer 3 and (*B*) variations in the amounts of groundwater from storage and depleted streamflow, and into storage and additional pumping, in response to an annual average increase of 10 ft^3/s in pumping from row 77, column 77, model layer 3, along the *N1–N1′* transect for the Pudding River in the Central Willamette subbasin, Willamette Basin, Oregon, for a 50-year simulation.

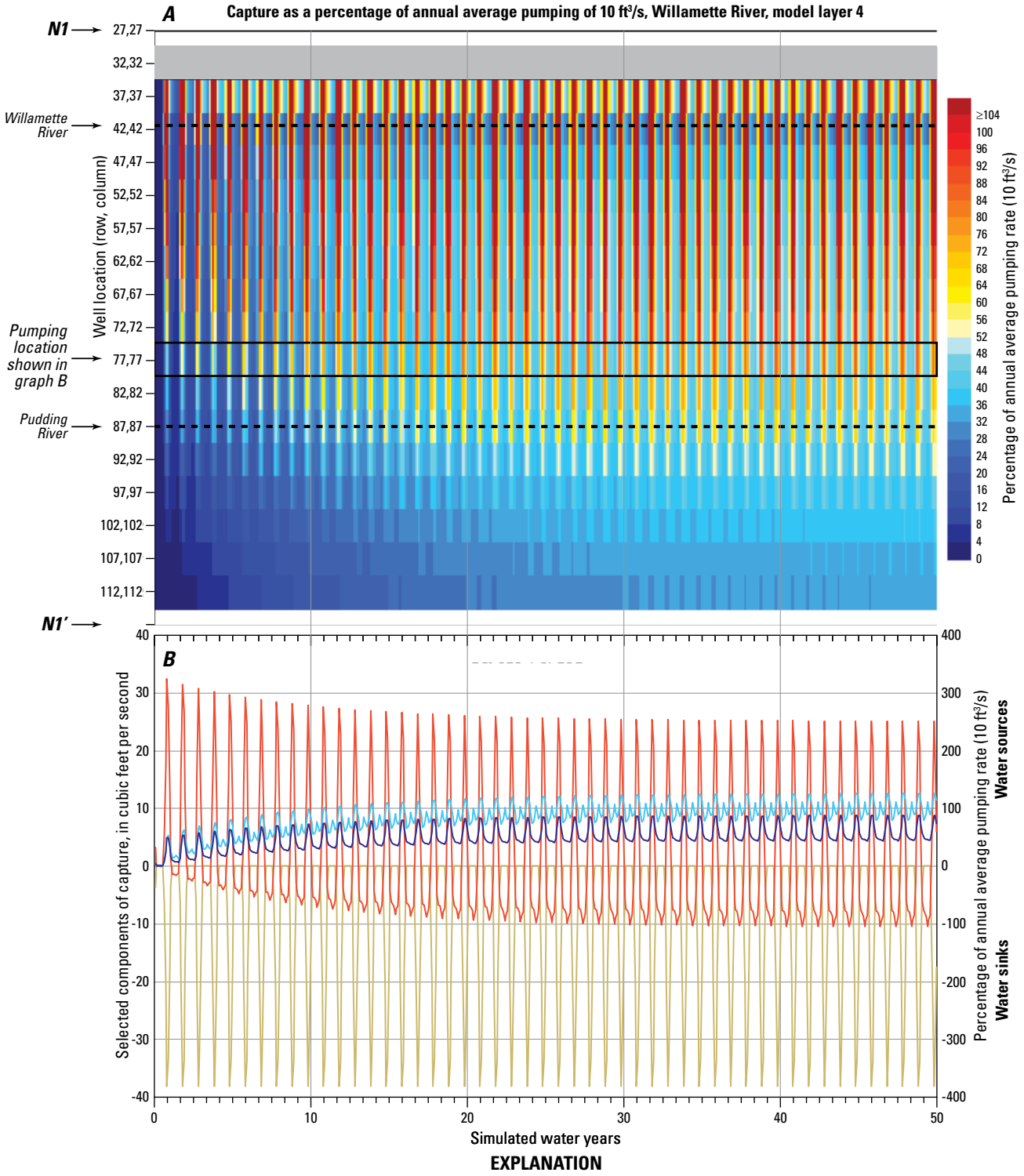

A Solid grey indicates areas where LSU is not present. Y-axis is position along *N1–N1′* line in figure 42. Willamette River capture for the pumping location shown in graph *B*; Willamette and Pudding River locations are noted along transect in black.

B **Selected components of capture for pumping at well location 77,77 in graph *A*—**Total capture is a summation of all stream capture, including Willamette River capture.

Figure 59. (*A*) Computed transient capture as a percentage of annual average pumping of 10 cubic feet per second (ft^3/s) that would result from additional simulated seasonal pumping from model layer 4 and (*B*) variations in the amounts of groundwater from storage and depleted streamflow, and into storage and additional pumping, in response to an annual average increase of 10 ft^3/s in pumping from row 77, column 77, model layer 4, along the *N1–N1′* transect for the Willamette River in the Central Willamette subbasin, Willamette Basin, Oregon, for a 50-year simulation.

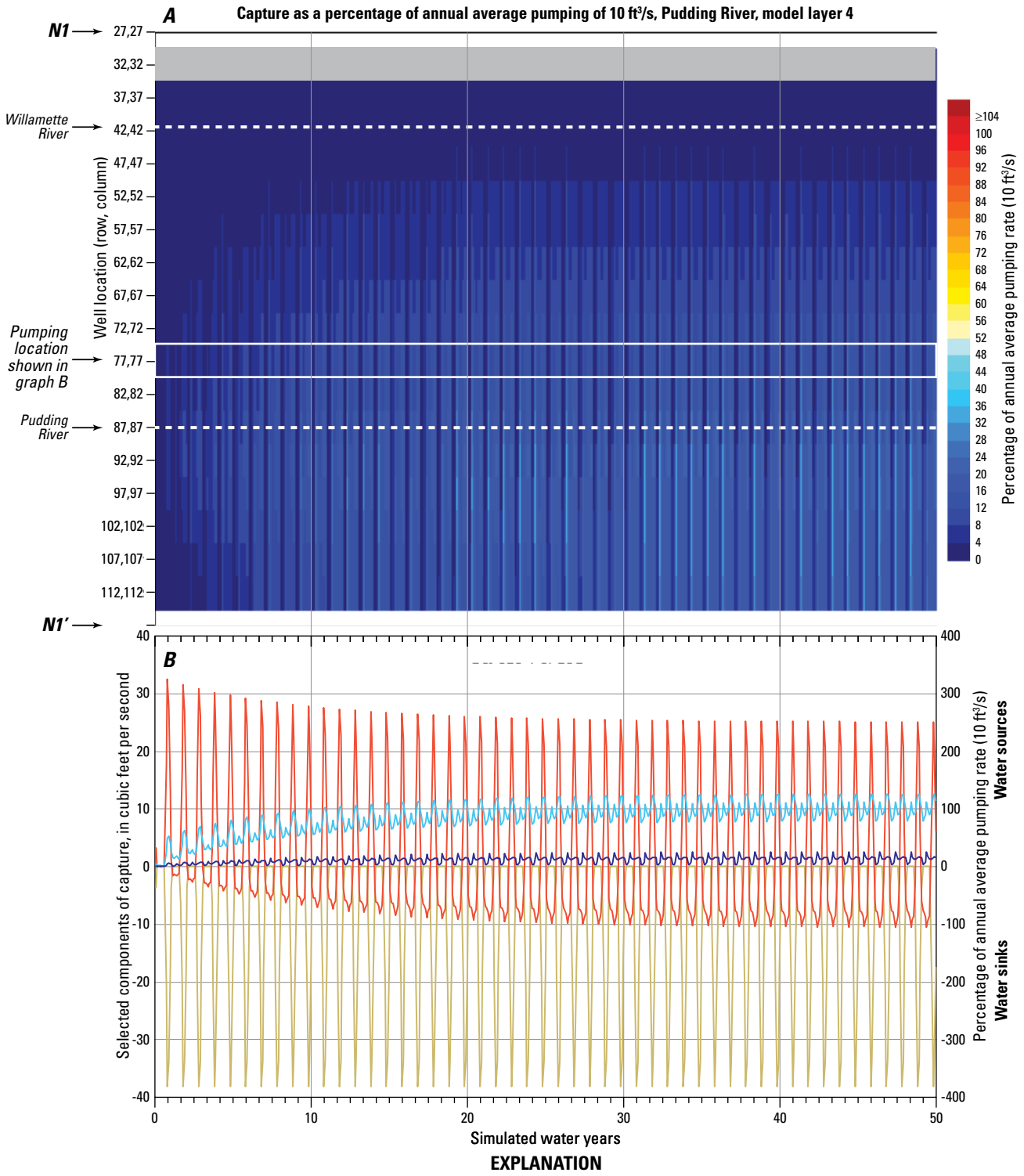

A Solid grey indicates areas where LSU is not present. Y-axis is position along *N1–N1′* line in figure 42. Pudding River capture for the pumping location shown in graph *B*; Willamette and Pudding River locations are noted along transect in white.

B **Selected components of capture for pumping at well location 77,77 in graph *A*—**Total capture is a summation of all stream capture, including Pudding River capture.

- Additional simulated seasonal pumping
- Simulated storage
- Total capture, all streams
- Capture, Pudding River

Figure 60. (*A*) Computed transient capture as a percentage of annual average pumping of 10 cubic feet per second (ft^3/s) that would result from additional simulated seasonal pumping from model layer 4 and (*B*) variations in the amounts of groundwater from storage and depleted streamflow, and into storage and additional pumping, in response to an annual average increase of 10 ft^3/s in pumping from row 77, column 77, model layer 4, along the *N1–N1′* transect for the Pudding River in the Central Willamette subbasin, Willamette Basin, Oregon, for a 50-year simulation.

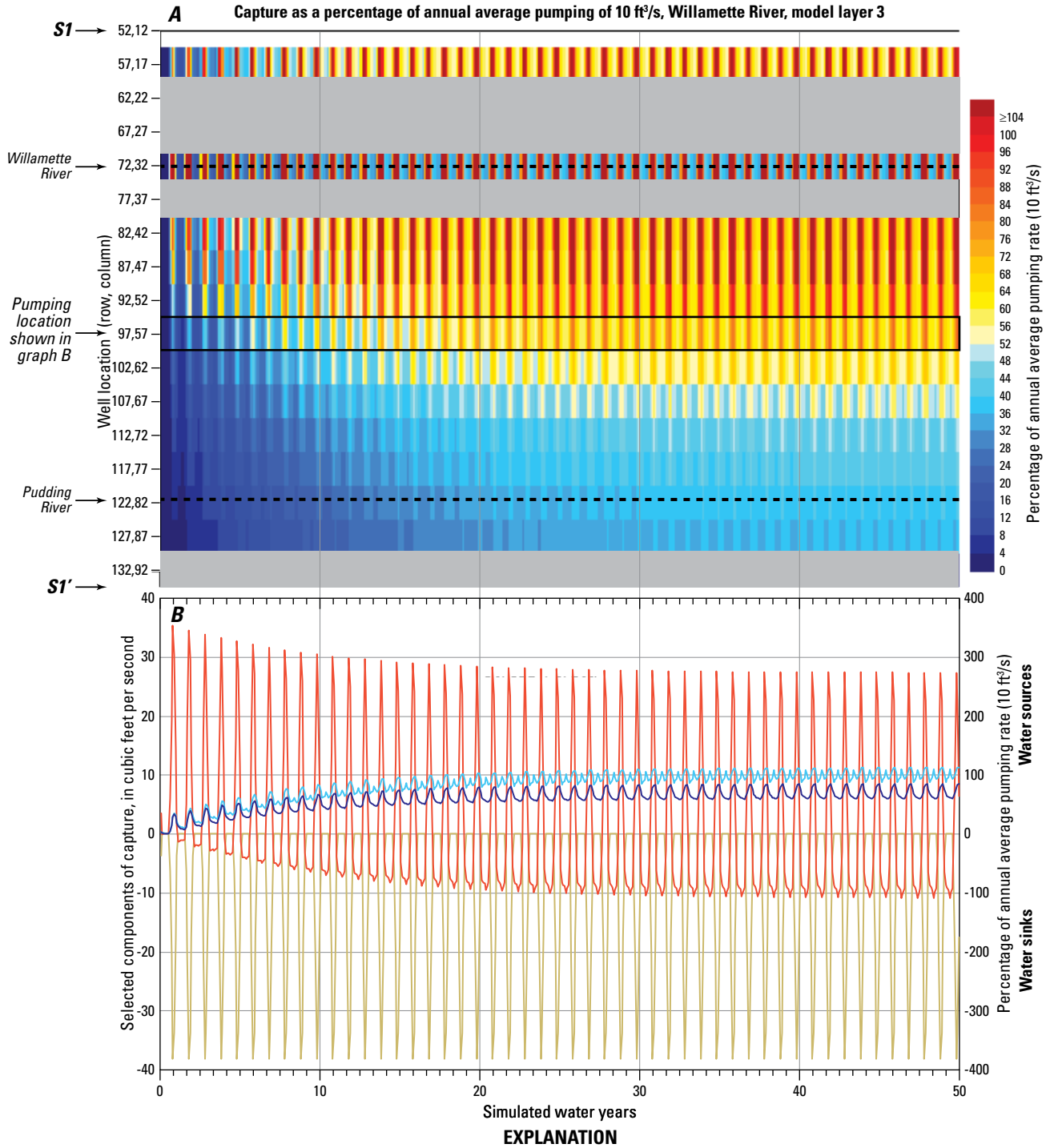

Figure 61. (*A*) Computed transient capture as a percentage of annual average pumping of 10 cubic feet per second (ft^3/s) that would result from additional simulated seasonal pumping from model layer 3 and (*B*) variations in the amounts of groundwater from storage and depleted streamflow, and into storage and additional pumping, in response to an annual average increase of 10 ft^3/s in pumping from row 97, column 57, model layer 3, along the *S1–S1′* transect for the Willamette River in the Central Willamette subbasin, Willamette Basin, Oregon, for a 50-year simulation.

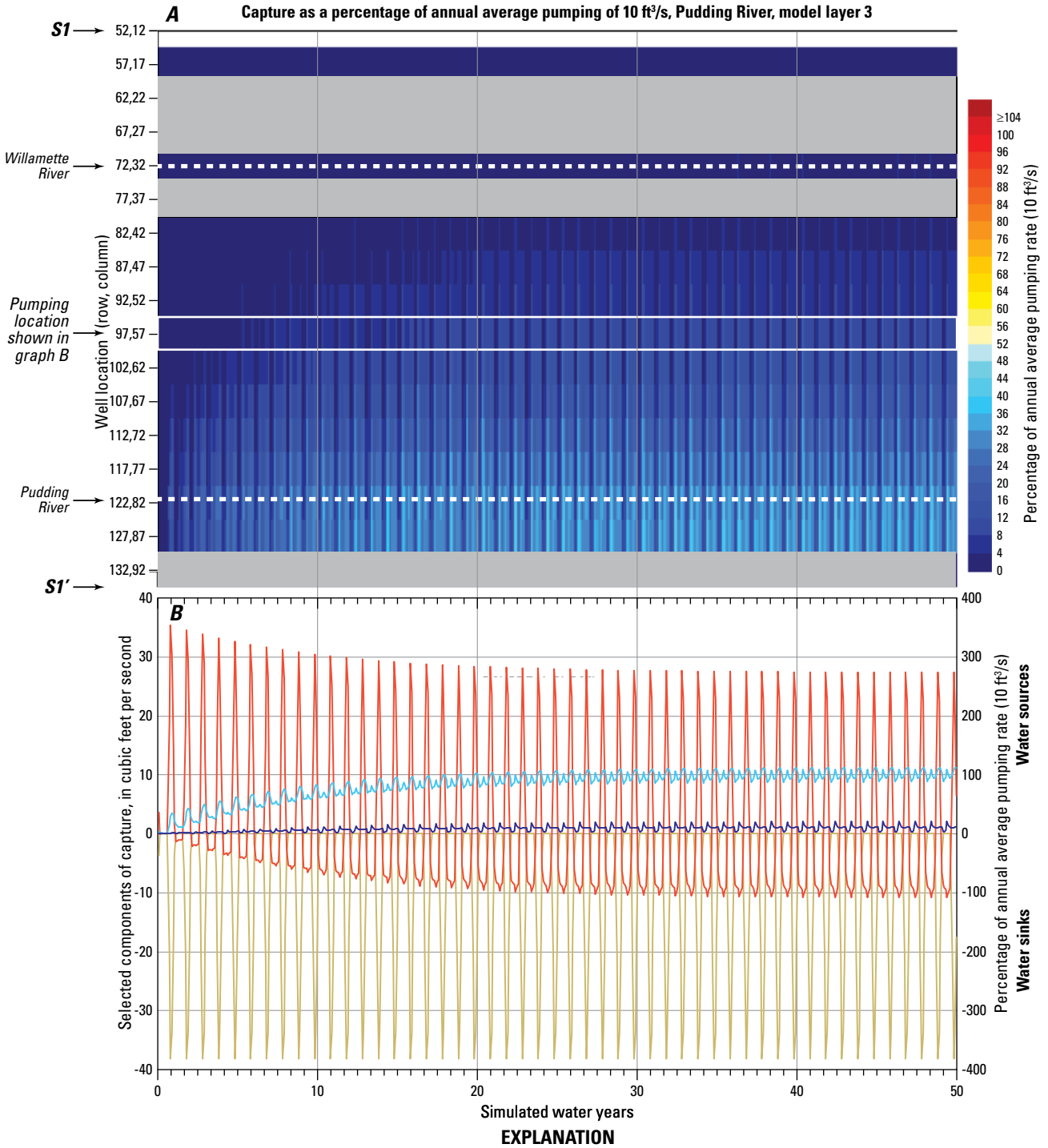

A Solid grey indicates areas where USU/MSU is not present. Y-axis is position along *S1–S1′* line in figure 42. Pudding River capture for the pumping location shown in graph *B*; Willamette and Pudding River locations are noted along transect in white.

B **Selected components of capture for pumping at well location 97,57 in graph *A*—**Total capture is a summation of all stream capture, including Pudding River capture.

Figure 62. (*A*) Computed transient capture as a percentage of annual average pumping of 10 cubic feet per second (ft^3/s) that would result from additional simulated seasonal pumping from model layer 3 and (*B*) variations in the amounts of groundwater from storage and depleted streamflow, and into storage and additional pumping, in response to an annual average increase of 10 ft^3/s in pumping from row 97, column 57, model layer 3, along the *S1–S1′* transect for the Pudding River in the Central Willamette subbasin, Willamette Basin, Oregon, for a 50-year simulation.

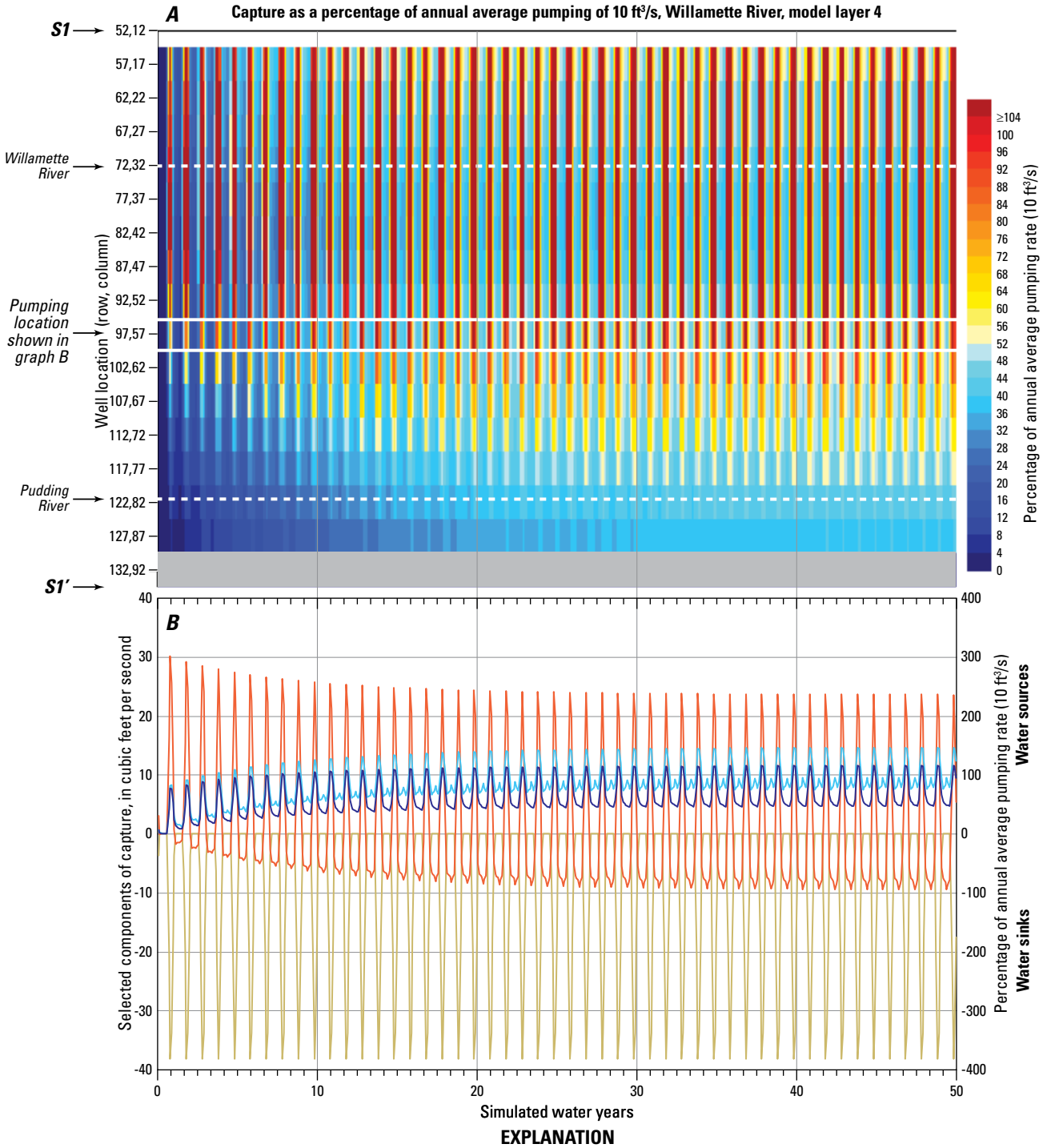

Figure 63. (*A*) Computed transient capture as a percentage of annual average pumping of 10 cubic feet per second (ft^3/s) that would result from additional simulated seasonal pumping from model layer 4 and (*B*) variations in the amounts of groundwater from storage and depleted streamflow, and into storage and additional pumping, in response to an annual average increase of 10 ft^3/s in pumping from row 97, column 57, model layer 4, along the *S1–S1′* transect for the Willamette River in the Central Willamette subbasin, Willamette Basin, Oregon, for a 50-year simulation.

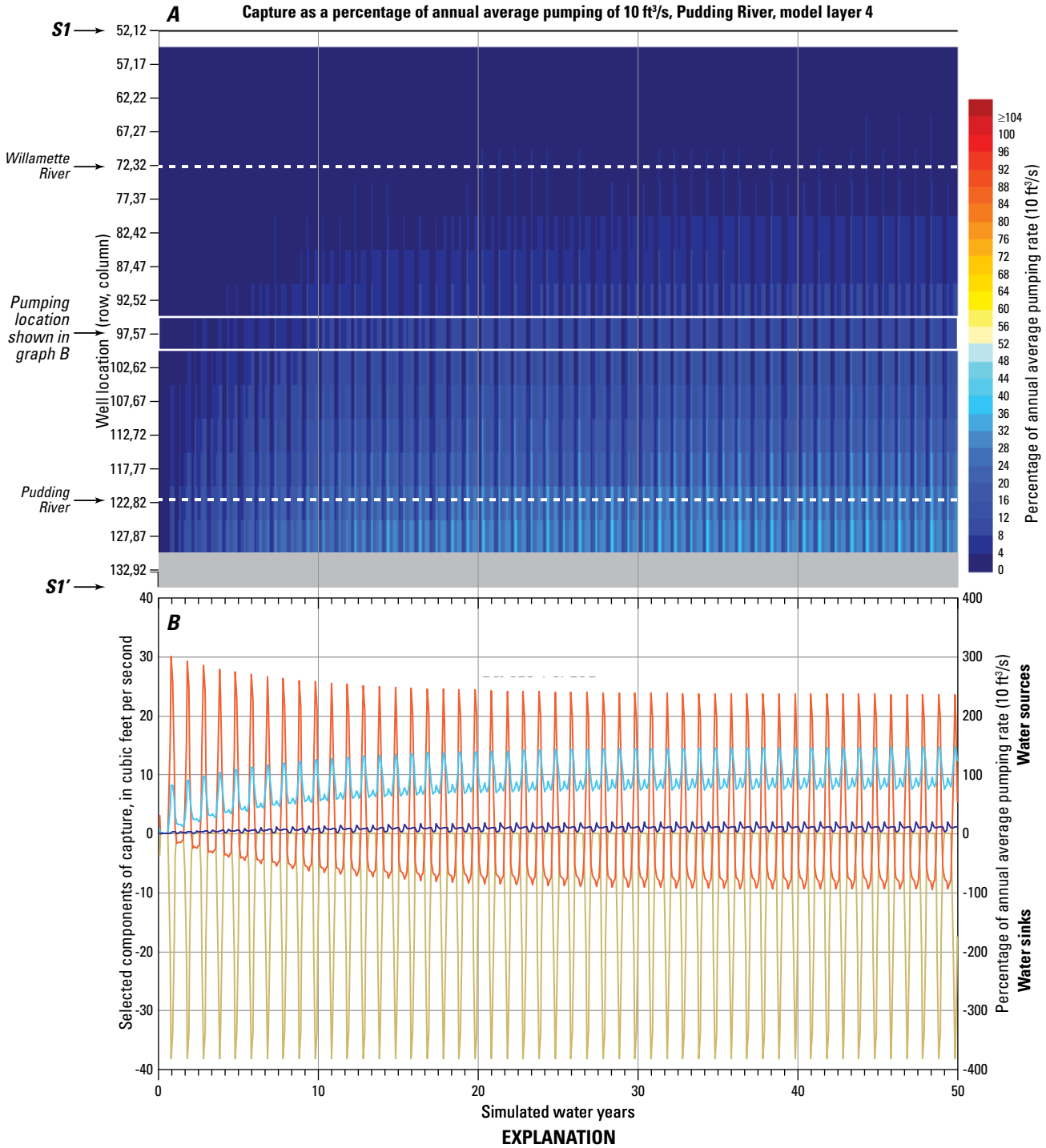

Figure 64. (*A*) Computed transient capture as a percentage of annual average pumping of 10 cubic feet per second (ft³/s) that would result from additional simulated seasonal pumping from model layer 4 and (*B*) variations in the amounts of groundwater from storage and depleted streamflow, and into storage and additional pumping, in response to an annual average increase of 10 ft³/s in pumping from row 97, column 57, model layer 4, along the *S1–S1′* transect for the Pudding River in the Central Willamette subbasin, Willamette Basin, Oregon, for a 50-year simulation.

Capture patterns for the Willamette River indicate that capture is directly related to seasonal pumping (figs. 57, 59, 61, and 63) in contrast to Pudding River capture, where pumping effects are impeded by the presence of the WSU and a direct influence from seasonal pumping is not present (figs. 58, 60, 62, and 64). Storage properties have a greater effect on Pudding River capture, whereas seasonal pumping requirements have a greater effect on Willamette River capture. Pudding River results consistently display greatest capture during winter (February) as flow is captured and replenishes storage (figs. 56, 60, 62, and 64). These results imply that careful location of a well can minimize the effects of pumping on stream capture during periods of historically high demand, and maximize stream capture during periods of historically high streamflows caused by precipitation and surface water runoff.

Local Assessment and Key Findings

Steady-state pumping simulations and capture fraction calculations provide information about stream capture and hydraulic head changes in the Central Willamette subbasin. Capture fraction calculations show that on a long-term, average annual basis, Willamette River capture will generally supply most of the groundwater for pumping in the Central Willamette subbasin, except for the northeast area of the subbasin near the Molalla River. Because the Molalla River flows primarily on the USU and MSU, Molalla River capture is readily available as a groundwater source. Pudding River capture is induced primarily by pumping wells in the USU or MSU and is small relative to Willamette River capture. In areas where the MSU is relatively thin, steep drawdowns occur in close proximity to pumping, inducing greater capture from the Pudding River and nearby streams. The thickness of the LSU in the Central Willamette subbasin results in a relatively high transmissivity value that allows effects of pumping to propagate more quickly to surface-water boundaries (primarily the Willamette River).

The area in the Central Willamette subbasin where the USU and MSU is absent provides a hydrologic barrier between the Willamette River and pumping in the MSU. This contributes to greater Pudding River capture for pumping located in the MSU compared to pumping in the LSU, which is mostly continuous throughout the Central Willamette subbasin. Pudding River capture increases in the northeastern part of the Central Willamette subbasin, where the WSU is absent. The increase in capture indicates that the WSU damps the hydrologic connection between the Pudding River and the underlying units. The hydrologic connection between the MSU and the Pudding River is poor along most of the stream area, but improves to the northeast near the confluence of the Pudding and Mollala Rivers where streams have incised through the WSU and are flowing on the USU and MSU. Areas in close proximity (within 2–3 mi) to the Pudding River show increased Pudding River capture that diminishes rapidly with increased distance. Capture fractions become more similar in the MSU and LSU in the southeastern part of the Central Willamette subbasin as the thickness of the LSU decreases and transmissivity values in the sedimentary units become uniform.

Results from transient simulations comparing pre-development and full use of groundwater rights with baseline (average annual) conditions indicate that groundwater levels and streamflows have changed since pre-development and would continue to change under full use of groundwater rights conditions. Baseline pumping and full-use conditions show monthly trends caused by consistent withdrawals in the Central Willamette subbasin. The pre-development condition shows monthly trends that reflect seasonal changes in recharge rather than changes induced by pumping. Minimum groundwater levels occur in October and maximum groundwater levels occur in February and March under pre-development conditions. These groundwater levels reflect the lag time in a natural system between when the rainy season begins and when recharge begins to affect the groundwater system. Baseline pumping and full use conditions move the maximum groundwater levels to March and April, and minimum groundwater levels to August. The delay in maximum groundwater levels is the result of depleted storage in the aquifer. Groundwater pumping practices result in the lowest groundwater levels during the time of greatest demand. Simulations indicate increases in seasonal groundwater-level fluctuations and a corresponding decline in average annual groundwater levels since pre-development in the Central Willamette subbasin. Groundwater-level fluctuations change with variations from baseline conditions. Full-use conditions result in a doubling of baseline fluctuations in groundwater levels, and cause further declines in average annual groundwater levels.

Development of groundwater use in the Central Willamette subbasin affects base flow, or groundwater discharge, to streams. Pre-development conditions present an autumn-low/winter-high base-flow pattern in the Willamette River that reflects natural seasonality. With groundwater pumping (baseline and full use of groundwater rights conditions), a summer-low/winter-high pattern occurs in Willamette River base flow from the Central Willamette subbasin, indicating influence by summer pumping. The base-flow patterns for the Pudding River under baseline conditions are similar to the base-flow patterns for pre-development conditions—an autumn-low/spring-high pattern—and indicate natural seasonal influences. Under full use conditions, the Pudding River transitions to a summer-low/spring-high base-flow pattern as base flow becomes increasingly influenced by pumping. When pumping is removed from the simulation (as in the pre-development condition), groundwater that would otherwise discharge to pumping remains in the groundwater system and maintains relatively higher base flows during the summer months.

Groundwater exchange, between streams that flow on the WSU and the underlying aquifers, is limited by this low permeability unit. Only the Willamette and Molalla Rivers have completely incised through the WSU. Steady-state simulations provide average annual values for capture

fractions in the Central Willamette subbasin. Monthly transient simulations clarify the timing of maximum and minimum capture. Initially during pumping, well discharge is supplied by aquifer storage, with the percentage supplied diminishing over the long term. The source of most summer pumping is water released from storage. Over time, the source of water to well pumping shifts from contributions from aquifer storage to contributions from stream capture—the average annual change in storage diminishes to zero as stream capture increases to fully supply pumping demands and a new equilibrium is reached. Additionally, storage tends to decrease with depth and smaller values of storage for the LSU result in less water available for release from the aquifer causing greater stream capture during summer to meet pumping demands, and increased capture during winter to replenish storage supplies. Consistently greater capture effects are shown in the Pudding River during winter as stream capture is used to replenish storage.

Simulated capture data for the Willamette River indicate that changes to base flow are directly related to seasonal pumping, which contrasts with results for the Pudding River, which indicate that changes to base flow and direct effects from seasonal pumping are limited. The continuous geometry of the LSU allows increased Willamette River capture, especially in areas where the USU and MSU are absent. Storage properties of the groundwater system have a greater effect on Pudding River capture, whereas seasonal pumping has a greater effect on Willamette River capture. This implies that careful consideration of pumping locations can minimize stream capture during times of historically high demand, and maximize stream capture during times of historically high streamflows.

The results of these local steady-state and transient simulations can be used by water-resource managers as a guide to evaluate possible long-term, short-term, and seasonal effects of changes in pumping in the Central Willamette subbasin. Effects of large declines in heads in the USU and MSU could cause increased pumping costs due to increased pumping lifts and concomitant power requirements, an increased number of dry wells during times of high demand, or increased seasonal changes in aquifer storage. Large declines also could lead to movement of low-quality water from the basement confining unit. Model simulations provide managers with a means to assess spatial and temporal pumping effects on groundwater levels and streamflows in the Central Willamette subbasin. Capture maps can be used as a tool to understand where groundwater pumping will affect flows in the Willamette River, the Pudding River, and other local rivers. Additionally, this study and the results may be used to identify areas where additional data are needed to understand groundwater and surface-water interactions better in the Willamette Basin.

The scenarios in this study consider only one aspect (changes in pumping) of possible effects to groundwater levels and flow direction, base flow, and stream capture in the Willamette Basin and Central Willamette subbasin. Other factors, such as climate cycles or significant changes in water-use patterns from current conditions can influence results. This study and the modeling tools it provides can be used as a starting point for climate and water-management studies and policy discussions, with close attention to strategy in the Central Willamette subbasin to optimize future water availability.

Acknowledgments

The authors acknowledge the collaboration, technical input, and support provided by U.S. Geological Survey colleagues: Marshall W. Gannett, Stephen R. Hinkle, Paul A. Hsieh, Stanley A. Leake, William D. McFarland, David S. Morgan, Jacqueline C. Olson, Leonard L. Orzol, Howard W. Reeves, Stewart A. Rounds, and Kenneth A. Skach, and Oregon Water Resources Department colleagues: Douglas E. Woodcock and Karl C. Wozniak.

References Cited

Bear, Jacob, 1979, Hydraulics of groundwater: McGraw-Hill, Inc., New York, 569 p.

Beeson, M.H., Tolan, T.L., and Anderson, J.L., 1989, The Columbia River Basalt Group in western Oregon—Geologic structures and other factors that controlled flow emplacement patterns, *in* Reidel, S.P., and Hooper, P.R., eds., Volcanism and tectonism in the Columbia River flood-basalt province: Boulder, Colo., Geological Society of America Special Paper 239, p. 223–246.

Bureau of Reclamation, 1985, Ground Water Manual—A water resources technical publication: Denver, Colorado, U.S. Bureau of Reclamation, 480 p.

Bureau of Reclamation, 2013, AgriMet irrigation guide—Root zone depths and management allowable depletion of Selected Crops: Bureau of Reclamation Web site, accessed July 24, 2013, at http://www.usbr.gov/pn/agrimet/irrigation.html#Root.

Conlon, T.D., Lee, K.K., and Risley, J.R., 2003, Heat tracing in streams in the central Willamette Basin, Oregon, *in* Stonestrom, D.A., and Constantz, Jim, eds., Heat as a tool for studying the movement of ground water near streams: U.S. Geological Survey Circular 1260, chap. 5, p. 29–34.

Conlon, T.D., Wozniak, K.C., Woodcock, D., Herrera, N.B., Fisher, B.J., Morgan, D.S, Lee, K.K., and Hinkle, S.R., 2005, Ground-water hydrology of the Willamette Basin, Oregon: U.S. Geological Survey Scientific Investigations Report 2005-5168, 83 p.

Fetter, C.W., 1994, Applied hydrogeology, 3d ed.: Upper Saddle River, N.J., Prentice-Hall, 691 p.

Frank, F.J., 1973, Ground water in the Eugene-Springfield area, southern Willamette Valley, Oregon: U.S. Geological Survey Water-Supply Paper 2018, 65 p.

Freeze, R.A., and Cherry, J.A., 1979, Groundwater: Prentice-Hall, Englewood Cliffs, N.J., 604 p.

Freeze, R.A., and Witherspoon, P.A., 1967, Theoretical analysis of regional ground water Flow—2. Effect of water-table configuration and subsurface permeability variation: Water Resources Research, v. 3, no. 2, p. 623–634.

Gannett, M.W., and Caldwell, R.R., 1998, Geologic framework of the Willamette lowland aquifer system, Oregon and Washington: U.S. Geological Survey Professional Paper 1424-A, 32 p.

Gannett, M.W., and Lite, K.E., Jr., 2004, Simulation of regional ground-water flow in the upper Deschutes Basin, Oregon: U.S. Geological Survey Water-Resources Investigations Report 03-4195, 84 p.

Gonthier, J.B., 1983, Ground-water resources of the Dallas-Monmouth area, Polk, Benton, and Marion Counties, Oregon: Oregon Water Resources Department Ground Water Report 28, 50 p.

Hampton, E.R., 1972, Geology and ground water of the Molalla-Salem slope area, northern Willamette Valley, Oregon: U.S. Geological Survey Water-Supply Paper 1997, 83 p.

Harbaugh, A.W., Banta, E.R., Hill, M.C., and McDonald, M.G., 2000, MODFLOW-2000, The U.S. Geological Survey modular ground-water model—User guide to modularization concepts and the ground-water flow process: U.S. Geological Survey Open-File Report 00–92, 121 p.

Hill, M.C., 1998, Methods and guidelines for effective model calibration: U.S. Geological Survey Water-Resources Investigations Report 98–4005, 90 p.

Hill, M.C., Banta, E.R., Harbaugh, A.W., and Anderman, E.R., 2000, MODFLOW-2000, The U.S. Geological Survey modular ground-water model—User guide to the observation, sensitivity, and parameter estimation processes and three post-processing programs: U.S. Geological Survey Open-File Report 00–184, 209 p.

Hill, M.C., and Tiedeman, C.R., 2007, Effective ground water model calibration—With analysis of data, sensitivities, predictions and uncertainty: Hoboken, N.J., John Wiley and Sons, Inc., 455 p.

Hinkle, S.R., and Polette, D.J., 1999, Arsenic in ground water of the Willamette Basin, Oregon: U.S. Geological Survey Water-Resources Investigations Report 98–4205, 28 p.

Hulse, David, Gregory, Stan, and Baker, Joan, eds., 2002, Willamette River Basin Planning Atlas, trajectories of environmental and ecological change: Corvallis, Oreg., Pacific Northwest Ecosystem Research Consortium, Oregon State University Press, 178 p.

Ingebritsen, S.E., Mariner, R.H., and Sherrod, D.R., 1994, Hydrothermal systems of the Cascade Range, north-central Oregon: U.S. Geological Survey Professional Paper 1044-L, 85 p.

Iverson, Justin, 2002, Investigation of the hydraulic, physical, and chemical buffering capacity of Missoula Flood deposits for water quality and supply in the Willamette Valley of Oregon: Corvallis, Oreg., Oregon State University, M.S. thesis, 147 p.

Leake, S.A., and Pool, D.R., 2010, Simulated effects of groundwater pumping and artificial recharge on surface-water resources and riparian vegetation in the Verde Valley sub-basin, Central Arizona: U.S. Geological Survey Scientific Investigations Report 2010–5147, 18 p.

Leake, S.A., Reeves, H.W., and Dickinson, J.E., 2010, A new capture fraction method to map how pumpage affects surface water flow: Ground water, v. 48, no. 5, p. 690–700.

Leavesley, G.H., Lichty, R.W., Troutman, B.M., and Saindon, L.S., 1983, Precipitation-runoff modeling system—User's manual: U.S. Geological Survey Water-Resources Investigations Report 83–4238, 207 p.

Lee, K.K., and Risley, J.C., 2001, Estimates of ground-water recharge, base flow, and stream reach gains and losses in the Willamette River Basin, Oregon: U.S. Geological Survey Water-Resources Investigations Report 01–4215, 52 p.

Lohman, S.W., Bennett, R.R., Brown, R.H., Cooper, H.H., Jr., Descher, W.J., Ferris, J.G., Johnson, A.I., McGuinness, C.L., Piper, A.M., Rorabaugh, M.I., Stallman, R.W., and Theis, C.V., 1972, Definitions of selected ground-water terms—Revisions and conceptual refinements: U.S. Geological Survey Water-Supply Paper 1988, 21 p.

McDonald, M.G., and Harbaugh, A.W., 1988, A modular three-dimensional finite-difference ground-water flow model: U.S. Geological Survey Techniques of Water-Resources Investigations, book 6, chap. A1, 586 p.

McFarland, W.D., and Morgan, D.S., 1996, A description of the ground-water flow system in the Portland Basin, Oregon and Washington: U.S. Geological Survey Water-Supply Paper 2470-A, 58 p., 7 pls.

Morgan, D.S., and Dettinger, M.D., 1996, Ground-water conditions in Las Vegas Valley, Clark County, Nevada—Part 2, Hydrogeology and simulation of ground-water flow: U.S. Geological Survey Water-Supply Paper 2320-B, 124 p., 2 pls.

Morgan, D.S., and McFarland, W.D., 1996, Simulation analysis of the ground-water flow system in the Portland Basin, Oregon and Washington: U.S. Geological Survey Water-Supply Paper 2470-B, 83 p.

O'Connor, J.E., Sarna-Wojcicki, A., Wozniak, K.C., Polette, D.J., and Fleck, R.J., 2001, Origin, extent, and thickness of Quaternary geologic units in the Willamette Valley, Oregon: U.S. Geological Survey Professional Paper 1620, 52 p.

Oregon Agricultural Statistics Service, 2007, Gross farm and ranch sales by county, 2007: Oregon Agricultural Statistics Service, accessed January 2010 at http://www.nass.usda.gov/or/grossfarmsales.pdf.

Oregon Agricultural Statistics Service, 2014, Gross farm and ranch sales by county, 2012: Oregon Agricultural Statistics Service, accessed August 18, 2014 at http://www.oregon.gov/ODA/docs/pdf/pubs/2013_agripedia_stats.pdf.

Orr, E.L., Orr, W.N., and Baldwin, E.M., 1992, Geology of Oregon, 4th ed.: Dubuque, Iowa, Kendall/Hunt Publishing Company, 254 p.

Orzol, L.L., Wozniak, K.C., Meissner, T.R., and Lee, D.B., 2000, Ground-water and water-chemistry data for the Willamette Basin, Oregon: U.S. Geological Survey Water-Resources Investigations Report 99–4036, 141 p.

Piper, A.M., 1942, Ground-water resources of the Willamette Valley, Oregon: U.S. Geological Survey Water-Supply Paper 890, 194 p, 10 pls.

Pollock, D.W., 1994, User's Guide for MODPATH/MODPATH-PLOT, Version 3—A particle tracking post-processing package for MODFLOW, the U.S. Geological Survey finite-difference ground-water flow model: U.S. Geological Survey Open-File Report 94–464, 248 p.

Price, Don, 1967a, Geology and water resources in the French Prairie area, northern Willamette Valley, Oregon: U.S. Geological Survey Water-Supply Paper 1833, 98 p.

Price, Don, 1967b, Ground water in the Eola-Amity hills area, northern Willamette Valley, Oregon: U.S. Geological Survey Water-Supply Paper 1847, 66 p.

Reilly, T.E., and Harbaugh, A.W., 2004, Guidelines for evaluating ground-water flow models: U.S. Geological Survey Scientific Investigations Report 2004–5038, 30 p.

Rutledge, A.T., 1998, Computer programs for describing the recession of ground-water discharge and for estimating mean ground-water recharge and discharge from streamflow records—Update: U.S. Geological Survey Water-Resources Investigations Report 98–4148, 43 p.

Snyder, D.T., Morgan, D.S., and McGrath, T.S., 1994, Estimation of ground-water recharge from precipitation, runoff into dry wells, and on-site waste-disposal systems in the Portland Basin, Oregon and Washington: U.S. Geological Survey Water-Resources Investigations Report 92–4010, 33 p.

Swanson, R.D., McFarland, W.D., Gonthier, J.B., and Wilkinson, J.M., 1993, A description of hydrogeologic units in the Portland Basin, Oregon and Washington: U.S. Geological Survey Water-Resources Investigations Report 90–4196, 56 p., 10 sheets, scale 1:100,000.

Tolan, T.L., Beeson, M.H., and DuRoss, C.B., 2000, Geologic map and database of the Salem East and Turner 7.5-minute quadrangles, Marion County, Oregon—A digital database: U.S. Geological Survey Open-File Report 00-351, scale 1:24,000.

Tolan, T.L., Beeson, M.H., and Wheeler, K.L., 1999, Geologic map of the Scotts Mills, Silverton, and Stayton Northeast 7.5-minute quadrangles, northwest Oregon—A digital database: U.S. Geological Survey Open-File Report 99–141, scale 1:24,000.

U.S. Census Bureau, 2014, Detailed tables of total population by county and census tract: U.S. Census Bureau data base, accessed August 18, 2014, at http://www.census.gov/.

Waitt, R.B., 1980, About forty last-glacial Lake Missoula jökulhlaups through Southern Washington: Journal of Geology, v. 88, p. 653–679.

Wentz, D.A., Bonn, B.A., Carpenter, K.D., Hinkle, S.R., Janet, M.L., Rinella, F.A., Uhrich, M.A., Waite, I.R., Laenen, Antonius, and Bencala, K.E., 1998, Water quality in the Willamette Basin, Oregon, 1991–95: U.S. Geological Survey Circular 1161, 34 p.

Wilson, D.C., 1997, Post-middle Miocene geologic history of the Tualatin Basin, Oregon with hydrogeologic implications: Portland, Oreg., Portland State University, Ph.D. dissertation, 321 p.

Woodward, D.G., Gannett, M.W., and Vaccaro, J.J., 1998, Hydrogeologic framework of the Willamette lowland aquifer system, Oregon and Washington: U.S. Geological Survey Professional Paper 1424-B, 82 p.

Yeats, R.S., Graven, E.P., Werner, K.S., Goldfinger, C., Popowski, T.A., 1996, Tectonics of the Willamette Valley, Oregon, *in* Rogers, A.M., Walsh, T.J., Kockelman, W.J., Priest, G.R., eds., Assessing earthquake hazards and reducing risk in the Pacific Northwest—Volume 1: U.S. Geological Survey Professional Paper 1560, p. 183–222.

Zaadnoordijk, W.J., 2009, Simulating piecewise-linear surface water and groundwater interactions with MODFLOW—Methods note: Ground Water, v. 47, no. 5, p 723–726.

Appendix A. Estimation of Recharge from Precipitation and Irrigation

A previous estimate of areally distributed estimates of recharge to the groundwater system in the Willamette Lowland based on PRMS models (Lee and Risley, 2001) was corrected to account for the presence of regional groundwater flow. The PRMS model used for the Willamette Lowland assumed that all groundwater recharge within each of the 216 subbasins in the area returned to streams within the same subbasin; however, preliminary regional groundwater modeling showed significant groundwater flow between PRMS modeling subbasins.

The assumption restricting regional groundwater flow between PRMS subbasins resulted in spatial bias of PRMS model simulation results, with systematic overprediction of flow in much of the Willamette Lowland and underprediction in the Cascade Range (Lee and Risley, 2001, fig. 7 and table 7). PRMS simulated flow is greater than measured flow in the sedimentary lowlands because all recharge is forced to return to the subbasin upstream of the streamgage. Simulated flow is less than measured flow for many Cascade Range streams because deeper groundwater flow from upslope subbasins is being forced into streams as the less permeable western Cascade Range deposits are met.

To remove bias and use the PRMS recharge estimates, the following physical assumptions were made:

Assumption 1: The PRMS model simulation results correctly incorporate the variability associated with all parameters used in the modeling process (such as land use, slope, and soils) except possibly surficial geology. For this reason, the model results provide the spatial pattern of potential recharge, although the magnitude of recharge might need to be adjusted to account for contributions to the regional groundwater-flow system.

Assumption 2: The primary control on how much of the recharge enters the regional groundwater system is surficial geology, or more precisely, the hydrogeologic units exposed at the ground surface.

Assumption 3: Only the Willamette River receives water lost to the regional groundwater system from the topographically higher rivers in the Willamette Lowland (groundwater in the Cascade Range is assumed to discharge to rivers before entering the lowland). This implies that a fraction of the groundwater recharge returns to the higher rivers, and a fraction leaks into the regional groundwater-flow system.

Assumption 4: All rivers in the Willamette Lowland generally act as drains of the groundwater system; that is, on an average annual basis, the few river reaches in the lowland that are losing flow to the groundwater system make up a negligibly small part of the river water budget.

The mathematical formulation of the above assumptions allows a systematic and unbiased correction to the recharge pattern and deep recharge to the regional groundwater-flow system as a function of surficial geology.

Five hydrogeologic units form the surficial geology in the Willamette Lowland: the Willamette silt unit (WSU), the lumped upper/middle sedimentary units (USU/MSU), the lower sedimentary unit (LSU), the Columbia River basalt unit (CRB), and the basement confining unit (BCU). Assuming that the PRMS model reflects rainfall-runoff processes associated with soil, land use, slope, and aspect, these hydrogeologic units are assumed to be the dominant control on partitioning flow into local rivers and the deep groundwater system. If there is no groundwater inflow to a gaged basin, by conservation of mass:

$$R^*_{WSU} + R^*_{USU/MSU} + R^*_{LSU} + R^*_{CRB} + R^*_{BCU} = B_{gage} \quad \text{(A1)}$$

where

B_{gage} is the base flow at the streamflow-gaging station and each one of the

R^*'s is the groundwater recharge to a hydrogeologic unit in the drainage basin that is returned to the river upstream of the streamgage (local groundwater return flow).

Each R^* is a fraction of the total groundwater recharge, because some groundwater flow also may contribute to the deeper, regional groundwater-flow system to be discharged into the Willamette River (per assumptions 3–4). Each true R^* is unknown, but it may be rewritten as a multiple of constant $R^* = \omega R^{PRMS}$ where the constant (R^{PRMS}) is the integral of average annual PRMS total groundwater recharge passing through the corresponding hydrogeologic unit over the area measured by the streamgage. The ω is an unknown weight that corrects the PRMS recharge estimate bias and represents the fraction of groundwater flow that returns "locally" to the river upstream of the streamgage. Equation A1 may be rewritten as:

$$\sum_i \omega_i R_i^{PRMS} = B_{gage} \quad \text{(A2)}$$

where

i = {WSU, USU/MSU, LSU, CRB, BCU}

Assuming that the bias is uniform across the PRMS model (assumption 1, which is reasonable, because PRMS used surficial geology as a conditioning variable) and that the surficial geology partitions flow between local and regional groundwater flow similarly throughout the model area (assumption 2), it is reasonable to postulate that each ω is only a function of the surficial geology, but otherwise does not vary across the model area. Under these assumptions, an equation may be written for each river streamgage:

$$\sum_i \omega_i R_{ik}^{PRMS} = B_k \quad \text{(A3)}$$

where

k is the streamgage number.

Using assumption 3, B_k in equation A3 is the measured base flow at all streamgages except those measuring flow in the Willamette River in the valley bottom. For each equation, the ω_i's are the only unknowns, so for the case where there are more linearly independent equations than unknowns, the solution to the system of equations is unique, and the solution is the best in the least-squares sense (Trefethen and Bau, 1997, p. 77–85).

Equation A3 describes only the part of recharge that returns to the stream upstream of each streamgage, but the total recharge is required for the regional groundwater model. Defining the total recharge into a hydrogeologic unit (R_i) as:

$$R_i = R_i^* + R_i^{deep} = \omega_i R_i^{PRMS} + R_i^{deep} \quad \text{(A4)}$$

Because the ω_i are uniquely determined above, and the partitioning between local groundwater return flow and deep recharge is assumed constant for each surficial hydrogeologic unit, R_i^{deep} may be rewritten in terms of a single unknown λ_i:

$$R_i^{deep} = \lambda_i \omega_i R_i^{PRMS} \quad \text{(A5)}$$

equation A4 becomes:

$$R_i = (1+\lambda_i)\omega_i R_i^{PRMS} \quad \text{(A6)}$$

where

$(1+\lambda_i)\omega_i$ is the total correction (array multiplier) needed for input to the groundwater model, and each λ_i may be viewed as a hydrologic unit "leakage" factor.

Under the assumption that the λ_i's also only depend on the hydrogeologic units, this results in five new unknowns, assuming there are five hydrogeologic units that leak to the regional groundwater system. Assuming there is negligible subsurface groundwater flow out of the drainage basin, upstream of each streamgage on the lower Willamette River (the regional drain), the following equation holds:

$$\sum_j (1+\lambda_j)\omega_j R_{jk}^{PRMS} + \sum_i \lambda_i R_{ik}^{PRMS} = \tilde{B}_k \quad \text{(A7)}$$

where

$\tilde{B}_k$ is the corrected base flow at streamgage k (corrected by subtracting base flow accounted for by other streamgages upstream of streamgage k),

i summation is the deep recharge from all gaged basins upstream of streamgage k, and

j summation is the total recharge for the drainage area upstream of streamgage k that is not included in the i summation.

This equation implies that the Willamette River will have a higher base flow than is predicted for the topographically higher rivers. This is consistent with the conceptual model of the Willamette River as a regional drain.

For the groundwater model, only two streamflow-gaging stations record flow through the lower Willamette River. The streamgage at Salem meets conditions used to derive equation A7, with geologic structural highs forcing most regional flow into the Willamette River upstream of the streamgage. The streamgage in Portland has various complications, including tidal influence and groundwater flow directly into the Columbia River, which decreases the confidence that equation A7 will yield accurate results for the streamgage. Only one streamgage with multiple unknown variables results in a non-unique solution for the λ_i's, requiring that the range of possible λ_i's be evaluated when computing recharge corrections. Table A1 summarizes the range of possible λ_i's (the recharge corrections) evaluated and the final selected values used for groundwater-flow simulation model calibration.

To constrain the analysis, physically based assumptions are used. The lower boundary of the model is no-flow, so "leakage" to a deeper groundwater system is zero ($\lambda_{BCU} = 0$). The CRB is more permeable than the BCU, so little leakage to the BCU occurs ($\lambda_{CRB} \approx 0$). The three sedimentary hydrogeologic units were analyzed to establish the range of allowable values of the λ_i's. The physically relevant upper bound is that recharge cannot exceed the sum of precipitation and irrigation. Both the WSU and USU/MSU could provide sufficient amounts of water to meet all

Table A1. Final multipliers used for recharge arrays and allowable range of multipliers for underdetermined parts of the groundwater-flow system, Willamette Basin and Central Willamette subbasin, Oregon.

[**High and low values:** Represent the uncertainty associated with the estimate of the array multiplier. The range was not computed for multipliers where the estimate is the best estimate in a least-squares sense (overdetermined parts of the system). **Abbreviations**: WSU, Willamette silt unit; USU, upper sedimentary unit; MSU, middle sedimentary unit; LSU, lower sedimentary unit, CRB, Columbia River basalt unit; BCU_cascades, basement confining unit Cascade Range; BCU_coast, basement confining unit Coast Range; –, no data]

	Recharge parameter (array multiplier) value	Low value	High value
WSU	0.58	0.17	1.11
USU/MSU	0.55	0.14	0.88
LSU	1.14	1.14	[1]***4.00***
CRB	1.08	–	–
BCU_cascades	1.05	–	–
BCU_coast	0.87	–	–

[1]Value is constrained by the criteria that recharge cannot exceed precipitation.

of the Willamette River base flow requirements. The LSU could not meet the requirements alone because the required recharge exceeded total precipitation/irrigation to this unit, and reasonable values of λ_{LSU} provided little of the required base flow. For this reason, a "balanced" scenario with the WSU and USU/MSU providing approximately equal amounts of the regional base flow was selected as the preliminary recharge estimate (table A1).

The remaining issue was to select base flow (B_k) targets for the above procedure. To accomplish this, PART-derived base flow estimates were computed. Lee and Risley (2001) found a systematic over-prediction of PART relative to PRMS base flow estimates (Lee and Risley, 2001, appendix 1), which implied that using PRMS recharge and PART base flow estimates will result in a water balance deficit. The PART to PRMS ratio has a mean and median value of 1.9 and a standard deviation of 0.4. To correct the bias the base flow targets may be divided by 1.9 or the PRMS recharge values may be multiplied by 1.9. Examination of Lee and Risley's (2001) figure 12 shows that the PART base flow separation retains higher frequency events than the PRMS separation. On the scale of the regional groundwater model, these high frequency events may be more appropriately classified as interflows (shallow flow that directly discharges to nearby streams) rather than deep recharge to groundwater. Nevertheless, both corrections were used to solve the system of equations defined by A3 and A7, and were tested as input to the regional model. Because most of the model inflow is from recharge, which is a prescribed flux, and discharge is controlled by head dependent boundaries; travel times in the steady-state model are dominated by recharge rates. Travel times were compared with chlorofluorocarbon (CFC) age dates, and it was determined that multiplying the PRMS recharge by 1.9 resulted in excessively short travel times that no amount of physically reasonable parameterization could correct. On the other hand, dividing PART base flow targets by 1.9 and leaving the corrected PRMS recharge alone resulted in reasonable modeled travel time estimates (table 4). As a final check on correction of recharge using the multipliers in table A1, the groundwater-flow simulation model also was calibrated using original PRMS modeled recharge (all recharge multipliers set to 1), and travel times were estimated with MODPATH. Original PRMS recharge also resulted in excessively short simulated travel times, indicating that correcting PRMS recharge was necessary.

References Cited

Lee, K.K., and Risley, J.C., 2001, Estimates of ground-water recharge, base flow, and stream reach gains and losses in the Willamette River Basin, Oregon: U.S. Geological Survey Water-Resources Investigations Report 01–4215, 52 p.

Trefethen, L.N., and Bau, D., 1997, Numerical linear algebra: Philadelphia, Society for Industrial and Applied Mathematics, 361 p.

Appendix B. Selected Observation Wells and Base-Flow Estimates, Willamette Basin, Oregon

Table B1. Groundwater-level data and simulations for the regional model from selected wells, Willamette Basin, Oregon.

[**Well location**: See section "Well- and Spring-Location System" for explanation.**Well log identifier**: Unique identifier combining a four-letter county code and a well-log number with as many as six digits, which is assigned to the well when a water well report is filed by the well driller with the Oregon Water Resources Department and recorded in Ground Water Resource Information Distribution (GRID), a statewide computer database maintained by Oregon Water Resources Department. **USGS site identification No.**: Site identification number permanently assigned to the well by the U.S. Geological Survey (USGS) and recorded in National Water Information System (NWIS), a national computer database maintained by USGS. **Layer**: Assigned layer in regional groundwater model. All observation wells simulated as open to only one layer (unit). **Row**: Assigned row in regional groundwater model. **Column**: Assigned column in regional groundwater model. **Head observation**: Mean annual water levels calculated using data from bimonthly, quarterly, or recorder well. Most water-level measurements made during, or near to, November 1996, to produce a synoptic measurent of water-level conditions throughout the Willamette Basin. **Scaled standard deviation**: Value from which the observation weight is calculated. **Measurement frequency**: B, bimonthly observation well for Willamette Basin study; Q, quarterly observation well for Willamette Basin study; R, observation well equipped with a digital recorder for Willamette Basin study; S, visited during November 1996 synoptic measurements. ft, foot]

Well location	Well log identifier	USGS site identification No.	Layer	Row	Column	Measured head (ft)	Scaled standard deviation (ft)	Measurement frequency	Simulated head (ft)
17S/05W-02BAC2	LANE 3203	440735123154601	1	95	19	372	6.09	B	OMITTED
03S/01E-27CBD	CLAC 9679	451640122403701	2	35	41	89	3.05	B	95.1
04S/02E-29ADC1	CLAC 17958	451141122345501	2	40	45	236	6.07	B	225
16S/04W-13DCC	LANE 752	441021123065601	2	93	25	346	1.89	B	348
16S/04W-04ACD	LANE 7719	441229123102801	2	91	23	320	1.86	B	323
17S/02W-30CAA2	LANE 10762	440341122584002	2	99	30	462	0.61	R	439
06S/03W-04ACD	MARI 4816	450451123031901	2	46	27	95.6	3.03	R	105
09S/01W-18ADA	MARI 13715	444723122504001	2	61	35	385	3.05	B	375
05S/02E-06BBB	CLAC 154	451018122370501	2	41	43	253	6.07	B	214
16S/05W-26AAD	LANE 8725	440915123145601	2	94	20	340	1.82	R	359
12S/02W-22BBB	LINN 8062	443109122552301	2	75	32	344	3.08	B	335
12S/03W-12BAA	LINN 10391	443252122595301	2	73	29	286	1.89	B	288
12S/04W-01ABB	LINN 50097	443343123070501	2	73	25	226	1.93	B	227
06S/02W-05CDD	MARI 3799	450423122573601	2	46	31	161	3.15	Q	120
06S/02W-17DAD	MARI 4160	450246122564801	2	47	31	154	3.17	Q	127
06S/02W-30ADB	MARI 4559	450122122581901	2	49	30	138	3.09	B	131
06S/03W-23CAA2	MARI 5030	450205123011201	2	48	28	113	6.07	B	114
07S/02W-04BDA	MARI 6564	445942122561801	2	50	31	152	3.09	Q	147
04S/01W-11CDA01	MARI 17545	451402122462501	2	38	38	129	3.03	R	105
10S/03W-30CAD	BENT 1557	444008123060001	3	67	25	180	1.89	Q	186
15S/05W-12BCB	BENT 6612	441701123145501	3	87	20	291	1.86	B	291
11S/05W-35DDD	LINN 10841	443349123150501	3	73	20	198	0.61	R	207
01N/02E-09CCB	MULT 1113	453449122342801	3	20	45	11.5	3.06	Q	10.1
05S/03W-22AAA	YAMH 6576	450745123015801	3	43	28	87	3.23	B	94.6
11S/04W-05CDD	BENT 2544	443812123120001	3	69	22	208	3.25	Q	248
02S/03E-06BDB	CLAC 4614	452539122291701	3	28	48	224	3.13	Q	218
02S/04E-29DAD	CLAC 6388	452033122195901	3	31	54	652	304	Q	440
03S/01W-25CBD	CLAC 8562	451642122453301	3	35	38	120	3.05	B	73.6
04S/01E-32ADD	CLAC 13378	451048122420501	3	40	40	134	3.06	B	150
16S/03W-17CDD	LANE 3382	441023123044001	3	93	26	370	6.06	R	369
17S/02W-30CAA1	LANE 10761	440341122584001	3	99	30	449	0.61	R	437
17S/04W-09DAD1	LANE 11804	440616123100701	3	97	23	371	6.09	B	376
17S/05W-02BAC1	LANE 12676	440736123154701	3	95	19	355	6.16	B	364
17S/05W-13BDD	LANE 13051	440534123142601	3	97	20	366	6.09	Q	375
18S/02W-35CAD	LANE 16030	435555123515701	3	104	33	636	6.08	Q	560
17S/02W-32BCC	LANE 51613	440304122573201	3	99	31	466	1.89	Q	441
11S/02W-15CB	LINN 6700	443646122552701	3	70	32	283	3.04	B	277

Table B1. Groundwater-level data and simulations for the regional model from selected wells, Willamette Basin, Oregon.—Continued

Well location	Well log identifier	USGS site identification No.	Layer	Row	Column	Measured head (ft)	Scaled standard deviation (ft)	Measurement frequency	Simulated head (ft)
11S/03W-26AAA	LINN 7478	443601123003501	3	71	29	262	1.88	Q	266
11S/04W-24CBD	LINN 8508	443547123073101	3	71	25	198	1.89	Q	204
12S/03W-29CDD	LINN 10562	442931123044801	3	76	26	248	1.86	Q	253
12S/04W-21CAB	LINN 10769	443042123110501	3	75	22	231	1.91	B	225
14S/04W-06ADD	LINN 13739	442300123123801	3	82	21	259	1.97	B	265
15S/03W-19ACD1	LINN 14047	441508123053001	3	89	26	322	3.04	Q	332
11S/04W-28CAA	LINN 14280	443500123105001	3	72	22	200	1.86	B	207
14S/03W-30DDC3	LINN 14778	441860123052201	3	85	26	293	3.07	B	306
04S/01W-12BBA	MARI 463	451437122453701	4	37	38	181	3.03	R	95.1
04S/01W-13BBB	MARI 479	451349122454301	3	38	38	99.5	3.04	B	108
04S/01W-32ADB	MARI 905	451052122512501	3	40	36	130	3.86	B	126
05S/01W-26DAB	MARI 1982	450627122460401	3	44	38	152	3.05	B	146
05S/02W-19DCC	MARI 2541	450758122590201	3	44	30	143	3.29	Q	103
06S/01W-06CCC	MARI 3054	450423122514701	3	46	34	127	3.44	Q	136
06S/01W-21CAD	MARI 3266	450200122485301	3	48	36	135	3.49	B	161
06S/01W-21CDC01	MARI 3280	450140122490701	3	48	36	142	3.03	R	160
06S/02W-06ABA	MARI 3803	450510122582901	3	45	30	140	3.44	B	113
07S/02W-28ADD	MARI 7883	445606122554101	3	53	32	182	3.27	B	184
08S/01W-30DDB1	MARI 8999	445032122505001	3	58	35	380	3.06	B	367
06S/03W-19AAD	POLK 1070	450227123052701	3	48	26	126	3.2	B	118
05S/04W-20CDC2	YAMH 2787	450658123123701	3	44	21	122	3.03	R	147
05S/03W-21CCD	YAMH 6572	450655123040601	3	44	27	120	6.15	Q	99.8
05S/05W-13ABC	YAMH 7310	450829123143801	3	43	23	136	3.07	Q	OMITTED
12S/05W-20DBA	BENT 50297	443310123183601	4	75	17	230	1.9	Q	241
05S/01E-18ACC	CLAC 2555	450812122435101	4	43	39	163	3.17	B	147
02S/01E-20CBD2	CLAC 3165	452249122430901	4	30	39	106	3.04	B	110
02S/01E-21CCC	CLAC 3246	452234122415901	4	30	40	98	3.07	B	108
02S/02E-15BBB	CLAC 4146	452407122332101	4	29	45	84.5	3.04	Q	68.5
02S/04E-05CBB	CLAC 5535	452528122205501	4	28	53	487	320	Q	418
02S/04E-05CCC	CLAC 5573	452510122210301	4	28	53	394	6.1	Q	420
03S/01W-24BCD	CLAC 8498	451752122453501	4	34	38	77.2	3.03	R	58
03S/01W-36DDD	CLAC 8794	451541122444301	4	36	39	88	3.17	B	83.4
03S/01E-17ACA	CLAC 9340	451845122423101	4	34	40	97	3.1	B	69.7
04S/03E-28CDA	CLAC 11435	451125122264801	5	40	50	523	6.06	B	437
03S/01E-36CCC	CLAC 12211	451536122382101	4	36	42	133	3.25	Q	158
04S/01E-20BAC	CLAC 13431	451251122425901	4	39	40	104	4.31	Q	131
04S/02E-04ABC	CLAC 13589	451520122340000	4	37	45	224	3.06	B	223
03S/04E-26CDB	CLAC 14665	451636122165701	4	35	56	1,060	306	Q	572
15S/05W-26BDC	LANE 6633	441416123154701	4	90	19	307	3.04	B	316
16S/04W-06BDA	LANE 7778	441237123130701	4	91	21	314	1.89	B	323
16S/04W-16CAC	LANE 8029	441035123105001	4	93	22	328	1.85	Q	343
12S/04W-35CDC	LINN 10817	442838123083001	4	77	24	244	1.89	Q	242
12S/05W-02AAA	LINN 12120	443348123150201	4	73	20	207	0.61	R	205
14S/03W-07DDC	LINN 13576	442140123052601	4	83	26	282	3.05	Q	292
14S/03W-30DDC1	LINN 13680	441902123052501	4	85	26	293	3.07	B	305
12S/03W-11BDD	LINN 50855	443231123011101	4	74	28	274	1.86	B	278
04S/01W-05CDC	MARI 308	451447122502101	4	37	35	124	4.31	Q	81.8
04S/02W-02BBD	MARI 1044	451528122541301	4	36	33	77.5	0.61	R	OMITTED
04S/02W-06DAA	MARI 1082	451509122580901	4	37	30	102	3.1	B	64.9
05S/02W-01DDA	MARI 2218	450939122520901	4	41	34	137	0.61	R	111
05S/02W-05BCC	MARI 2331	450958122580201	4	41	30	149	3.15	Q	91.4
05S/02W-25CBD	MARI 2666	450620122530501	4	44	33	145	3.65	Q	119
05S/03W-13CBA	MARI 2910	450808123002601	4	43	29	103	6.24	B	83.2

Table B1. Groundwater-level data and simulations for the regional model from selected wells, Willamette Basin, Oregon.—Continued

Well location	Well log identifier	USGS site identification No.	Layer	Row	Column	Measured head (ft)	Scaled standard deviation (ft)	Measurement frequency	Simulated head (ft)
04S/02W-19AAA	MARI 17671	451259122581101	4	39	30	125	3.65	B	82.4
05S/02W-08CCA2	MARI 52504	450851122575801	4	42	30	149	303	R	93.6
05S/02W-08CCB1	MARI 52597	450851122580101	4	42	30	123	3.03	R	93.4
01S/03E-10CCA	MULT 2164	452938122254801	4	24	50	267	307	Q	184
01N/02E-23AACB1	MULT 52396	453338122311001	2	21	47	11	3.04	Q	22.7
01N/03W-30BDB1	WASH 146	453242123062201	4	21	25	172	6.06	B	187
01N/02W-08BCA	WASH 5173	453514122575801	4	19	30	195	3.2	Q	190
01N/02W-17ACC	WASH 5382	453417122572901	4	20	31	180	3.13	B	186
01N/03W-36DDC	WASH 6528	453117122593602	4	23	29	166	3.05	Q	159
01S/01W-33CBC	WASH 9205	452619122492401	4	27	36	143	303	R	217
01S/01W-34DAA	WASH 9228	452623122470801	4	27	37	186	3.06	B	208
01S/02W-16DAC	WASH 9903	452854122555601	4	25	32	141	3.06	B	142
01S/02W-31DCA	WASH 10446	452610122582901	4	27	30	166	3.08	B	139
03S/03W-36DCB	YAMH 4669	451545123000001	4	36	29	61	3.17	B	54.5
04S/03W-33DBA	YAMH 5484	451045123032701	4	41	27	148	3.07	Q	82.2
04S/01W-15BDD	CLAC 1952	451333122474901	5	38	37	102	3.08	B	106
05S/01E-27BCB	CLAC 2950	450634122404601	5	44	41	99	3.13	B	163
03S/01W-15CAC	CLAC 8184	451747122484801	5	34	37	87	3.09	Q	109
03S/01E-16DDD	CLAC 9327	451815122405401	5	34	41	107	3.06	B	52.1
03S/01E-26BCD	CLAC 9648	451656122391801	5	35	42	82	3.05	Q	103
02S/01E-20CBD1	CLAC 12346	452249122430801	5	30	40	106	3.06	B	133
04S/04E-22BBC2	CLAC 18382	451242122183601	5	39	55	1,290	618	B	937
04S/04E-22BBC3	CLAC 20423	451241122183601	5	39	55	1,140	6.09	B	937
03S/01W-14ABA	CLAC 50585	451903122460801	5	33	38	84.8	3.03	R	85.5
09S/01W-14DCA	LINN 2705	444700122460701	5	61	38	407	307	Q	467
04S/01W-05CDB	MARI 290	451454122502401	5	37	35	111	8.23	B	79
05S/01W-28DBB	MARI 2035	450623122484901	5	44	36	76	3.65	B	126
06S/01W-25ADA	MARI 3346	450122122443601	5	49	39	151	6.09	B	324
07S/01W-02CAA01	MARI 5904	445923122462501	5	50	38	146	303	R	332
07S/02W-13CAC	MARI 7019	445734122524301	5	52	34	164	3.15	B	168
07S/02W-26CCB	MARI 7736	445544122541601	5	54	33	168	3.17	B	228
08S/01W-14CDC	MARI 8695	445205122463501	5	57	37	592	3.24	B	580
08S/01W-30DDB2	MARI 8971	445033122505101	5	58	35	358	3.14	B	382
08S/02W-11CDA	MARI 9897	445304122535101	5	56	33	430	3.56	Q	440
08S/02W-31DCA	MARI 11229	444936122582801	5	59	30	290	3.34	B	298
08S/03W-11CCC	MARI 11727	445304123014101	5	56	28	407	1.82	R	437
08S/03W-21DAB	MARI 12216	445139123031101	5	57	27	449	1.85	Q	485
08S/03W-33DAB	MARI 12958	444956123031701	5	59	27	606	1.84	Q	531
08S/03W-35DDD	MARI 12984	444935123003701	5	59	29	444	1.82	R	513
09S/02W-06ACD	MARI 13943	444906122582401	5	59	30	314	3.11	B	344
09S/01E-05CDA	MARI 15589	444844122424301	5	60	40	725	6.58	Q	672
06S/01E-20CDA	MARI 17959	450150122424401	5	48	40	364	3.05	B	410
05S/01W-33CDD1	MARI 18242	450510122485401	5	45	36	76	3.6	B	125
07S/01W-07DD1	MARI 19644	445819122505601	5	51	35	152	3.2	B	164
07S/01W-19BAC02	MARI 53069	445706122512701	5	52	34	194	3.03	R	192
07S/03W-05CCA2	POLK 125	445913123051101	5	51	26	328	3.03	R	261
07S/03W-05CCA1	POLK 881	445918123050801	5	50	26	228	3.03	R	246
06S/03W-07DCD	POLK 992	450328123054601	5	47	26	230	6.07	B	193
06S/04W-35DAA	POLK 1253	450023123075401	5	50	24	345	6.39	B	372
07S/03W-18BAD	POLK 1777	445803123060701	5	52	25	497	2.73	B	370
07S/03W-18BAD01	POLK 1781	445804123061201	5	52	25	550	303	R	377
01S/03W-28DBD	WASH 4236	452708123033201	5	26	27	668	606	R	408
01N/02W-17DAB	WASH 5377	453414122571001	5	20	31	128	3.24	B	194

Table B1. Groundwater-level data and simulations for the regional model from selected wells, Willamette Basin, Oregon.—Continued

Well location	Well log identifier	USGS site identification No.	Layer	Row	Column	Measured head (ft)	Scaled standard deviation (ft)	Measurement frequency	Simulated head (ft)
02N/03W-35CDD	WASH 5956	453628123012101	5	18	28	97	3.03	R	199
01N/04W-02BBC1	WASH 6543	453615123090601	5	18	24	223	1,215	B	284
01S/03W-17DDD2	WASH 10758	452842123042201	5	25	26	225	6.15	B	250
01S/03W-17DDD1	WASH 10760	452840123042101	5	25	27	230	6.12	B	248
02S/03W-13ABC	WASH 13506	452405122595000	5	29	29	359	3.1	B	344
05S/04W-14AB1	YAMH 672	450826123082601	5	43	24	321	3.03	R	246
02S/03W-15BBD	YAMH 946	452410123025500	5	29	27	1,330	646	B	538
03S/02W-17AAB	YAMH 2410	451900122571001	5	33	31	231	3.04	Q	245
03S/03W-35DCA2	YAMH 2925	451546123005701	5	36	29	129	6.08	B	97.6
04S/03W-03BAC	YAMH 5161	451523123024401	5	37	28	210	7.03	B	141
05S/04W-13DAD	YAMH 7924	450807123065201	5	43	25	183	6.09	B	158
11S/07W-28BDA	BENT 403	443523123324701	6	71	9	700	22.12	R	633
10S/06W-30DDB	BENT 2326	444008123273801	6	67	12	324	16.06	R	349
12S/06W-11DDA	BENT 5672	443217123222301	6	74	15	258	11.82	R	273
16S/03W-22CBA	LANE 7413	440951123023501	6	93	28	433	16.06	R	519
16S/05W-28BBB	LANE 8733	440925123182501	6	94	18	382	16.12	B	372
19S/02W-07DDA	LANE 20028	435513123013401	6	106	30	546	22.13	Q	559
20S/03W-11BAB	LANE 22027	435024123053401	6	110	28	584	16.06	R	631
13S/03W-27ABD	LINN 1993	442455123020101	6	80	28	286	11.82	R	343
12S/01W-30DDD	LINN 9725	442929122504801	6	76	35	428	16.06	R	467
13S/03W-36ADA	LINN 11999	442351122592301	6	81	30	300	16.07	Q	333
07S/01W-01CDC1	MARI 5895	445907122451801	6	51	38	366	13.03	R	381
08S/03W-05DDD	MARI 11420	445357123041801	6	55	27	202	11.83	Q	355
06S/04W-17DDB	POLK 1192	450300123121001	6	47	22	198	13.07	Q	221
01N/04W-28BAD1	WASH 1664	453249123111701	6	21	22	244	34.28	B	286
01S/03W-19CAD1	WASH 10784	452801123061901	6	26	25	311	16.09	B	211
05S/04W-24BBA2	YAMH 599	450740123074401	6	43	24	284	16.06	R	253
15S/04W-17DBC	LANE 5976	441545123114801	2	88	22	292	10	S	300
17S/03W-16BCA	LANE 11159	440543123034201	2	97	27	400	10	S	404
10S/03W-12DDDD	MARI 16246	444230122592201	2	65	30	234	10	S	231
NONE	BENT 6275	NONE	2	79	20	230	10	S	244
NONE	BENT 6310	NONE	2	80	20	245	10	S	252
16S/03W-32DBB	LANE 7596	440803123042601	2	95	26	369	10	S	380
16S/04W-16ACC	LANE 7996	441046123103701	2	93	23	330	10	S	339
08S/02W-33DCB	MARI 11267	444939122560301	2	59	32	305	10	S	321
04S/03E-06ADC	CLAC 11035	451510122284000	2	37	48	775	1,000	S	377
03S/04E-29BAC	CLAC 14861	451708122204801	2	35	53	594	1,000	S	427
03S/02E-35ABA	CLAC 16383	451620122312000	2	36	47	628	1,000	S	307
03S/03E-34ADC	CLAC 17076	451600122250301	2	36	51	980	1,000	S	401
04S/01E-36BAB	CLAC 18748	451110122375601	2	40	43	236	10	S	203
03S/01E-14ADC	CLAC 19411	451839122384001	2	34	42	220	10	S	118
13S/03W-07BBC2	LINN 12050	442733123063101	2	78	25	257	10	S	257
13S/04W-24CDD	LINN 12089	442507123071301	2	80	25	264	10	S	265
12S/03W-07CCB	LINN 50103	443211123062901	2	74	25	231	10	S	242
12S/03W-07BCC2	LINN 50852	443234123063101	2	74	25	233	10	S	239
12S/03W-09BDC2	LINN 50853	443232123034501	2	74	27	255	10	S	265
07S/03W-01ADA	MARI 30	445939122592001	2	50	30	139	10	S	134
05S/02W-31DBB	MARI 2760	450535122584601	2	45	30	145	10	S	112
06S/03W-36AAD	MARI 5425	450041122592701	2	49	30	139	10	S	128
09S/02W-15DBB2	MARI 14171	444714122545102	2	61	32	334	10	S	351
11S/04W-01CBB	BENT 961	443834123073501	3	68	24	183	10	S	OMITTED
15S/04W-07ADB2	BENT 1444	441656123124202	3	87	21	291	10	S	291
10S/04W-10CDB	BENT 1695	444238123100101	3	65	23	165	10	S	189

Table B1. Groundwater-level data and simulations for the regional model from selected wells, Willamette Basin, Oregon.—Continued

Well location	Well log identifier	USGS site identification No.	Layer	Row	Column	Measured head (ft)	Scaled standard deviation (ft)	Measurement frequency	Simulated head (ft)
12S/05W-13DDC2	BENT 5182	443117123140101	3	75	20	209	10	S	213
15S/04W-29ACD	LANE 6212	441414123121001	3	90	22	302	10	S	310
15S/04W-26BCC	LINN 163	441415123084801	3	90	24	319	10	S	313
10S/03W-07BDA	LINN 4570	444308123060501	3	65	25	170	10	S	182
10S/04W-12CDA	LINN 5344	444242123072401	3	65	25	167	10	S	178
12S/05W-01BCB	LINN 10846	443330123145901	3	73	20	194	10	S	204
07S/04W-36BCD	POLK 2188	445512123074501	3	54	24	115	10	S	131
09S/04W-12ACD	POLK 3835	444815123070001	3	60	25	154	10	S	154
NONE	BENT 5297	NONE	3	75	19	213	10	S	225
13S/05W-07DAD	BENT 6251	442704123200001	3	78	17	243	10	S	263
02S/02E-14CBC	CLAC 4126	452335122320801	3	29	46	46.9	10	S	120
03S/03E-03BCD	CLAC 14047	452025122255001	3	32	50	309	10	S	285
16S/03W-09BAC	LANE 7371	441152123033101	3	92	27	366	10	S	378
16S/05W-03CCC	LANE 8406	441206123171101	3	91	18	319	10	S	336
17S/03W-15ADA1	LANE 11099	440541123013701	3	97	28	416	10	S	413
17S/05W-08CBC	LANE 12862	440618123194501	3	96	17	380	10	S	406
18S/02W-34DBD	LANE 15943	435726122544301	3	104	33	612	10	S	548
13S/04W-08CDC	LINN 91	442653123121301	3	79	22	233	10	S	235
14S/04W-20AAD	LINN 1091	442036123112301	3	84	22	276	10	S	280
12S/04W-34BCB	LINN 1332	442910123101301	3	77	23	239	10	S	235
14S/04W-36BCC	LINN 2140	441838123073801	3	86	24	293	10	S	294
11S/04W-28BDD1	LINN 4146	443512123105001	3	71	22	191	10	S	205
11S/04W-34CDA	LINN 8753	443358123093601	3	72	23	216	10	S	215
13S/03W-30BCC	LINN 11952	442442123063001	3	81	25	270	10	S	276
15S/04W-09ADD1	LINN 14111	441649123101101	3	87	23	293	10	S	293
06S/01W-28ACB	MARI 3471	450121122485001	3	49	36	155	10	S	163
09S/02W-15DBB	MARI 14169	444714122545101	3	61	32	334	10	S	348
09S/03E-30DBD	MARI 15956	444522122285901	3	63	48	792	10	S	874
09S/01W-04CCD	MARI 17154	444915122493801	3	60	36	412	10	S	377
05S/03W-36DAA	MARI 17239	450535122593201	3	45	29	104	10	S	106
06S/02W-06DAC	MARI 17263	450432122582001	3	46	30	141	10	S	116
09S/04W-15AAB	POLK 71	444744123092302	3	61	23	160	10	S	OMITTED
08S/04W-21DBC	POLK 219	445133123105701	3	57	22	149	10	S	145
06S/03W-17DCB	POLK 1090	450240123044801	3	48	26	118	10	S	117
06S/03W-29ACC	POLK 1109	450120123045001	3	49	26	97.3	10	S	116
06S/05W-09AAC	POLK 1277	450412123175501	3	46	18	158	10	S	191
NONE	POLK 50073	NONE	3	52	27	115	10	S	OMITTED
03S/04W-05CCC2	YAMH 4725	452000123125001	3	33	21	143	10	S	206
05S/04W-24ACD	YAMH 7043	450723123120701	3	43	22	125	10	S	OMITTED
05S/05W-01CAB	YAMH 7318	450957123150201	3	41	20	123	10	S	163
05S/03W-34CBB	YAMH 50041	450531123025901	3	45	27	91.6	10	S	103
10S/04W-23ABB	BENT 1805	444136123082401	3	66	24	184	10	S	OMITTED
13S/05W-03AAA	BENT 6206	442833123162401	3	77	19	229	10	S	247
14S/05W-08AAB	BENT 6693	442226123184901	3	82	17	254	10	S	295
16S/04W-33CDC	LANE 88	440744123105301	3	95	22	355	10	S	363
17S/06W-24DCB2	LANE 14118	440422123213701	3	98	16	405	10	S	409
14S/01W-07CCD	LINN 13101	442139122513101	3	83	34	489	10	S	465
12S/03W-34BDD	LINN 50854	442900123021701	3	77	28	265	10	S	286
05S/01W-10ADD	MARI 1728	450908122470801	3	42	37	121	10	S	130
05S/01W-19BAD	MARI 1886	450734122512601	3	43	34	138	10	S	130
05S/01W-26BDC	MARI 1984	450632122463201	3	44	37	144	10	S	145
09S/03W-08ABB	MARI 14890	444837123044201	3	60	26	168	10	S	154
07S/05W-35CAB	POLK 88	445509123161001	3	54	19	232	10	S	245

Table B1. Groundwater-level data and simulations for the regional model from selected wells, Willamette Basin, Oregon.—Continued

Well location	Well log identifier	USGS site identification No.	Layer	Row	Column	Measured head (ft)	Scaled standard deviation (ft)	Measurement frequency	Simulated head (ft)
06S/05W-02DCA	POLK 1278	450427123153401	3	46	20	142	10	S	163
06S/05W-01CCB	POLK 1293	450441123151401	3	46	20	152	10	S	152
08S/04W-19BCA	POLK 2914	445152123134701	3	57	21	173	10	S	214
06S/06W-05DDB1	YAMH 7815	450443123264801	3	46	13	234	10	S	242
10S/04W-17AAA2	BENT 1750	444227123113701	4	65	22	85.7	10	S	222
12S/06W-12CDD	BENT 7884	443209123214701	4	74	16	253	10	S	275
02S/02E-34BDA	CLAC 4450	452125122322000	4	31	46	91.1	10	S	184
02S/03E-31CAA	CLAC 5246	452107122291501	4	31	48	260	10	S	215
02S/03E-36CBD	CLAC 5311	452102122231701	4	32	52	310	10	S	232
02S/03E-36CAC	CLAC 5318	452102122230701	4	32	52	195	1,000	S	229
04S/01E-02BDB	CLAC 12869	451520122391701	4	37	42	125	10	S	143
04S/01E-07CCB	CLAC 12968	451359122442501	4	38	39	82.8	10	S	108
04S/02E-07CAD	CLAC 13661	451411122364001	4	38	43	171	10	S	194
04S/02E-29AAD	CLAC 14212	451154122344901	4	40	45	220	10	S	224
06S/01E-10BCC	CLAC 15181	450415122411101	4	46	41	294	10	S	271
06S/02E-14ABA	CLAC 15413	450321122312801	4	47	47	1,440	10	S	OMITTED
03S/03E-07AAD	CLAC 16533	451941122283901	4	33	48	333	10	S	239
05S/03E-17DAC	CLAC 18994	450802122273001	4	43	49	863	10	S	OMITTED
03S/01W-22DDA	CLAC 20233	451729122470101	4	35	37	77.3	10	S	58.8
16S/05W-24AAB2	LANE 8712	441018123135501	4	93	21	328	10	S	348
15S/04W-07DDD	LANE 50039	441630123123201	4	88	21	280	10	S	297
15S/04W-09DAB	LINN 2123	441647123101401	4	87	23	291	10	S	299
10S/01W-16ADA	LINN 3778	444213122481301	4	65	36	363	10	S	364
10S/02W-24AAC	LINN 4295	444128122520901	4	66	34	307	10	S	295
12S/04W-33ADA	LINN 10808	442910123101401	4	77	23	236	10	S	233
14S/03W-02DBA	LINN 13545	442252123004201	4	82	29	305	10	S	310
14S/02W-10BDC	LINN 14614	442205122550401	4	83	32	396	10	S	421
04S/02W-22ACA	MARI 1258	451242122544601	4	39	32	124	10	S	94.6
04S/02W-28CDB	MARI 1331	451124122563801	4	40	31	127	10	S	92.2
04S/01W-17DAD	MARI 2234	451317122493101	4	38	36	144	10	S	107
05S/02W-10CDB2	MARI 2360	450853122552902	4	42	32	153	10	S	103
06S/01W-01CDD	MARI 2978	450418122451201	4	46	38	175	10	S	172
06S/02W-17DBC	MARI 4092	450248122572601	4	47	31	125	10	S	120
07S/04W-21DCC2	POLK 2031	445631123105101	4	53	23	162	10	S	249
07S/04W-30DAD	POLK 2129	445551123125301	4	53	21	188	10	S	198
08S/04W-07CCA2	POLK 3227	445308123134701	4	56	21	196	10	S	215
09S/04W-28DBA	POLK 3950	444531123104501	4	62	23	197	10	S	OMITTED
10S/04W-04ABC2	POLK900003	444406123105501	4	64	22	191	10	S	185
01S/01W-01BB1	WASH 89	453103122443401	4	23	39	554	10	S	OMITTED
NONE	WASH 747	NONE	4	28	32	126	10	S	125
01N/01W-21CAB	WASH 4787	453315122491201	4	21	36	270	10	S	216
01N/03W-04CCC	WASH 5967	453540123041101	4	19	27	162	10	S	194
01N/03W-07CCD01	WASH 6037	453445123063201	4	20	25	161	10	S	194
01N/04W-01ABC1	WASH 6532	453614123072102	4	18	25	154	10	S	205
02N/04W-03DAA1	WASH 7726	454106123092001	4	14	24	583	10	S	OMITTED
01S/01W-13CCB1	WASH 8801	452843122454201	4	25	38	214	10	S	222
01S/02W-02CBB2	WASH 9314	453043122542501	4	23	33	165	1,000	S	170
01S/02W-02CBB1	WASH 9320	453040122542301	4	23	33	200	10	S	170
01S/02W-18AAC	WASH 9959	452916122582001	4	24	30	163	1,000	S	138
01S/02W-18ABD	WASH 9987	452917122583201	4	24	30	118	10	S	138
01S/02W-21AAB	WASH 10042	452836122555001	4	25	32	154	10	S	140
01S/02W-21BBA	WASH 10062	452831122564501	4	25	31	156	10	S	133
01S/02W-28CAB	WASH 10348	452713122563001	4	26	31	143	10	S	131

Table B1. Groundwater-level data and simulations for the regional model from selected wells, Willamette Basin, Oregon.—Continued

Well location	Well log identifier	USGS site identification No.	Layer	Row	Column	Measured head (ft)	Scaled standard deviation (ft)	Measurement frequency	Simulated head (ft)
01S/02W-29DBD	WASH 10406	452707122572201	4	26	31	148	10	S	129
02S/02W-05BBA	WASH 10477	452558122575201	4	27	31	128	10	S	132
01S/03W-02DDA	WASH 10569	453031123004201	4	23	29	157	10	S	154
01S/03W-13BAD	WASH 10686	452917123000601	4	24	29	152	10	S	146
01S/04W-02ADD	WASH 11109	453020123063601	4	23	24	162	10	S	213
02S/02W-11CCD01	WASH 12572	452416122541601	4	29	33	118	10	S	120
05S/03W-09ACD	YAMH 147	450906123033601	4	42	27	84.3	10	S	83.1
03S/02W-18ABB	YAMH 2424	451856122584401	4	33	30	189	10	S	180
04S/03W-02DCB	YAMH 5151	451451123011401	4	37	28	131	10	S	68.1
04S/04W-14BDA	YAMH 5712	451341123084601	4	38	24	81.9	10	S	128
05S/05W-13ABA	YAMH 7306	450833123143701	4	42	20	128	10	S	129
05S/01E-22DCC	CLAC 2616	450655122401101	5	44	41	103	10	S	165
03S/01W-10CCD	CLAC 8009	451905122475801	5	33	37	129	10	S	152
03S/01W-27DDB	CLAC 8638	451636122471801	5	35	37	83.1	10	S	73
03S/01E-01BCD	CLAC 8824	452027122380701	5	32	43	54.6	10	S	54.3
05S/02E-14BBD01	CLAC 10188	450824122320401	5	43	46	346	10	S	379
03S/02E-15ABC	CLAC 18421	451856122324701	5	33	46	104	10	S	205
03S/01W-10CAA	CLAC 18836	451923122474601	5	33	37	130	10	S	163
04S/01W-10DDC	MARI 405	451354122471701	5	38	37	91	10	S	103
06S/01W-02BCD	MARI 3003	450444122464501	5	46	37	78.6	10	S	141
06S/01E-06CDD	MARI 5539	450418122440201	5	46	39	70.2	10	S	187
06S/01E-17BDA	MARI 5576	450311122424801	5	47	40	194	10	S	263
07S/01W-27CCC	MARI 6404	445546122480201	5	54	37	533	10	S	497
07S/02W-26CCB2	MARI 7741	445549122541701	5	54	33	177	10	S	231
08S/02W-14BAA	MARI 10239	445255122534401	5	56	33	417	10	S	450
09S/01W-31ACD	MARI 13834	444443122510401	5	63	35	354	10	S	359
09S/03W-03BCB	MARI 14847	444913123025201	5	59	27	590	10	S	537
09S/01E-03BCC	MARI 15579	444903122404501	5	59	41	1,050	10	S	1,060
09S/01E-03CB1	MARI 15581	444858122404901	5	59	41	1,060	10	S	1,040
06S/01W-03ACA	MARI 17676	450456122472501	5	46	37	77.9	10	S	137
06S/03W-07ADD	POLK 1003	450406123052601	5	46	26	176	10	S	155
06S/03W-08DCD	POLK 1008	450333123043701	5	47	26	137	10	S	120
06S/03W-32DBA	POLK 1150	450023123043901	5	50	26	111	1,000	S	137
02S/02W-08ACB	WASH 943	452452122573101	5	28	31	133	10	S	149
NONE	WASH 1364	NONE	5	33	34	178	10	S	212
02S/02W-02BDB	WASH 1686	452545122540801	5	28	33	166	10	S	199
03S/02W-11DDC	WASH 2003	451906122532801	5	33	33	306	10	S	287
02N/03W-25BBB1	WASH 3779	453805123003201	5	17	29	536	10	S	291
01N/02W-28DAB	WASH 5586	453230122555701	5	22	32	136	10	S	181
01N/03W-16AAB	WASH 6150	453441123032001	5	20	27	132	10	S	188
02N/02W-31CCD01	WASH 7101	453630122590501	5	18	30	161	10	S	210
02N/02W-32AAD1	WASH 7121	453705122570201	5	18	31	279	1,000	S	449
02N/02W-33ACD1	WASH 7155	453655122561301	5	18	31	281	1,000	S	467
02N/02W-33BBB1	WASH 7175	453709122564701	5	18	31	230	1,000	S	466
01S/01W-17AAD1	WASH 8851	452916122493401	5	24	36	177	10	S	215
01S/01W-21CDD2	WASH 8988	452751122485401	5	26	36	165	10	S	225
01S/01W-24BBC1	WASH 9027	452831122454201	5	25	38	176	10	S	216
01S/01W-24BBD2	WASH 9029	452830122454401	5	25	38	206	10	S	216
01S/01W-31DAB	WASH 9162	452623122510101	5	27	35	151	10	S	279
NONE	WASH 10189	NONE	5	25	34	180	10	S	214
01S/02W-31BA1	WASH 10450	452641122584701	5	27	30	143	10	S	154
NONE	WASH 10496	NONE	5	27	32	155	10	S	179
NONE	WASH 10509	NONE	5	27	33	163	10	S	202

Table B1. Groundwater-level data and simulations for the regional model from selected wells, Willamette Basin, Oregon.—Continued

Well location	Well log identifier	USGS site identification No.	Layer	Row	Column	Measured head (ft)	Scaled standard deviation (ft)	Measurement frequency	Simulated head (ft)
NONE	WASH 11106	NONE	5	28	36	123	10	S	220
NONE	WASH 11467	NONE	5	27	36	129	10	S	241
02S/01W-06BCC	WASH 11510	452536122515501	5	28	34	150	10	S	252
02S/01W-07ACD1	WASH 11516	452443122510301	5	28	35	132	10	S	186
02S/01W-16ABB	WASH 11552	452415122485101	5	29	36	136	10	S	123
02S/01W-10BAB	WASH 11592	452501122475701	5	28	37	127	10	S	203
02S/01W-10ADA	WASH 11594	452351122465901	5	28	37	124	10	S	185
02S/01W-14AAB	WASH 11707	452411122460701	5	29	38	129	10	S	150
02S/01W-18DAD	WASH 11875	452336122504901	5	29	35	128	10	S	111
02S/02W-02BBD1	WASH 12399	452549122541301	5	27	33	168	10	S	199
02S/02W-02DCC1	WASH 12405	452514122534301	5	28	33	130	10	S	185
02S/02W-06BBB	WASH 12442	452556122592001	5	27	30	146	10	S	191
NONE	WASH 12457	NONE	5	28	30	168	10	S	252
02S/02W-16CCA	WASH 12679	452335122564301	5	29	31	170	10	S	220
02S/03W-11DDC	WASH 13438	452424123005301	5	29	29	652	1,000	S	428
NONE	WASH 50346	NONE	5	27	33	157	10	S	199
01S/02W-15ACB	WASH 51495	452911122545901	5	25	32	126	10	S	166
03S/02W-23BBA	YAMH 168	451805122541801	5	34	33	449	10	S	231
05S/03W-06CBD	YAMH 1928	450949123062901	5	41	25	124	10	S	99.1
03S/02W-14BCB	YAMH 2345	451850122542201	5	34	33	219	10	S	251
03S/02W-19CCB	YAMH 2428	451730122591500	5	35	30	100	10	S	85.8
03S/02W-24BAD	YAMH 2544	451804122524001	5	34	34	517	10	S	266
03S/02W-13CCD	YAMH 2549	451814122525901	5	34	33	653	1,000	S	276
03S/02W-26BDA	YAMH 2599	451705122540000	5	35	33	286	10	S	189
03S/02W-36ACA	YAMH 2685	451611122522601	5	36	34	141	10	S	148
03S/02W-36ABA	YAMH 2703	451626122522001	5	36	34	356	1,000	S	170
10S/05W-14ABC	BENT 176	444222123154401	6	65	19	229	20	S	395
NONE	BENT 755	NONE	6	74	16	253	10	S	256
12S/05W-18ABA	BENT 768	443158123201801	6	74	17	239	20	S	257
11S/07W-08CAB	BENT 1205	443742123341001	6	69	8	704	20	S	660
NONE	BENT 1402	NONE	6	77	18	231	10	S	252
13S/06W-22DAD	BENT 1408	442523123234401	6	80	14	437	20	S	603
10S/07W-27CCD	BENT 1479	444002123321501	6	67	9	699	20	S	1,230
10S/04W-19ABD	BENT 1487	444131123131201	6	66	21	287	20	S	324
10S/04W-16BBC	BENT 1751	444224123113201	6	65	22	202	10	S	223
10S/04W-27CDA	BENT 1899	444004123095201	6	67	23	287	20	S	232
10S/06W-23BCC1	BENT 2309	444116123234101	6	66	15	786	20	S	525
10S/06W-30DCA	BENT 2334	444011123280201	6	67	12	355	20	S	382
11S/05W-23AC	BENT 3838	443609123153101	6	71	20	301	20	S	332
11S/06W-14CCC	BENT 4268	443630123232701	6	70	15	580	20	S	731
12S/05W-06DCA	BENT 4951	443304123201701	6	73	17	277	20	S	397
13S/06W-06ABA	BENT 6475	442831123273801	6	77	12	435	20	S	562
14S/05W-06ACA1	BENT 6679	442309123200801	6	82	17	310	20	S	347
14S/06W-22BDC1	BENT 7238	442024123241301	6	84	14	598	20	S	598
14S/06W-26ADA2	BENT 7383	441933123222201	6	85	15	295	20	S	332
15S/05W-09BCB	BENT 7691	441643123181501	6	87	18	467	20	S	371
10S/04W-24AD	BENT 7800	444126123140601	6	66	20	298	20	S	311
12S/06W-34ABB	BENT 7842	442924123240801	6	76	14	451	20	S	463
NONE	BENT 50096	NONE	6	81	14	428	10	S	515
05S/03E-32DBB	CLAC 50106	450530122274501	6	45	49	658	20	S	772
18S/05W-12ADC	LANE 2328	440112123135901	6	101	20	414	20	S	563
17S/06W-07DDD	LANE 3479	440601123270901	6	97	12	581	20	S	470
18S/03W-15AAD	LANE 4663	440031123013801	6	101	28	542	20	S	517

Table B1. Groundwater-level data and simulations for the regional model from selected wells, Willamette Basin, Oregon.—Continued

Well location	Well log identifier	USGS site identification No.	Layer	Row	Column	Measured head (ft)	Scaled standard deviation (ft)	Measurement frequency	Simulated head (ft)
15S/06W-24DBD	LANE 4857	441459123212701	6	89	16	358	20	S	388
15S/05W-09ADC	LANE 6478	441653123173601	6	87	18	313	20	S	314
15S/05W-09ACD	LANE 6479	441657123174701	6	87	18	323	20	S	312
15S/05W-09BCD2	LANE 6483	441657123182301	6	87	18	438	20	S	368
15S/05W-20CDD	LANE 6584	441448123190801	6	89	17	340	20	S	349
15S/05W-31ABD	LANE 6678	441342123201101	6	90	17	529	20	S	443
16S/03W-09AAC2	LANE 7370	441152123030001	6	92	27	351	20	S	523
16S/05W-04AAB2	LANE 8411	441255123173401	6	91	18	319	20	S	325
16S/05W-30DCA	LANE 8773	440845123201001	6	94	17	692	20	S	537
16S/06W-33AAA	LANE 9114	440831123244301	6	95	14	538	20	S	623
17S/03W-30AAD	LANE 11461	440405123051301	6	98	26	408	20	S	407
17S/04W-30CCA	LANE 12505	440331123133001	6	99	21	401	20	S	472
17S/04W-31CAB2	LANE 12554	440255123131701	6	99	21	498	20	S	540
17S/05W-06BCB	LANE 12844	440726123205601	6	95	16	434	20	S	625
17S/05W-34DCC	LANE 13575	440232123164101	6	100	19	371	20	S	391
17S/06W-36CDD2	LANE 14458	440232123214301	6	100	16	438	20	S	461
17S/06W-36CDD	LANE 14459	440235123214101	6	100	16	448	20	S	464
18S/02W-14CCC	LANE 15398	435953122541201	6	102	33	522	20	S	528
18S/03W-23AAC	LANE 16438	435939123003701	6	102	29	487	20	S	539
18S/04W-14BBA	LANE 16780	440036123083201	6	101	24	651	20	S	944
18S/04W-14ACA	LANE 17048	440029123080301	6	102	24	738	20	S	933
18S/06W-08ABA	LANE 18864	440131123260901	6	101	13	492	20	S	489
18S/06W-24BBBD	LANE 18890	435948123220801	6	102	15	505	20	S	558
19S/01W-03ADB	LANE 19429	435656122471801	6	105	37	642	20	S	665
19S/03W-15AAB	LANE 20567	435525123014601	6	106	28	518	10	S	549
19S/03W-14BCC	LANE 20573	435504123012701	6	106	28	523	10	S	555
12S/03W-25ABB1	LINN 832	443014122594801	6	76	29	284	20	S	306
13S/02W-20BBC3	LINN 935	442549122575001	6	80	31	384	20	S	648
14S/02W-21AAA	LINN 1070	442040122552901	6	84	32	415	20	S	500
11S/02W-12ADC	LINN 1643	443743122520201	6	69	34	271	20	S	294
14S/01W-08ADD	LINN 2571	442206122492701	6	83	36	599	20	S	583
11S/01W-01CAD	LINN 5572	443824122451501	6	69	38	393	20	S	463
12S/01W-12BCD	LINN 6586	443234122453301	6	74	38	470	20	S	614
12S/02W-19CCB1	LINN 8054	443028122590901	6	76	30	318	20	S	315
13S/01W-07BCC	LINN 11056	442716122514901	6	78	34	813	20	S	745
13S/01W-07CBB	LINN 11061	442746122514701	6	78	34	822	20	S	751
13S/02W-20BBC2	LINN 11661	442547122575501	6	80	30	434	20	S	640
14S/02W-10DBD2	LINN 13434	442150122543801	6	83	33	417	20	S	436
14S/02W-21ADC	LINN 13508	442020122554901	6	84	32	507	20	S	579
14S/03W-13BBC	LINN 13620	442123123001901	6	83	29	423	20	S	384
12S/02W-12DAD	LINN 14489	443216122515201	6	74	34	456	20	S	436
06S/01W-36DDC	MARI 3652	445959122445001	6	50	39	238	20	S	390
06S/01W-36DBC2	MARI 3693	450010122450401	6	50	38	349	20	S	359
08S/01W-01BAD	MARI 8594	445433122451201	6	55	38	813	20	S	654
09S/03W-23DDB	MARI 15218	444608123004401	6	62	29	237	10	S	267
09S/02E-10DCC	MARI 15788	444741122325201	6	61	46	717	20	S	760
06S/01E-34CAA2	MARI 18158	450019122402301	6	50	41	394	20	S	512
07S/06W-24CDC2	POLK 31	445636123221501	6	53	15	693	20	S	596
07S/05W-05DDA	POLK 373	445917123185901	6	50	17	433	20	S	236
06S/03W-08DDA	POLK 1023	450333123041301	6	47	27	118	10	S	121
06S/04W-24ADB	POLK 1232	450218123064901	6	48	25	230	20	S	187
06S/05W-33ACC	POLK 1317	450031123181701	6	49	18	443	20	S	243
06S/06W-17DDB	POLK 1368	450248123262601	6	47	13	285	20	S	306

Table B1. Groundwater-level data and simulations for the regional model from selected wells, Willamette Basin, Oregon.—Continued

Well location	Well log identifier	USGS site identification No.	Layer	Row	Column	Measured head (ft)	Scaled standard deviation (ft)	Measurement frequency	Simulated head (ft)
06S/06W-22BDC1	POLK 1393	450214123244201	6	48	14	473	20	S	360
07S/05W-06BBC	POLK 2208	445950123211901	6	50	16	235	20	S	267
08S/05W-07BBB	POLK 3477	445352123212201	6	55	16	397	20	S	469
09S/04W-18ABB	POLK 3899	444744123132401	6	61	21	231	20	S	246
07S/06W-12ADC	POLK 4293	445845123213001	6	51	16	524	20	S	471
01S/05W-13DAA1	WASH 1510	452901123141301	6	25	21	295	20	S	342
01S/04W-14DCD2	WASH 3235	452844123082301	6	25	24	91.3	20	S	291
01S/04W-18BCC1	WASH 3506	452908123140801	6	25	21	333	20	S	335
01S/04W-18BAC1	WASH 3765	452922123135201	6	24	21	336	20	S	321
01N/04W-06DAC1	WASH 14009	453546123131601	6	19	21	309	20	S	314
01N/04W-31CBD1	WASH 50022	453130123135801	6	23	21	1,200	20	S	550
04S/05W-22DA	YAMH 536	451222123165701	6	39	19	388	20	S	350
05S/06W-32DAC	YAMH 666	450526123264401	6	45	13	191	20	S	206
02S/03W-31ABC	YAMH 1124	452128123060701	6	31	25	181	20	S	255
02S/03W-31ACB	YAMH 1127	452120123060500	6	31	25	174	20	S	261
03S/03W-09DAB	YAMH 4100	451927123032301	6	33	27	179	10	S	175
03S/03W-30DAB	YAMH 4591	451650123054501	6	35	26	183	20	S	355
03S/04W-18BDC	YAMH 4867	451838123135001	6	34	21	293	20	S	339
03S/05W-12DCD	YAMH 5046	451906123143901	6	33	20	219	20	S	414
04S/03W-05DBB02	YAMH 5189	451514123045201	6	37	26	220	20	S	215
04S/04W-07ACC	YAMH 5590	451418123133501	6	37	21	177	20	S	151
05S/04W-36DDB	YAMH 7222	450518123070401	6	45	25	216	20	S	256
05S/06W-26AAA	YAMH 7529	450654123225401	6	44	15	523	20	S	270
05S/05W-32BBA2	YAMH 7608	450600123201001	6	45	17	199	20	S	174
05S/06W-32CDA	YAMH 7610	450519123271201	6	45	12	193	20	S	210
06S/06W-05DDB2	YAMH 7813	450443123264501	6	46	13	208	20	S	227
04S/05W-24DBD	YAMH 7992	451222123143901	6	39	20	187	20	S	225

Table B2. Base-flow estimates from selected streamgages, Willamette Basin, Oregon.

[**USGS** station No.: Site identification number permanently assigned to the surface-water site by the U.S. Geological Survey (USGS) and recorded in National Water Information System (NWIS), a national computer database maintained by USGS. **Short name**: Unique name derived from station name. Station **name**: Unique site name permanently assigned to a surface-water gaging station. **Estimated surface-water body gain**: Mean annual base flow derived by PART (a streamflow partitioning computer program; Rutledge, 1998, and Lee and Risley, 2001). **Scaled standard deviation**: Value from which the observation weight is calculated. ft^3/s, cubic foot per second]

USGS station No.	Short name	Station name	Estimated surface-water body gain (ft^3/s)	Adjusted estimated surface-water body gain (ft^3/s)	Scaled standard deviation (ft^3/s)	Simulated surface-water body gain (ft^3/s)
14211500	JHNSN_SYCMR	Johnson Creek at Sycamore, Oregon	37	19	2.2	0
14211550	JHNSN_MILW	Johnson Creek at Milwaukie,Oregon	26	14	4.4	9
14207500	TUAL_WLINN	Tualatin River at West Linn,Oregon	1,414	742	224.8	713
14203500	TUAL_DILLEY	Tualatin River near Dilley, Oregon	398	209	48.2	190
14200000	MOLAL_CANBY	Mollala River near Canby, Oregon	800	421	370.9	357
14198500	MOLAL_WILHT	Mollala River above Pine Creek near Wilhoit, Oregon	605	318	146.8	363
14202000	PUDD_AUR	Pudding River at Aurora, Oregon	281	148	191.5	82
14201000	PUDD_MT_ANG	Pudding River Near Mount Angel, Oregon	466	245	172.1	196
14200300	SILVER_SILVE	Silver Creek at Silverton, Oregon	211	111	51.2	117
14194150	SYAM_MCMINN	South Yamhill River at McMinnville, Oregon	525	276	163.8	371
14192500	SYAM_WLLMNA	South Yamhill River near Willamina, Oregon	545	287	132	342
14193000	WLLMNA_WLLMN	Willamina Creek near Willamina, Oregon	232	122	56.3	110
14190700	RICKRL_DLLS	Rickreall Creek near Dallas,Oregon	117	62	28.3	79
14201500	BUTTE_MONTR	Butte Creek at Monitor,Oregon	266	140	64.6	105
14209700	FISH_3LNX	Fish Creek near Three Lynx, Oregon	170	89	10.3	140
14210000	CLACK_ESTCDA	Clackamas River at Estacada, Oregon	387	204	412.8	262
14190500	LUCKMT_SUVER	Luckiamute River near Suver, Oregon	750	395	45.4	430
14171000	MARYS_PHLMTH	Marys River near Philomath, Oregon	575	303	139.4	277
14170000	LTOM_MONROE	Long Tom River at Monroe, Oregon	260	137	90.1	209
14166500	LTOM_NOTI	Long Tom River near Noti, Oregon	214	113	13	159
14167000	COYOTE_CROW	Coyote Creek near Crow, Oregon	174	92	42.2	107
14189000	SANT_JFFSN	Santiam River at Jefferson, Oregon	229	121	858.2	391
14182500	L_NSANT_MHMA	Little North Santiam River near Mehama, Oregon	201	106	29.7	151
14183000	NSANT_MHMA	North Santiam River at Mehama, Oregon	372	196	453	170
14188800	THOM_SCIO	Thomas Creek near Scio,Oregon	390	205	94.7	241
14191000	WILL_ABV_SALEM	Willamette River at Salem, Oregon	[1]1,513	–	217.3	1,167
14211720	WILLAMETTE	Willamette River at Portland, Oregon	[1]3,247	–	2,173	2,874

[1]Estimated based on base flow separation methods (K. Lee, U.S. Geological Survey, written commun., 2006).

Table B3. Groundwater-level data for the local model from selected wells, Willamette Basin, Oregon.

[**Well location**: See section Well- and Spring-Location System for explanation. **Well log identifier:** Unique identifier combining a four-letter county code and a well-log number with as many as six digits, which is assigned to the well when a water well report is filed by the well driller with the Oregon Water Resources Department and recorded in Ground Water Resource Information Distribution (GRID), a statewide computer database maintained by Oregon Water Resources Department. **USGS site identification No.**: Site identification number permanently assigned to the well by the U.S. Geological Survey (USGS) and recorded in National Water Information System (NWIS), a national computer database maintained by USGS. **Layer**: Assigned layer in local groundwater model. ALL, well open to all units, CRB, well open to layers 5, 6, and 7. All other observation wells simulated as open to only one layer (unit). **Row**: Assigned row in local groundwater model. **Column**: Assigned column in local groundwater model. **Average annual head estimate:** Mean annual water levels calculated using data from bimonthly, quarterly, or recorder well. **Scaled standard deviation**: Value from which the observation weight is calculated. ft, foot]

Well location	Well log identifier	USGS site identification No.	Layer	Row	Column	Average annual head estimate (ft)	Scaled standard deviation (ft)	Simulated head (ft)
06S/01W-01ADB	MARI 2979	450452122444901	ALL	101	107	187	3.03	179
03S/01W-14ABA	CLAC 50585	451903122460801	CRB	15	101	36.4	3.03	90.1
08S/03W-11CCC	MARI 11727	445304123014101	CRB	173	34	347	3.03	411
07S/02W-26CCB	MARI 7736	445544122541601	CRB	157	66	173	3.03	225
06S/01W-08DAD06	MARI 55017	450340122493404	1	109	86	134	3.03	140
06S/01W-08DAD04	MARI 54953	450339122492801	1	109	87	156	3.03	149
03S/01W-24DDD01	CLAC 54227	451722122443501	2	26	107	110	3.03	88
05S/03W-22AAA	YAMH 6576	450745123015801	2	84	33	87.2	6.06	93
06S/03W-04ACD	MARI 4816	450451123031901	2	102	27	94.1	3.03	105
06S/01W-08DAD03	MARI 54952	450340122493402	2	109	86	119	3.03	150
06S/01W-08DAD05	MARI 55015	450339122492802	2	109	87	116	3.03	151
03S/01W-25CBD	CLAC 8562	451642122453301	3	30	103	117	3.03	83.8
04S/01W-12BBA	MARI 463	451437122453701	3	42	103	181	3.03	106
04S/01W-11CDA01	MARI 17545	451402122462501	3	46	100	133	3.03	118
04S/01E-20BAC	CLAC 13431	451251122425901	3	53	114	111	3.03	138
04S/01W-32ADB	MARI 905	451052122512501	3	64	86	141	3.03	123
04S/01E-32ADD	CLAC 13378	451048122420501	3	65	118	134	3.03	165
05S/02W-01DDA	MARI 2218	450939122520901	3	73	75	137	3.03	122
05S/02W-08CCA2	MARI 52504	450851122575801	3	77	50	152	3.03	102
05S/02W-19DCC	MARI 2541	450758122590201	3	88	47	140	3.03	103
05S/01W-26BCC	MARI 1980	450628122465801	3	92	97	138	3.03	149
06S/03W-04ACD	MARI 4816	450451123031901	3	102	27	96.1	3.03	105
06S/02W-05CDD	MARI 3799	450423122573601	3	104	52	163	3.03	121
06S/01W-06CCC	MARI 3054	450423122514701	3	105	77	128	3.03	135
06S/02W-17DAD	MARI 4160	450246122564801	3	114	55	154	3.03	127
06S/03W-19AAD	POLK 1070	450227123052701	3	116	18	127	3.03	126
06S/01W-21CDC01	MARI 3280	450140122490701	3	121	88	144	3.03	165
06S/02W-30ADB	MARI 4559	450122122581901	3	123	49	147	3.03	130
07S/02W-04BDA	MARI 6564	445942122561801	3	133	57	153	3.03	146
07S/02W-28ADD	MARI 7883	445606122554101	3	155	60	188	3.03	191
07S/02W-32ABC01	MARI 16424	445528122574501	3	159	53	196	3.03	198
03S/01W-24BCD	CLAC 8498	451752122453501	4	23	103	75.2	3.03	75.2
04S/02W-02BBD	MARI 1044	451528122541301	4	37	66	78.9	3.03	71.5
04S/01W-05CDC	MARI 308	451447122502101	4	41	83	132	3.03	104
04S/02W-01CDD01	CSCH DP	451444122524701	4	42	72	82.2	3.03	89.2
04S/03W-33DBA	YAMH 5484	451045123032701	4	66	27	149	6.06	89.2
05S/02W-05BCC	MARI 2331	450958122580201	4	71	50	151	3.03	99.4
05S/02W-08CCB1	MARI 52597	450851122580101	4	77	50	128	3.03	101
05S/01E-18ACC01	CLAC 2555	450812122435101	4	81	111	169	3.03	162
05S/03W-21ACB	YAMH 6565	450733123034101	4	85	25	108	3.03	97.3
05S/02W-25CBD	MARI 2666	450620122530501	4	93	71	145	3.03	124
03S/01E-26BCD	CLAC 9648	451656122391801	5	28	130	82.2	3.03	184
05S/01W-28DBB	MARI 2035	450623122484901	5	92	89	76.8	3.03	133
07S/01W-19BAC02	MARI 53069	445706122512701	6	149	78	195	3.03	223
07S/03W-05CCA2	POLK 125	445913123051101	6	136	19	329	1.82	287

Table B3. Groundwater-level data for the local model from selected wells, Willamette Basin, Oregon.—Continued

[**Well location**: See section Well- and Spring-Location System for explanation. **Well log identifier:** Unique identifier combining a four-letter county code and a well-log number with as many as six digits, which is assigned to the well when a water well report is filed by the well driller with the Oregon Water Resources Department and recorded in Ground Water Resource Information Distribution (GRID), a statewide computer database maintained by Oregon Water Resources Department. **USGS site identification No.**: Site identification number permanently assigned to the well by the U.S. Geological Survey (USGS) and recorded in National Water Information System (NWIS), a national computer database maintained by USGS. **Layer**: Assigned layer in local groundwater model. ALL, well open to all units, CRB, well open to layers 5, 6, and 7. All other observation wells simulated as open to only one layer (unit). **Row**: Assigned row in local groundwater model. **Column**: Assigned column in local groundwater model. **Average annual head estimate:** Mean annual water levels calculated using data from bimonthly, quarterly, or recorder well. **Scaled standard deviation**: Value from which the observation weight is calculated. ft, foot]

Well location	Well log identifier	USGS site identification No.	Layer	Row	Column	Average annual head estimate (ft)	Scaled standard deviation (ft)	Simulated head (ft)
03S/01W-15CAC	CLAC 8184	451747122484801	7	19	93	86.4	3.03	112
03S/01W-16DDD	CLAC 8231	451813122481801	7	20	91	87.3	3.03	119
07S/01W-02CAA01	MARI 5904	445923122462501	7	135	100	144	6.06	345
07S/03W-18BAD01	POLK 1781	445804123061201	7	143	15	548	3.03	403
07S/03W-05CCA1	POLK 881	445918123050801	7	135	19	230	6.06	269
05S/04W-14AB1	YAMH 672	450826123082601	7	80	5	323	6.06	254
05S/04W-24BBA2	YAMH 599	450740123074401	8	84	8	254	6.06	239

Appendix C. Estimation of Prescribed Fluxes for Local Model

The Central Willamette subbasin is completely contained within the regional model grid boundary, and the subbasin boundary crosses active coarse-grid regional model cells, some of which have nonnegligible fluxes. For the Central Willamette subbasin model (referred to as the local model), the flux across the local model boundary was estimated using the regional model. The flux from the coarse-grid regional model was divided equally among the finer grid of the boundary cells of the local model. The WELL package in MODFLOW was used to simulate these fluxes.

To compute the flux across the new boundary, a mass balance was calculated for the active local cells within each active regional cell that intersects the Central Willamette subbasin boundary (fig. C1). For the example shown in figure C1, the flux across the boundary (fig. C1*A*) plus the flux leaving the area of the regional model cell occupied by active local model cells (fig. C1*B*) plus the sum of the remaining fluxes (such as vertical fluxes, recharge, rivers, and wells) in the regional model cell must equal zero to maintain the mass balance. Generally, this is given by the equation:

$$Q_A + Q_B + \{\text{Sum of Remaining Fluxes}\}_{\text{Active Local Cells}} = 0 \qquad \text{(C1)}$$

where

Q_A is the flux (shown in figure C1*A*) to be estimated for simulation as a prescribed flux boundary condition, and

Q_B is the sum of the fluxes shown in figure C1*B*.

After Q_A is estimated, it is divided equally between the new boundary cells (fig. C1*C*).

The regional cell flux through any face is known from the steady-state simulation. The part of Q_B passing through any cell face is estimated as the regional cell flux through that face multiplied by the fraction of the regional cell face occupied by active local cells. For each regional cell, summing the fluxes over all regional cell faces that intersect active local cells (for example, two faces are intersected in figure C1) yields the total Q_B.

For the regional scale cell, mass also must be conserved. This implies that the sum of the fluxes through the four plan view sides (these are known from the regional steady-state simulation) must equal the "Sum of the Remaining Fluxes" for the whole regional cell, allowing computation of the following estimate:

$$\{\text{Sum of Remaining Fluxes}\}_{\text{Local Cells}} = \text{Active Fraction} \times \{\text{Sum of Remaining Fluxes}\}_{\text{Regional Cell}} \qquad \text{(C2)}$$

where the

"Active Fraction" is the number of new active cells divided by the total number of local cells in a regional cell.

Using the previous estimates, equation (C1) is used to compute Q_A, which is subsequently divided by the total number of new boundary cells within the regional cell (see fig. C1*C*) yielding the flux to be injected/extracted from each new boundary cell. This procedure works for all new layers except the layer representing the CRB. Because this layer is divided into three layers for the local scale model, the flux also must be divided into three for each plan view cell shown in figure C1. This is accomplished by further dividing the flux into three parts weighted by thickness of each CRB layer.

The algorithm described above generates a specified flux boundary condition for the local Central Willamette subbasin model. Model calibration did not indicate the model was sensitive to variation in boundary flux conditions; therefore, flux was applied at a constant average annual rate in each cell. Most boundary flux indicated flow into the Central Willamette subbasin, except areas where a stream was close to a boundary, or crossed a boundary. In some of these areas, net flux was out of the Central Willamette subbasin (flow entered the model through 1,626 cells; flow exited the model through 295 cells). Total flux rate into the Central Willamette subbasin per month is 158 ft^3/s, and total flux rate out of the Central Willamette subbasin per month about 7 ft^3/s. The largest amount of net flux (about 100 ft^3/s) enters the Central Willamette subbasin from the northeast through layer 4 (LSU) (fig. C1 and table 6). The second largest contributor is the BCU (38 ft^3/s), with net flux distributed fairly evenly around the perimeter of the study area. Net contribution from the WSU is negligible (0.1 ft^3/s).

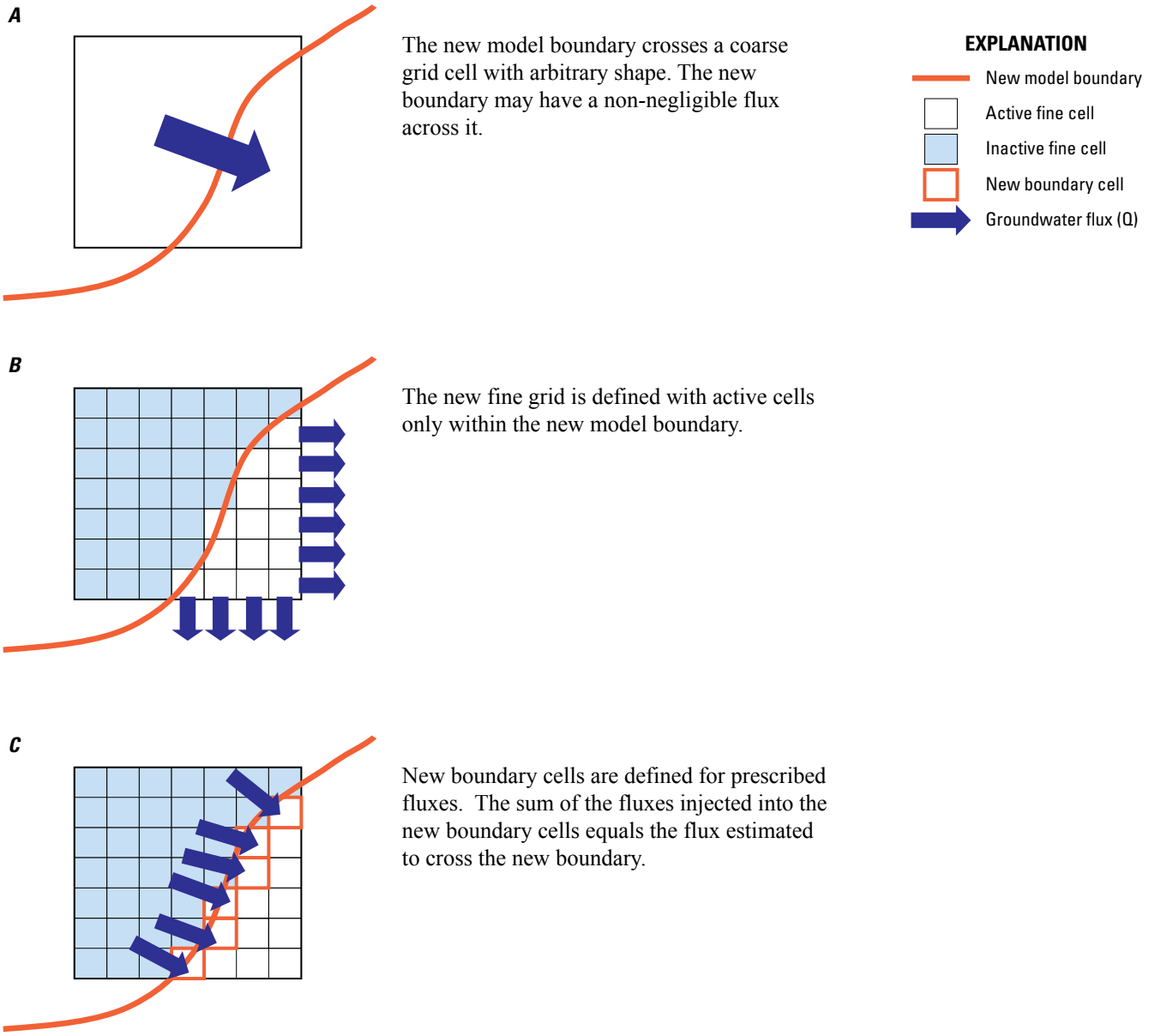

Figure C1. Plan view grid refinement from the regional coarse grid model to the refined fine scale model. (*A*) A new model boundary crosses a coarse grid cell with arbitrary shape. The new boundary may have a non-negligible flux across it. (*B*) The new fine grid is defined with active cells only within the new model boundary. (*C*) New boundary cells are defined for prescribed fluxes. The sum of the fluxes injected into the new boundary cells equals the flux estimated to cross the new boundary.

Publishing support provided by the U.S. Geological Survey
Publishing Network, Tacoma Publishing Service Center

For more information concerning the research in this report, contact the
Director, Oregon Water Science Center
U.S. Geological Survey
2130 SW 5th Avenue
Portland, Oregon 97201
http://or.water.usgs.gov

ISSN 2328-0328 (online)
http://dx.doi.org/10.3133/sir20145136